New insights into the gene regulatory network that regulates dorsoventral axis patterning in *Oncopeltus fasciatus*

I n a u g u r a l – D i s s e r t a t i o n

zur

Erlangung des Doktorgrades

der Mathematisch-Naturwissenschaftlichen Fakultät

der Universität zu Köln

vorgelegt von

Kai Hans Conrads

aus Neuss

Köln, 2023

Berichterstatter/in: Herr Prof. Dr. Siegfried Roth
Herr Prof. Dr. Matthias Hammerschmidt

Tag der letzten mündlichen Prüfung: 26. Februar 2024

Table of Contents

Zusammenfassung

Die Toll-abhängige dorsoventrale Achsenbildung in Drosophila ist eines der am besten verstandenen genregulatorischen Netzwerke. Außerhalb der Insekten ist Toll jedoch nicht für eine achsenbildende Funktion bekannt, sondern für eine Rolle bei der Pathogenabwehr. Bei den meisten anderen Tieren wird die dorsoventrale Achsenbildung durch eine BMP-Signalkaskade induziert. Wie sich die Verschiebung von einer BMP-basierten zu einer Toll-dominierten Form der dorsoventralen Achsenbildung innerhalb der Insektenlinie evolviert hat, ist noch nicht ausreichend erforscht. Frühere Arbeiten haben gezeigt, dass in der Wanze *Oncopeltus fasciatus* Toll nur zur Polarisierung eines dynamischen BMP-Signalkaskadennetzwerks erforderlich ist, einer Architektur, die den Merkmalen der dorsoventralen Achsenbildung bei Wirbeltieren und anderen Tieren ähnlicher ist als bei jedem anderen bisher untersuchten Insekt.

In dieser Arbeit habe ich ein embryonales Mikroinjektionsprotokoll zur Injektion von Komponenten des Toll- und BMP-Signalwegs entwickelt, um diese Signalkaskaden ektopisch in Wildtyp- und dorsalisierten Toll-Knockdown-Embryonen zu aktivieren, und die induzierten Genexpressionsmuster mittels In-situ-Hybridisierungen analysiert. Zusammen mit phänotypischen Analysen zeigen meine Experimente, dass der Transkriptionsfaktor Snail eine entscheidende Komponente des BMP/Sog-Systems von *Oncopeltus* ist und damit eine Achsenbildungsfunktion hat, die für keinen anderen Organismus beschrieben ist. Ich schlage ein genregulatorisches Netzwerk mit Snail vor, das das bisherige BMP/Sog-System von *Oncopeltus* erweitert und in der Lage ist, das Mesoderm, Ektoderm und Mesectoderm zu induzieren.

Darüber hinaus habe ich Transkriptome von Wildtyp- und RNAi-vermittelten Knockdown-Embryonen erstellt, die auf wichtige dorsoventrale Musterbildungsgene des Toll- und BMP-Signalwegs abzielen. Ich führte RNAseq durch und analysierte eine Untergruppe von unterschiedlich exprimierten Genen durch In-situ-Hybridisierung und RNAi-vermittelte Knockdown-Generation. Mehrere in der Literatur noch nicht beschriebene Expressionsmuster wurden dabei entdeckt, unter anderem für die Serosa, für die es bisher keinen eigenständigen Marker gab.

Abstract

Toll-dependent dorsoventral axis patterning in *Drosophila* represents one of the best understood gene regulatory networks. However, outside the insects Toll is not known for a patterning function, but rather for a role in pathogen defense. In most other animals the dorsoventral axis is patterned by BMP signaling. How the shift from a BMP-based to a Toll-dominated mode of dorsoventral axis patterning within the insect lineage evolved has remained elusive. Previous work has shown that in the milkweed bug *Oncopeltus fasciatus* Toll is only required to polarize a dynamic BMP signaling network, an architecture that resembles characteristics of dorsoventral axis patterning in vertebrates and other animals more than any other insect studied so far.

In this work, I established an embryonic microinjection protocol to inject Toll and BMP pathway components to ectopically activate these pathways in wild-type and dorsalized Toll knockdown embryos and analyzed the induced gene expression patterns via in situ hybridizations. Together with phenotypic analysis my experiments revealed, that the transcription factor Snail is a crucial component of the BMP/Sog system of *Oncopeltus* and thus has an axis patterning function that is not described for any other organism. I propose a gene regulatory network including Snail that extends the previous BMP/Sog system of *Oncopeltus* and is able to pattern the mesoderm, ectoderm and mesectoderm.

In addition, I generated transcriptomes of both wild type and RNAi-mediated knockdown embryos, targeting essential dorsoventral patterning genes of the Toll and BMP pathway. I performed RNAseq and analysed a subset of differentially expressed genes via in situ hybridizations and RNAi-mediated knockdown generation. Several expression patterns were found that have never been described before, including two markers of the serosa, an embryonic fate that lacked a distinct marker in *Oncopeltus* as of yet.

1. Introduction

1.1. The conservation of body axis formation in animals

The number of body plans, shapes and sizes among animals is incredibly divers, yet in the vast majority of phyla animals possess two major body axes, the anteroposterior (AP) and the dorsoventral (DV) axis. How animals establish and pattern their primary body axis is one of the most fundamental problems in biology. The signaling pathways and gene regulatory networks underpinning axis formation seem to be well conserved among animals. For example, the conservation of positional roles for Hox genes suggests the existence of an AP axis patterning system used by most if not all bilaterally symmetric animals (Slack et al., 1993; Holland, 2013). Data from diverse deuterostomes and from protostomes suggest that Wnt signaling through β-catenin controls posterior identity during AP axis formation in most bilaterally symmetric animals (Petersen and Reddien, 2009). DV axis patterning mechanisms are highly conserved as well and most animals use BMP signaling to pattern their DV axis (Fig. 1) (Little and Mullins, 2006; De Robertis, 2008; Bier, 2011; Bier and De Robertis, 2015). A substantial amount of work is published for the role of BMP signaling in axis patterning of diploblasts [e.g., cnidarians (Genikhovich et al., 2015; Niehrs, 2010)], lophotrochozoa [e.g., planaria (Reddien et al., 2007; Molina et al., 2011; Gaviño et al., 2011) and annelids (Denes et al., 2007; Kuo and Weisblat, 2011)], arthropods [e.g., spiders (Akiyama-Oda and Oda, 2003; Akiyama-Oda and Oda, 2006; Pechmann et al., 2017; Pechmann, 2020)] and deuterostomes [e.g., echinoderms and nonvertebrate chordates like amphioxus (Lapraz et al., 2009; Yu et al., 2007)]. However, in the following I will focus on reviewing the existing knowledge on DV axis patterning of vertebrates and insects as it seems to be most relevant for understanding the DV patterning mechanisms of *Oncopeltus fasciatus*.

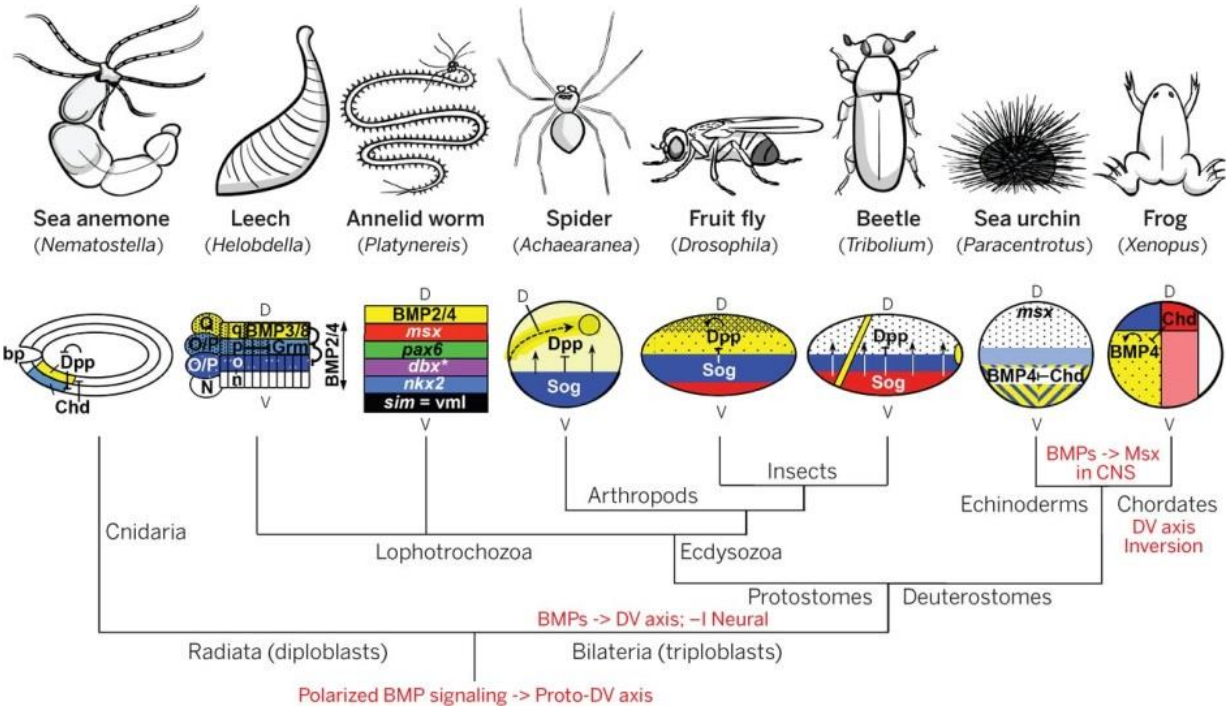

Figure 1: Phylogeny of animals using BMP signaling to pattern body axes

Phylogeny of selected animals in which substantial data for BMP-mediated axes patterning is available. Despite many alterations in expression pattern profiles of BMP signaling components, the developmental outcome of

this signaling pathway has remained conserved across diverse phyla (e.g., suppression of neural fates by BMP signaling). Red text indicates nodes at which specific changes in BMP signaling may have occurred (Figure taken from Bier and De Robertis, 2015).

1.2 Dorsoventral axis establishment in vertebrates

Classic graft manipulation experiments by Spemann and Mangold in which the dorsal blastopore lip of donor newt embryos was transplanted into recipient newt embryos lead to a secondary axis induction (Spemann and Mangold, 1924). Since two different newt species with different degrees of pigmentation were used in these grafting experiments it was possible to distinguish between the mesodermal-derived notochord which developed from donor cells and ectodermal-derived neuronal tube which developed from the host cells within the graft-induced duplicated axis. Hence the transplanted blastopore lip induced neuronal fates in tissues that were originally fated to become epidermis. The dorsal blastopore lip seemingly emitted a neuralizing signal to its surrounding tissue. Spemann later named the dorsal blastopore lip the organizer. Later, various experiments conducted in several vertebrate species revealed that also fish, frog, chick and mouse possess a Spemann organizer-like structure (the shield in zebrafish, node in mouse, and Henson's node in chick) which produced neural-inducing signals. These signals were found to act by inhibiting the bone morphogenetic protein (BMP) pathway. Although there is elaborate research data available for mice and chicken (Coffinier et al., 2002; Moser et al., 2003; Kamimura et al., 2004; Timmer et al., 2002; Wilson and Maden, 2005; Le Dréau and Martí, 2012), BMP-mediated DV patterning in vertebrates is best understood in the African clawed frog *Xenopus laveis* and the zebrafish *Danio rerio*.

BMP ligand genes are expressed in a dynamic manner in the early *Xenopus* embryo (Nishimatsu et al., 1992; Dale et al., 1992; Fainsod et al., 1994; Clement et al., 1995; Hemmati-Brivanlou and Thomsen, 1995; Schmidt et al., 1995; Wang et al., 1997; Fritz and Sheets, 2001). mRNAs encoding *bmp2*, *bmp4*, and *bmp7* are maternally contributed to the egg and are found ubiquitously throughout the early embryo. Maternal *bmp2* transcript is degraded during mid-blastula stage, and *bmp2* is not transcribed zygotically until mid-gastrulation. Zygotic transcription of *bmp7* and *bmp4* is activated at the midblastula transition and both are expressed throughout the embryo, but get degraded dorsally at the early gastrula stage. As gastrulation proceeds, the domain of BMP gene expression is gradually reduced from a broad domain encompassing the ventral and lateral regions to a ventrally-restricted segment near the end of gastrulation. Thus, the early ubiquitous domain of maternal BMP expression becomes restricted zygotically, beginning with a clearing on the dorsal side at midblastula, and gradually moving into more lateral domains as gastrulation proceeds.

A similar pattern of BMP ligand expression is found in zebrafish embryos (Kishimoto et al., 1997; Martinez-Barbera et al., 1997; Nikaido et al., 1997; Dick et al., 2000; Schmid et al., 2000; Furthauer et al., 2004). mRNAs coding for *bmp4* and *bmp7* are found in immature oocytes (Kramer et al., 2002), but are either weakly detected or are absent at the two to four cell stage (Dick et al., 2000). *bmp2b* and *bmp7* are expressed throughout the early blastula and are then cleared from the dorsal side. *bmp4* is expressed ventrally just prior to the onset of gastrulation, so that during gastrulation all three BMP ligands are broadly expressed in the ventral half of the embryo.

BMP signaling itself regulates BMP ligand gene expression in a positive feedback loop, thus ensuring continued BMP activity (Metz et al., 1998). Maternal signaling via Smad5 likely initiates embryo-wide zygotic expression of *bmp2b* and *bmp7* in zebrafish, and *bmp4* and *bmp7* in *Xenopus* (Kramer et al., 2002). Disruption of BMP-mediated positive feedback is essential for the loss of *bmp* expression from

the dorsal side. The initial dorsal clearance of *bmp* expression is mediated by various overlapping mechanisms, involving transcriptional repression dependent on the homeodomain protein Bozozok, β-catenin, Wnt and FGF signaling, as well as MAP Kinases, which leads to the establishment of broad BMP-positive and BMP-negative regions demarcating initial dorsal and ventral domains in the late blastula stage embryo (Lemaire et al., 1995; Furthauer et al., 1997; Kretzschmar et al., 1997; Baker et al., 1999; Koos and Ho, 1999; Fekany-Lee et al., 2000; Gomez-Skarmeta et al., 2001; Furthauer et al., 2001; Lekven et al., 2001; Leung et al., 2003; Pera et al., 2003; Furthauer et al., 2004; Tsang et al., 2004; Ramel and Lekven, 2004; Stern, 2005; Kuroda et al., 2005; Ramel et al., 2005).

However, these mechanisms of transcriptional BMP ligand repression acting on the dorsal domain do not explain the classic observations of Spemann and Mangold that transplanted dorsal organizer tissue can redirect the development of ventral host tissue to take on dorsal fates. In addition, supplying BMP ligand mRNA ubiquitously throughout a zebrafish embryo can rescue *bmp2b* and *bmp7* mutants to wild-type, indicating that additional mechanisms must regulate DV axis patterning (Kishimoto et al., 1997; Nguyen et al., 1998). Moreover, the broad ventral expression of BMP ligand genes does not explain how BMP signaling acts in a graded fashion along the DV axis.

These properties are mediated by dorsal organizer-derived BMP signaling antagonists. Two such antagonists are Chordin (Chd) and Noggin (Nog) which are secreted by and produced within the organizer at the start of gastrulation (Sasai et al., 1994; Smith and Harland, 1992). Those inhibitors can induce dorsal fates in ectoderm and mesoderm in a dose-dependent manner and produce a secondary axis when ectopically expressed ventrally, thus mimicking the activity of organizer tissue (Dosch et al., 1997; Wilson et al., 1997; Bauer et al., 1998; Eimon and Harland, 1999; Furthauer et al., 1999). Chordin and Noggin themselves do not directly specify cell fates, but instead block BMP signaling by directly binding BMP ligands extracellularly and BMP ligands bound to these antagonists cannot interact with receptors and thus cannot signal (Smith and Harland, 1992; Sasai et al., 1994; Piccolo et al., 1996; Zimmerman et al., 1996). *chordin* expression extends outside the organizer into future neural tissue in both *Xenopus* and zebrafish, as well as into marginal dorsolateral regions well outside the organizer in zebrafish (Schulte-Merker et al., 1997; Miller-Bertoglio et al., 1997; Kuroda et al., 2004). Zebrafish embryos that lack Chordin display reduced neural plate, reduced paraxial tissue, and slight reduction of the dorsal-most axial mesoderm, with expansion of ventral fates, indicating excess BMP signaling (Hammerschmidt et al., 1996; Oelgeschlager et al., 2003). Lack of Chordin also attenuates the ability of the organizer to induce a secondary axis in transplant experiments (Oelgeschlager et al., 2003). However, overexpression of *chordin* induces dorsal fates in a dose-dependent manner, and this can occur at a distance from the site of *chordin* expression (Jones and Smith, 1998; Blitz et al., 2000). The restricted expression of *chordin* and *noggin* on the dorsal side, combined with the broad expression of BMP ligands ventrally, has led to a model in which BMP antagonists diffuse laterally from their sites of expression (Thomsen, 1997). The ventrally-directed movement of Chordin and Noggin causes a DV gradient of anti-BMP activity, resulting in an inverse gradient of BMP activity with high levels ventrally and decreasing levels in progressively more lateral regions. Thus, the movement of BMP antagonists from dorsal to ventral sets up a BMP activity gradient, which establishes differential cell fates in an activity-level dependent manner. An antibody which specifically detects phosphorylated Smads, the effectors of vertebrate BMP signaling, reveals high levels of pSmad ventrally and no staining near the organizer, consistent with the proposed gradient (Faure et al., 2000; Mintzer et al., 2001; Schohl and Fagotto, 2002).

Extracellular antagonism of BMP signaling is indispensable for DV patterning. The triple depletion of Chordin, Nogggin, and Follistatin, another extracellular BMP antagonist (Hemmati-Brivanlou et al., 1994), causes a complete loss of neural tissue and dorsal mesoderm in *Xenopus*, demonstrating a

certain degree of redundancy between the extracellular antagonists The establishment of the organizer is not affected by this triple antagonist knockdown, however, the dorsalizing activities of β-catenin signaling are not sufficient to maintain any dorsal identity if BMP antagonists are absent (Khokha et al., 2005). In zebrafish, lack of Chordin and the transcriptional repressor Bozozok massively derepress BMP expression and lead to radialized ventral fates (Gonzalez et al., 2000). Thus, both extracellular antagonists and transcriptional repression are required to repress ventralizing BMP signals to allow dorsal development.

Many additional factors influence BMP signaling at the extracellular level. Among them are members of the Tolloid family, that promote BMP signaling via inactivation and degradation of Chordin. Multiple homologs of the metalloprotease Tolloid are found in vertebrates (Ge and Greenspan, 2006). The first vertebrate Tolloid-related protease identified, BMP1, was purified along with BMP ligands from demineralized bone extracts (Wozney et al., 1988). BMP1 homologs have been identified in fish, frog, mouse, and human. Additional related genes are, in *Xenopus*, *Xolloid* (*Xld*) and *Xolloid-related* (*Xlr*) (Goodman et al., 1998; Dale et al., 2002), and in zebrafish, *tolloid-like 1* (*tll1*), *bmp1a*, and *bmp1b* (Blader et al., 1997; Muraoka et al., 2006). Of these factors, those studied most intensely for their role in DV patterning have been, in frog, *Xld* and *Xlr*, and in zebrafish, *bmp1a* and *tll1* (Connors et al., 1999). These genes are members of the "BMP synexpression group" of genes that are expressed ventrally and are positively regulated by BMP signaling (Karaulanov et al., 2004). The anti-Chordin activity of Tolloid can be interpreted as sink for Chordin by which the diffusing BMP antagonist can be destroyed, thus maintaining a gradient of BMP activity.

1.3 Dorsoventral axis establishment in *Drosophila melanogaster*

While most animals employ BMP signaling to pattern their DV axis, extensive amounts of research since the 1970s revealed that in the fly *Drosophila* the Toll signaling pathway gained dominance over BMP signaling in DV axis establishment (Stein and Stevens, 2014; Sachs et al., 2015). In *Drosophila* BMP signaling also plays a crucial, but spatially restricted role in patterning the most dorsal fates, in particular the amniosera and the dorsal ectoderm (O'Connor et al., 2006).

This is somehow surprising since Toll signaling itself is a highly conserved pathway from Hydra to human, providing innate immunity (Lemaitre et al., 1996; Leulier and Lemaitre, 2008; Franzenburg et al., 2012; Gilmore and Wolenski, 2012).

Genetic screens carried out largely in the 1970s and 1980s identified a group of genes collectively referred to as the dorsal group (Nüsslein-Volhard, 1979; Nüsslein-Volhard et al., 1980; Anderson and Nüsslein-Volhard, 1984a; Anderson and Nüsslein-Volhard, 1984b; Nüsslein-Volhard et al., 1987; Schüpbach and Wieschaus, 1989; Luschnig et al., 2004). Among this group is a ubiquitously expressed gene called *Toll*, which codes for a leucine-rich repeat-bearing single-pass transmembrane receptor (Hashimoto et al., 1988). Toll is uniformly distributed throughout the plasma membrane of the syncytial blastoderm stage embryo (Hashimoto et al., 1991). The molecular events which occur up and downstream of the Toll receptor are known in great detail (Fig. 2).

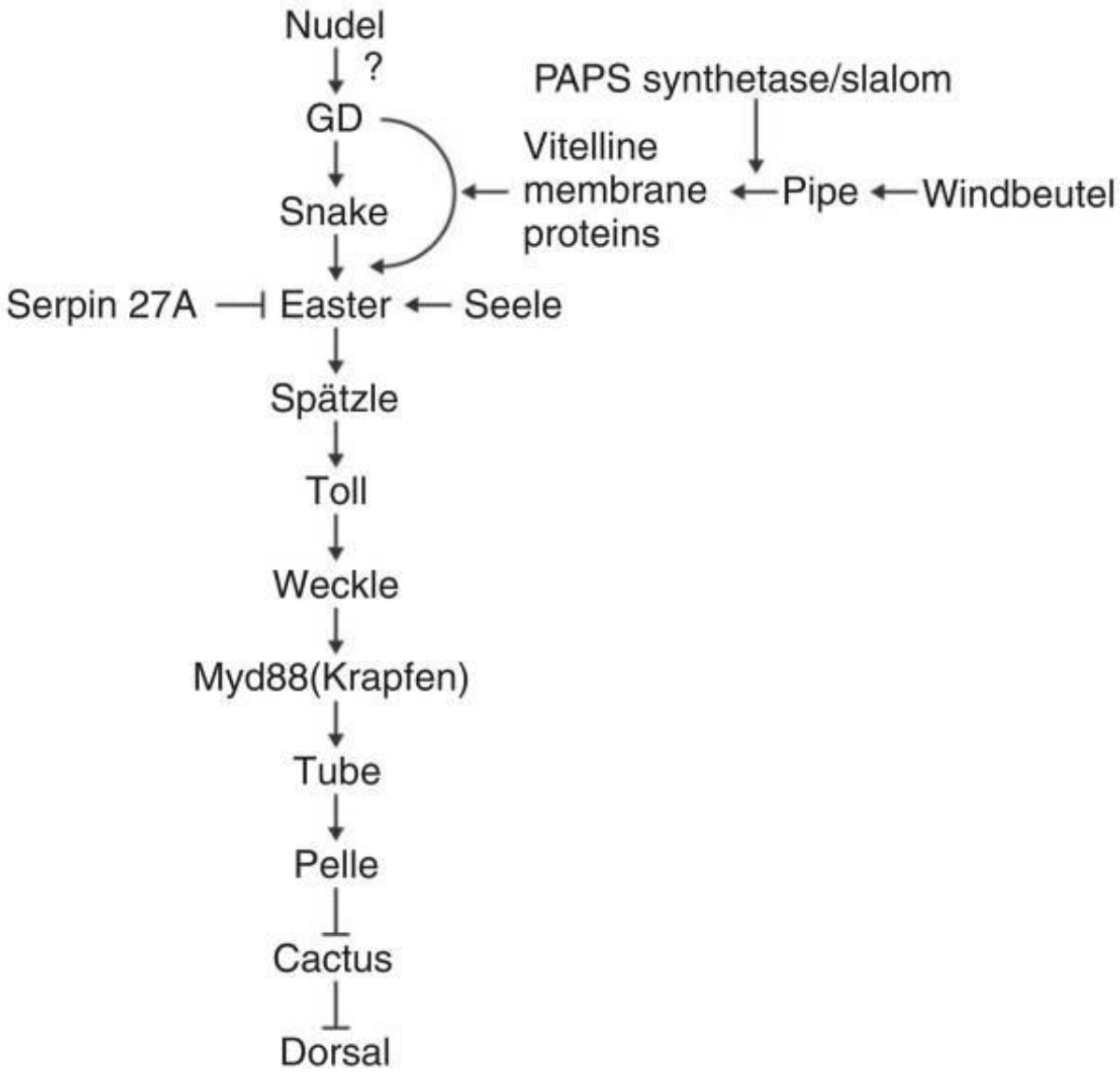

Figure 2: Components of the Toll signaling pathway
Overview of the gene products known to be involved in dorsoventral patterning of the *Drosophila* embryo in their order of action and epistatic relationship (Figure taken from Stein and Stevens, 2014).

Upstream of the Toll receptor, within the perivitelline space between the eggshell and the embryonic membrane, acts a protease cascade that processes the ligand of the Toll receptor into its active form. The activity of the protease cascade is restricted to the ventral side of developing embryos. The mechanisms that establish this ventral activity restriction are known in great detail (Fig. 3).
In order to achieve the ventral activity restriction of proteolytic events upstream of Toll during embryo development, a molecular cue in the egg that transmits spatial information is already established in the oocyte (Schüpbach, 1987). During oogenesis, *gurken* mRNA, coding for an TGF-α-like secreted peptide growth factor, is expressed by the nurse cells and then transported into the oocyte (Neuman-Silberberg and Schüpbach, 1993). At stage 8, the oocyte nucleus has migrated from its original position at the posterior of the oocyte to an anterior position adjacent to the oocyte/nurse cell boundary and *gurken* mRNA localizes in association with the oocyte nucleus (Neuman-Silberberg and Schüpbach, 1996; Saunders and Cohen, 1999; Thio et al., 2000; Caceres and

Nilson, 2005). Gurken protein is synthesized within and secreted from this corner of the oocyte, and subsequently activates Torpedo in the overlying follicle cells, defining the dorsal side of the follicular epithelium (Neuman-Silberberg and Schüpbach, 1996; Peri et al., 1999; Bökel et al., 2006; Castro et al., 2007). Torpedo is the *Drosophila* homologue of the Epidermal Growth Factor Receptor (Price et al., 1989; Schejter et al., 1989). Activation of Torpedo results in the phosphorylation and inactivation of Capicua, a HMG-Box protein that acts as repressor of *mirror* (Astigarraga et al., 2007; Atkey et al., 2006; Goff et al., 2001). Torpedo signaling-mediated inactivation of Capicua in dorsal and lateral follicle cells leads to the expression of the transcription factor encoding gene *mirror*, which in turn represses *pipe* transcription (Andreu et al., 2012). However, in ventral follicle cells Capicua represses *mirror* and *pipe* is expressed (Andreu et al., 2012, Atkey et al., 2006; Goff et al., 2001).

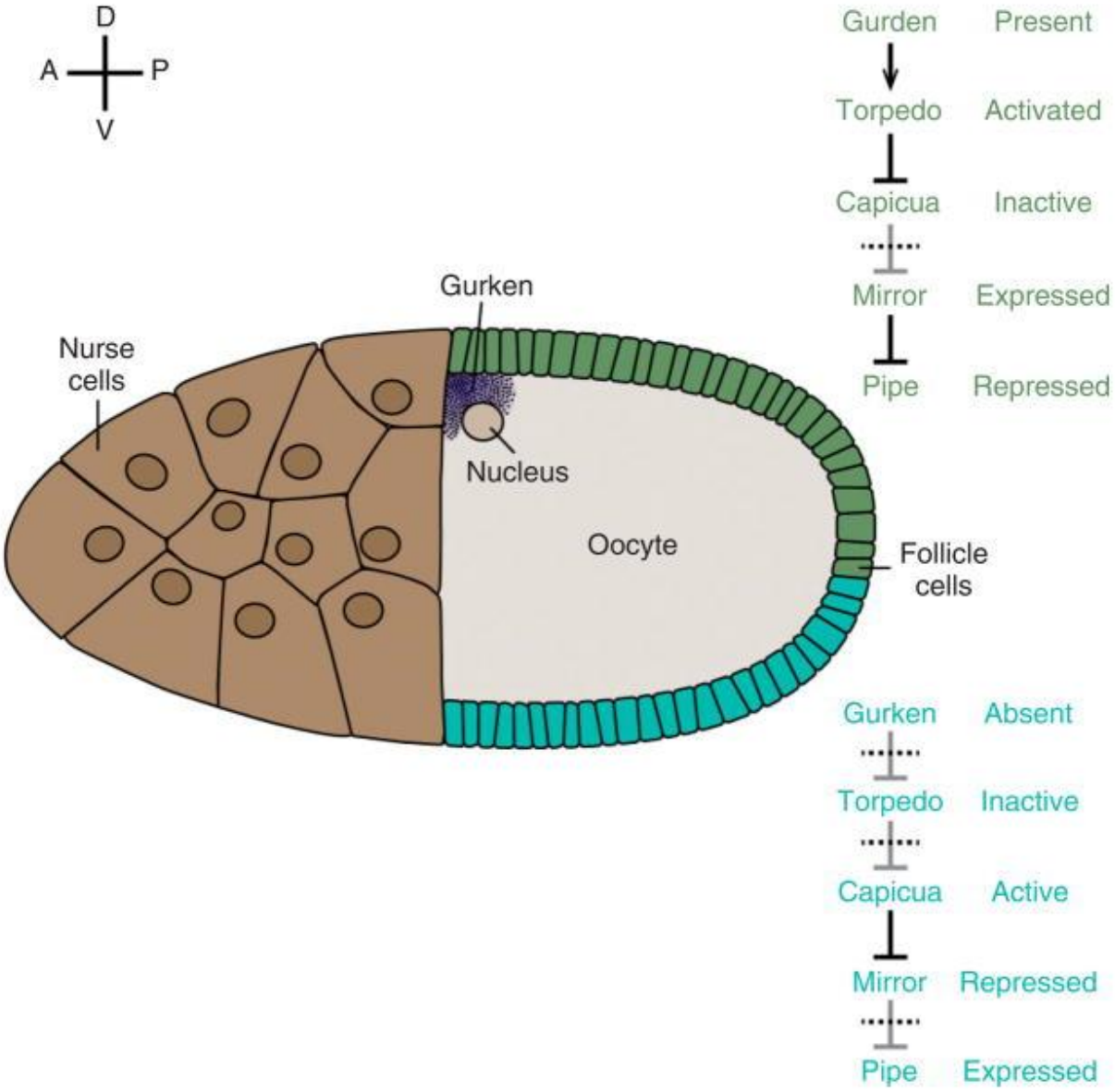

Figure 3: EGFR signaling ventrally restricts expression of *pipe* in the follicle cell layer during oogenesis
Schematic drawing of a stage 10 oocyte. *pipe* is expressed in the ventrally (blue), but repressed in the dorsal epithelium (green). Relevant effector peptides and their activation states in ventral and dorsal follicle cells are indicated at right (Figure taken from Stein and Stevens, 2014).

pipe codes for a sulfate 2-O-sulfotransferase that exhibits a type II transmembrane topology, consistent with its localization to the Golgi apparatus (Sen et al., 1998; Kobayashi et al., 1997; Kobayashi et al., 1999). Golgi localization of Pipe requires chaperone activity of Windbeutel, a dorsal group protein and *Drosophila* homologue of the vertebrate chaperone ERp29 (Sen et al., 2000; Konsolaki et al., 1998). The question of the substrate of Pipe remains controversial (Park et al., 2008; Zhu et al., 2005). However, despite the uncertainty about Pipes target carbohydrate, there is strong evidence that Pipe-associated sulfotransferase activity is necessary for the formation of embryonic DV polarity as hypomorphic *pipe* mutations lead to weak dorsalization that can be enhanced by feeding mutant female flies an inhibitor of the enzyme PAPS synthetase (Anderson and Nüsslein-Volhard, 1984; Zhu et al., 2005). PAPS is a cosubstrate and source of activated sulfate for sulfotransferases (Robbins and Lipmann, 1957; Kobayashi et al., 1996; Kobayashi et al., 1999). In addition, female flies bearing follicle cell clones lacking the function of either PAPS Synthetase or Slalom, a transporter of PAPS from the cytoplasm to the Golgi produce dorsalized progeny embryos (Zhu et al., 2007; Lüders et al., 2003; Kamiyama et al., 2003). Thus, Pipe-mediated sulfation in the follicular epithelium is required for the establishment of the DV axis in Drosophila embryos.

A protein target of Pipe sulfotransferase activity is the Vitelline Membrane-Like (VML) protein (Zhang et al., 2009). Sulfated VML is secreted by the follicle cells and becomes stably associated with the region of the vitelline membrane that lies adjacent to the site of *Vml* expression in the follicular epithelium (Zhang et al., 2009; Alartortsev, 2006; Scherer et al., 1988). Other vitelline membrane associated proteins that undergo Pipe-dependent sulfation have been identified (Zhang et al., 2009; Burke et al., 1987; Popodi et al., 1988; Gigliotti et al., 1989; Elalayli et al., 2008). Embryos from mothers homozygous for a mutation that eliminates VML or other vitelline membrane associated proteins are not dorsalized. However, the hypomorphic *pipe* phenotype is enhanced by a reduction in the gene dosage of VML or the other vitelline membrane associated proteins sulfated by Pipe suggesting that these other Pipe substrates act redundantly with VML to influence Toll signaling (Zhang et al., 2009). In summary, it is thought that VML and other glycosylated vitelline membrane components are sulfated by Pipe and then secreted and incorporated into the vitelline membrane, where they comprise a ventrally localized cue that restricts the activity of the protease cascade that processes the Toll ligand.

It has been shown experimentally that GD, a member of the protease cascade upstream of Toll interacts with Pipe-sulfated molecules that are embedded in the ventral vitelline membrane and thereby accumulates on the ventral side of developing *Drosophila* embryos (Cho et al., 2012). In addition, processing of the Easter zymogen, another member of the protease cascade, requires Pipe activity (Cho et al., 2010; LeMosy, 2006; Steen et al., 2010).

In summary, DV polarity of the embryo is dependent upon prior DV polarity establishment within the follicle cell layer surrounding the oocyte. In this process Pipe is a central component that links EGFR-mediated DV polarity from the egg chamber to Toll-mediated DV polarity of the embryo by providing a spatial cue that restricts Toll activity to the ventral side.

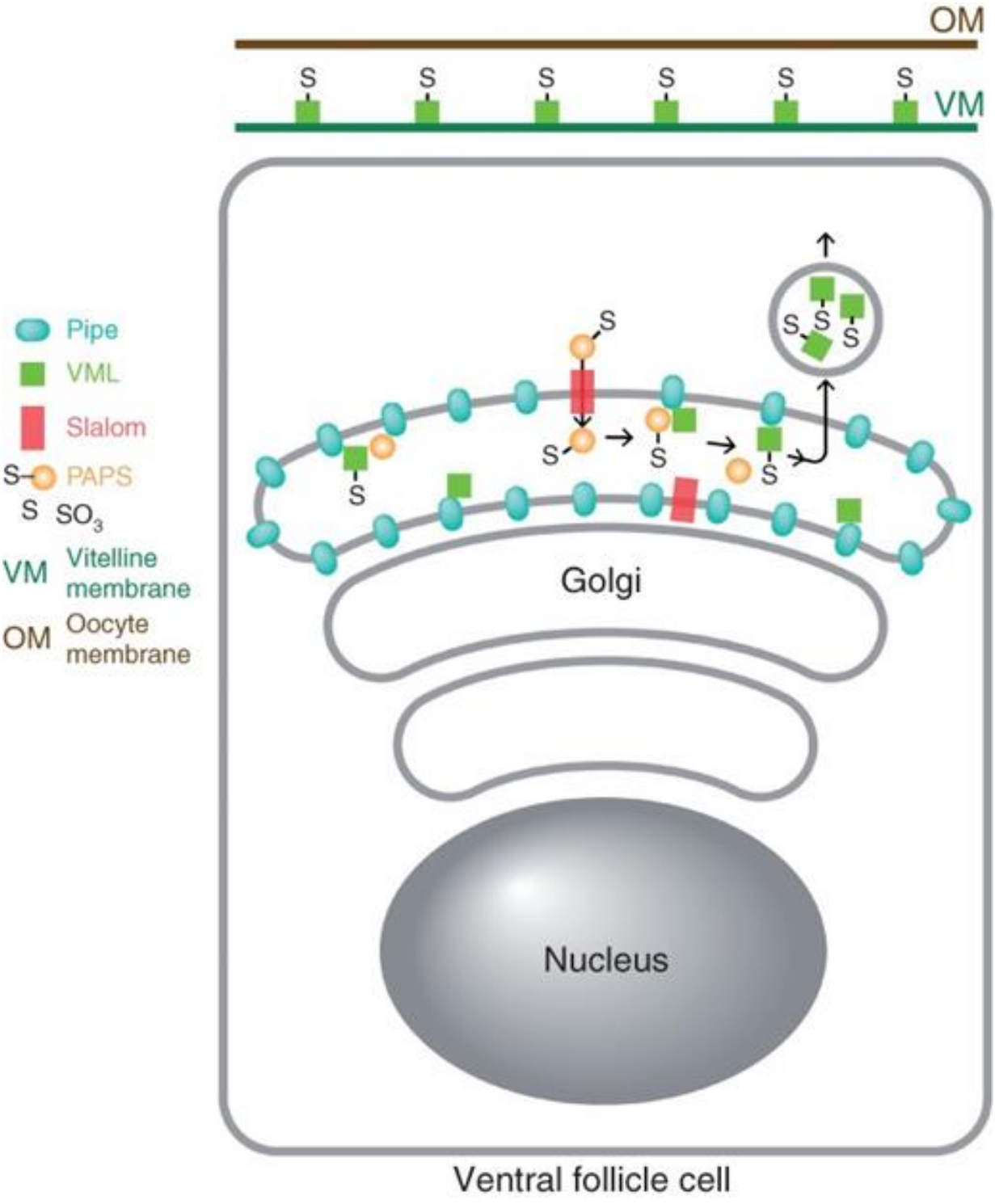

Figure 4: Sulfation of VML by Pipe in a ventral follicle cell

PAPS is transported into the Golgi apparatus by Slalom. Pipe present in the Golgi apparatus transfers sulfate from PAPS to VML. Sulfated VML is then secreted and incorporated into the vitelline membrane layer of the egg (Figure taken from Stein and Stevens, 2014).

The protease cascade upstream of Toll consists of three distinct serine proteases, Gd, Snake and Easter. The presence of signal peptides in GD, Snake and Easter suggested that they are secreted from the embryo and function within the perivitelline fluid that surrounds the developing embryo (Stein and Stevens, 2014). Both *snake* and *easter* are expressed in the germline and code for trypsin-like serine proteases (DeLotto and Spierer, 1986; Chasan and Anderson, 1989). They are expressed as inactive zymogens and are both activated by a cleavage reaction that cuts the backbone of the protein between an N-terminal segment, the prodomain, and the catalytic region in the C-terminus. Although the proteolytic function of Easter and Snake is activated by the cleavage event, the prodomain and catalytic fragments remain linked by a disulfide bond. The prodomains of both Snake and Easter carry six cysteine residues that are predicted to form three intra-chain disulfide bridges that form a structure termed Clip domain because of its resemblance to a paper clip (Muta et al, 1990; Smith and DeLotto, 1992; Jiang and Kanost, 2000). The Clip domain was first found in the proclotting enzyme of the horseshoe crab, *Tachypleus tridentus* (Muta et al, 1990). The Horseshoe crab proclotting enzyme functions in the hemolymph coagulation system and is considered to be the counterpart of prothrombin in the mammalian blood clotting reaction (Miyata et al., 1983). The Clip domain is thought to function as a recognition site for activators or other components of the hemolymph clotting system (Muta et al, 1990; Smith and DeLotto). *gd* also codes for a protease, but rather than a trypsin-type protease, GD instead exhibits limited structural similarity to two serine proteases of the mammalian complement system, factors C2 and B (Konrad et al., 1998; DeLotto, 2001). *gd* is both expressed in the germline and follicle cells where accumulation of mRNA appears to be somewhat graded along the dorsal–ventral axis with marginally higher levels of mRNA in the ventral follicle cells (Konrad et al., 1998).

Various genetic and biochemical experiments revealed the epistatic relationships within the proteolytic cascade upstream of Toll and support a model in which GD acts on Snake, Snake on Easter, and Easter cleaves and thereby activates Spätzle, the ligand for Toll (Chasan et al., 1992; Smith and DeLotto, 1995; Dissing et al., 2001; LeMosy et al., 2001; Stein and Nüsslein-Volhard, 1992). Spätzle is a neurotrophin-like signaling peptid and the C-terminus of Easter-processed Spätzle forms a disulfide-linked homodimer that acts as active Toll ligand (Stein et al., 1991; Morisato and Anderson, 1994; Schneider et al., 1994; Weber et al., 2003; Lemaitre et al., 1996; DeLotto and DeLotto, 1998).

Besides proteolytic activation by Snake, Easter activity is regulated by various mechanisms. Processed Easter is rapidly bound and inactivated by the inhibitor Serpin 27A. *serpin 27A* mRNA is maternally provided and Serpin 27A is uniformly distributed along the DV axis, thereby preventing activated Easter from diffusing to lateral and dorsal regions (Misra et al., 1998; Ligoxygakis et al., 2003; Hashimoto et al., 2003). Easter is also regulated at the level of secretion by Seele, an endoplasmic reticulum-localized saposin-like protein. In embryos lacking Seele the secretion of Easter, but not of other secreted dorsal group proteins, is disrupted, leading to a weakly dorsalized embryonic phenotype (Stein et al., 2010). Hence, Easter can be seen as a critical control point for regulation of Toll pathway activity.

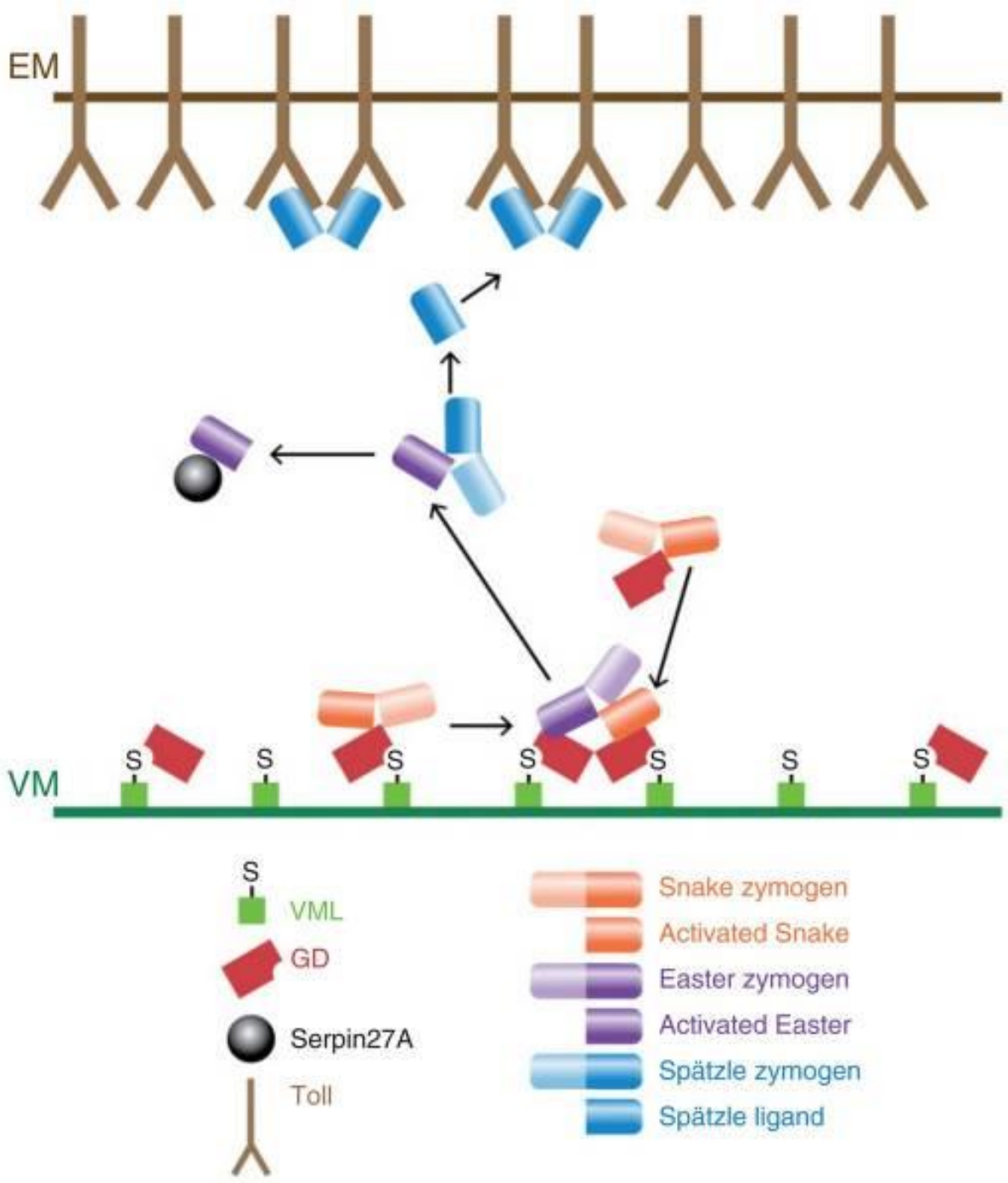

Figure 5: Processing of Spätzle by a ventrally active protease cascade

The Spätzle ligand is processed within the ventral perivitelline space. VML-associated and free GD processes and thereby activates Snake. Only GD which is associated with Pipe-sulfated VML promotes the interaction between activated Snake and unprocessed Easter zymogen, which leads to Easter cleavage and activation. Activated Easter then processes Spätzle into the active Toll ligand. Active Easter is bound and inactivated by Serpin 27A (Figure taken from Stein and Stevens, 2014).

The signaling cascade events downstream of Toll are also known in detail (Fig. 5). Binding of activated Spätzle ligand to Toll induces dimerization of the receptor. Active Toll simultaneously recruits the adaptor proteins Myd88 and Weckle to form a stable complex with Tube that activates Pelle (Towb et al., 1998; Grosshans et al., 1994; Galindo et al., 1995; Sun et al., 2004; Charatsi et al., 2003; Chen et al., 2006). The formation of this complex transmits signaling that is dependent upon the Pelle kinase. Pelle phosphorylates Toll, Tube, Cactus, Dorsal and itself (Reach et al., 1996; Fernandez et al., 2001; Grosshans et al., 1994; Shen and Manley, 1998; Towb et al., 2001; Shen and Manley, 2002; Daigneault et al., 2013). The phosphorylation, ubiquitination and subsequent degradation of Cactus, a *Drosophila* homologue of vertebrate IκB proteins that regulate NFκB activity, leads to nuclear uptake of Dorsal, a *Drosophila* homologue of vertebrate Rel and NFκB proteins (Steward et al., 1987; Bours et al., 1990; Ghosh 1990; Kieran et al., 1990; Nolan et al., 1991; Ruben et al., 1991; Hayden and Ghosh, 2012). In the absence of active Toll signaling Cactus acts as repressor by sequestering Dorsal within the cytoplasm and therefore inhibiting Dorsal from entering the nucleus (Roth et al., 1991; Geiseler et al., 1992; Kidd, 1992; Belvin et al., 1995; Bergmann et al., 1996; Reach et al., 1996).

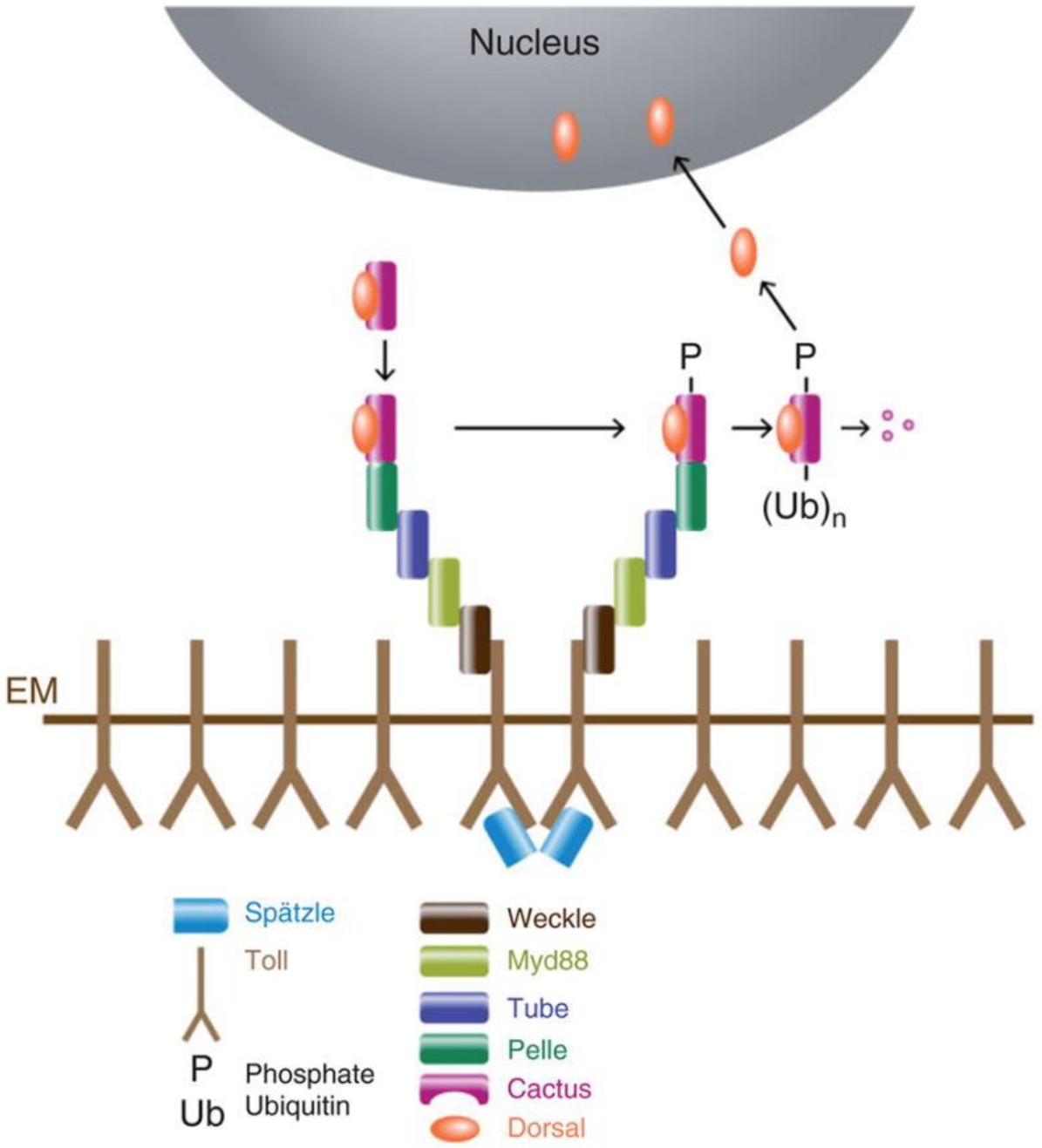

Figure 6: Toll activation and signaling leads to nuclear uptake of Dorsal
Binding of activated Spätzle to Toll leads to the Weckle-dependent recruitment of a complex comprised of Myd88, Tube, and Pelle. Toll activation leads to the phosphorylation, ubiquitination and degradation of Cactus, releasing Dorsal to enter the nucleus (Figure taken from Stein and Stevens, 2014).

The outcome of ventrally active Toll signaling establishes a gradient of nuclear Dorsal exhibiting peak levels at the ventral-most side, intermediate levels at the lateral sides and low levels on the dorsal-most side (Rushlow et al., 1989; Steward, 1989; Roth et al., 1989; Liberman et al., 2009; Reeves et al., 2012; Reeves and Stathopoulos, 2009; DeLotto et al., 2007) (Fig. 7). A complete understanding of the formation of the Dorsal nuclear gradient is still a work in progress, however, the current understanding suggests an extracellular Spätzle gradient that results in graded Toll activity (Stein and Stevens, 2014). As nuclei enter mitotic prophase, the gradient disappears, then reappears at the end

of mitosis and the gradient must re-form multiple times during the nuclear division cycles 10 through 14 (DeLotto et al., 2007; Kanodia et al., 2009).

The nuclear concentration of Dorsal along the embryonic DV axis defines the transcriptional state of Dorsal target genes in a threshold-dependent manner (Roth et al., 1989; Stathopoulos and Levine, 2002; Reeves and Stathopoulos, 2009) (Fig. 7). Type 1 target genes like *twist* and *snail* bear low affinity binding sites for Dorsal and are activated only in cells containing high levels of Dorsal, which will form ventral mesoderm. Type 2 target genes, such as *rhomboid*, *vnd*, and *brinker*, bear high affinity binding sites for Dorsal and are expressed in the ventral domain of the neurogenic ectoderm, where nuclear Dorsal is present at intermediate levels (Jiang and Levine 1993; Papatsenko and Levine 2005).

Beside the affinity and number of Dorsal bindings sites, the boundaries of Dorsal target genes are defined by binding sites for additional transcription factors. For example the regulatory regions of the type 2 target *rhomboid* contain both binding sites for Dorsal and Twist, Daughterless, Scute and Su(H), which all co-activate *rhomboid*, while Snail represses (Bier et al., 1990; Ip et al., 1992; Jiang and Levine, 1993; Markstein et al., 2004).

Gene expression in dorsolateral regions of the embryos (Type 3+, e.g. *sog*) requires the function of both Dorsal and Zelda, while in dorsal regions (Type 3−, e.g. *zen*, *dpp* and *tld*), Dorsal activity must be essentially absent but Zelda is still required (Liang et al., 2008; Liberman and Stathopoulos 2009).

Dorsal's intrinsic activity is to turn on gene expression, but Dorsal can function as repressor for type 3- targets by facilitating the binding of co-repressor proteins to neighboring AT-rich regions within the Ventral Repression Elements (VREs) of *zen, tld* and *dpp* (Kirov et al., 1993; Huang et al., 1993; Jiang et al., 1993; Kirov et al., 1994; Lehming et al., 1994; Huang et al., 1995; Cai et al., 1996; Valentine et al., 1998).

While it seems that only three distinct Dorsal-mediated activation thresholds exist, up to six different gene-expression patterns have been identified that are generated by additional activators or repressors downstream of Dorsal. Besides the already described patterns two additional gene expression patterns, Type 1A (e.g. *sim*) and Type2A (e.g. *ind*), have been described, that in addition to Dorsal involve Notch or EGF signalling, respectively (Hong et al., 2008).

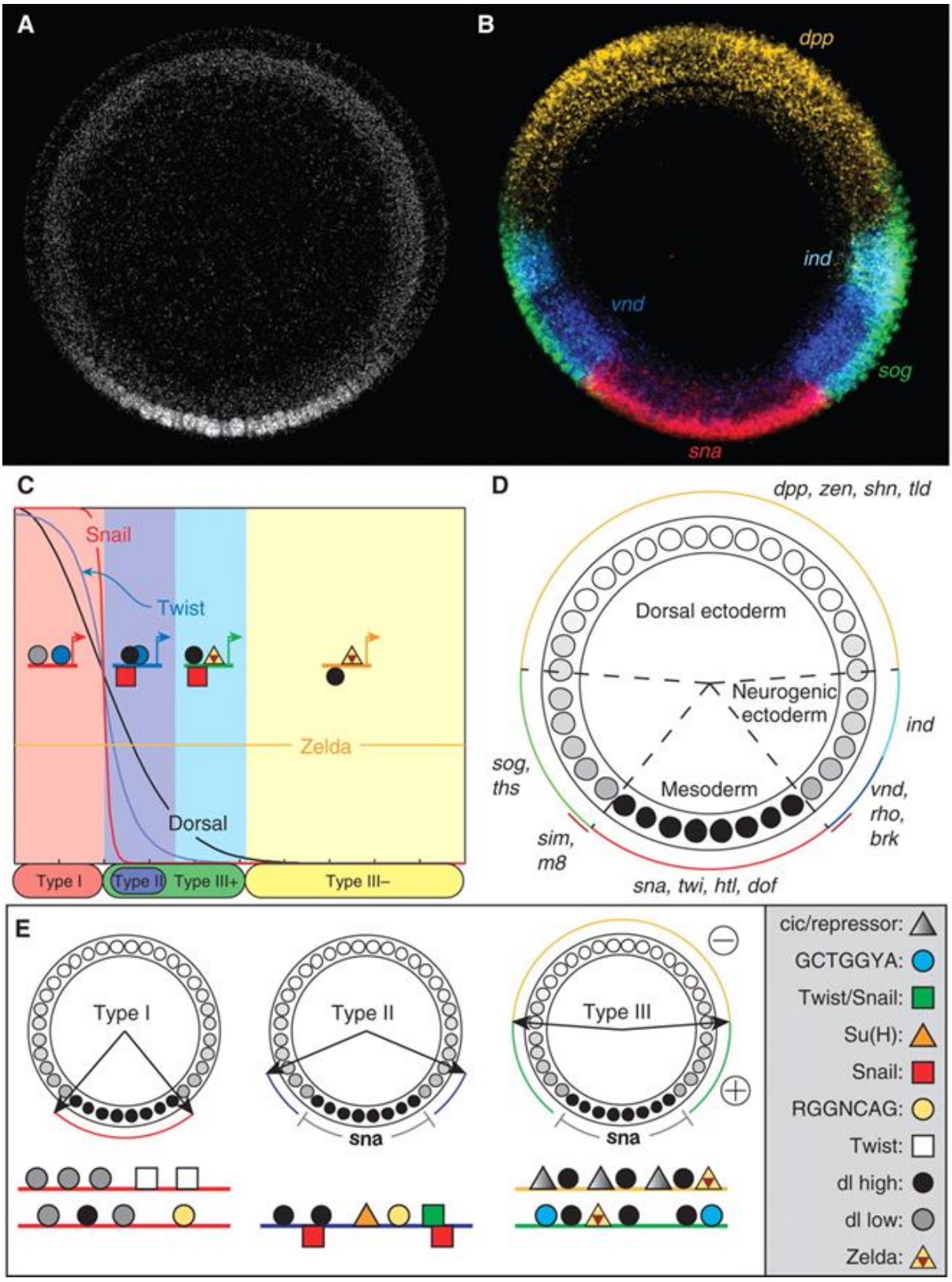

Figure 7: Dorsal target genes and their threshold levels

(A) Cross section of Stage 5 *Drosophila* embryo, stained with an α-Dorsal antibody. **(B)** Cross section of Stage 5 *Drosophila* embryo, stained by ISH to detect the Dorsal target gene transcripts *dpp*, *ind*, *vnd*, *sog* and *sna*. **(C)** Dorsal and Twist cooperate to specify Type I and Type II Dorsal target genes. Dorsal functions together with Zelda to support expression of Type III target genes. **(D)** Fate map schematic. The nuclear Dorsal gradient divides the embryo into three main subtissues: mesoderm, neurogenic ectoderm, and dorsal ectoderm. The neurogenic ectoderm can be divided into ventral and dorsal halves. **(E)** Groupings of Dorsal target gene

thresholds. Type I genes are expressed in the ventral-most cells of the embryo, where Dorsal nuclear levels are the highest. Type II genes have dorsal borders in the middle of the neurogenic ectoderm and are repressed by Snail. Type III genes have their dorsal (+) or ventral (−) borders at roughly 50% DV axis, and contain sites for both Dorsal binding as well as a Zelda, a uniformly expressed activator (Figure taken from Reeves and Stathopoulos, 2009).

1.4 Dorsoventral axis establishment in *Oncopeltus fasciatus* and other insects

The early embryonic development of *Drosophila* displays many derived features compared to other insects. The beetle *Tribolium castaneum* exhibits a more representative mode of embryogenesis for insects in general (Brown et al., 2009). In *Tribolium* Toll signaling is also essential for mesoderm specification and polarization of BMP signaling. However, in contrast to *Drosophila* Toll signaling is only weakly polarized by maternal cues in *Tribolium*. Instead, Toll gradient formation in *Tribolium* is dynamic and depends on extensive zygotic feedback mechanisms (Nunes da Fonseca et al., 2008). The Toll gradient in *Tribolium* provides less spatial information for direct target gene control compared to *Drosophila* (Chen et al., 2000). Accordingly, the number of Toll target genes is smaller than in *Drosophila* (Stappert et al., 2016). Among the BMP signaling components of *Tribolium* only *sog* has been identified as direct Toll target (van der Zee et al., 2006).
In the jewel wasp *Nasonia vitripennis*, a representative of Hymenoptera, the most basal branching line within the Holometabola (insects with complete metamorphosis) Toll's role in DV patterning is even less pronounced (El-Sherif et al., 2012; Schmidt-Ott and Lynch, 2016). In *Nasonia*, Toll signaling seems to be active only in a narrow domain of cells along the ventral midline (Buchta et al., 2013; Özüak et al., 2014b). In this domain Toll initiates mesoderm specification, but does not determine the final size of the mesodermal region which depends on inhibition by BMP signaling. Like in other insects, BMP also specifies the cell fates of the dorsal half of the *Nasonia* embryo, and therefore provides patterning information along the entire DV axis. In addition, BMP gradient formation in *Nasonia* is independent of Toll and possesses its own maternal source along the dorsal midline (Özüak et al., 2014a). Thus, DV axis patterning in *Nasonia* is dominated by BMP signaling while Toll's function is reduced to being a local inducer instead of a long-rang morphogen.
A common feature of all holometabolous insects studied so far is the strict reliance on Toll signaling for mesoderm specification.
However, in the milkweed bug *Oncopeltus fasciatus* (Hemiptera), a representative of the Hemimetabola (insects with incomplete metamorphosis) Toll signaling is only employed as a polarity cue for a self-organizing system of BMP signaling components (Sachs et al., 2015). In *Oncopeltus* Toll signaling never refines to form a steep long-range gradient like in *Drosophila* and *Tribolium* or a pattern of local activation like in *Nasonia*. Instead, Toll rather provides a weak activating function for the BMP inhibitor *sog*. Since in *Oncopeltus* BMP signaling itself represses *sog* transcription a self-regulatory double-negative feedback loop is established which leads to a stable long-range pattern of BMP signaling. As a consequence, all cell fates along the DV axis depend on BMP signaling. The presumptive mesoderm is entirely defined by BMP repression and does no longer require an additional input from Toll (Sachs et al., 2015).
Thus, the *Oncopeltus* BMP system might has preserved regulatory features of an ancestral BMP-based mechanism of DV axis formation more similar to vertebrates like *Xenopus* and zebrafish then to *Drosophila*.

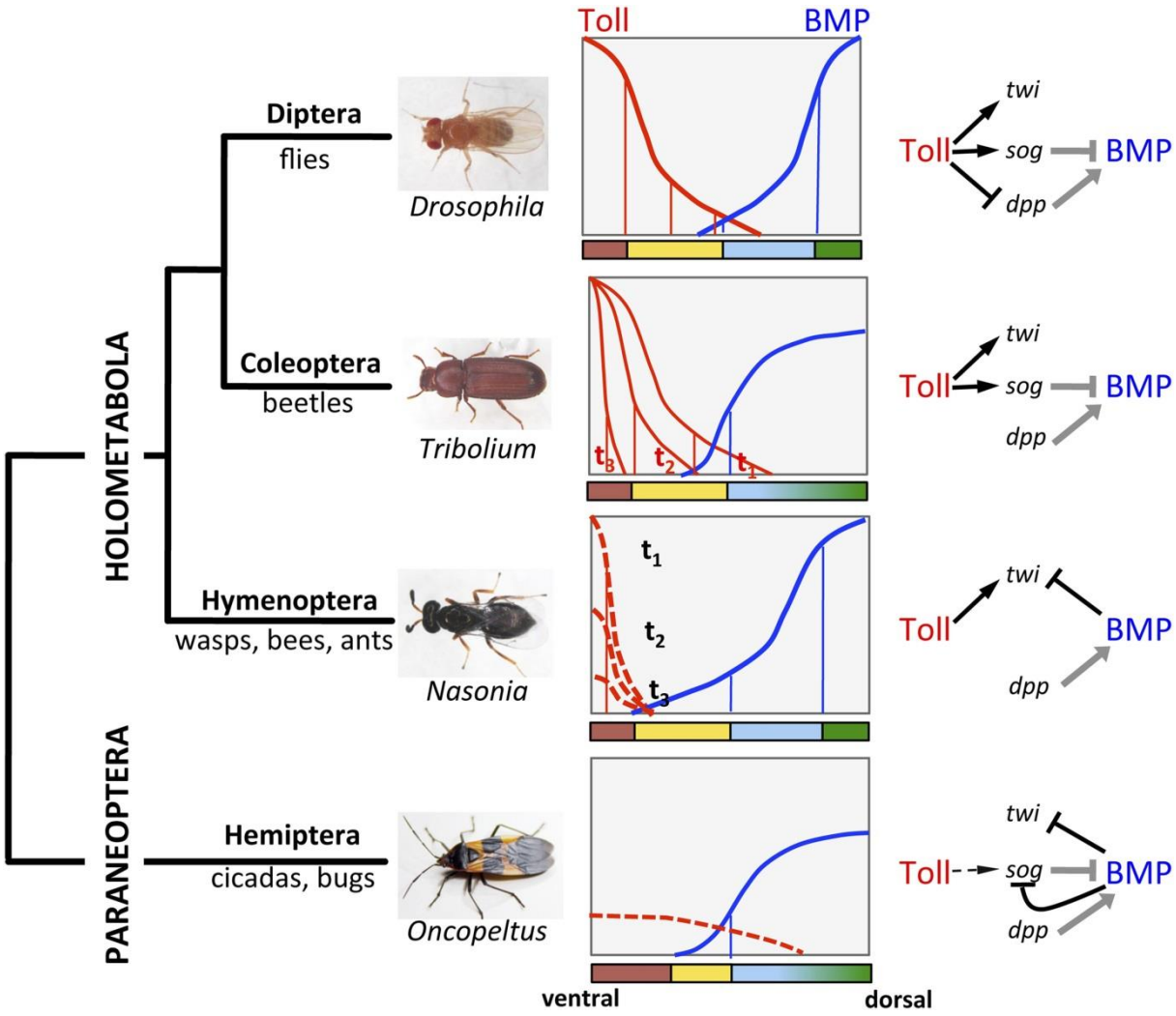

Figure 8: Toll's role in DV patterning across different insects

In holometabolous insects Toll signaling is ventrally activated and forms an activity gradient (red) that is essential at the very least for specifying the ventral-most cells on the DV axis, giving rise to the mesoderm (brown), by activating the gene *twist*. In *Drosophila* Toll signaling not only determines the mesoderm, but also the neuroectoderm (yellow) and restricts BMP signaling to the dorsal side through several parallel mechanisms, including the activation of the BMP inhibitor short gastrulation (*sog*) and repression of the major BMP ligand decapentaplegic (*dpp*). On the dorsal side a BMP gradient (blue) is established that specifies non-neurogenic ectoderm (blue) and extraembryonic tissues (green). In *Tribolium* Toll signaling is dynamic and polarizes BMP signaling only by activating *sog*. BMP signaling in turn has an increased role in ectodermal patterning compared to flies. In contrast to *Drosophila* and *Tribolium* Toll signaling in the wasp *Nasonia* appears to be restricted to a narrow ventral domain where it is only transiently active. In this domain Toll signaling is required to induce mesodermal and mesectodermal fates. But the size of the mesodermal region as well as the fate and position of all other regions along the DV axis are determined by a BMP signaling gradient originating from the dorsal side by an unknown Toll-independent mechanism. Thus, in holometabolous insects BMP signaling gets increasingly more important towards basally branching groups, whereas Toll's role is decreased, but remains essential for ventral-most cell fates. *Oncopeltus* uses Toll signaling only as spatial cue to polarize a dynamic BMP signaling network that establishes a gradient responsible for patterning all cell fates along the entire DV axis. The key regulatory element of this network is the transcriptional repression of *sog* by BMP signaling in a double-negative feedback (Figure taken from Sachs et al., 2015).

1.5 Aim of the study

Sachs et al. provides a theoretical framework for DV axis patterning in *Oncopeltus,* based on phenotypic analysis of core components of BMP and Toll signaling and theoretic modeling approaches (Sachs et al., 2015). The authors propose a system with self-regulatory properties in which the entire DV axis is patterned by a double negative feedback loop comprised of BMP signaling and Sog inhibiting each other. In this system the initial symmetry is broken by ventrally active Toll signaling that only acts as a local inducer of *sog* expression.

To test this hypothesis this study presents experiments in which an ectopic source of BMP inhibition is introduced into both wild-type and embryos lacking Toll via microinjection of the *sog* homolog *chordin*. To examine the injection-induced effects on the DV patterning network different markers where used in ISH experiments. Similar simulations of microinjection experiments were executed within the theoretical model to compare the *in vitro* with the *in silicio* data. Additionally, differential expression analysis by RNAseq of distinct phenotypic transcriptomes of Toll and BMP signalling core components was performed in order to discover new marker genes of embryonic fates and potentially novel components of axis patterning.

2. Materials and Methods

2.1 Materials

2.1.1 Chemicals

Chemicals were purchased from Ambion, BAUER, Merck, PFALTZ, Roche, Roth, Sigma and VWR. Chemicals ordered from other companies were marked as such.

2.1.2 Reagent Kit

Table 1: Reagent Kits used during experiments

Reagent Kit	Company
QUIAGEN Plasmid Miniprep Kit	Quiagen
TOPO™ TA Cloning™ Kit (pCR™II TOPO® TA vector)	Invitrogen
SuperScript® VILO™ cDNA Synthesis Kit	Life Technologies
MEGAscript ® KIT	Ambion
MAXIscript™ T7 Transcription Kit	Ambion
High-Fidelity PCR Kit	Invitrogen
5x MEGAscript T7 Kit	Invitrogen
mMessage mMachine™ SP6	Invitrogen
Advantage® 2 PCR Kit	Clontech
ZR Plasmid Miniprep Classic	Zymo Research
mMessage mMachine® T7 Kit	Ambion
mMessage mMachine® SP6 Kit	Ambion

2.1.3 Solutions and Buffers

Applied water was purified by double filtration and autoclaved afterwards. If necessary, the pH was adjusted with HCl or NaOH.

For general use:

<u>Phosphate buffered saline (PBS), 1 x</u>

NaCl	137 mM
KCl	2.7 M
$NaHPO_4$	8 mM
KH_2PO_4	1.7 mM

<u>Phosphate buffered saline with Tween-20 (PBST), 1 x</u>

NaCl	137 mM

KCl	2.7 M
$NaHPO_4$	8 mM
KH_2PO_4	1.7 mM
Tween-20	0.1 %

Sodium Dodecyl Sulfate (SDS), 10 %

$C_{12}H_{25}SO_4Na$	10 %

Saline sodium citrate (SSC), 20 x, pH 5

NaCl	3 M
$Na_3C_6H_5O_7$	300 mM

Injection buffer

KCl	5 mM
Na_2HPO_4	0.1 mM

Tris-acetate-EDTA buffer (TAE)

Tris	40 mM
acetic acid	20 mM
EDTA	1 mM

Lysogeny broth (LB) medium, pH 7

yeast extract	0.5 %
NaCl	1 %
tryptone	1 %

Super-optimal broth with catabolite repression (SOC) medium

bacto-tryptone	2 %
bacto-yeast extract	0.5 %
NaCl	10 mM
KCl	2.5 mM
$MgCl_2$	10 mM
glucose	20 mM

Fuchsin staining solution:

Alcoholic fuchsin staining solution

Pararosaniline	5 mg/ml
Ethanol	80 %

store at room temperature

Solution C

Ethanol	50 %
Solution D/BBBA	50 %

Solution D/BBBA

Benzyl benzoate	80 %
Benzyl alcohol	20 %

In situ Hybridization and antibody staining solutions:

Hybridization buffer

Formamide	50 %
SSC, pH	5 5 x
Heparin	100 µg/ml
salmon sperm DNA (ssDNA)	100 µg/ml
transfer-RNA (tRNA)	100 µg/ml
SDS	1 %
Tween-20	0.1 %

Blocking solution

PBS	1 x
Bovine serum albumin (BSA)	2 mg/ml
Goat serum	5 %
Tween-20	0.1 %

Alkaline phosphatase (AP) buffer, pH 9.5

Tris, pH 9.5	0.1 M
$MgCl_2$	50 mM
NaCl	100 mM
Tween-20	0.05 %

Probe resuspension buffer

Formamide	50 %
SSC, pH 5	2 x

2.1.4 Oligonucleotides

All oligonucleotides were purchased from Sigma-Aldrich. Primers were designed using the online browser-based version of Primer3web, version 4.1.0 (https://primer3.ut.ee/) (Rozen and Skaletsky, 2000).

The Gene ID indicates the gene name or OFAS-number of the official *Oncopeltus fasciatus* gene set (Panfilio et al., 2019). F and R stand for forward and reverse, respectively. The last number indicates the fragment length in nucleotides that is amplified by a pair of primers. Adapters like the T7 adapter sequence are written in lower case letters.

Table 2: Oligonucleotides used for PCR

Gene ID	Sequence 5'-3'
Of_Tl1_F_1068	ggccgcggTTGGGGAATCTCACATGGCT
Of_Tl1_R_1068	cccggggcGCTAAGGTCGGCTGTCAGTA
Of_DPP_F_1041	ggccgcggCTCTCGCCAGCACAACTTAC
Of_DPP_R_1041	cccggggcTACATCCACAGCCAACCACA
Of_GBB_F_1060	ggccgcggTTTTGCTGCACTGTCTGGTC
Of_GBB_R_1060	cccggggcGGAGCACAACAAGGCTTAGG
Of_Sog_F_1073	ggccgcggGTCCAAACCCCTCCAGAAGA
Of_Sog_R_1073	cccggggcGCTAGGTTGGCAAGGGAAAC
Of_tld_F831	ggccgcggATGGATGAATGTGCGATCAA
Of_tld_R831	cccggggcGCTTGATGAATCCACTGCTG
Of_snail_F731	ggccgcggCTGGAGCCGTCTGAAGATCA
Of_snail_R731	cccggggcAAGGTCTTGCTGCAATTCGG
Of_snail_F550	ggccgcggTGGGCAGTACTTCTTCCTGG
Of_snail_R550	cccggggcTGGGAGTACTCGTGCTTGAA
Of_twist_F736	ggccgcggAGTTTGCCTTCGGAGCTTTG
Of_twist_R736	cccggggcACATTTCTGGCTTGGGGAAG
Of_1sna_F396	ggccgcggCTGGAGCCGTCTGAAGATCA
Of_1sna_R396	cccggggcGCCGGAATAGGTGGAGTAGG
Of_2sna_F407	ggccgcggGAGTCCTCGGCCAAGAAGA
Of_2sna_R407	cccggggcTGGGAGTACTCGTGCTTGAA
Of_13549_F865	ggccgcggACCGGCAAAATGAGGTTACG
Of_13549_R865	cccggggcTGCACTTAGGTCCCTCAGTG
Of_1789_F846	ggccgcggAGCCCTACTGACCTTGCATT
Of_1789_R846	cccggggcTTCAATTTGAGGGTGGCTGC
Of_25202_F841	ggccgcggAAAGACCCGACGAGTAAGCA
Of_25202_R841	cccggggcTGCTCAGTGAATGGGATCGT
Of_627_F784	ggccgcggTACACAGGCGACAGATCCAG
Of_627_R784	cccggggcACTTAGTGAACACAGGGGCA
Of_16851_F996	ggccgcggTACTTCTGGCTCCCACACTG
Of_16851_R996	cccggggcTTGAAGACACCGGCGAAAAG
Of_10790_F954	ggccgcggCATCGTACGTGTGTGAGCAG
Of_10790_R954	cccggggcTAATCCCGACTGCACCATGT
Of_9424_F837	ggccgcggGTGACCGTGGTGTTTGTTGA
Of_9424_R837	cccggggcCTCCGCTCACTCAGTACAGT
Of_10201_F823	ggccgcggGACTGTCCCCGGTTCTAACA
Of_10201_R823	cccggggcGGGGTAGGCGCTTTAGAGAT
Of_423_F364	ggccgcggGGATACGACTGAGCATCTGAC
Of_423_R364	cccggggcGCCTGCTCTGCCATGAAGTA
Of_81_F949	ggccgcggCGCTTTAACCGCCACATGAT
Of_81_R949	cccggggcAGCAGACTCTAGCACCATGG
Of_13274_F904	ggccgcggTCTATGGCACCGGTGAAACT
Of_13274_R904	cccggggcGCGGGATCAGCATTTCGAAT
Of_1714_F823	ggccgcggCACTATGGACCTCACCCTCC
Of_1714_R823	cccggggcAGTGTGTCTGTGGGATGAGG

Of_9838_F888	ggccgcggGGTCTCATGGTCCTATCCGG
Of_9838_R888	cccggggcTGACCCAGTCCACAAAGTGT
Of_25328_F756	ggccgcggATATGGAAGACGCGGGGTAC
Of_25328_R756	cccggggcAGGAAGAAGCCCCTTTCAAGT
Of_7959_F669	ggccgcggACTGGTAAAATGGACAGGTCTG
Of_7959_R669	cccggggcCAGCAGGAGTGGCTTCTTTT
Of_9879_F928	ggccgcggGCATCGTCTCTGGAAAGCTG
Of_9879_R928	cccggggcTCCCTGAGCTCTGAGACTCT
Of_6907_F792	ggccgcggGAAAGTGCACTCCTGATGGC
Of_6907_R792	cccggggcCCAAAATCCAAGGTGACAAGGT
Of_16797_F983	ggccgcggCGAGAGTGGTCCATCTGTGA
Of_16797_R983	cccggggcTTGGGCAGTGGTGGTTATCT
Of_1225_F753	ggccgcggGCTATCGCTGTCAAGGAAGC
Of_1225_R753	cccggggcGGCTGCTATTTTGATTGGGGA
Of_13115_F602	ggccgcggGAATGGCCGAGAACTGCAG
Of_13115_R602	cccggggcCGGACTTCCTCGTTTGCC
Of_9611_F1172	ggccgcggGGCCAAAGTGTCCTGGATTC
Of_9611_R1172	cccggggcTTAGTGTCCTGTGAGCTGCA
Of_6404_F941	ggccgcggAGAAAGGACGGGATTGGAGG
Of_6404_R941	cccggggcTCGCCCACCACATCAAATTC
Of_25039_F1132	ggccgcggCTCTTCATTCGCCTGCCATC
Of_25039_R1132	cccggggcGGGCAAGCACTAACCACAAT
Of_13115_F599	ggccgcggGAGAACTGCAGGTCTCGAAC
Of_13115_R599	cccggggcTATGGCGGACTTCCTCGTTT
Of_8642_F884	ggccgcggACCATTGACATCTTGCATCACA
Of_8642_R884	cccggggcACCTTGACTGAACCCCAACA
Of_8467_F827	ggccgcggCGTCCTCATGCGAAAGACTG
Of_8467_R827	cccggggcCCAAGAAGACAAGCAGCTCC
Of_9611_F1179	ggccgcggTGGCAGTCGATATCCCCATC
Of_9611_R1179	cccggggcACCTCCCACTGTTTGATGGT
Of_15144_F876	ggccgcggTGGACCGAAAAGCTGATCCT
Of_15144_R876	cccggggcAGCTCTCAACATTGGCTCCT
Of_4252_F782	ggccgcggAAGAAGAGGTGGGTGAAGGG
Of_4252_R782	cccggggcTTGAGACAATGGGCGTGTTC
Of_6404_F1042	ggccgcggAAGGACGGGATTGGAGGAAG
Of_6404_R1042	cccggggcTGTTCTTCTGGACTGGGCAA
Of_17639_F1016	ggccgcggAACAGGCACATGAGGATCCA
Of_17639_R1016	cccggggcACTGGGCTAGGGGTCTTTTC
Of_3526_F789	ggccgcggTCGCTGGATGATGACTCTCC
Of_3526_R789	cccggggcCTTCTCGGCAGCAACCATTT
Of_10790_F593	ggccgcggTCATCAATGTGTGGCTGGAC
Of_10790_R593	cccggggcTTTCTTCCCCAAAAGTTTCA
Of_10091_F400	ggccgcggTGAATTATTTTCCTGCCAATTT
Of_10091_R400	cccggggcCCAGACCCAGAGGTCCTATTT
Of_6476_F311	ggccgcggACTGTCTGCCTTCGTAATTGG
Of_6476_R311	cccggggcACCAACCTCTCCTCCAACAC

Of_9045_F914	ggccgcggTCAAGTGGAGAGCGAAGTGT
Of_9045_R914	cccggggcGCTTGGTCGTTTTGATGGGT
Of_13272_F1077	ggccgcggAAACAGCAACAGCAATGGGA
Of_13272_R1077	cccggggcGCAGCATCCTTCCCAGTTTC
Of_8638_F862	ggccgcggCCAAAACCCGTGGCTGTTAA
Of_8638_R862	cccggggcTCGTTTGATCAGGCTCACTT
Of_12526_F536	ggccgcggAGTTCGATTGATGCGCTAGA
Of_12526_R536	cccggggcTGCACAGCCCATTAGTTTTCC
Of_2807_F515	ggccgcggACAGAACGTCTCCAGCAAGA
Of_2807_R515	cccggggcCCTCCAAAACCAGAAAATCCCA
Of_8316_F953	ggccgcggGTGATTACGAACCTTTGCCTGA
Of_8316_R953	cccggggcAGGCCCCAGAAGCTCTAAAG
Of_16399_F987	ggccgcggGGCTCTTCACGGTTATGCAG
Of_16399_R987	cccggggcTTGACATCCCACAGAGCCAT
Of_9423_F922	ggccgcggAACGGAATGAATCACGCTCG
Of_9423_R922	cccggggcAGTGCTTGGGGTTGTTGAAC
Of_3124_F502	ggccgcggTGGGAATAGTCAAACAAGTGGA
Of_3124_R502	cccggggcATACAGCCACGACCTCAAAG
Of_25201_F1093	ggccgcggGCCTTGCAAGAACAACGGTA
Of_25201_R1093	cccggggcCTCGGTGTTGAGCTGCTTTT
Of_6887_F851	ggccgcggGTGGCAGAACTGAACTCGC
Of_6887_R851	cccggggcTGCAGTTCATCAGACCTCGT
Of_9422_F324	ggccgcggCTTCAACCTCAACGCTGCTT
Of_9422_R324	cccggggcAGCTTCCAGTCACCAACAGT
Of_7134_F334	ggccgcggTGGACGTGAAGCATTGCAAA
Of_7134_R334	cccggggcATCTGCATTGAACACGTCGG
Of_18575_F278	ggccgcggAGTATCACAGTGGACCAGGG
Of_18575_R278	cccggggcATTTCAGACCCACGAAGAGTT
Of_625_F356	ggccgcggCTGTCCAAATGCAAGGCGTA
Of_625_R356	cccggggcGATCTTCGTGCAGCAGTCG
Of_6375_F1064	ggccgcggGGTGTCAGGTTGCTGGATTC
Of_6375_R1064	cccggggcGACTCGGGGTTGTTTTCACC
Of_18840_F488	ggccgcggTCAATATATGGCATCCTCTCGG
Of_18840_R488	cccggggcATTCCGCACCACTTAGCCAA
17639OF1500	TTAGCTCTCCCGACGAATCC
17639OR1500	GAGGTCATCTGCCACTTCCT
17639IF1084	CCCTCCATCCCTGCATTACT
17639IR1084T7	taatacgactcactatagggTCACAGCCACATCTTCAACC
17639IF1084T7	taatacgactcactatagggCCCTCCATCCCTGCATTACT
627OF1019	ATGTGGGAGCGCCTTGTT
627OR1019	ACTTAGTGAACACAGGGGCA
627IF853	GACTGGGAGAGCTGGCAA
627IR853T7	taatacgactcactatagggGTCAGCTGAGCATGTACACA
627IF853T7	taatacgactcactatagggGACTGGGAGAGCTGGCAA
18039OF606	TCACGGGACCAAGGAAAACC
18039OR606	GCAAATGTGTCTAAGGGAGGC

18039IF548	CATATGGTGGGGAGAGAGCT
18039IR548T7	taatacgactcactatagggAGAAGCAGGATATGGGCGAG
18039IF548T7	taatacgactcactatagggCATATGGTGGGGAGAGAGCT
3579OF1836	ACTGGGGTGATTAATTTTGGGT
3579OR1836	TTGAGGTTGAGGGAATGGCT
3579IF1030	GGTTGGGAGGAGAGATGCTT
3579IR1030T7	taatacgactcactatagggAAGATGGTGGAAGAGGTGGG
14828OF1327	TGAGATGCAGCCACCTACAA
14828OR1327	CTCACATTAAGACTGCCACACA
14828IF1083	GGAAAGTAATGAGCGGCCTG
17639IR1083T7	taatacgactcactatagggGTGACCAACTCGAACCACTG
25202OF1159	GCCAAGCGGAAAGAGATACA
25202OR1159	CGCCAAGAGTAATTCGGTCA
25202IF1001	ACAAGTGTCGCAGCAAGTAC
25202IR1001T7	taatacgactcactatagggTTGACGGTGTTCCTCTTCCT
10513OF1121	TTTCGGAGTTGGTGTTCCTC
10513OR1121	TCATGGATGGACCCTCTGA
10513IF918	CTTGCCAAATGGTTGTGTTG
10513IR918T7	taatacgactcactatagggTGGGTTTGGAATAGGGATGA
10513IF918T7	taatacgactcactatagggCTTGCCAAATGGTTGTGTTG
9851OF1392	CCCACTTGAGGTTCACTTGC
9851OR1392	AAGTCTTCTCGGTCAGCTCC
9851IF1020	GCAACTGAGCCTCAAATGGT
9851IR1020T7	taatacgactcactatagggTGGATTGTTGCCCTTGTCAG
9851IF1020T7	taatacgactcactatagggGCAACTGAGCCTCAAATGGT
25131OF1603	GGTAGGAGTAGGCACAGCAT
25131OR1603	TGTAGCTCCACTTGTCGGTT
25131IF1003	TGTGTGGTGTTTGGAGGAGA
25131IR1003T7	taatacgactcactatagggTGCACAGTAATGACCCCTGA
13273OF1307	TATGCCCGTGGTTTTGAGTC
13273OR1307	TCCTGACAATAGCGACAAGG
13273IF1107T7	taatacgactcactatagggCAGCAGCACCGTGATACTAA
13273IR1107T7	taatacgactcactatagggCACAAATTCGACAGTTTCCAGT
1002OF1346	ATCGGAATGGGAGCAAACAC
1002OR1346	ATAAGAGTCCGTGGCGTCTG
1002IF1009	CGCTGGAACACCTGGAAGTA
1002IR1009T7	taatacgactcactatagggAATCAGGGTGGGAGGAGAGG
14448OF1320	CCCAGCAATACCATTCCAGC
14448OR1320	AGTGCTGCCTAGTGTGACTT
14448IF1000	TTTTAGCCAGCCTCCACCTT
14448IR1000T7	taatacgactcactatagggAGCTGTTGTTGGAGTGATTGA
14448IF1000T7	taatacgactcactatagggTTTTAGCCAGCCTCCACCTT
10383OF1278	CTCCGACTGACTCAACTGGT
10383OR1278	TGGCTGCTTCTTCTTTGCTC
10383IF1056	GGAACTACCCATGTCGTGAT
10383IR1056T7	taatacgactcactatagggCTTGAGTCACATCCCCATTGT

10383IF1056T7	taatacgactcactatagggGGAACTACCCATGTCGTGAT
16851OF1131	TGTTGTTGGCGGTATTTCCTG
16851OR1131	AGGAAACAGGGTCTAGTGGG
16851IF1025	CAGCAAATGATCTGTCTCCCC
16851IR1025T7	taatacgactcactatagggAGTGGTGCCTTCTTCATCCA
T7 5' universal (fwd)	gagaattctaatacgactcactatagggccgcgg
T7 3' universal (rev)	agggatcctaatacgactcactatagggcccggggc

2.2 Methods

2.2.1 Culturing and husbandry of *Oncopeltus fasciatus*

Oncopeltus fasciatus was cultured at 25 °C, fed with sunflower seeds and supplied with tap water-filled erlenmeyer flask that were plugged with paper towels to enable the bugs to drink and prevent them from drowning. Small petri dishes with cotton were supplied in which the females laid their eggs. Detailed husbandry conditions for *O. fasciatus* are described in Liu and Kaufmann, 2009.

2.2.2 Embryo fixation

The embryo fixation protocol for *O. fasciatus* is adapted from Liu and Kaufman, 2004. The space between the chorion and the embryo of *O. fasciatus* is under relatively high pressure. Initially the eggs were heat-fixed to prevent the embryo from being damaged during the eggshell cracking process. Therefore the eggs were transferred into screw top tubes and covered with 1.2 ml distilled H_2O. The tubes were submerged into boiling water for 90 seconds. Afterwards the tubes were immediately cooled down in ice water for 5 minutes. Subsequently the eggs were vortexed in 600 µl heptane and 600 µl 1x PBS with 5 % formaldehyde for 5 minutes. The lower aqueous phase was removed, 600 µl ice cold methanol (-20 °C) were added and the tube was shaken vigorously for 1 minute. Afterwards all liquid was removed and the embryos were again shaken vigorously in 1.2 ml of ice cold methanol. The addition of methanol in combination with vigorously shaking initiated the cracking of the chorion. The embryos were fixed in 1x PBS with 5 % formaldehyde for at least 2 hours. The fixation works via a nucleophile attack of primary amino functional groups, which are mainly found in lysine side chains, to carbonyl functional groups of formaldehyde. This leads to hemiaminals that condensate with further amino functional groups. Thus the proteins become connected to each other. The fixed embryos were stored in methanol at -20 °C.

2.2.3 RNA extraction

Wild-type or knockdown embryos were transferred into a 1.5 ml tube and homogenized with a micro pestle (Eppendorf) in 100 µl TRIzol (Ambion). 900 µl TRIzol were added and the tube was briefly vortexed. Following homogenization the sample was centrifuged at 12000 x *g* for 10 minutes at 4 °C. The cleared supernatant was transferred into a new tube, while solid components were discarded. In TRIzol homogenized embryos could be optionally stored at -80 °C. The homogenized sample was

incubated for 5 minutes at room temperature. 200 µl chloroform were added and the tube was vortexed for 15 seconds. After incubation at room temperature for 3 minutes the sample was centrifuged at 12000 × *g* for 15 minutes at 4 °C. The upper aqueous phase was transferred into a new tube by angling the tube at 45° and pipetting the solution out. Afterwards the aqueous phase was mixed with 500 µl of 100% isopropanol by inverting the tube. In order to precipitate the RNA the sample was incubated for 1 hour to overnight at -20 °C. The sample was centrifuged at 12000 × *g* for 15 minutes at 4 °C. The supernatant was removed and the RNA-pellet was washed with 1 ml of 75% ethanol for 5 minutes at room temperature. The sample was vortexed briefly and then centrifuged at 7500 x *g* for 5 minutes at 4 °C. The ethanol was removed and the pellet was allowed to dry on air. Afterwards the pellet was resuspended in nuclease-free water and incubated at 55 °C for 5 minutes. Concentration and quality was estimated by measuring the absorption at 230, 260 and 280 nm with a NanoDrop (Thermo Scientific). In addition, the RNA was monitored on an agarose gel to confirm that the isolated RNA was not degraded. The isolated RNA was stored at -80 °C. This protocol was adapted from the Ambion TRIzol® Reagent manual.

2.2.4 cDNA synthesis

The SuperScript® VILO™ cDNA Synthesis Kit (Life Technologies) was used for cDNA synthesis. Synthesis was carried out according to the manufacturer's manual. cDNA was used as template for cloning, the generation of single-stranded antisense in situ hybridization probes and double-stranded RNA fragments for RNAi. cDNA was stored at -20°C or -80°C.

2.2.5 Polymerase chain reaction (PCR)

All PCRs were performed on a C1000 or S1000 Thermal Cycler (Bio Rad, Hercules, US). REDTaq® ReadyMix™ (Sigma-Aldrich) was used to amplify fragments. cDNA or linearized plasmids were used as template. The components for a PCR reaction were pipetted on ice in a 0.2 ml PCR-tube. Table 3 shows a detailed list of components used for a PCR reaction.
After pipetting of all components the tube was transferred to a thermal cycler and the PCR reaction was carried out. Table 4 shows a typical PCR program. The elongation time was 1 min per 1 kb of desired product. The PCR product was checked on an agarose gel and if needed sequenced. The PCR products were kept at -20 °C.

Table 3: PCR components

Component	Amount per reaction
REDTaq® ReadyMix™	12.5 µl
Primers (20 µM)	0.5 µl of each
cDNA template (50 ng/µl)	1 µl
H_2O	Up to 25 µl
Total	25 µl

Table 4: Standard PCR program

Cycle number	Denature	Anneal	Elongate	Hold
1	94°C, 5 min			
2-36	94°C, 30 s	55-57°C, 30 s	72°C, 1 min	
37			72°C, 5 min	
38				4°C, forever

2.2.6 electrophoresis separation

To determine the presence and size of a particular PCR product, 5 µl of the reaction was run on a 1% agarose gel in 0.5x Tris-acetate-EDTA buffer at 135 V. To visualize the DNA 2 to 3 drops of 0.025 % ethidium bromide solution per 50 ml agarose were used. To identify the approximate size of a DNA fragment 2.5 µL of Smart Ladder MW 1700-10 (Eurogentec) was used as a molecular-weight size marker.

2.2.7 Cloning of PCR products

2.2.7.1 Transformation via electroporation

The Invitrogen™ TOPO™ TA Cloning™ Kit in combination with DH5α component *E. coli* cells were used and the instructions from the manuals were followed. Competent *E. coli* bacteria were stored at -80 °C and thawed on ice. After adding the ligation reaction, the bacteria were electro shocked at 1700 V. Immediately after the electroporation the cells were transferred into SOC medium and incubated at 37 °C for at least 1 h on a shaking incubator. Afterwards the bacteria were spread on LB-agar plates (LB medium plus 1.5% agar) with kanamycin, isopropyl β-D-1-thiogalactopyranoside (IPTG) and 5-Brom-4-chlor-3-indoxyl-β-D-galactopyranosid (X-Gal) and grown at 37 °C overnight. The pCR™II TOPO® TA vector contains a kanamycin resistance gene and the cloning site is located within the LacZ gene. Therefore bacteria with the pCRII vector were selected positively and it was possible to distinguish between colonies with an insertion in the pCRII vector (white) and with an empty vector (blue).

2.2.7.2 Extraction, purification, linearization and sequencing of plasmids

White colonies were picked and each was allowed to grow in 3 ml of LB medium with kanamycin at 37 °C overnight on a shaking incubator. The picked colonies were additional used as templates for colony PCRs with gene specific or M13 primers. For plasmid extraction the QUIAGEN Plasmid Miniprep Kit was used and all instructions from the manuals were followed. To examine the length of the cloned PCR products extracted plasmids were linearized with EcoRI and subsequent gel electrophoresis separation was performed. Finally the cloned PCR products were sequenced to confirm the cloning of the desired DNA fragments.

2.2.8 Template generation for RNAi and ISH

A two-step PCR strategy was used to amplify cDNA fragments with added T7 linkers as templates for either double-stranded RNA fragments for RNAi or single-stranded antisense mRNA probes for ISH. To each gene specific primer a linker sequence was added on the 5' end of each primer; for the forward (sense) primer "ggccgcgg" and for the reverse (antisense) primer "cccggggc" was added. The first PCR was carried out using standard PCR parameters (denaturation at 94 °C, annealing at 55 to 57 °C, elongation at 72 °C, 35 cycles), cDNA as template and gene specific primers with the described linkers for the gene of interest. The PCR products from the first PCR could be used to generate a template for both labeled antisense probes for ISH and double-stranded RNA fragments for RNAi, respectively. To generate a template for a labeled antisense probe a second PCR (using standard PCR parameters) was performed in which the PCR product from the first PCR was used as template together with the gene specific forward primer and the 3' T7 universal primer (agggatcctaatacgactcactatagggcccggggc). To generate a template for a double-stranded RNA fragment both the 3' T7 universal primer and the 5' T7 universal primer (gagaattctaatacgactcactatagggccgcgg) were used together with the PCR product from the first PCR as template (using standard PCR parameters). The PCR products from the second PCR were used as templates for subsequent ISH probe and double-stranded RNA fragment synthesis, respectively.

2.2.9 Synthesis of dsRNA fragments for RNAi

To generate double-stranded (ds) RNA fragments the MEGAscript ® KIT (Ambion) was used. First, a mastermix was prepared on ice containing 2 µl of each NTP (ATP, CTP, GTP and UTP), 2 µl T7 RNA Polymerase Enzyme Mix and 2 µl supplied 10x reaction buffer per reaction. The mastermix was briefly vortexed and quickly pipetted in individual reaction tubes (12 µl each). The gene-specific PCR templates (see section 2.2.8) or linearized plasmid were diluted with an equal amount of nuclease-free water and 8 µl of the diluted gene-specific PCR template was added. The reaction tubes were incubated overnight at 37 °C. The reaction was stopped by adding 115 µl water and 15 µl 10x ammonium acetate stop solution (5 M ammonium acetate, 100 mM EDTA). The dsRNA fragments were purified by adding 150 µl phenol/chloroform/isoamylalkohol (25:24:1). The reaction tube was vortexed for 1 minute and centrifuged at 5000 rpm for 5 minutes at 4 °C. The upper aqueous phase was transferred into a new tube by angling the tube at 45° and pipetting the solution out. Afterwards the aqueous phase was mixed with 150 µl of 100% isopropanol by inverting the tube. In order to precipitate the dsRNA the sample was incubated for 1 hour to overnight at -20 °C. The sample was centrifuged at 12000 rpm for 15 minutes at 4 °C. The supernatant was removed and the RNA-pellet was washed with 300 µl of 70% ethanol. The sample was again centrifuged at 12000 rpm for 5 minutes at 4 °C. The ethanol was removed via pipetting and the pellet was allowed to dry on air. Afterwards the pellet was resuspended in 50 µl nuclease-free water. Concentration and quality was estimated by measuring the absorption at 230, 260 and 280 nm with a NanoDrop (Thermo Scientific). In addition, the RNA was monitored on an agarose gel to confirm that the dsRNA was not degraded. The dsRNA was stored at -20 °C. This protocol was adapted from the MEGAscript ® KIT (Ambion) manual.

2.2.10 Synthesis of labeled ISH probes

To generate single-stranded (ss) digoxigenin (DIG)-labeled antisense RNA in situ hybridization (ISH) probes reagents from Roche were used. First, a mastermix was prepared on ice containing 7.5 µl nuclease-free water, 2 µl DIG RNA labeling mix (Roche), 0.5 µl Protector RNase-Inhibitor (Roche), 2 µl T7 RNA Polymerase and 2 µl supplied transcription buffer (both from Roche) per reaction. The mastermix was briefly vortexed and quickly pipetted in individual reaction tubes (14 µl each). 6 µl gene-specific PCR template (see section 2.2.8) or linearized plasmid was added. The reaction tubes were incubated for 4 hours at 37 °C. The reaction was stopped by adding 30 µl water and 50 µl 2x ammonium acetate stop solution (10x ammonium acetate stop solution: 5 M ammonium acetate, 100 mM EDTA). 5 µl tRNA, 10 µl lithium chloride precipitation solution (7.5 M lithium chloride, 50 mM EDTA) and 300 µl ethanol (100%) were added and the probe was precipitated for 1 hour to overnight at -20 °C. Then the probe was centrifuged at 14000 rpm for 15 minutes at 4 °C. The supernatant was discarded and 300 µl ethanol (70%) was added. The reaction tube was briefly vortexed and again centrifuged at 14000 rpm for 5 minutes at 4 °C. All supernatant was discarded via a pipette and the pellet was allowed to air dry. Finally the pellet was resuspended by pipetting in 100 µl probe resuspension buffer (formamide 50 %, 2x SSC). The resuspended probes were stored at -20°C. This protocol was adapted from the MEGAscript ® KIT (Ambion) manual.

2.2.11 Generation of parental RNA interference knockdown embryos

To generate parental RNA interference (pRNAi) knockdown embryos for a particular gene of interest 5 µl dsRNA at concentrations of 1000 ng/µl was injected into adult virgin females of *Oncopeltus*. Injections were performed using a 10 µl syringe (Hamilton). The method of RNAi knockdown generation exploits an ancient defense mechanism against double-stranded (ds) RNA viruses that is thought to be present in most multicellular organisms (Jinek and Doudna, 2009). dsRNAs that often result from viral infection and transcription are recognized and cleaved by Dicer, an RNAse III family protein. Thereby small dsRNAs (21-25 nucleotides) are generated, which are labeled via mono-phosphate groups on their 5'-ends and dinucleotide overhangs on their three 3'-ends. These small dsRNAs are bound by argonoute proteins. This association forms the core complex of the RNA induced silencing complex (RISC). The argonoute proteins are responsible for the cleavage and binding of the target single-stranded RNA (ssRNA).This mechanism can be experimentally used to knock down gene expression by injection of long dsRNA molecules (about 200 bp to 1.5 kb) corresponding to an exonic region of the respective target gene. This leads to a knockdown of the target gene via mRNA degradation. This method is very successful and easy to apply in *Oncopeltus*. It is possible to perform (pRNAi) knockdowns via injection of dsRNA into adult females. Embryos with a loss of function phenotype can be obtained for up to four weeks (Liu and Kaufman 2004), except immunity-relevant genes are targeted, e.g. *Toll,* which leads to drastically increased mortality of injected female after about one week and therefore decreases knockdown embryo yield.

2.2.12 In situ hybridization protocol

This in situ hybridization (ISH) protocol was adapted from the previously published ISH protocol for *O. fasciatus* by Liu and Kaufman, 2005. The ISH protocol was always performed within a timeframe of 3 days.

2.2.12.1 Embryo preparation before hybridization

The embryos were stepwise transferred from 100% methanol to 1x PBST and then washed with 1x PBST (2x 5 minutes, 1x 1 hour). Subsequently the embryos were gradually transferred into hybridization buffer and washed twice in hybridization buffer for 5 minutes. In order to inactivate the endogenous alkaline phosphatase the embryos were incubated at 70 °C for 30 minutes. Subsequently the embryos were prehybridized by incubation at 60 °C for at least 30 minutes.

2.2.12.2 Hybridization reaction

5 µl probe was added to 495 µl hybridization buffer. Hybridization was performed at 60 °C overnight (end of day 1). The specificity of the hybridization of nucleic acids depends largely on an appropriate concentration of formamide, salts and on a suitable temperature. Salt (SSC, SDS) promoted hybridization because the positively charged cations neutralized the negative charge of the phosphate backbone of nucleic acids. Additionally, formamide is a hydrogen bond breaking substance that prevented unspecific hybridization. A high temperature also hindered unspecific hybridization. Moreover, ssDNA also inhibited unspecific hybridization because it blocks and saturates nucleic acids via unspecific bindings which then are replaced by specific bindings from the antisense probe to sense mRNA. tRNA is added to protect the RNA probe against nucleases by competitive inhibition. Since the concentration of tRNA was much higher than the probes concentration, tRNA was more likely a substrate for nucleases then the probe was.

2.2.12.3 Removal of excessive probe

Excessive probe was removed by six washes in hybridization buffer at 60 °C (2x rinsed, 4x 20 minutes) and two subsequent washings at room temperature (2x 5 minutes) first in 5x SSC/ 50% formamide/ 0.1% Tween-20 and second in 2x SSC/ 50% formamide/ 0.1% Tween-20. Afterwards the embryos were gradually transferred into 1x PBST and then washed in 1x PBST (2x rinsed, 2x 20 minutes). Afterwards the embryos were once rinsed and subsequently blocked for 2 hours at room temperature in blocking solution.

2.2.12.4 Probe detection

The anti-digoxigenin::alkaline phosphatase (α-DIG::AP) antibody (Roche, Fab fragments from sheep, applied dilution 1:2000) and the nucleic acid stain SYTOX-green (Nuclear probes) was added in fresh

blocking solution. The embryos were incubated overnight at 4 °C (end of day 2). The excessive antibody was removed by several washes in 1x PBST at room temperature (4x rinsed, 4x 20 minutes). The embryos were stepwise transferred into alkaline phosphatase (AP) buffer. This buffer contains ions and has an alkaline pH, which enables the enzyme to catalyze efficiently. After several washings in AP buffer (2x rinsed, 1x 30 minutes) nitro blue tetrazolium chloride/5brome-4chlor-3indolylphosphate (NBT/BCIP; Sigma-Aldrich) solution was added in fresh buffer to initiate the color reaction. Alkaline phosphatase dephosphorylates BCIP which becomes then oxidized by NBT and adds to a blue indigo colorant while NBT is reduced to a blue diformazan. The reaction was stopped by several washes in 1x PBST.

2.2.13 Fuchsin staining

Fixed embryos (see section 2.2.2) were transferred into glass vials and washed in 70% ethanol (4x 20 minutes). The ethanol was removed, 2 N HCl were added and the embryos were incubated at 60 °C for 10 minutes. Afterwards one washing with distilled H_2O (5 minutes) and two with 70% ethanol (2x 5 minutes) were performed. Subsequently the embryos were incubated in alcoholic fuchsin staining solution for 30 minutes. Then excessive color was removed by washing in 95% ethanol (3x 20 minutes). Afterwards the embryos were dehydrated by washing in 100% ethanol (2x 3 minutes). The ethanol was removed and solution C was added. As soon as the embryos sank to the bottom of the tubes, solution C was substituted by solution D. The BBBA alcohol mixture is responsible for optical clearing of the yolk. The stained embryos were stored at 4 °C, protected from light. This protocol was based on Lena Sachs fuchsin staining protocol (Sachs, PhD thesis, 2014).

2.2.14 mRNA synthesis protocol

The mMessage mMachine® SP6/T7 Kit (Ambion) was used for capped mRNA synthesis. Synthesis was carried out according to the manufacturer's manual. Linearized plasmids were used as templates. The plasmid pCS2-zfChd (vector: pCS2+; insert: *Danio rerio chordin* cDNA; bacterial resistance: ampicillin; linearized with: NotI; sense transcription with: SP6) was kindly provided by the Matthias Hammerschmidt lab. The plasmid pUC57-Eos-NLS-PolyA (vector: pUC57; insert: *Eos-NLS* cDNA; bacterial resistance: ampicillin; linearized with: BamHI; sense transcription with: SP6 or T7) was kindly provided by Matthias Pechmann. Capped mRNA was microinjected into O. *fasciatus* blastoderm stage embryos at concentrations between 1500 to 3000 ng/µl. Capped mRNA was stored at -20°C and thawed not more than 3 times before being discarded.

2.2.15 Dechorionation of *Of* embryos for microinjections

In order to perform embryonic microinjections *Oncopeltus* embryos were partially dechorionated to enable needle penetration. Complete dechorionation established for other insect embryos like *Drosophila* or *Tribolium* was not possible in *Oncopeltus* since the dechorionation agent enters *Oncopeltus* embryos trough the micropyles and completely dissolved the entire embryo before dechorionation was achieved.

Partial dechorionation was achieved with two different methods. For a strong but less uniform partial dechorionation two small stripes of cellulose filter paper (Whatman) were saturated with DanKlorix (Colgate-Palmolive). The embryos were lined up on the first stripe in a way in which the most anterior part including the micropyles was not touching the stripe. The second stripe was placed on top in an analogous manner. After 5 minutes of exposure to DanKlorix embryos were rinsed with water 3 times. For a more uniform but less strong partial dechorionation embryos were transferred into 50% DanKlorix for 5 minutes and subsequently rinsed with water 3 times to remove DanKlorix.

2.2.16 Needle preparation for embryonic microinjections

Our lab routinely microinjects embryos from various arthropods with borosilicate glass needles. Unfortunately the chorion of *Oncopeltus* embryos is too resistive to be penetrated with such needles even after partial dechorionation. Instead I used quartz glass needles (with filament; outer diameter 1 mm; inner diameter 0,5 mm; length 100 mm; Sutter Instrument item #: QF100-50-10). Those needles were pulled on a P-2000 micropipette puller (Sutter Instrument) using the following quarz glass specific program:

Heat	Filament	Velocity	Delay	Pull
825	5	50	145	175

Unlike borosilicate glass needles which can be opened by polishing on a grinder quarz glass needles had to be cut open with a razor blade since they were too rigid to be polished.

2.2.17 Embryonic microinjections

1% agarose gel was poured into a Petri dish and long slits were cut into the cooled down gel with a razor blade. Partially dechorionated embryos (see 2.2.15) were pushed into these slits with a brush and covered with halocarbon oil (Voltalef H10S, Arkema). Protein or mRNA was backloaded into quartz glass needles which were cut open with a razor blade. Embryos were injected under a microscope using a microinjector (PLI-100A Pico-Injector, Warner Instruments). After injection embryos were left within the agrose slits and placed into their regular incubator.
Several parameters within this injection protocol could not be standardized and therefore the injection amount was necessarily variable and difficult to quantify, ranging from about 0.05 % to 5 % of overall egg volume. Varying parameters included depth of injection and bevel angle of the needles.

2.2.18 RNA sequencing

RNA was isolated and purified as described in 2.2.3. RNA quantity and quality was checked using a Thermo Scientific Nanodrop 2000C Spectrophotometer and 2 µg was sent for sequencing by the Cologne Centre for Genomics (CCG) on an Illumina HiSeq 2000 sequencer after sample preparation using a TruSeq RNA Library Preparation Kit (Illumina). Samples were sequenced on one lane per

species. Adaptor trimming and initial quality control was performed by the provider according to their proprietary standards, and after exclusion of complete reads, no orphan reads were kept. This cleaned data was then made available to us for download from an external server. Paired end read quality after sequencing was assessed using the FastQC program (Andrews, 2010) and no residual adaptor was observed.

2.2.19 Transcript Quantification and Differential Expression Analyses

Transcript Quantification was made using the Trinity toolkit together with the alignment-based quantification method RSEM (Grabherr et al., 2011; Li and Dewey, 2011). Trimmomatic (Bolger et al., 2014) was assayed (Illuminaclip Leading:3 Trailing:3 Slidingwindow:4:15 Minlen:36) but not utilized. DeconSeq standalone version 0.4.3 (Schmieder and Edwards, 2011) was run on full assemblies with settings -i 95 -c 95, using the bact, fungi, hsref, and prot databases. Differential expression analyses were performed by mapping reads from individual samples (RNAi knockdowns and wild-type) to the Official Gene Set (OGS v1.2) of *Oncopeltus fasciatus* (Panfilio et al., 2019) using RSEM with Bowtie (Langmead at al., 2009) as packaged in the Trinity module (align_and_estimate_abundance.pl script,—est_method RSEM—aln_method bowtie) to compare the individual samples with each other. The abundance_estimates_to_matrix.pl script was then run (cross sample normalization: Trimmed Mean of M-values). edgeR (Robinson et al., 2010) was then run using the run_DE_analysis.pl script and the most differentially expressed transcripts were extracted and clustered using the analyze_diff_expr.pl script, p-value cut off for FDR of 0.05 and fold change of 2, with—gene_dist euclidean and—gene_clust.complete.

3. Results

3.1 Knockdown of *Of-snail*

Most of the conserved components of insect DV axis patterning had been analyzed in *Oncopeltus* in previous work (Sachs, PhD thesis, 2014; Chen, PhD thesis, 2015; Sachs et al., 2015). However, a knockdown of *Of-snail* was never described. I performed a pRNAi-mediated *Of-snail* knockdown and analyzed the phenotype by fuchsin staining (Fig. 9 E) and ISH experiments with DV and AP marker genes (Fig. 9 A-D). Embryos lacking Sna exhibited a strong lethal phenotype in which a head was formed at the posterior end but thoracic and abdominal segments seemed to be lacking, indicating impaired germ band formation and defective katatrepsis (Fig. 9 E). The expression of *OFAS016851* in *Of-snail* knockdown embryos is similar to its wild-type expression pattern (Fig. 9 C, compare to Fig. 26 A). However, the expression of the mesodermal markers *sog* and *twi*, and of the mesectodermal marker *sim* was derepressed in *Of-sna* knockdown embryos, that is, their expression was uniform around the embryonic circumference (Fig. 9 A, B, C). While the derepression of *sog* and *twist* is seen in several knockdown conditions which lack BMP signaling (e.g. in *dpp* and *tld* knockdown embryos) (Sachs et al., 2015), the expression of *sim* within the derepressed mesoderm is a distinctive characteristic of *snail* knockdown embryos.

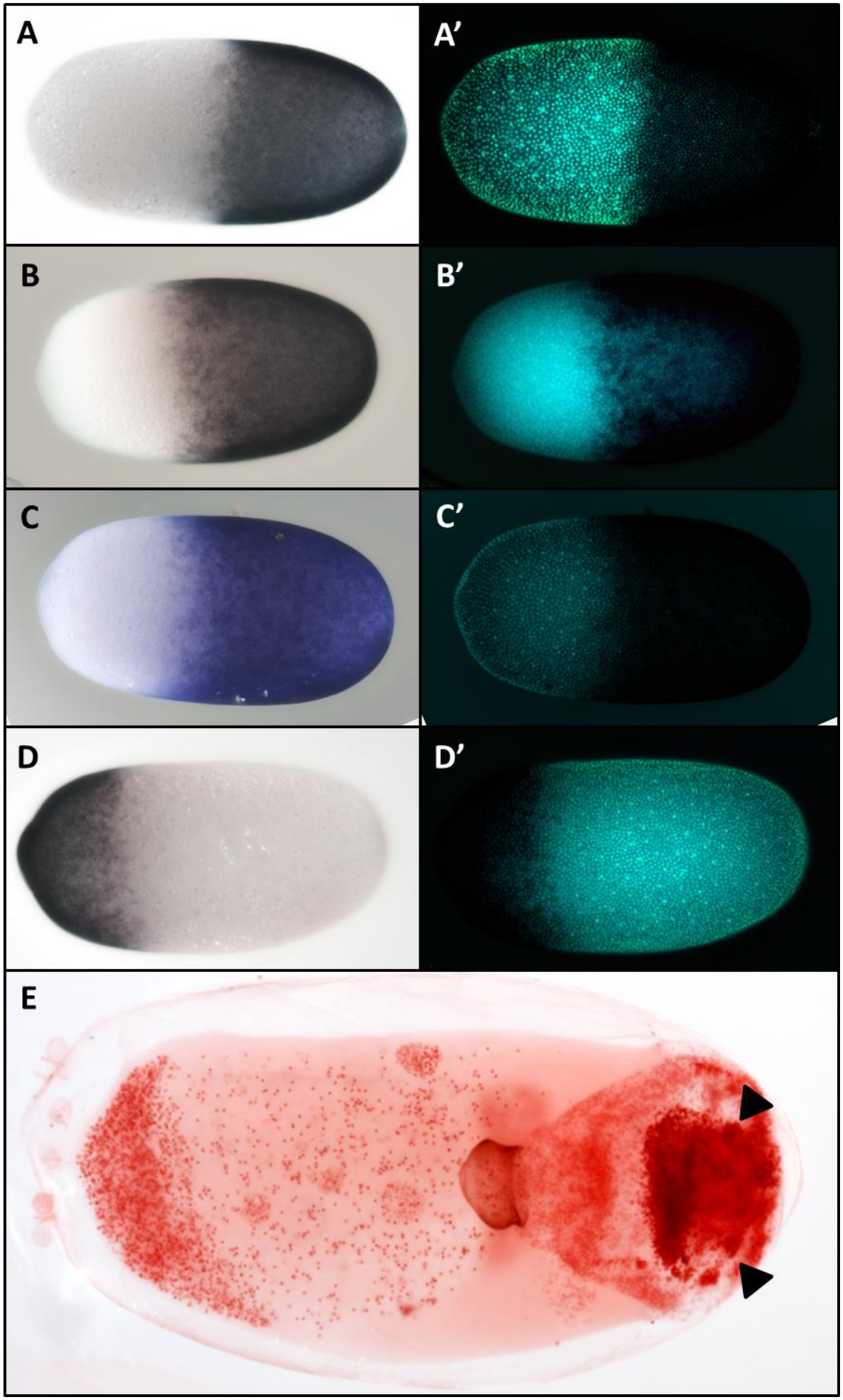
A
A’
B
B’
C
C’
D
D’
E

Figure 9: pRNAi-mediated knockdown of *Of-snail*
(A-E) *Of* embryos lacking Snail, anterior to the left; **(A-D)** embryos were fixed 24-30 hpf (hours post fertilization); **(A)** expression of *sog*; **(B)** expression of *twist*; **(C)** expression of *sim*; **(D)** expression of *OFAS016851*; **(A'-D')** same embryo as depicted in pictures labeled with corresponding capital letters, nuclei stained with SYTOX Green; **(E)** fuchsin staining. Embryo was fixed 144 hpf. Position of the eyes is marked with black arrowheads.

3.2 Establishment of embryonic injections

In order to perform the desired DV network manipulations in *Of* blastoderm embryos a practical injection method had to be developed (see 2.2.15 – 2.2.17). To test the injection method early blastoderm stage embryos (18 - 24 hpf) were injected with dd H_2O as negative control (Fig. 10). The injected embryos developed and hatched wild-type-like in 91,76% of observed cases (n=182). 8,24% of injected embryos exhibited unspecific developmental arrests before or during germ band formation, presumptively caused by the injection process itself. Hughes and Kaufman who first published a similar though less sophisticated injection protocol for *Of* reported a 50% rate of developmental arrests in their negative control experiments (Hughes and Kaufman, 2000).
The location of needle penetration for these initial and each of the following injection experiments was between 25 and 50 % of egg length (posterior is 0%) from lateral positon to ensure injections into presumptive mesodermal or ectodermal regions. Anterior and posterior of *Oncopeltus* embryos were easy to distinguish by the anterior positioned micropyles. Unfortunately the embryos looked uniform along their DV axis during blastoderm stage. Therefore it was not possible to aim injections specifically for distinct regions along the DV axis like for example the mesoderm. However, in nuclear staining of embryos fixed 6h after injection an injection-wound was frequently visible and therefore allowed to locate the site of injection.

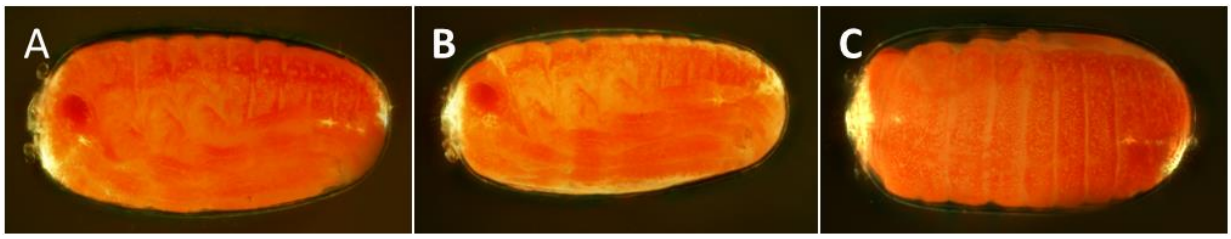

Figure 10: *Of* embryos after injection of water
(A - C) *W*ater-injected *Of* wild-type embryos shortly before hatching, anterior to the left. Injections were performed at early blastoderm stage between 18 - 24 hpf; **(A)** lateral view; **(B)** ventrolateral view; **(C)** dorsal view.

3.3 Microinjection of human BMP4 protein into *Of* embryos

The first successful embryonic microinjections which induced DV aberrations during axis formation in *Oncopeltus* were performed using commercially available human BMP4 protein (Thermo Fisher Scientific; PHC9534) (Fig. 11 - 13). It has been shown before that vertebrate BMP4 is able to activate the BMP signaling pathway in arthropod species and vice versa (Padgett et al., 1993; Pechmann, 2020; Sampath et al., 1993). Early blastoderm stage embryos (18 - 24 hpf) were microinjected with

different BMP4 concentrations and either fixed at late blastoderm stage (24 - 30 hpf) for ISH experiments (Fig. 13) or photographed after 6 more days of development, when the negative controls were about to hatch (Fig. 11 - 12). As negative control to exclude unspecific protein injection effects like an immune response I injected BSA at similar concentrations which did not seem to disturb embryogenesis.

Embryos injected with high concentrations (100 µg/ml) of BMP4 show strong phenotypes in which the embryo developed into a large agglutination of yolk connected with a small cuticulized part of embryonic tissue (94,77 % n=153) (Fig. 11). Injections with moderate concentrations of BMP4 (10 - 20 µg/ml) lead to milder but nevertheless still strong phenotypes in which the embryos developed heads with visible eyes and mouthparts, but thoracic and abdominal segments failed to develop correctly (Fig. 12 A - B). Defective katatrepsis occurred as well (Fig. 12 A). In some cases the embryos injected with moderate concentrations of BMP4 hatched wild-type-like or showed late developmental arrests after katatrepsis (Fig. 12 C - D).

In situ hybridization for *sog* transcripts revealed that around the injection site of moderate BMP4 concentrations the endogenous expression of *sog* is disturbed (Fig. 13). Cells in proximity to the injection site show either weaker or no staining, indicating reduced or absent *sog* expression (Fig. 13). In situ hybridizations for *sog* transcripts performed on embryos which were injected with high concentrations of BMP4 do either not show visible staining or chaotic and disorganized patches of *sog* expression (data not shown).

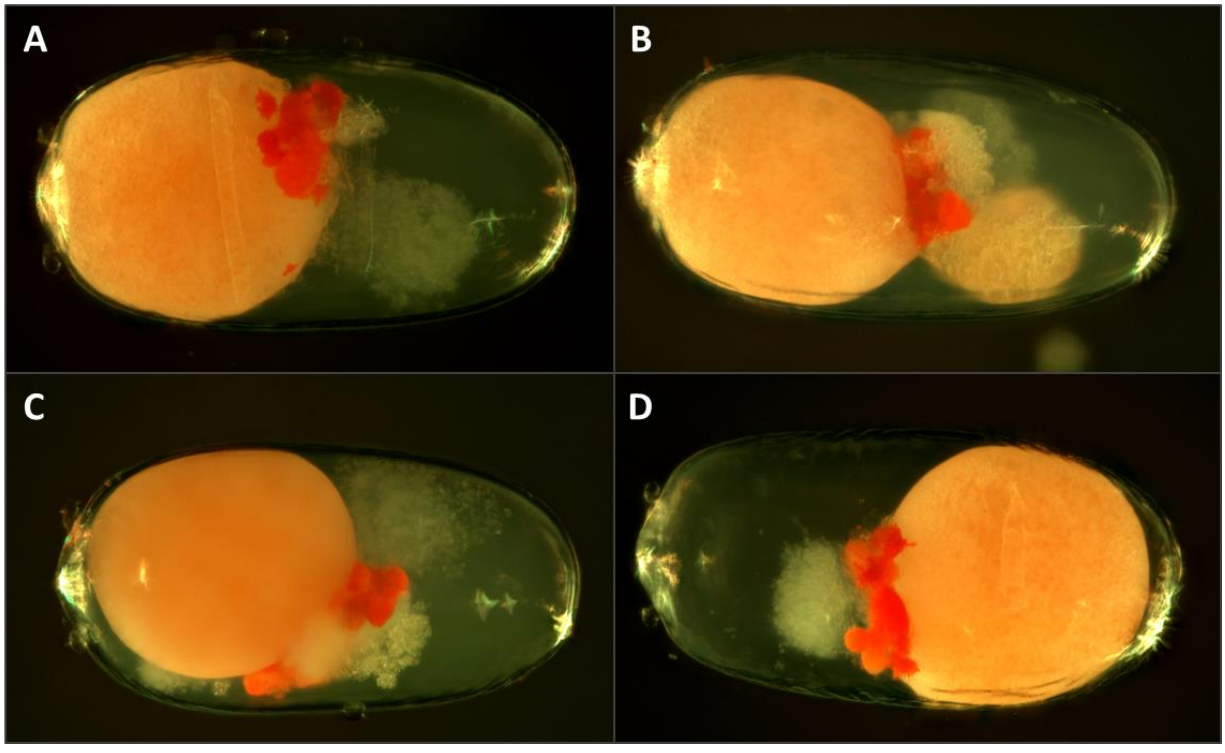

Figure 11: *Of* embryos after injection with high concentration of human BMP4

(A - D) Embryos were injected with high concentrations of human BMP4 18 - 24 hpf and photographed 96 h later, anterior to the left.

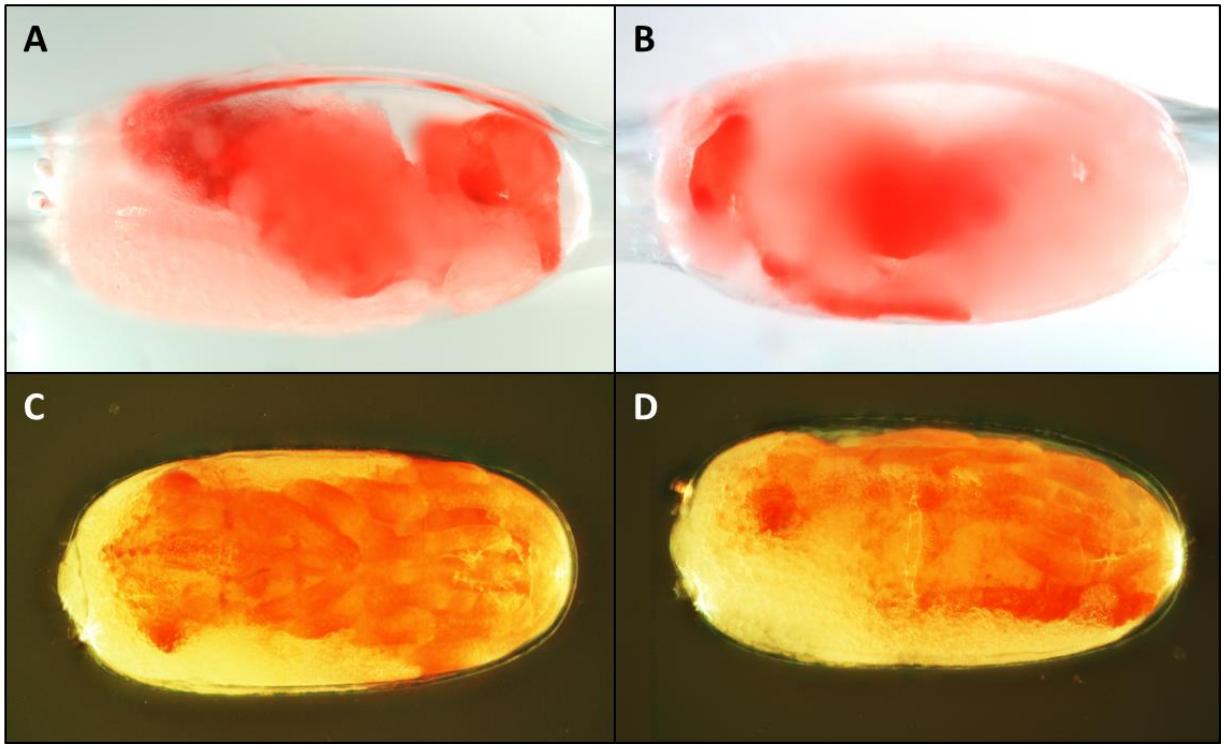

Figure 12: *Of* embryos after injection with moderate concentrations of human BMP4
(A - D) Embryos were injected with moderate concentrations of human BMP4 18 - 24 hpf and photographed 96 h later, anterior to the left.

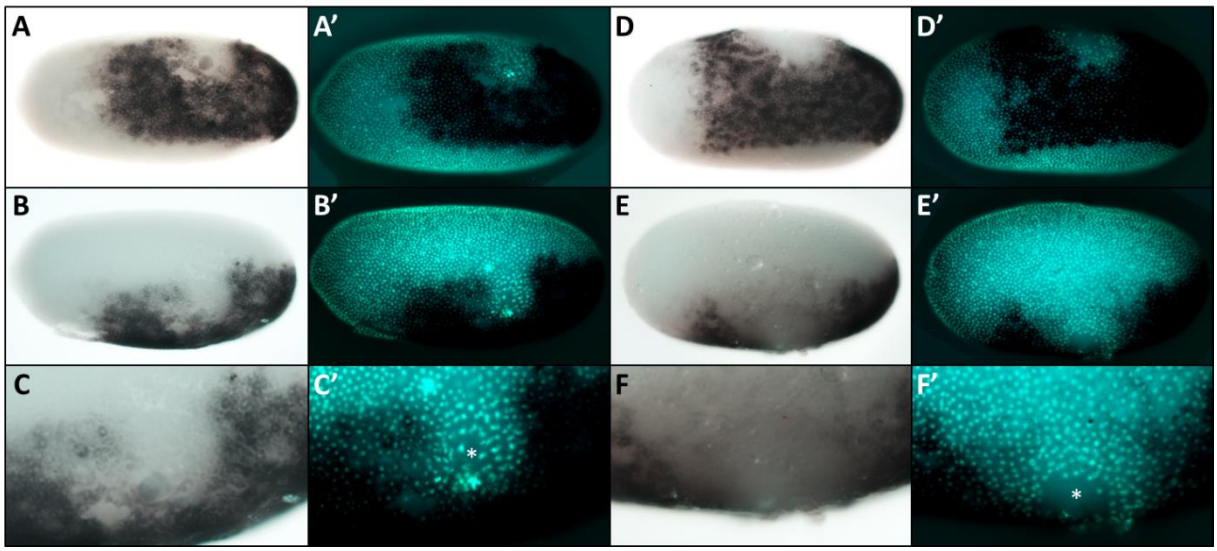

Figure 13: *sog* expression after injection of BMP4
(A - F) *sog* expression in late blastoderm stage embryos fixed 24 - 30 hpf after injection of human BMP4 at 18 – 24 hpf, anterior to the left; **(A' - F')** same embryo as depicted in pictures labeled with corresponding capital letters, nuclei stained with SYTOX Green; **(A - F')** A - C' and D - F' show the same embryo, respectively; **(A, A', D and D')** ventral view; **(B, B', E and E')** lateral view; **(C, C', F and F')** magnification of corresponding lateral views **(C' and F')** location of injection marked with white asterisk.

3.4 Microinjection of *eosFP-nls* mRNA into *Of* embryos

After successful embryonic microinjections of proteins, I tried mRNA injections. To test whether the injected mRNA remained rather local or tended to distribute throughout embryos I injected *eosFP-nls* mRNA into *Of* blastoderm embryos 18 - 24 hpf. *eosFP-nls* mRNA codes for a fluorescent marker protein and contains a nuclear localization sequence. 2 - 6 h after injection the *eosFP-nls* mRNA was translated into detectable protein (Fig. 14 B - D). The localization of EosFP-positiv nuclei depends on the depth of injection. Deep injections into the yolk generate EosFP-positiv yolk nuclei (Fig. 14 B), whereas injections close to the egg surface induce spatially restricted EosFP-positiv blastodermal nuclei (Fig. 14 C - D).

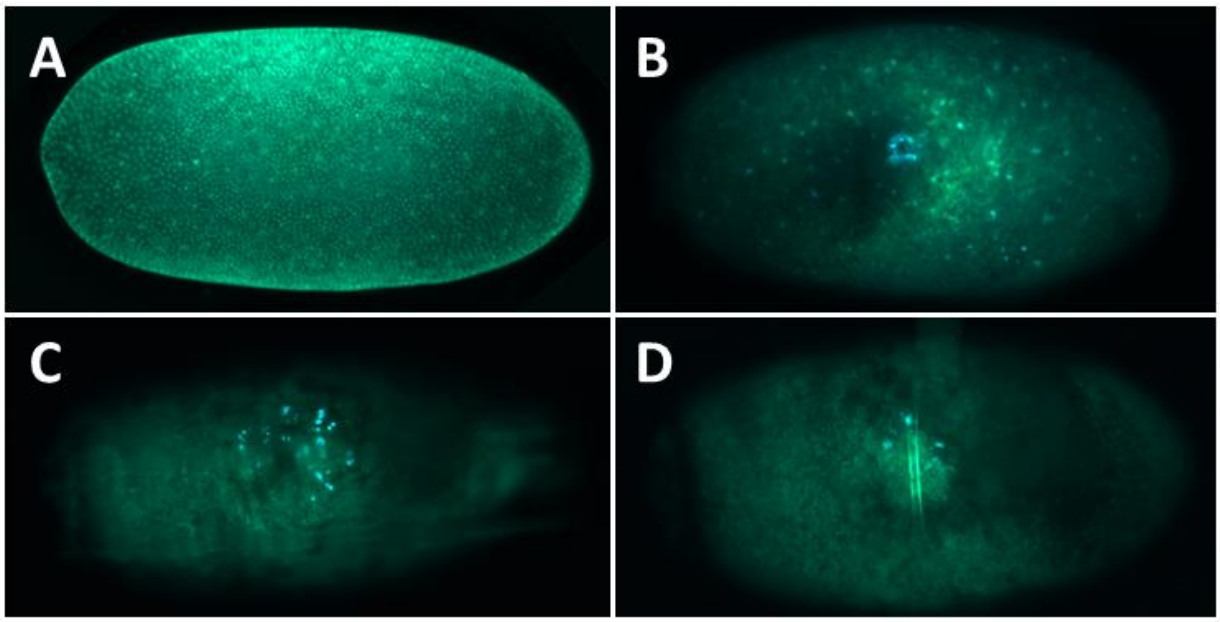

Figure 14: *Of* embryos injected with *eosFP-nls* mRNA
(A) Wild-type *Of blastoderm stage* embryo stained with SYTOX Green; **(B - D)** embryos injected with *eosFP-nls* mRNA 18 - 24 hpf and photographed while alive 2 - 6 h after injection; **(B)** localization of EosFP in yolk nuclei; (**C - D)** EosFP-positive blastodermic nuclei are spatially restricted around the injection site.

3.5 Microinjection of *Danio rerio chordin* mRNA into *Of* wild-type embryos and embryos lacking Toll

After successful manipulations of the DV network during *Of* embryogenesis via microinjections of BMP components which lead to disturbance of the mesoderm, I planned DV manipulations via injections of BMP antagonists. A previous published *eLife* article shows that in *Oncopeltus* the BMP antagonist Sog polarizes the BMP network and that mesodermal fates are not strictly reliant on Toll (Sachs et al., 2015). Following the logic of the article an injection of *sog* into the dorsal side of wild-type *Of* embryos should be sufficient to induce ventral fates. In addition an injection of *sog* into dorsalized *Of* embryos lacking Toll should also induce ventral fates. I show here that these inductions of ventral fates via ectopic polarization of the BMP gradient by microinjection of BMP antagonists are indeed possibly, both in wild-type and in a dorsalized embryonic phenotype (Fig. 15 - 22).

Since *sog* itself is expressed in the ventral ectoderm and presumptive mesoderm of Oncopeltus embryos it is often used in ISH experiments as ventral marker. mRNA microinjections of *Of-sog* would not allow to distinguish microinjected *sog* from endogenous *sog* produced by the embryo itself in ISH experiments. To overcome this problem I injected *Danio rerio chordin*, the vertebrate homolog of *sog* into *Of* embryos. Vertebrate BMP antagonists like Chordin and Noggin have been shown to repress BMP activity in insects and vice versa (Holley et al., 1996; Yu et al., 2000; Schmidt et al., 1995).

Dr-chordin was microinjected at concentrations between 1500 - 3000 ng/ml into early blastoderm stage embryos (18 - 24 hpf), which were either fixed at late blastoderm stage (24 - 30 hpf) for ISH experiments (Fig. 18 - 22) or photographed after 6 more days of development, when the negative controls were about to hatch (Fig. 15 -17).

Microinjections with *chordin* caused a range of different injection phenotypes. The strongest injection phenotypes were lethal and showed defective gross morphology (Fig. 15), sometimes including defective katatrepsis (Fig. 15 A - B). Moderate injection phenotypes were lethal as well and showed defective segmentation boundaries leading to fused tergites (Fig. 16 C, E and F) and fused legs (Fig. 16 B and D). The weakest injection phenotypes were viable and showed irregular shortened and thickened appendages (Fig. 17 A - C) or dented tergites (Fig. 17 D). This range of phenotypic effects and severity was most likely caused by the location of the injection site (dorsal, lateral or ventral) and the necessarily variable injection amount (see 2.2.17).

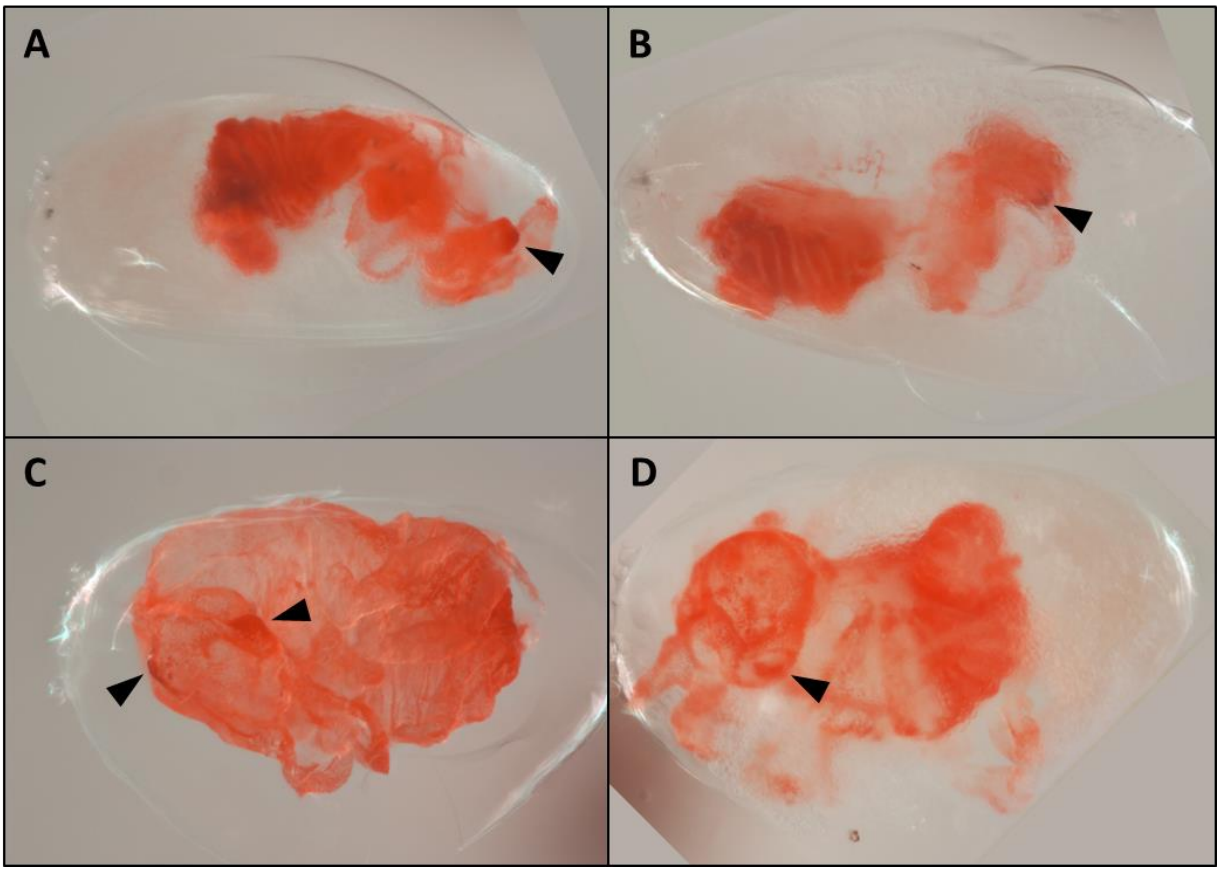

Figure 15: Cuticle preparations of strong *chordin* injection phenotypes

(A - D) Wild-type embryos were injected with *Dr chordin* 18 - 24 hpf and mounted in Hoyer's medium 96 h later, anterior to the left. Position of the eyes is marked with black arrowheads.

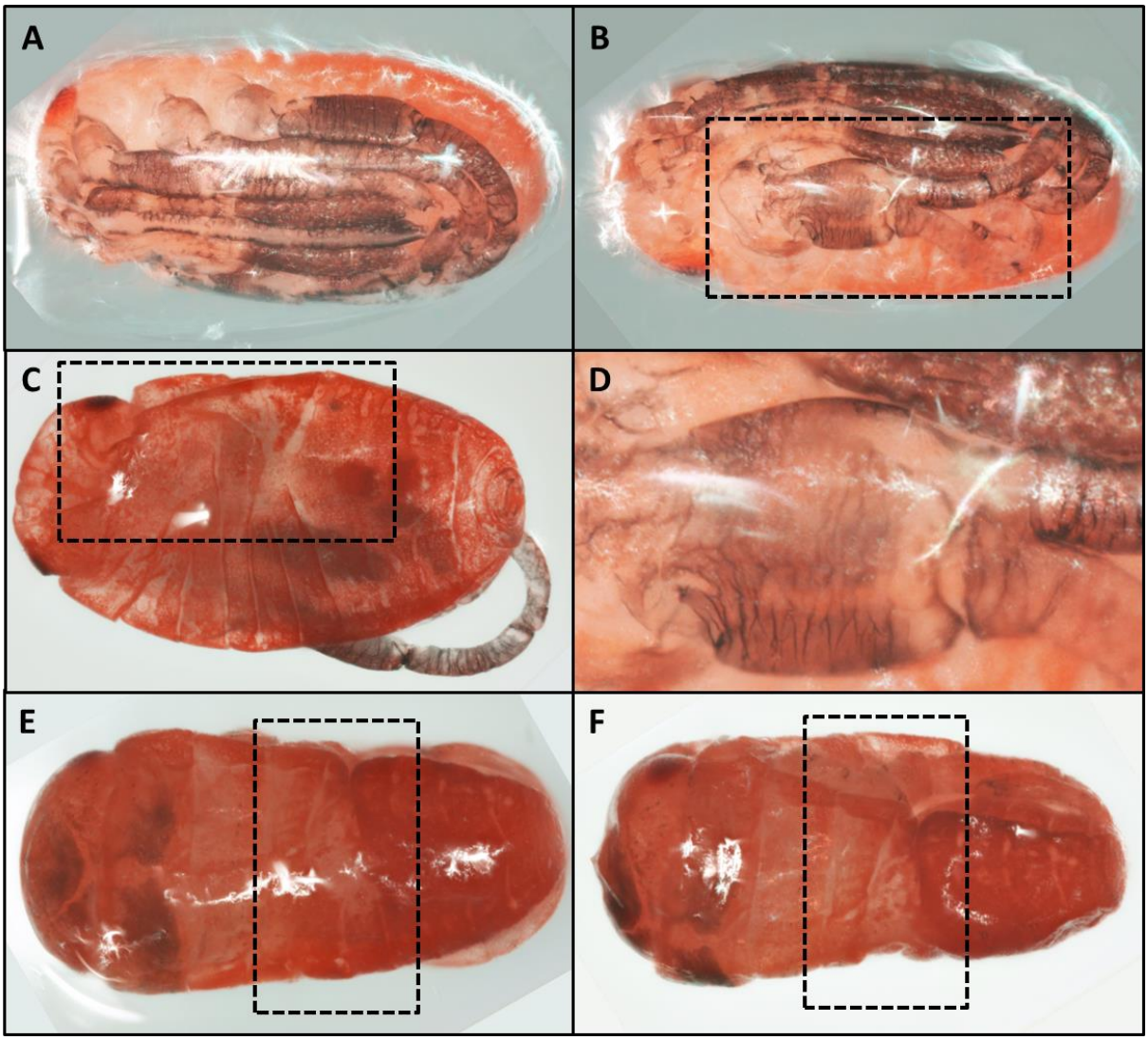

Figure 16: Moderate *chordin* injection phenotypes

(A - F) Wild-type embryos were injected with *Dr chordin* 18 - 24 hpf and photographed 96 h later, anterior to the left. Irregular formed structures are marked with black dotted boxes. A - D and E - F show the same embryo, respectively; **(D)** magnification of B.

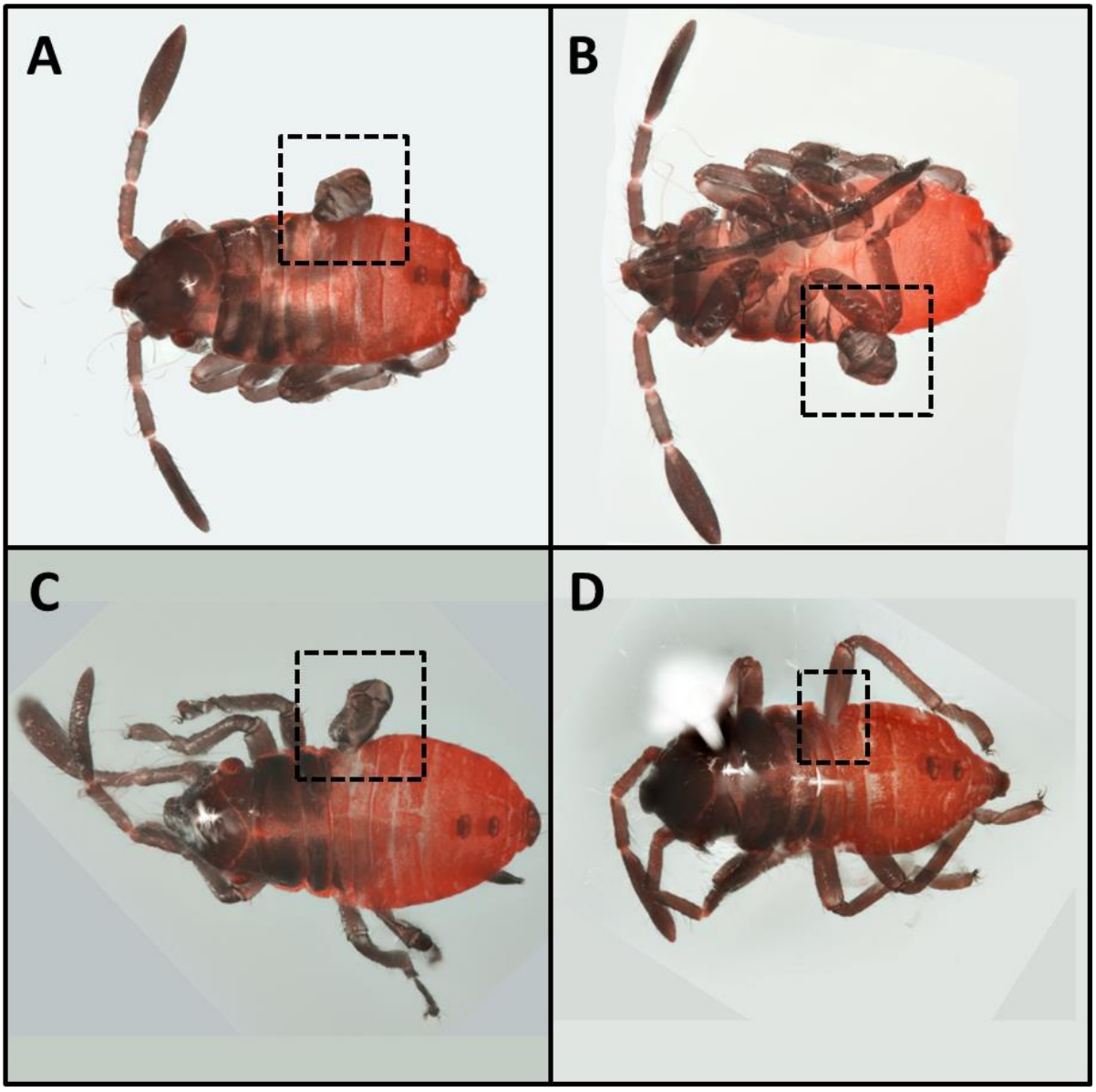

Figure 17: Weak *chordin* injection phenotypes
(A - D) Wild-type embryos were injected with *Dr chordin* 18 - 24 hpf and photographed 96 h later, anterior to the left. Irregular formed structures are marked with black dotted boxes.

ISH experiments on microinjected *Of* wild-type embryos revealed that the presence of ectopic *chordin* is sufficient to induced the expression of mesodermal marker genes *twist* (Fig. 18)and *sog* localized around the site of injection (Fig. 19 and 20). Lateral microinjections induced an expansion of the ventral expression domain of *sog* to the lateral side (Fig. 19 c and c'). Dorsal microinjections induced ectopic expression of *twi* (Fig. 18) and *sog* (Fig. 19 D - F' and 20) on the dorsal side.
The area of ectopic *twi*-positive and *sog*-positive cells on the dorsal side was frequently shaped either like a small solid patch (Fig. 19 D - F') or like a ring with *twi*-negative and *sog*-negative cells in its center (Fig. 18 and 20). Some embryos showed a fading weak sporadic expression of mesodermal markers within such rings (Fig. 20). It could be possible that these embryos were fixed during a transition process from a small solid spot to a wider ring of ectopic mesodermal marker gene expression.

Nuclear density within the region of ectopic *twi* (Fig. 18 C, C', F, F', I and I') and *sog* (Fig. 20 C, C', E, E', F and F') expression on the dorsal side was lower than in the surrounding *twi*-negative and *sog*-negative dorsal region, respectively. Nuclear density can be used to distinguish dorsal and ventral regions of *Oncopeltus* embryos. At the dorsal side nuclear density is higher than at the ventral side (Sachs et al., 2015). Thus the ectopic *twi*-positive and *sog*-positive regions on the dorsal side resembled a more ventral-like nuclear density.

Oncopeltus embryos lacking Toll are dorsalized and do not express *sog*, *twi* and *sim* along their DV axis (Sachs et al., 2015). However, after injection of *chordin* into *Of-Toll* pRNAi knockdown embryos ISH experiments revealed that around the site of injection expression of *sog* and *sim* is induced (Fig. 21 and 22). *sog* was expressed either in a large solid patch or a ring with a patch in its center (Fig. 21). *sim* was expressed in wide rings with single *sim*-positive cells within those rings (Fig. 22). The injection-induced expression patterns in embryos lacking Toll were similar to those of dorsally injected wild-type embryos. However, the observed patches and rings were wider in embryos lacking Toll than in wild-type embryos. Similar to observations made in dorsally injected wild-type embryos, nuclear density within the patches and rings of *sog* and *sim* expression is lower than in the unstained regions of *chordin*-injected dorsalized *Toll*-knockdown embryos (Fig. 21 and 22).

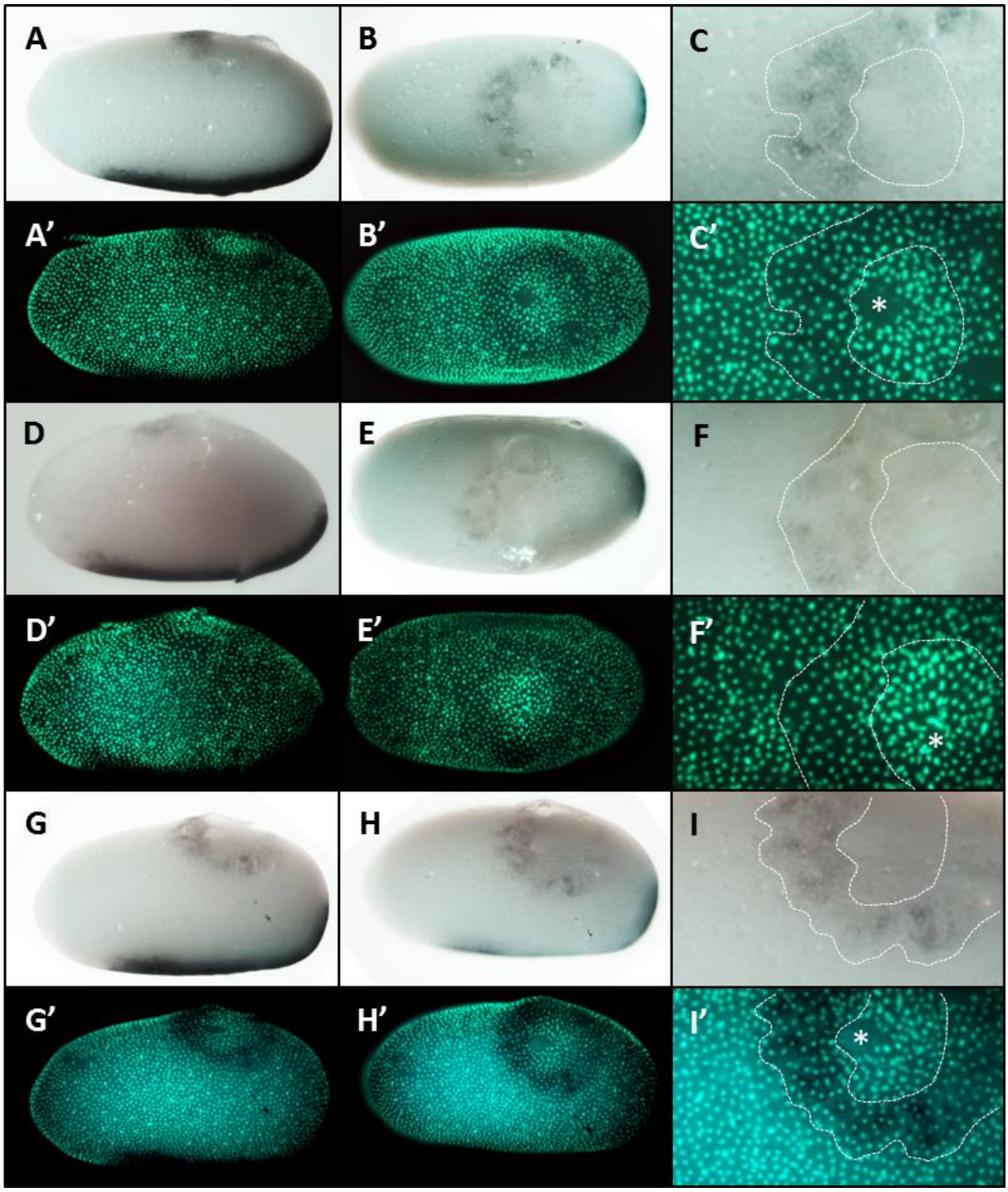

Figure 18: *twi* expression after injection of *Danio rerio chordin* mRNA into *Of* wild-type embryos
(A - I) *twi* expression in late blastoderm stage embryos fixed 24 - 30 hpf after injection of *Dr chordin* at 18 – 24 hpf, anterior to the left; **(A' - I')** same embryo as depicted in pictures labeled with corresponding capital letters, nuclei stained with SYTOX Green; **(A - I')** A - C', D - F' and G - I' show the same embryo, respectively; **(A, A', D, D', G and G')** lateral view; **(B, B', E, E', H and H')** dorsal view; **(C, C', F, F', I and I')** magnification of corresponding dorsal views, *twi* staining enframed by white dotted line; **(C' F' and I')** location of injection marked with white asterisk.

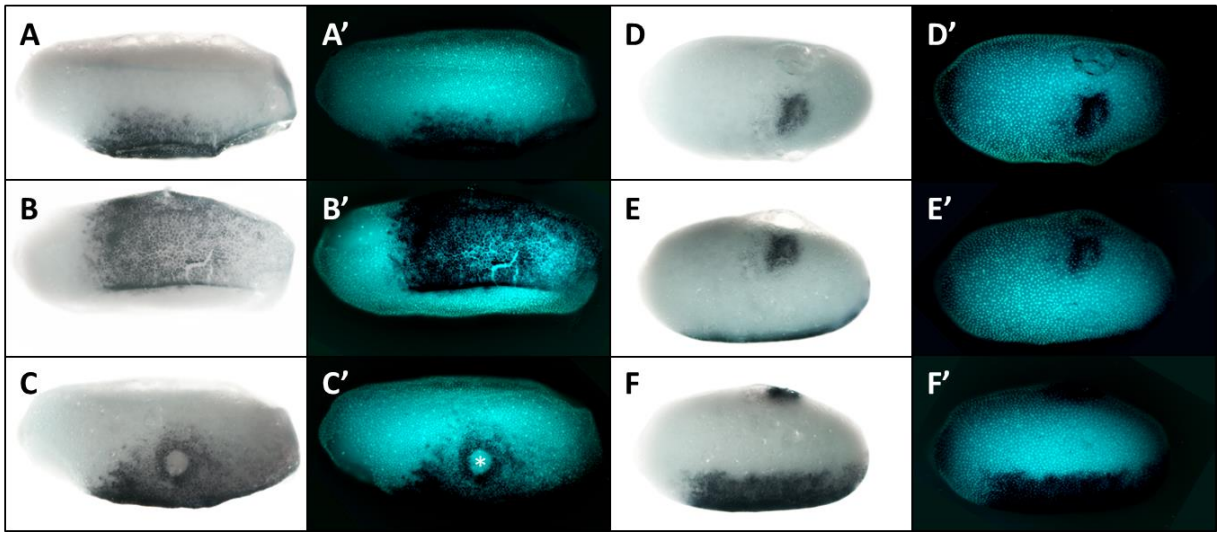

Figure 19: *sog* expression after injection of *Danio rerio chordin* mRNA into *Of* wild-type embryos
(A - F) *sog* expression in late blastoderm stage embryos fixed 24 - 30 hpf after injection of *Dr chordin* at 18 – 24 hpf, anterior to the left; **(A' - F')** same embryo as depicted in pictures labeled with corresponding capital letters, nuclei stained with SYTOX Green; **(A - F'**) A - C' and D - F' show the same embryo, respectively; **(A, A', C, C', F and F')** lateral view**; (B and B')** ventral view; **(D - E')** dorsal view; **(C')** location of injection marked with white asterisk.

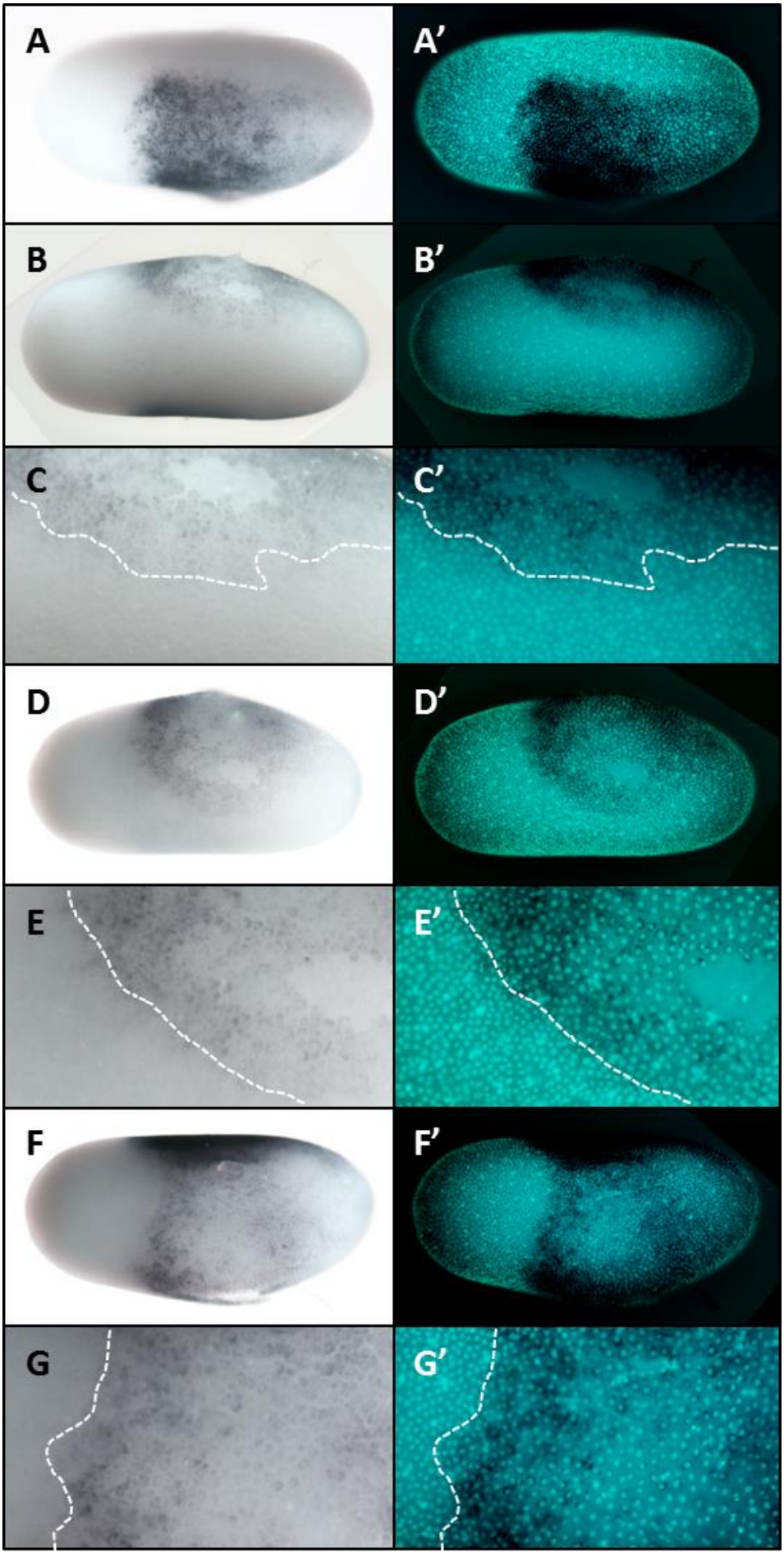

Figure 20: *sog* expression after injection of *Danio rerio chordin* mRNA into *Of* wild-type embryo (A - G) *sog* expression in late blastoderm stage embryo fixed 24 - 30 hpf after injection of *Dr chordin* at 18 – 24 hpf, anterior to the left; **(A' - G')** same embryo as depicted in pictures labeled with corresponding capital letters, nuclei stained with SYTOX Green; **(A and A')** dorsal view; **(B - E')** lateral view; **(F - G')** dorsal view; **(C, C', E, E', G and G')** magnification of corresponding views, *sog* staining enframed by white dotted line.

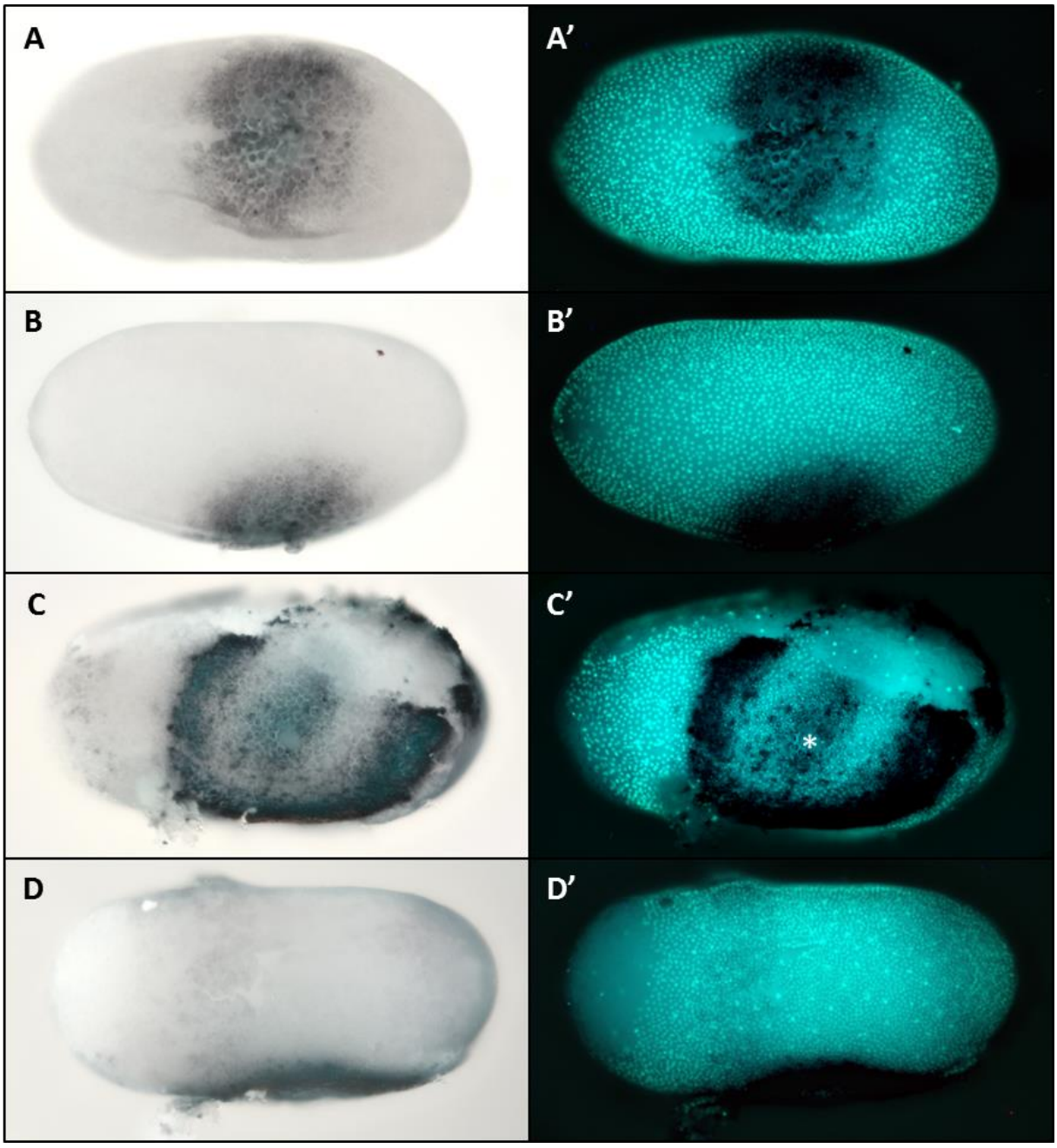

Figure 21: *sog* expression after injection of *Dr chordin* mRNA into *Toll* pRNAi embryos

(A - D) *sog* expression in late blastoderm stage embryos lacking Toll fixed 24 - 30 hpf after injection of *Dr chordin* at 18 – 24 hpf, anterior to the left; **(A' - D')** same embryo as depicted in pictures labeled with corresponding capital letters, nuclei stained with SYTOX Green; **(A - D')** A - B' and C - D' show the same embryo, respectively.

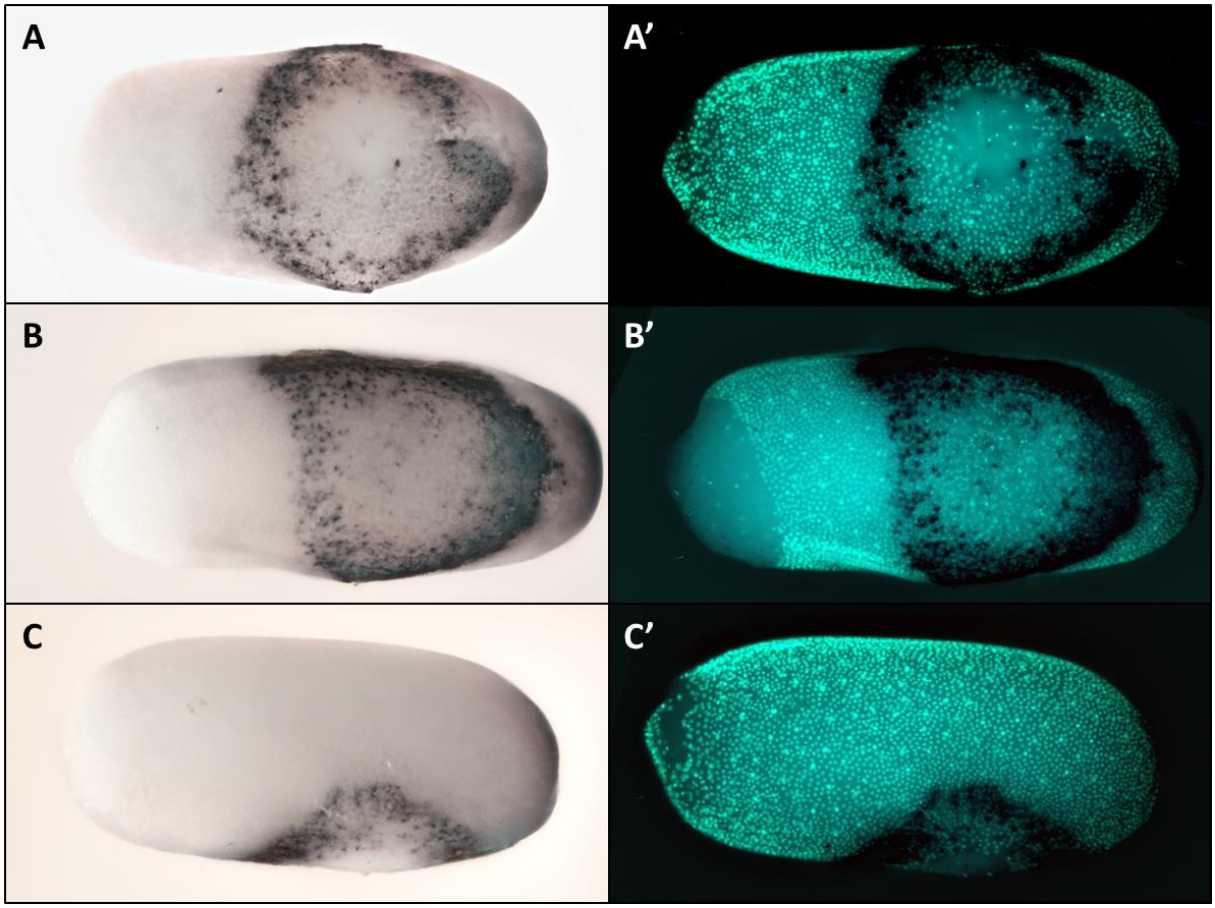

Figure 22: *sim* expression after injection of *Dr chordin* mRNA into *Toll* pRNAi embryos
(A - C) *sim* expression in late blastoderm stage embryos lacking Toll fixed 24 - 30 hpf after injection of *Dr chordin* at 18 – 24 hpf, anterior to the left; **(A' - C')** same embryo as depicted in pictures labeled with corresponding capital letters, nuclei stained with SYTOX Green.

3.6 Differential expression analysis (RNAseq) of dorsalized and ventralized *Oncopeltus* embryos

Changes in gene expression, induced via genetic manipulations, can be investigated by differential expression analysis (Wang et al., 2009; Stappert et al., 2016). To identify differentially expressed transcripts, the transcriptomes of manipulated specimens are compared to wild-type transcriptomes. I generated transcriptomes of ventralized and dorsalized phenotypes by knocking down crucial components of Toll and BMP signaling by parental RNA interference (pRNAi) in the large milkweed bug *Oncopeltus fasciatus* in order to find new marker genes of the embryonic fate map and potentially identify novel components of DV signaling that were not found before by using the candidate gene approach. For each knockdown condition I generated a triplicate of biological replicates to make the subsequent analysis more robust. The different knockdown conditions were: (1) a pRNAi *Toll* knockdown which led to a complete dorsalization and a loss of the most anterior fate of *Oncopeltus* embryos, (2) a pRNAi *sog* knockdown which also led to a complete dorsalization but without any anterior-posterior patterning effect, (3) a pRNAi *tld* knockdown which led to a complete ventralization similar to *dpp* knockdowns (*dpp* knockdown embryos were considered as an transciptome candidate but collection of embryos was discontinued because of a sterility effect in *dpp* pRNAi injected females), (4) a pRNAi *gbb* knockdown which lead to a weaker pronounced

dorsalization/lateralization, (5) a pRNAi *gfp* knockdown as negative control to account for unspecific pRNAi effects, (6)and a wild-type control from untreated mothers. All embryos were collected between 24 and 30 hpf at 25 °C which corresponded to a time frame from differentiated blastoderm stage, when important DV genes like *sog* were expressed robustly in the presumptive mesoderm, to late blastoderm stage, when the embryo started to condense and invaginate at the posterior. The embryo collection was tightly staged for each knockdown condition and the total RNA was isolated using standard TRIzol protocols. The isolated total RNA was brought to the Cologne Center for Genomics (CCG) which synthesized cDNA from the total RNA and sequenced it on a single lane on an Illumina HiSeq4000 sequencer. Paired-end sequencing technique was used with read lengths of 75 bp per end and a total insert size of 180 bp. Subsequent RNA-seq analysis was carried out in collaboration with Nathan J. Kenny (PostDoc at Oxford Brookes University). A subsequent in situ hybridization screen was carried out in order to identify genes with an asymmetric localization along the DV axis among the candidates gained by differentially expression analysis. Differentially expressed genes for the ISH screen were chosen by several criteria; genes with potentially interesting gene products (i.e. transcription factors or components of signaling pathways); strongly differential expressed genes based on different thresholds of fold changes (FC); genes that overlapped in several knockdown conditions in Venn diagrams (i.e. down-regulated in dorsalized but up-regulated in ventralized embryos) (Fig. 23). False discovery rate (FDR) cut-off was at least ≤0.05 for each criteria. Genes achieved from ISH screening with spatial restricted expression along the dorsoventral axis (Fig. 24 – 26 and 28) were additionally tested for a knockdown phenotype via pRNAi (Fig. 27).

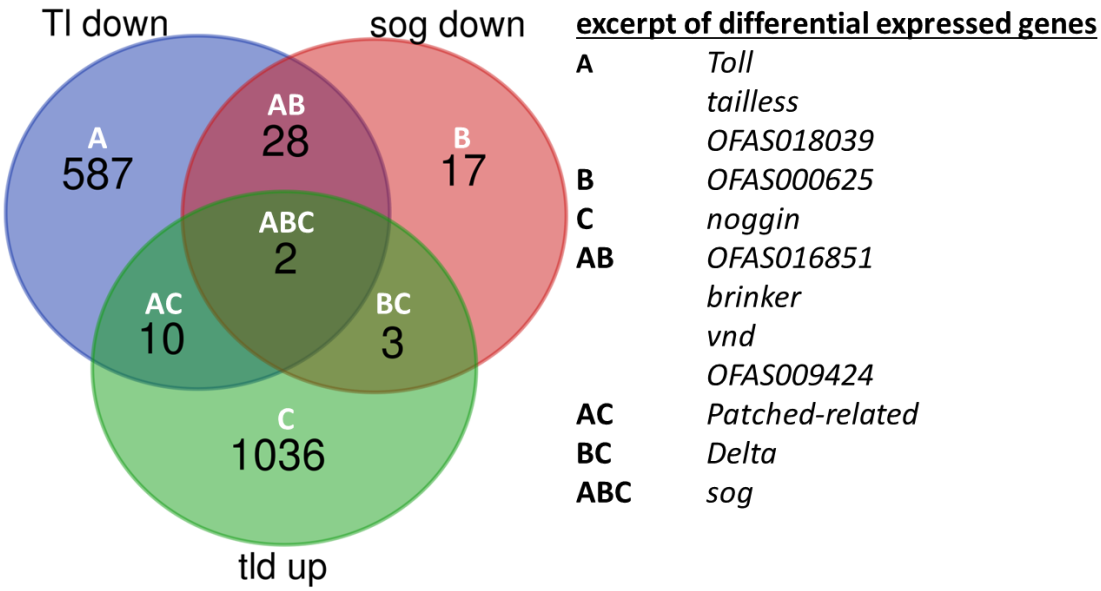

Figure 23: Venn diagram for mesodermal candidate genes

Venn diagram of differential expressed genes from various pRNAi knockdown embryos compared to wild-type embryos; knockdown conditions were: *Tl* knockdown (dorsalized), *sog* knockdown (dorsalized) and *tld* knockdown (ventralized); blue circle displays genes that are upregulated upon Tl knockdown compared to wild-type blastoderm stage embryos; red circle displays genes that are upregulated upon sog knockdown compared to wild-type blastoderm stage embryos; green circle displays genes that are upregulated upon sog knockdown compared to wild-type blastoderm stage embryos; fold change cut-off was ≥2; false discovery rate cut-off was ≤0.05.

Knockdown embryos that lack *Tl* or *sog* underexpress genes that are normally expressed within the mesoderm, while embryos that lack *tld* overexpress mesodermal localized gene transcripts. Vice versa ectodermal localized gene transcripts should be upregulated in dorsalized and downregulated in ventralized embryos. A useful strategy to narrow down potential candidate genes, besides increasing the FC and decreasing the FDR, is to create Venn diagrams and focus on genes that overlap in more than one knockdown condition. A similar approach using microarray assays was successfully used in *Drosophila* to identify new Dorsal target genes (Stathopoulos et al., 2002). By generating Venn diagrams with this approach and subsequent ISH screening I identified four novel genes, *OFAS000625*, OFAS009424, *OFAS016851* and *OFAS018039,* which exhibit localized expression patterns in *Oncopeltus* blastoderm stage embryos (Fig. 24 – 26 and 28).

Figure 23 shows a Venn diagram that was used to identify mesodermal candidate genes in which genes that were downregulated in *Toll* and *sog*, but upregulated in *tld* knockdowns compared to wild-type embryos were overlapped against each other. Among the differential expressed genes was the known DV patterning key component *sog*, which was downregulated in *Toll* and *sog* knockdown, but upregulated in *tld* knockdown, which is consistent with in situ hybridization experiments in these knockdown conditions and wild-type embryos (Sachs et al., 2015). However, *Toll* was not downregulated in *sog*, but only in *Toll* knockdown which was expected for the ubiquitous expressed receptor. The anteriorly expressed gene *tailless* was downregulated in *Toll*, but not in *sog* knockdown embryos. This is consistent with the observation that in *Toll* knockdown embryos, besides dorsalization, the most anterior fates are lost, a region of the embryo which is thought to give rise for the serosa and parts of the head fate map (Sachs et al., 2015). Also downregulated in *Toll* knockdown were *OFAS018039* and *OFAS016851,* and subsequent in situ screening identified both as anterior expressed genes, and their expression profiles, gene products and phenotypes are described later in section 3.8 and 3.9 (Fig. 26 - 28). Like *tailless, OFAS018039* was only downregulated in *Toll*, but not downregulated in *sog* knockdown, which is consistent with the observed loss of the most anterior fates in *Toll* knockdown embryos. However, *OFAS016851* was downregulated in both *Toll* and *sog* knockdown embryos, which was unexpected since the anterior fates are usually not affect by a lack of Sog. Downregulated in both *Toll* and *sog* knockdown were *vnd* and *brk* which are known Type 2 Dorsal target genes in *Drosophila*. However, in *Oncopeltus vnd* is expressed in an anteroventral domain (Chen, PhD Thesis, 2015) and a localized expression of *brk* was not detectable via ISH (data not shown). However, a downregulation of both *vnd* and *brk* in dorsalized *Toll* and *sog* knockdown embryos would be consistent with the current understanding of *Oncopeltus* DV axis patterning. *noggin*, a BMP signaling antagonist which is not present in *Drosophila*, but in vertebrates was upregulated in *tld* knockdown embryos. In *Xenopus noggin* is expressed in the Spemann organizer region, promotes mesodermal cell fates and induces neural formation in the overlying ectoderm (Holley et al., 1996). A localized expression pattern of *noggin* was not detectable via ISH (data not shown), however an upregulation of *noggin* in mesodermalized *Oncopeltus* embryos would be consistent with the expression patterns of *noggin* in vertebrates. pRNAi knockdowns of *noggin* and *brinker* were performed, but did not led to a notable phenotype (data not shown). Downregulated in *sog* knockdown was *OFAS000625*, a gene which has an expression pattern similar to *sog* in *Oncopeltus* blastoderm stage embryos. *OFAS000625* gene product and expression pattern profile is described in more detail later in section 3.7 (Fig. 24).

Another gene whose transcripts turned out to be localized in blastoderm stage embryos was *OFAS009424*. *OFAS009424* expression seems to be associated with nuclear density and was strongly localized on the lateral sides, but expression on the dorsal and ventral side, where the nuclear density is lower, was weaker (Fig. 25). The condensation of the lateral sides of blastoderm stage

embryos which forms a region of high nuclear density was disturbed in dorsalized embryos and therefore a downregulation of *OFAS009424* in *Toll* and *sog* knockdown embryos is consistent with the observed interrelation of transcript expression and nuclear density.
Delta (*Dl*) was downregulated in *sog* but upregulated in *tld* knockdown, which is comparable to RNAseq and ISH data from *Tribolium*, where *Delta* is expressed in the presumptive mesoderm and repressed in the ectoderm (Stappert et al., 2016). However, in *Drosophila Delta* is repressed in the presumptive mesoderm and shows graded expression in the neurogenic ectoderm (Vassin et al., 1987). A localized expression of *Delta* was not detectable via ISH in *Oncopeltus* blastoderm stage embryos (data not shown). *Patched-related* (*Ptr*) was downregulated in *Toll* but upregulated in *tld* knockdown embryos, which seems to be strikingly different from Drosophila, where *Ptr* is expressed in the ventral and dorsal ectoderm (Fisher et al., 2012). A localized expression of *Ptr* was not detectable via ISH in *Oncopeltus* blastoderm stage embryos (data not shown).
A complete list of all differential expressed genes within this Venn diagram is enclosed in the appendix.

3.7 Analysis of *OFAS000625*

OFAS000625 was downregulated in *sog* knockdown embryos compared to wild-type control embryos of *Oncopeltus*. Therefore it was selected as an ISH screen candidate. The spatial and temporal expression patterns of *OFAS000625* in *Oncopeltus* late blastoderm stage wild-type embryos are shown in Figure 24.
At 24 hpf *OFAS000625* was expressed similar to transcripts of *sog* in a broad ventral stripe encompassing approximately 60 % of the embryo from posterior while omitting the anterior 40 % of the embryo. In between 24 to 30 hpf a ring-like second domain of transcript expression emerged which encompassed 70 to 80 % of egg length from anterior and spanned around the whole DV axis of the embryo. Expression patterns similar to *OFAS000625* late blastodermic expression have never been reported for *Oncopeltus* embryos in the literature before.
Because of *OFAS000625* asymmetric expression pattern along the DV axis it was further analyzed via pRNAi-mediated knockdown. However, the knockdown did not result in a developmental or otherwise notable phenotype.
Bioinformatic analysis with various tools like BLAST and Conserved Domain Search showed that *OFAS000625* exhibits homologies to genes of several insect orders (Lepidoptera, Coleoptera and Hymenoptera, Hemiptera, and Blattodea). However, bidirectional BLAST could not find a clear ortholog for *OFAS000625*. The only conserved domain that was detected in *OFAS000625* is the Baculo_F super family domain which is found in a variety of baculoviruses and some presumed transposons (Pearson et al., 2000).

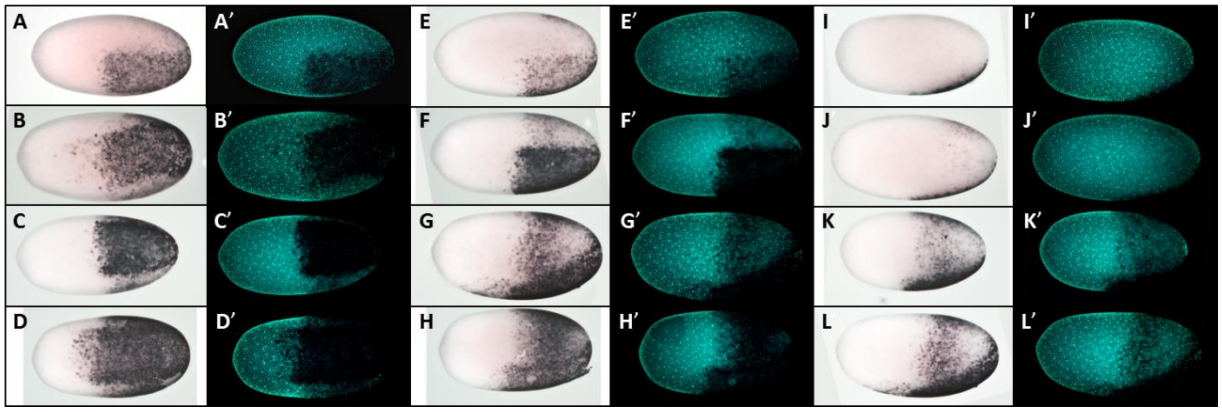

Figure 24: Spatial and temporal expression patterns of *OFAS000625*

(A - L) Expression patterns of *OFAS000625* revealed by ISH in *Of* late blastoderm stage wild type embryos, 24-30 hpf, anterior to the left; **(A' - L')** same embryo as depicted in pictures labeled with corresponding capital letters, nuclei stained with SYTOX Green; **(A - D')** ventral view, age is increasing; **(E - H')** lateral view, age is increasing; **(I - L')** dorsal view, age is increasing.

3.8 Analysis of *OFAS009424*

Compared to wild-type control embryos *OFAS009424* transcript expression was downregulated in *sog* and *Toll* knockdown embryos. Therefore *OFAS009424* was selected for ISH screening. The spatial expression patterns of *OFAS009424* in late blastoderm stage embryos are shown in Figure 25.

In late blastoderm stage embryos *OFAS009424* was expressed strongly on the lateral sides, moderately on the dorsal side and only weakly on the ventral side in a "salt and pepper"-like expression pattern (Fig. 25). This expression pattern seemed to be correlated with nuclear density which is highest on the lateral sides and lowest on the ventral side of *Oncopeltus* embryos. *OFAS009424* was not expressed in the anterior region of blastoderm embryos, omitting about 40 % of the anterior pole. Expression patterns similar to *OFAS009424* late blastodermic expression have never been reported for *OF* embryos in the literature before.

Because of its asymmetric expression pattern along the DV axis *OFAS009424* was further analysed via pRNAi-mediated knockdown, but the knockdown did not result in a developmental or otherwise notable phenotype.

Bioinformatic analysis of *OFAS009424* with various tools like BLAST and Conserved Domain Search showed that the gene is highly conserved in several insect orders (Diptera, Siphonaptera, Lepidoptera, Trichoptera, Coleoptera, Hymenoptera, Phthiraptera, Hemiptera, Thysanoptera and Blattodea). *OFAS009424* putative *Drosophila* homolog *CG8646* is expressed in various tissues during embryonic development (ectoderm, posterior endoderm, Malpighian tubule, ring gland, midgut and hindgut primordia) according to various ISH screens (Tomancak et al., 2002; Tomancak et al., 2007; Lecuyer et al., 2007; Hammonds et al., 2013; Wilk et al., 2016), but has not been object of any detailed characterization or phenotypic analysis. *OFAS009424* contains the conserved domain of the ALP_like super family. This family includes alkaline phosphatases and sulfatases. Alkaline phosphatases are non-specific phosphomonoesterases that catalyze the hydrolysis reaction via a phosphoseryl intermediate to produce inorganic phosphate and the corresponding alcohol, optimally at high pH. Sulfatases catalyze the hydrolysis of sulfate esters from wide range of substrates, including steroids, carbohydrates and proteins. The biological roles of sulfatases include the degradation of sulfated glycosaminoglycans and glycolipids in the lysosome and the remodeling of

sulfated glycosaminoglycans in the extracellular space. Both alkaline phosphatases and sulfatases are essential for metabolism (Peter et al., 1990; Coleman, 1992).

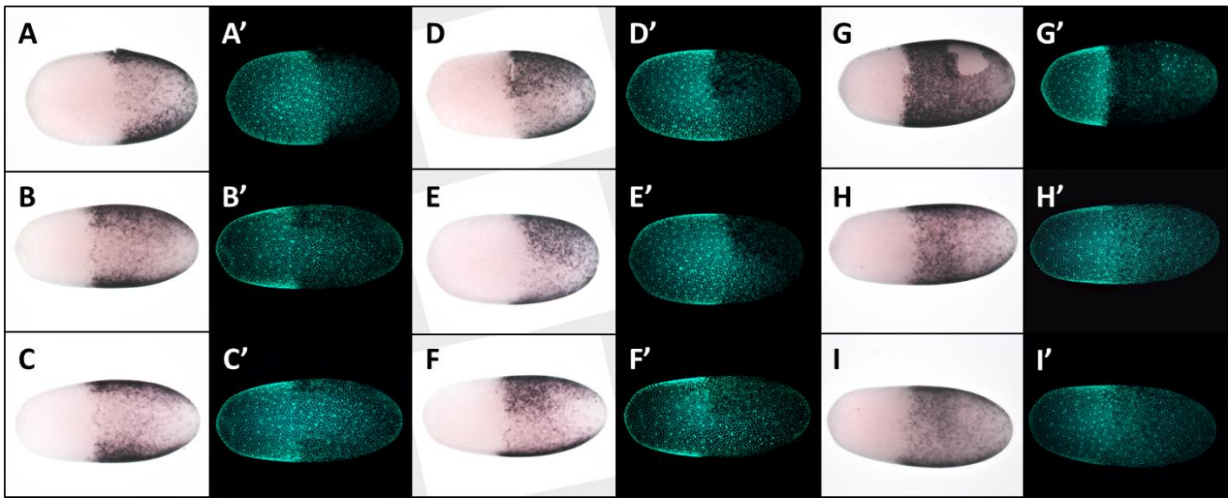

Figure 25: Spatial expression pattern of *OFAS009424*
(A - I) Expression pattern of *OFAS009424* revealed by ISH in *Of* late blastoderm stage wild type embryos, 24-30 hpf, anterior to the left; **(A' - I')** same embryo as depicted in pictures labeled with corresponding capital letters, nuclei stained with SYTOX Green; **(A - C')** ventral view; **(D - F')** ventrolateral view; **(G - I')** dorsal view.

3.9 Analysis of *OFAS016851*

OFAS016851 was downregulated in *Toll* and *sog* knockdown embryos compared to wild-type control embryos of *Of*. *OFAS016851* putative *Drosophila* ortholog, identified by reciprocal BLAST, is *Serpin 88Ea*, a negative regulator of Toll immune signaling in the fly (Ahmad et al., 2009).
Therefore it was selected as an ISH screen candidate. The spatial expression pattern of *OFAS016851* in late blastoderm stage and early germ band stage embryos is shown in figure 26.
In late blastoderm stage embryos *OFAS016851* was expressed in an anterior cap region, encompassing about 10 to 20 % of the embryo from anterior (Fig. 26 A-A'). In invaginating germ band stage embryos *OFAS016851* was expressed in extraembryonic serosa cells (Fig. 26 B-B'). Transcript expression in the anterior cap region of blastoderm stage embryos has been reported for *tailless*, *Toll8* and *Toll10* (Weisbrod et al., 2013; Benton et al., 2016). Transcript expression in spread serosa cells has been reported for *hb*, *zen*, *Toll8* and *Toll10* (Liu and Kaufmann, 2004; Panfilio et al., 2006; Benton et al., 2016; unpublished data of M.A. Benton, Y.-T. Chen and K. H. Conrads).
Knockdown of *OFAS016851* resulted in a lethal phenotype in all observed embryos (n=183, 3 independent experiments). The phenotypic embryos did not show obvious developmental defects until enclosure. After enclosure phenotypic first instar nymphs had their mandibles and maxillae not detached from a cuticle (Fig. 27 A - B'). In contrast; antennas, labium and labrum were detached from this cuticle.
The nature of this cuticle is difficult to determine since many insect embryos including *Oncopeltus* secrete three embryonic cuticles after the serosal cuticle is secreted by the extraembryonic serosa during embryogenesis (Konopová and Zrzavý, 2005). It is not clear if the first embryonic cuticle is digested before enclosure or shed at enclosure but at least the second cuticle is shed during enclosure in many insects. The third cuticle constitutes the first instar cuticle. It is thought that those

first and second embryonic cuticles are secreted before the appendages including the mouthparts are fully elongated. Thus, the observed cuticle could be of embryonic but also serosal origin. The nature of the irregular attachment is unclear as well. It could be a pure mechanical attachment in which the mouthparts become entangled with the cuticle, possibly because the cuticle, the mouthparts or both are misshaped at their surface. Another possibility could be a chemical bounding in which the mouthparts are fused to the cuticle, possibly because of irregular overactive sclerotization. The phenotypic embryos were alive after enclosure but died within 48 h, presumably because they were disabled in their feeding abilities.

Since serosally expressed serpins are known from other insects to be involved in negatively regulating the melanization cascade (Jacobs et al., 2014), I tested if the melanization cascade in embryos in which *OFAS016851* was knocked down was overactive. I pricked both wild-type embryos and embryos lacking *OFAS016851* but I did not observe any increased melanization around the injection wound in *OFAS016851* knockdown embryos (data not shown).

Bioinformatic analysis via BLAST showed that *OFAS016851* is highly conserved in several insect orders (Diptera, Siphonaptera, Lepidoptera, Trichoptera, Coleoptera, Hymenoptera, Phthiraptera, Hemiptera, Thysanoptera and Blattodea).

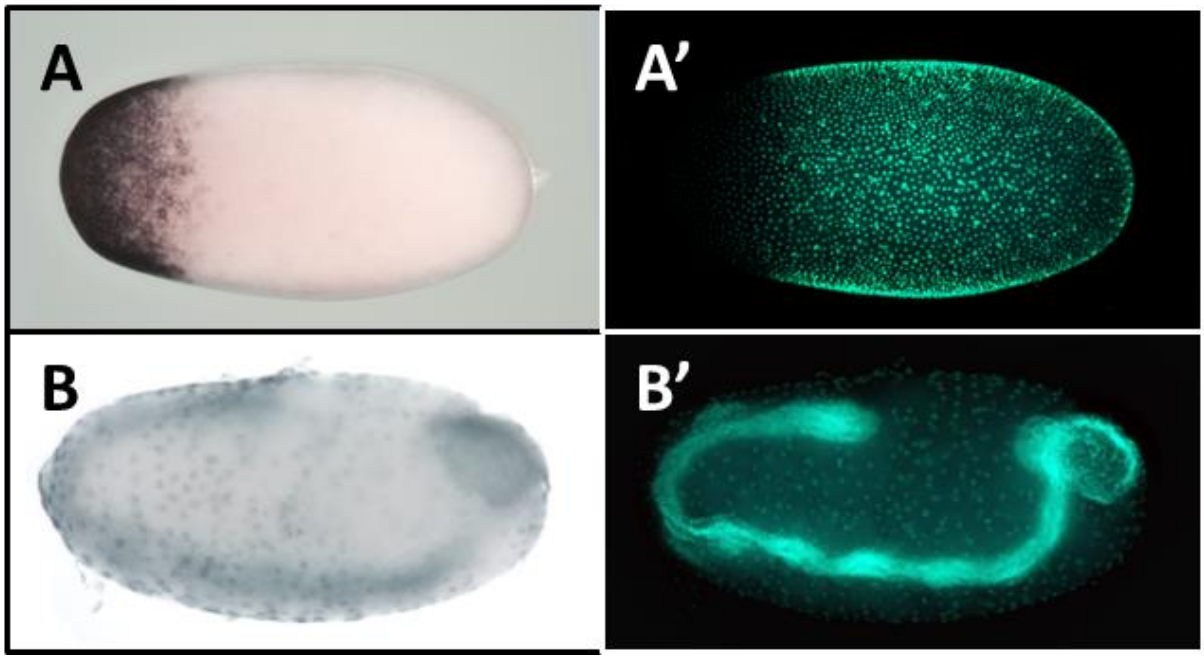

Figure 26: Expression patterns of *OFAS016851*

(A - B) Expression pattern of *OFAS016851* revealed by ISH in *Of* wild type embryos, anterior to the left; **(A' - B')** same embryo as depicted in pictures labeled with corresponding capital letters, nuclei stained with SYTOX Green; **(A - A')** In blastoderm stage embryos *OFAS016851* is expressed in an anterior cap region; **(B - B')** In early germband stage embryos *OFAS016851* is expressed in the serosa.

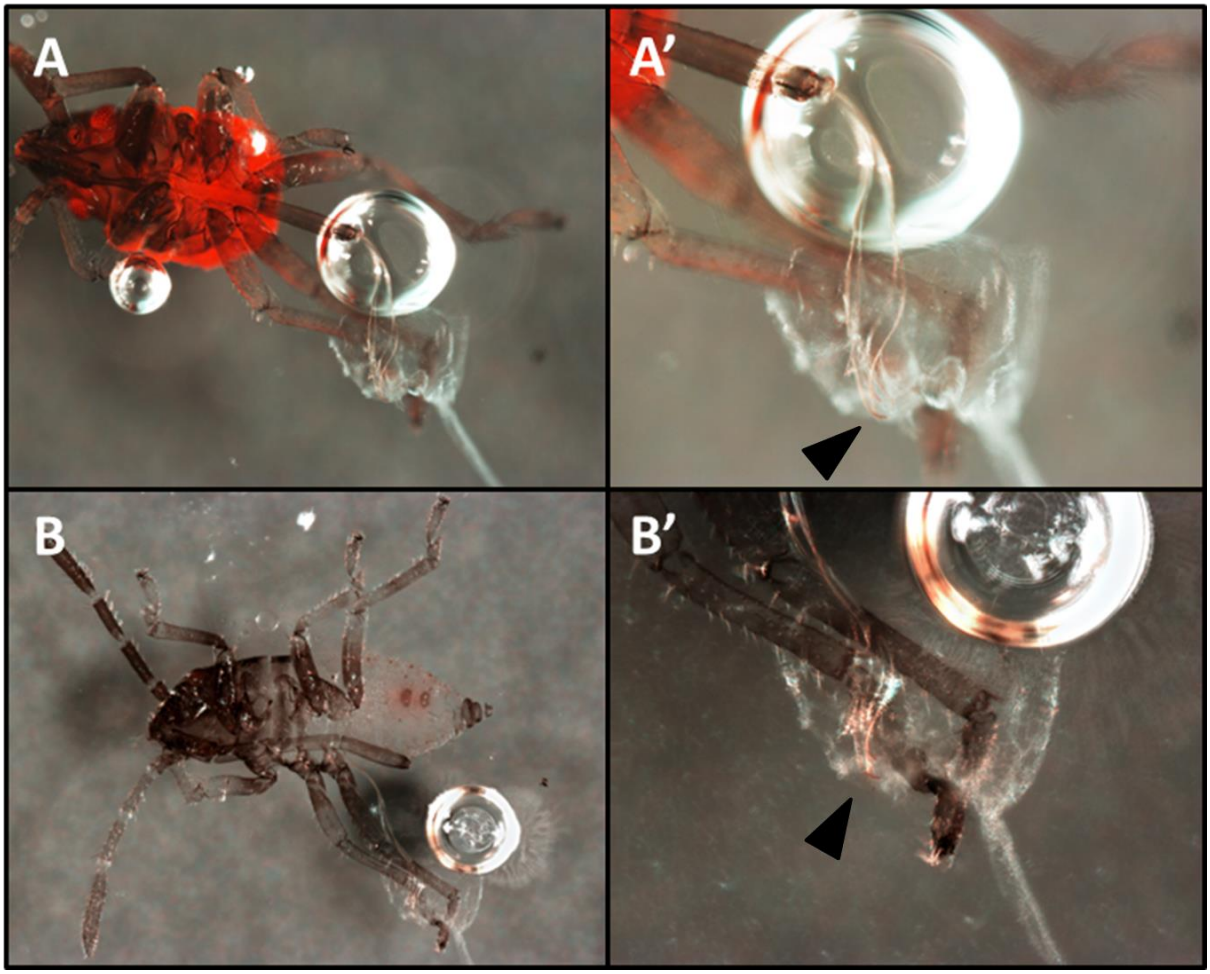

Figure 27: *OFAS016851* RNAi defects

(A) *Of'OFAS016851* RNAi hatchling in which the mandibles and maxillae are not detached from a cuticle in an irregular fashion; **(B)** *Of'OFAS016851* RNAi hatchling mounted in Hoyers's medium; **(A' and B')** same hatchling as in corresponding picture, close up on the cuticle, black arrowhead points towards the irregular connection of mouthparts and cuticle.

3.10 Analysis of *OFAS018039*

OFAS018039 was downregulated in *Toll* knockdown embryos compared to wild-type control embryos. Therefore it was selected as an ISH screen candidate. The spatial expression pattern of *OFAS018039* in late blastoderm stage embryos is shown in figure 28.

Similar to *OFAS016851 OFAS018039* was expressed in the most anterior part of late blastoderm stage embryos. In contrast to *OFAS016851* transcript expression of *OFAS018039* was not detectable via ISH in germ band stage embryos.

Because of its asymmetric expression pattern along the DV axis *OFAS018039* was further analyzed via pRNAi-mediated knockdown, but the knockdown did not result in a developmental or otherwise notable phenotype.

Bioinformatic analysis of *OFAS018039* with various tools like BLAST, Conserved Domain Search and OrthoDB shows that the gene is conserved in several insect orders (Diptera, Siphonaptera, Lepidoptera, Coleoptera, Hymenoptera, Hemiptera, Isoptera and Blattodea). *OFAS018039* reciprocal/bidirectional best BLAST hit in *Dm* is *CG33290*, an understudied gene for which no

expression or phenotypic data is available in the literature. Conserved domains or motifs have not been identified neither for *OFAS018039* nor for *CG33290* using various bioinformatics tools.

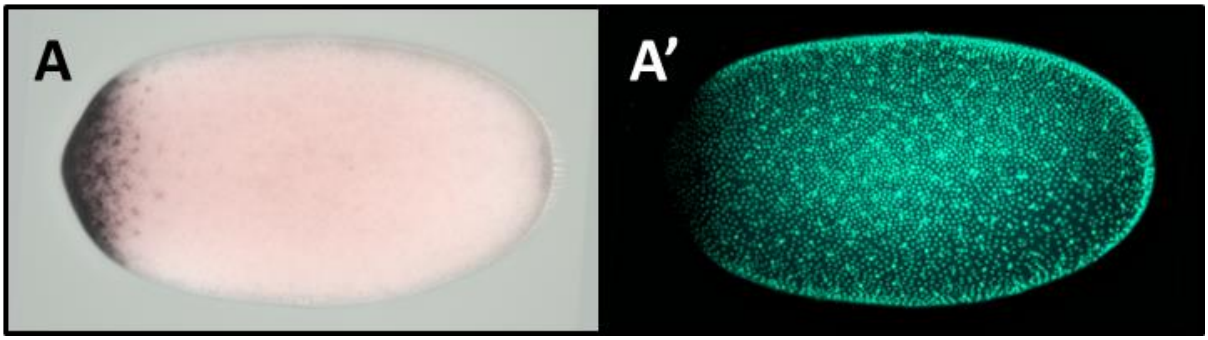

Figure 28: Expression pattern of *OFAS018039*

(A) Expression pattern of *OFAS018039* revealed by ISH in *Of* late blastoderm stage wild type embryo, 24-30 hpf, anterior to the left; **(A’)** same embryo as in A, nuclei stained with SYTOX Green; **(A - A’)** in blastoderm stage *OFAS018039* is expressed in the most anterior part of the embryo.

4. Discussion

4.1 Snail is necessary for a correct formation of the opposing Sog and BMP gradients

Snail is a transcription factor and part of a conserved family of C2H2 zinc finger proteins that have been extensively studied for their role in development, cell morphogenesis, and tumor metastasis (Barrallo-Gimeno and Nieto, 2005). During early embryogenesis of *Drosophila* and *Tribolium*, the described functions of Snail are specification and internalization of the mesoderm (Simpson, 1983; Leptin and Grunewald 1990; Rao et al., 1991; Ip et al. 1994; Seher et al. 2007; von Levetzow, PhD thesis, 2008).

In *Drosophila, Anopheles*, *Tribolium*, *Nasonia*, *Apis* and *Oncopeltus snail* is expressed in a broad ventral domain within the presumptive mesoderm of blastoderm stage embryos (Leptin and Grunewald 1990; Buchta et al., 2013; Goltsev et al., 2007; Wilson et al., 2014; Chen, PhD thesis, 2015).

In both *Drosophila* and *Tribolium* a lack of Snail does not affect ectodermal fates but rather leads to an expansion of the mesectoderm into mesodermal territory (Leptin, 1991; Rao et al., 1991; von Levetzow, PhD thesis, 2008), consistent with Snail's function as repressor of non-mesodermal genes like *sim* (Leptin, 1991; Rao et al., 1991; Reeves and Stathopoulos, 2009).

However, the knockdown of *Oncopeltus snail* led to a derepression of the presumptive mesoderm markers *twist* and *sog,* and of the mesectodermal marker *sim* along the entire DV axis (Fig. 9), indicating a crucial difference in the mechanisms of DV axis patterning between *Oncopeltus* and other insects. A known distinctive particularity of DV axis patterning in *Oncopeltus* is that mesodermal and mesoectodermal gene expression is not strictly reliant on Toll/Dorsal signaling, as it is in other insects, but rather on the absence of BMP signaling (Sachs et al., 2015).

The temporal expression profile of *sog* during *Oncopeltus* wild-type development seems to indicated the presence of a moderate repression of *sog* within the mesoderm; in mid blastoderm stage embryos *sog* is expressed in a broad ventral stripe, but in late blastoderm stage embryos *sog* expression is moderately weakened within the presumptive mesoderm and enhanced within the mesectoderm (Sachs, PhD thesis, 2014; Chen, PhD thesis, 2015; Sachs et al., 2015). While Toll/Dorsal signaling activates *sog* expression within the mesoderm and mesectoderm (Sachs et al., 2015), Snail could moderately repress *sog* expression in the mesoderm as Snail also represses *sog* during *Drosophila* development (Reeves and Stathopoulos, 2009).

A lack of *Oncopeltus* Snail could lead to increased Sog production within the mesoderm that in turn could extend the Sog gradient to the dorsal side at the expense of the BMP gradient. A subsequent collapse of the BMP gradient and thus absence of BMP signaling along the entire DV axis would lead to a derepression of mesodermal marker genes as exposed by the *Oncopeltus dpp* knockdown (Sachs et al., 2015).

In wild-type *Oncopeltus* embryos *sim* exhibits a temporal expression dynamic similar to those of *sog*; in mid blastoderm stage embryos *sim* is expressed in a broad ventral domain, which clears ventrally during development and eventually flanks the presumptive mesoderm in narrow stripes (Yen-Ta Chen, PhD thesis, 2015). A similar temporal expression profile of *sim* was described for *Tribolium* and *Nasonia* (Buchta et al., 2013). A lack of *Oncopeltus* Snail could lead to the expansion of the mesectodermal marker *sim* into the derepressed mesoderm (Fig. 9 C), comparable to the lack of Snail

phenotypes in *Drosophila* and *Tribolium* (Leptin, 1991; Rao et al., 1991; von Levetzow, PhD thesis, 2008).

How is *Oncopeltus snail* regulated? During early development of *Drosophila* and *Tribolium snail* is activated by high levels of nuclear Dorsal and, as secondary input, by Twist (Leptin, 1991; Reeves and Stathopoulos, 2009; Stappert, PhD thesis, 2014; Stappert et al., 2016). However, the *Toll dpp* double knockdown of *Oncopeltus* seems to indicate a derepressed expression of *snail* within the expanded mesoderm as *sim* is expressed in an anterior mesectodermal domain bordering the derepressed mesoderm (Sachs et al., 2015). Thus, like *twist* and *sog*, the expression of *Oncopeltus snail* seems not to strictly rely on Toll/Dorsal signaling, but on the absence of BMP signaling.

In summary, *Oncopeltus snail* has two functions during blastoderm stage: moderate repression of *sog* within the mesoderm to buffer the self-regulatory BMP/Sog system and repression of mesectodermal genes to ensure the integrity of the mesoderm. While the second function seems to be conserved across insects, the first function seems to be a crucial element of the distinctive BMP/Sog DV axis patterning system of *Oncopeltus*.

In zebrafish, organizer-derived Bmp2b (the zebrafish homolog of Dpp) represses *chordin* transcription in the organizer and contributes to the control of the Chordin gradient (Xue et al., 2014). A lack of organizer-derived Bmp2b causes an increase of Chordin protein and transcript along the dorsoventral axis of zebrafish embryos and leads to a complete mesodermalization (Xue et al., 2014). It has been experimentally shown, that the *chordin* gene is transcriptionally repressed by Bmp/Smad signaling in zebrafish (Xue et al., 2014) and a similar mechanism was proposed for *Oncopeltus* (Sachs et al., 2015). Thus, Organizer-derived Bmp2b signaling is a mesoderm-derived source of Chordin repression which acts and is needed in parallel to the ectoderm-derived sinks of Chordin repression (e.g. cleavage by Tolloid). It seems that correct Sog/Chordin gradient formation does need both an ectodermal sink and a mesodermal impediment in both fish and bug.

4.2 New insights into BMP/Sog gradient formation extend the GRN controlling DV axis patterning in *Oncopeltus*

As phenotypic analysis revealed (see section 4.1 and Fig. 9), Snail seems to repress *sog* and *sim* within the presumptive mesoderm, while *snail* seems to be repressed by BMP signaling. The knowledge about these interactions allows extending of the GRN regulating DV axis formation of *Oncopeltus*, which was originally proposed by Sachs et al., 2015. Fig. 29 shows how the primary GRN discriminates between mesoderm and ectoderm and Fig. 30 shows how in secondary diversification the primary GRN can also pattern the mesectoderm. While the extracellular ligands of BMP signaling and the BMP antagonist Sog are diffusible components, Snail acts as immobile transcriptional repressor.

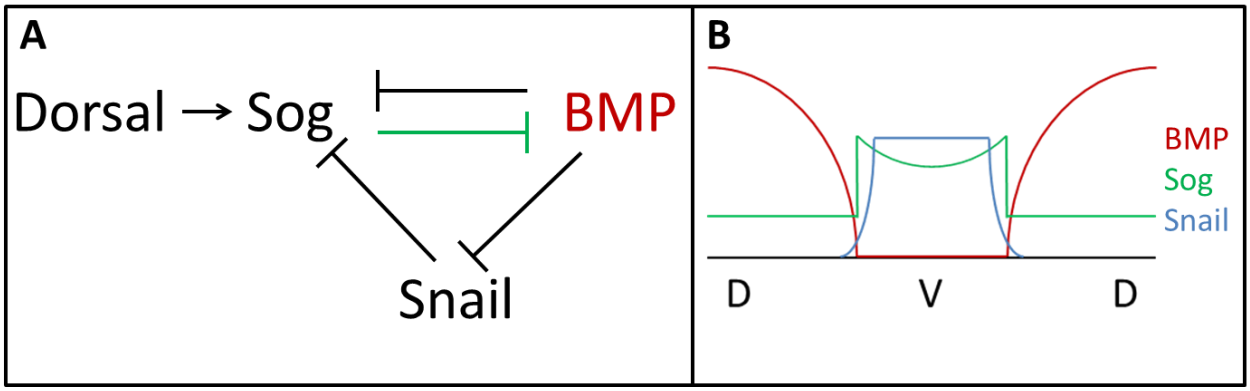

Fig. 29 Primary GRN regulating DV axis patterning in *Oncopeltus*

(A) Ventrally restricted Toll/Dorsal signaling initiates *sog* expression and thus cues the self-regulatory network. Sog forms an inhibitory complex with BMP ligands, and thus indirectly autoactivates and maintains its own expression by repression of its own inhibitor. Absence of BMP signaling is sufficient to activate *sog* and *snail* expression without any additional activator. Thus, BMP signaling transcriptionally represses both *sog* and *snail* expression and thus indirectly autoactivates itself. Expression of BMP signaling component transcripts (ligands, receptors, transcription factors) is ubiquitous, but active BMP signaling is restricted to the ectoderm by Sog inhibition. Once Sog has established its ventral expression domain by repressing BMP signaling, *snail* expression is activated. Thus, Sog indirectly activates *snail* expression, by repressing *snails* repressor BMP signaling. In turn, Snail transcriptionally represses *sog* expression and causes a moderate depression of *sog* transcript within the presumptive mesoderm. Through Snail's interposed position, between Sog and BMP signaling, Snail buffers the self-regulatory network and prevents an expansion of the ventral mesoderm and collapse of BMP signaling. In contrast to both Sog and BMP signaling, Snail does not autoactivate itself, but rather represses its own indirect activator Sog. Arrows indicate activation; T-bars indicate repression; black lines indicate transcriptional activation/repression; green line indicates protein-protein interaction; black text indicates individual proteins; red text indicates entire signaling pathway. **(B)** Schematic drawing of DV axis patterning in steady state, the individual concentrations of active BMP signaling, Sog and Snail are plotted on the y-axis. The x-axis shows the circumference of the embryo, with the dorsal and ventral sides marked as D and V, respectively.

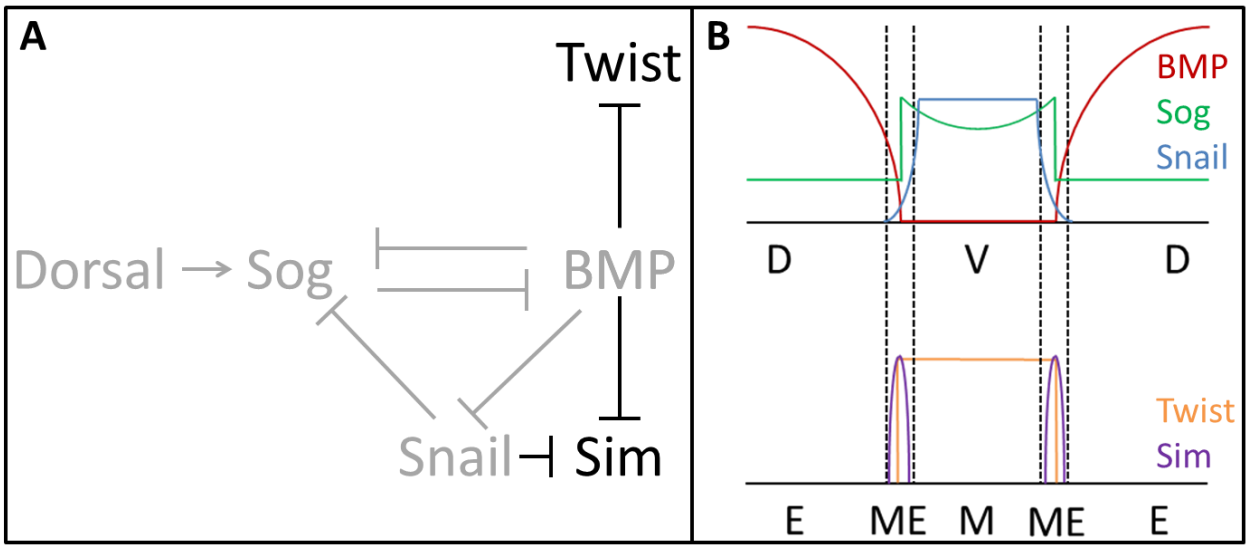

Fig. 30 GRN in secondary diversification controls mesectoderm patterning in *Oncopeltus*

(A) The primary GRN that regulates DV axis patterning in *Oncopeltus,* consisting of Dorsal, Sog, Snail and BMP signaling, is not only able to pattern the mesoderm and the ectoderm, but also the mesectoderm. The primary GRN in steady state generates a small space at the border of the mesoderm and the ectoderm in that the

concentrations of both Snail and active BMP signaling (pMad) is low. Within this space, the mesectodermal marker *sim* is expressed. Within the mesectoderm *sog* expression is not depressed by Snail, which leads to an enhancement of the lateral boarders of the *sog* expression profile. The low concentration of active BMP signaling within the mesoderm and mesectoderm is sufficient to activate *twist* expression in a broad ventral domain; an input of an activator is not necessary. Arrows indicate activation; T-bars indicate repression; black lines indicate transcriptional activation/repression; black text indicates individual proteins; the primary network is grayed out for reasons of clarity and comprehensibility. **(B)** Schematic drawing of DV axis patterning in steady state, the individual concentrations of active BMP signaling, Sog, Snail, Twist and Sim are plotted on the y-axis. Top: The x-axis shows the circumference of the embryo, with the dorsal and ventral sides marked as D and V, respectively. Bottom: The x-axis shows the circumference of the embryo, with the ectoderm, mesectoderm and mesoderm marked as E, ME and M, respectively.

4.3 Microinjection of BMP4 can disturb mesoderm development

Injections with high concentrations of human BMP4 lead to a strong phenotype in which the embryo developed into a large agglutination of yolk connected with a small cuticulized part of embryonic tissue (Fig. 11). This injection phenotype is similar to the most severe *sog*, *tsg* and *dpp* knockdown phenotypes in which BMP signaling is either globally activated (*sog* and *tsg* knockdown) or suppressed (*dpp* knockdown) (Sachs, PhD thesis, 2014).

Since *Oncopeltus* embryos look uniform along their DV axis during blastoderm stage it was not possible to aim injections specifically for distinct regions along the DV axis, but on the basis of more than 150 individual injected embryos it is most likely that mesodermal as well as ectodermal regions were injected with high amounts of BMP4. However, I did not observe any phenotypic range and the observed injection phenotypes did not seem to effectively differ from each other when injected with high concentrations of BMP4 (Fig. 11). It is thus likely that due to the high abundance of ectopic BMP4, the protein diffused within the perivitelline space around the entire DV axis of injected embryos, which resulted in a uniform level of high BMP4 concentration independent of the initial site of injection. High concentrations of ectopic BMP4 most likely interfere with canonical endogenous BMP signalling by BMP4 binding to BMP receptors and extracellular BMP signaling components like Sog, Tsg and Tld. Heterodimer formation of endogenous Dpp and Gbb with ectopic BMP4 could occur as well. High uniform levels of BMP4 likely activate BMP signaling in the entire embryo which would disturb the formation of the endogenous pMad gradient and lead to an entirely symmetric pMad distribution that would lack DV polarity. The consequences of ubiquitously activated BMP signaling can be observed in strong *Toll*, *tsg* and *sog* knockdown embryos. These knockdown embryos show a complete loss of the mesoderm and mesectoderm in blastoderm and germ band stage, and gastrulation and all subsequent morphogenetic movements lack DV asymmetry (Sachs et al., 2015).

However, the observed BMP4-injection phenotype seems to be more severe than phenotypes derived from partial knockdowns of *Toll*, *tsg* and *sog* in that BMP4-injected embryos exhibit a strongly reduced and often fragmented germ band and no visible head whereas *Toll*, *tsg* and *sog* knockdown embryos often develop a head and a continuous germ band. The phenotypic severity of BMP4-injected embryos could be caused by a stronger BMP signaling activation than in partial *Toll*, *tsg* and *sog* knockdown embryos which often possess slight DV asymmetries in their pMad gradient and residual *twi, sog* or *sim* expression (Sachs, PhD thesis, 2014).

However, injections with moderate concentrations of BMP4 (1:10) lead to a range of milder phenotypes. Observed phenotypic traits included abnormally formed thoracic and abdominal segments, defective katatrepsis and late developmental arrests after katatrepsis (Fig. 12). The range

of phenotypic severity and different phenotypic traits indicates that the site of injection combined with a lower BMP4 concentration affected the phenotypic characteristics potentially by locally disturbing the canonical pMad gradient. This assumption is supported by ISH staining that show a local disturbance of mesodermal *sog* expression after BMP4 injections into mesodermal regions (Fig. 13).

Similar defects in formation of thoracic and abdominal segments are also observed in *sog* or *tsg* knockdown phenotypes and could be caused by a local dorsalization of such segments in BMP4 injected embryos. Defective katatrepsis is observed in many knockdown phenotypes of genes with dorsalizing and ventralizing effects like *sog*, *tsg*, *tld* and *dpp* (Sachs, PhD thesis, 2014). Katatrepsis is dependent on a functional amnion in *Oncopeltus* (Panfilio et al., 2006). It is assumed that the amnion anlage is located dorsally in the early *Oncopeltus* embryo and that the correct development of the amnion is dependent on a canonical pMad gradient (Sachs, PhD thesis, 2014). Defective formation of the amnion caused by a globally disturbed pMad gradient like in strong *sog*, *tsg*, *tld*, *dpp* and *gbb* knockdown phenotypes or a locally disturbed pMad gradient like in *Oncopeltus* embryos injected with BMP4 in moderate concentrations is likely to be the reason for defective katatrepsis.

Although BMP4-injection phenotypes are comparable to pRNAi-mediated *sog* and *tsg* knockdown phenotypes they do not phenocopy each other. On the one hand pRNAi mediated gene knockdown implemented in virgin females affects already oogenesis and, from the very beginning, embryogenesis whereas microinjections of proteins or mRNA implemented at 24 – 30 hpf can only affect embryogenesis from this point onwards. Shallow pMad gradients can already be detected around 26 hpf in wild-type embryos although cell fates are not fixed unalterably during blastoderm stage in the self-organizing DV patterning system of *Oncopeltus* (Sachs et al., 2015). On the other hand especially microinjections at moderate concentrations affect embryogenesis rather local, spatially dependent on the site of injection, whereas pRNAi affects embryogenesis on a global level.

4.4 An ectopic source of *chordin* induces mesodermal cell fates independent of Toll

Microinjections of *chordin* into both dorsalized Toll knockdown embryos and into the dorsal side of *Oncopeltus* wild-type embryos induced the expression of the ventral marker genes *sim*, *sog* and *twist* and mesoderm-like nuclear density patterns (Fig. 18 - 22). Thus, a local depression of BMP signaling induces ventral cell fates even in a BMP dominated background that lacks endogenous Toll/Dorsal signaling.

However, the injection-induced domains of ventral marker transcript expression suggest a fading over time resulting in a transition from patch-like to ring-like domains which suggests that the ectopic mesodermal domain tends to be instable and seems to decompose and become ectodermal again (Fig. 18 - 22). If the ventral marker gene expression within such rings has entirely faded, accordingly nuclear density increases to ectodermal levels again, which further indicates the instability of the injection-induced mesodermal domains and their tendencies to decompose and become ectodermal again (Fig. 18).

As phenotypic analysis suggests *snail* is a crucial component of the BMP/Sog system of *Oncopeltus* (see section 4.1, 4.2 and Fig. 9). The GRN incorporating Snail shows, that Sog indirectly activates its own inhibitor *snail* (Fig. 29). Such an activation of *snail* within the injection-induced mesodermal domain, subsequent repression of *sog* and thus, reactivation of BMP signaling can explain a transition from mesodermal to ectodermal fates. The observed “patch-within-ring” patterns (Fig. 9 C) can be explained as well with the same GRN; once Snail has repressed *sog* and BMP signaling gained

dominance again, in turn, BMP signaling represses *snail* and thus, *sog* becomes activated again. Apparently the self-regulatory network cannot enter steady state but oscillates between Sog/mesoderm and BMP/ectoderm dominance. Within the endogenous mesoderm in *Oncopeltus* wild-type embryos a continuous activation of *sog* by Toll/Dorsal signaling could prevent such oscillation and facilitate steady state establishment.

4.5 *OFAS016851* and *OFAS018039* are potential serosa markers

OFAS016851 and *OFAS018039* are expressed in the early embryo at blastoderm stage in the anterior cap and *OFAS016851* is additionally expressed later during germ band stage in spreading serosa cells (Fig. 26 and 28). It has been proposed before that the regions of the blastoderm stage embryo of *Oncopeltus* that do not express *engrailed*, namely the anterior cap and the most dorsal part of the embryo, could be presumed as extraembryonic territories (Liu and Kaufman, 2004; Panfilio et al., 2006). The expression pattern of *OFAS016851* indeed seems to suggest that the presumptive serosa is patterned in the anterior cap of *Oncopeltus* blastoderm stage embryos.
However, work from the Chipman lab shows that in blastoderm stage embryos *tailless* is expressed in the anterior cap region. As the blastoderm starts to invaginate at the posterior the expression of *tailless* refines to a pair of lateral patches while the most anterior 10 % stop to express *tailless*. In developing germ bands *tailless* is expressed in the head lobes. In embryos that lack Tailless the head lobes including the eyes are missing (Weisbrod et al., 2013). It is possible that during early blastoderm stage *tailless* and *OFAS016851* are coexpressed and that their expression refines and splits shortly before or at the onset of the posterior blastoderm invagination into the yolk and the anterior serosa expansion on top of the yolk.
Both *OFAS016851* and *OFAS018039* could turn out to be useful serosa markers, especially *OFAS016851* since it is expressed not only in blastoderm stage but also in spreading serosa cells.
It has been proposed before that from the anterior region of the early *Oncopeltus* egg the presumptive serosa emerges whereas the amnion is thought to emerge from the most dorsal part of the embryo itself (Panfilio et al., 2006). Similar fate maps in which the serosa emerges anterior of the condensing germ band are realized in hemimetabolus insects like *Schistocerca* (Dearden et al., 2000) and potentially *Gryllus* (Nakamura et al., 2010) and this architecture could be a plesiomorphic character. In contrast, in insects of most major holometabolous orders like hymenoptera (*Apis* and *Nasonia*), lepidoptera (*Bombyx*), coleopteran (*Tribolium*) and diptera (*Drosophila*, *Megaselia* and *Anopheles*) the anlage of the serosa and amnion or the amnioserosa, respectively, seems to have a derived position within the embryonic fate map (Amanai et al., 1994; van der Zee et al., 2005; Goltsev et al., 2007; Rafiqi et al., 2008; Rafiqi et al., 2012; Panfilio, 2008; Buchta et al., 2013; Wilson et al., 2014).

4.6 *OFAS016851* RNAi phenotype

Oncopeltus embryos in which *OFAS016851* was knocked down died within 48 h after enclosure, presumably because their mandibles and maxillae were not detached from their embryotic cuticles, which seemed to disable them from feeding (Fig. 27). *OFAS016851* codes for a member of the serpin family. The serpin gene family is the largest family of protease inhibitors, present in animals, plants,

bacteria, archea and poxviruses (Law et al., 2006). The majority of serpins inhibits serine proteases. Serpins are central in controlling many proteolytic cascades including the blood clotting cascade, the protease cascade upstream of Toll and Toll-like receptors and the cascade which proteolytically activates many phenoloxidases, which are involved in melanization and sclerotization (De Gregorio et al., 2002; Ligoxygakis et al., 2003; Zou et al., 2005; Rau et al., 2007; Scherfer et al., 2008; Tang et al., 2008).

It is difficult to speculate about the causes of the *OFAS016851* knockdown phenotype. First, the nature of the irregular attachment of the mouthparts to the cuticle is unknown. Second, it is unknown if the cuticle is of serosal or embryonic origin. Third, the role of serpins is divers and several distinct functions of various serosal serpins are described. Serosally expressed serpins are thought to function in immunity by regulating Toll signaling and the melanization cascade, and in wound healing also by regulation of the melanization cascade (Jacobs et al., 2014). However, loss of these functions cannot explain the phenotype. Besides providing immunity and wound healing capacities the serosa secrets the serosal cuticle which provides desiccation resistance (Jacobs et al., 2013). The mechanical properties of cuticles are determined by the interplay of many factors including the degree of sclerotization (Arakane et al., 2005; Andersen, 2010). Central players in sclerotization are phenoloxidases which are proteolytically activated by serin protease cascades which in turn are negatively regulated by serpins (Kanost and Gorman, 2008). Overactive sclerotization of serosal or embryonic cuticles caused by a lack of OFAS016851 could possibly explain the attachment of mouthparts to cuticle.

OFAS016851 Drosophila ortholog *Serpin 88Ea* was determined via bidirectional BLAST. Carron and colleagues report, that in *Drosophila Serpin 88Ea* is expressed in ovaries, at all embryonic stages except between five and fifteen hours of development, throughout larval and pupal development and in adults. Homozygous mutant lines for *Serpin 88Ea* are not viable. However, heterozygous lines are viable and RNAi silencing turned out to be difficult in that several RNAi transgene copies were needed to achieve a detectable decrease of *Serpin 88Ea* mRNA levels. The only conspicuous phenotype that was observed following RNAi-mediated perturbation of *Serpin 88Ea* expression was a defect in wing development, specifically in the unfolding and expansion of the wings (Charron et al., 2008). Interestingly, the few Spn27A deficient flies that enclose also show a defect in wing expansion (De Gregorio et al., 2002). It seems that there are many redundancies and shared functions between the different serpins, yet many knockouts of single serpins are lethal.

Outlook

As the integration of Snail into the BMP/Sog system of *Oncopeltus* leads to an extended GRN for DV axis patterning, it is of great interest to simulate the new GRN *in silico* to test if it can pattern mesoderm, ectoderm and mesectoderm as hypothesized. Another important experiment would be the detection of *snail* transcripts via ISH in *Toll* and *dpp* single knockdowns as well as in the *Toll*/*dpp* double knockdowns as the repression of snail by BMP signaling is not shown directly, but rather hypothesized by phenotypic analysis. In addition, the expression of *snail* in *chordin*-injected wild-type and *Toll* knockdown embryos should be detected by ISH and analyzed as well, together with the expression of *sim* in *chordin*-injected wild-type and *twist* in *chordin*-injected *Toll* knockdown embryos. However, the detection of *snail* transcripts around the site of *chordin*-injection might be hard to realize; as soon as Snail is synthesized it will repress *sog* and facilitate BMP signaling and thus repress its own transcription.
Another interesting experiment would be to generate *Toll*/*snail* double knockdown embryos and analyze their fate map, as it is not clear how the GRN would perform in such a background. A *Toll*/*snail* double knockdown could potentially phenocopy a *Toll*/*dpp* knockdown (except expansion of mesectoermal markers into the derepressed mesoderm).
However, a *Toll*/*snail* double knockdown could also phenocopy a *dpp* knockdown, as the BMP network would lack a polarization via Toll that is needed to express *sog* within a BMP-rich background. If this would be the case, *chordin*-injections into *Toll*/*snail* double knockdown embryos could lead to a stabile induction of ectopic mesodermal domains or even an entire collapse of BMP signaling in line with derepression of mesodermal fates along the entire DV axis.
Finally, as new version of the *Oncopeltus* genome is to be released, mapping of the RNAseq reads to the latest *Oncopeltus* official gene set could potentially increase the RNAseq analysis by a large magnitude.

References

Ahmad ST, Sweeney ST, Lee JA, Sweeney NT, Gao FB. Genetic screen identifies serpin5 as a regulator of the toll pathway and CHMP2B toxicity associated with frontotemporal dementia. Proc Natl Acad Sci U S A. 2009 Jul 21;106(29):12168-73. doi: 10.1073/pnas.0903134106. Epub 2009 Jul 6. PMID: 19581577; PMCID: PMC2715505.

Akiyama-Oda Y, Oda H. Axis specification in the spider embryo: dpp is required for radial-to-axial symmetry transformation and sog for ventral patterning. Development. 2006 Jun;133(12):2347-57. doi: 10.1242/dev.02400. PMID: 16720876.

Akiyama-Oda Y, Oda H. Early patterning of the spider embryo: a cluster of mesenchymal cells at the cumulus produces Dpp signals received by germ disc epithelial cells. Development. 2003 May;130(9):1735-47. doi: 10.1242/dev.00390. PMID: 12642480.

Alatortsev VE. [New genes coding for vitelline membrane proteins in Drosophila]. Mol Biol (Mosk). 2006 Mar-Apr;40(2):375-7. Russian. PMID: 16637280.

Altschul SF, Gish W, Miller W, Myers EW, Lipman DJ. Basic local alignment search tool. J Mol Biol. 1990 Oct 5;215(3):403-10. doi: 10.1016/S0022-2836(05)80360-2. PMID: 2231712.

Amanai K, Suzuki Y, Ohtaki T. Involvement of a maternally transcribed lectin gene in the early development of Bombyx mori. Rouxs Arch Dev Biol. 1994 Aug;203(7-8):397-401. doi: 10.1007/BF00188688. PMID: 28305945.

Andersen SO. Cuticular sclerotization and tanning. Comprehensive Molecular Insect Science, Vol. 4, Elsevier, Oxford. 1995. pp. 79-110. ISBN 9780123847478. https://doi.org/10.1016/B978-0-12-384747-8.10006-6.

Andersen SO. Insect cuticular sclerotization: a review. Insect Biochem Mol Biol. 2010 Mar;40(3):166-78. doi: 10.1016/j.ibmb.2009.10.007. Epub 2009 Nov 20. PMID: 19932179.

Anderson KV, Nüsslein-Volhard C. Genetic analysis of dorsal-ventral embryonic pattern in Drosophila. In: Malacinsky GM, Bryant SV, eds. Pattern Formation. New York: MacMillan; 1984, 269–289.

Anderson KV, Nüsslein-Volhard C. Information for the dorsal--ventral pattern of the Drosophila embryo is stored as maternal mRNA. Nature. 1984 Sep 20-26;311(5983):223-7. doi: 10.1038/311223a0. PMID: 6434989.

Andreu MJ, González-Pérez E, Ajuria L, Samper N, González-Crespo S, Campuzano S, Jiménez G. Mirror represses pipe expression in follicle cells to initiate dorsoventral axis formation in Drosophila. Development. 2012 Mar;139(6):1110-4. doi: 10.1242/dev.076562. Epub 2012 Feb 8. PMID: 22318229.

Andrews S. FastQC: A Quality Control Tool for High Throughput Sequence Data [Online]. 2010. Available online at: http://www.bioinformatics.babraham.ac.uk/projects/fastqc/

Arakane Y, Muthukrishnan S, Beeman RW, Kanost MR, Kramer KJ. Laccase 2 is the phenoloxidase gene required for beetle cuticle tanning. Proc Natl Acad Sci U S A. 2005 Aug 9;102(32):11337-42. doi: 10.1073/pnas.0504982102. Epub 2005 Aug 2. PMID: 16076951; PMCID: PMC1183588.

Arakane Y, Muthukrishnan S, Kramer KJ, Specht CA, Tomoyasu Y, Lorenzen MD, Kanost M, Beeman RW. The Tribolium chitin synthase genes TcCHS1 and TcCHS2 are specialized for synthesis of epidermal cuticle and midgut peritrophic matrix. Insect Mol Biol. 2005 Oct;14(5):453-63. doi: 10.1111/j.1365-2583.2005.00576.x. PMID: 16164601.

Astigarraga S, Grossman R, Díaz-Delfín J, Caelles C, Paroush Z, Jiménez G. A MAPK docking site is critical for downregulation of Capicua by Torso and EGFR RTK signaling. EMBO J. 2007 Feb 7;26(3):668-77. doi: 10.1038/sj.emboj.7601532. Epub 2007 Jan 25. PMID: 17255944; PMCID: PMC1794389.

Atkey MR, Lachance JF, Walczak M, Rebello T, Nilson LA. Capicua regulates follicle cell fate in the Drosophila ovary through repression of mirror. Development. 2006 Jun;133(11):2115-23. doi: 10.1242/dev.02369. Epub 2006 May 3. Erratum in: Development. 2006 Dec;133(23):4794. PMID: 16672346.

Baker JC, Beddington RS, Harland RM. Wnt signaling in Xenopus embryos inhibits bmp4 expression and activates neural development. Genes Dev. 1999 Dec 1;13(23):3149-59. doi: 10.1101/gad.13.23.3149. PMID: 10601040; PMCID: PMC317181.

Barrallo-Gimeno A, Nieto MA. The Snail genes as inducers of cell movement and survival: implications in development and cancer. Development. 2005 Jul;132(14):3151-61. doi: 10.1242/dev.01907. PMID: 15983400.

Bauer H, Meier A, Hild M, Stachel S, Economides A, Hazelett D, Harland RM, Hammerschmidt M. Follistatin and noggin are excluded from the zebrafish organizer. Dev Biol. 1998 Dec 15;204(2):488-507. doi: 10.1006/dbio.1998.9003. PMID: 9882485.

Belvin MP, Jin Y, Anderson KV. Cactus protein degradation mediates Drosophila dorsal-ventral signaling. Genes Dev. 1995 Apr 1;9(7):783-93. doi: 10.1101/gad.9.7.783. PMID: 7705656.

Benton MA, Pechmann M, Frey N, Stappert D, Conrads KH, Chen YT, Stamataki E, Pavlopoulos A, Roth S. Toll Genes Have an Ancestral Role in Axis Elongation. Curr Biol. 2016 Jun 20;26(12):1609-1615. doi: 10.1016/j.cub.2016.04.055. Epub 2016 May 19. PMID: 27212406.

Benton MA. A revised understanding of Tribolium morphogenesis further reconciles short and long germ development. PLoS Biol. 2018 Jul 3;16(7):e2005093. doi: 10.1371/journal.pbio.2005093. PMID: 29969459; PMCID: PMC6047830.

Bergmann A, Stein D, Geisler R, Hagenmaier S, Schmid B, Fernandez N, Schnell B, Nüsslein-Volhard C. A gradient of cytoplasmic Cactus degradation establishes the nuclear localization gradient of the dorsal morphogen in Drosophila. Mech Dev. 1996 Nov;60(1):109-23. doi: 10.1016/s0925-4773(96)00607-7. PMID: 9025065.

Bier E, De Robertis EM. EMBRYO DEVELOPMENT. BMP gradients: A paradigm for morphogen-mediated developmental patterning. Science. 2015 Jun 26;348(6242):aaa5838. doi: 10.1126/science.aaa5838. PMID: 26113727.

Bier E, Jan LY, Jan YN. rhomboid, a gene required for dorsoventral axis establishment and peripheral nervous system development in Drosophila melanogaster. Genes Dev. 1990 Feb;4(2):190-203. doi: 10.1101/gad.4.2.190. Erratum in: Genes Dev 1990 Apr;4(4):680-1. PMID: 2110920.

Blader P, Rastegar S, Fischer N, Strähle U. Cleavage of the BMP-4 antagonist chordin by zebrafish tolloid. Science. 1997 Dec 12;278(5345):1937-40. doi: 10.1126/science.278.5345.1937. PMID: 9395394.

Blitz IL, Shimmi O, Wünnenberg-Stapleton K, O'Connor MB, Cho KW. Is chordin a long-range- or short-range-acting factor? Roles for BMP1-related metalloproteases in chordin and BMP4 autofeedback loop regulation. Dev Biol. 2000 Jul 1;223(1):120-38. doi: 10.1006/dbio.2000.9740. PMID: 10864466.

Bökel C, Dass S, Wilsch-Bräuninger M, Roth S. Drosophila Cornichon acts as cargo receptor for ER export of the TGFalpha-like growth factor Gurken. Development. 2006 Feb;133(3):459-70. doi: 10.1242/dev.02219. Epub 2006 Jan 5. PMID: 16396907.

Bolger AM, Lohse M, Usadel B. Trimmomatic: a flexible trimmer for Illumina sequence data. Bioinformatics. 2014 Aug 1;30(15):2114-20. doi: 10.1093/bioinformatics/btu170. Epub 2014 Apr 1. PMID: 24695404; PMCID: PMC4103590.

Bours V, Villalobos J, Burd PR, Kelly K, Siebenlist U. Cloning of a mitogen-inducible gene encoding a kappa B DNA-binding protein with homology to the rel oncogene and to cell-cycle motifs. Nature. 1990 Nov 1;348(6296):76-80. doi: 10.1038/348076a0. PMID: 2234062.

Buchta T, Ozüak O, Stappert D, Roth S, Lynch JA. Patterning the dorsal-ventral axis of the wasp Nasonia vitripennis. Dev Biol. 2013 Sep 1;381(1):189-202. doi: 10.1016/j.ydbio.2013.05.026. Epub 2013 Jun 2. PMID: 23735637.

Burke T, Waring GL, Popodi E, Minoo P. Characterization and sequence of follicle cell genes selectively expressed during vitelline membrane formation in Drosophila. Dev Biol. 1987 Dec;124(2):441-50. doi: 10.1016/0012-1606(87)90497-0. PMID: 3119397.

Cáceres L, Nilson LA. Production of gurken in the nurse cells is sufficient for axis determination in the Drosophila oocyte. Development. 2005 May;132(10):2345-53. doi: 10.1242/dev.01820. Epub 2005 Apr 13. PMID: 15829517.

Cai HN, Arnosti DN, Levine M. Long-range repression in the Drosophila embryo. Proc Natl Acad Sci U S A. 1996 Sep 3;93(18):9309-14. doi: 10.1073/pnas.93.18.9309. PMID: 8790326; PMCID: PMC38424.

Castro CP, Piscopo D, Nakagawa T, Derynck R. Cornichon regulates transport and secretion of TGFalpha-related proteins in metazoan cells. J Cell Sci. 2007 Jul 15;120(Pt 14):2454-66. doi: 10.1242/jcs.004200. PMID: 17607000.

Cerenius L, Söderhäll K. The prophenoloxidase-activating system in invertebrates. Immunol Rev. 2004 Apr;198:116-26. doi: 10.1111/j.0105-2896.2004.00116.x. PMID: 15199959.

Charatsi I, Luschnig S, Bartoszewski S, Nüsslein-Volhard C, Moussian B. Krapfen/dMyd88 is required for the establishment of dorsoventral pattern in the Drosophila embryo. Mech Dev. 2003 Feb;120(2):219-26. doi: 10.1016/s0925-4773(02)00410-0. PMID: 12559494.

Charron Y, Madani R, Combepine C, Gajdosik V, Hwu Y, Margaritondo G, Vassalli JD. The serpin Spn5 is essential for wing expansion in Drosophila melanogaster. Int J Dev Biol. 2008;52(7):933-42. doi: 10.1387/ijdb.072419yc. PMID: 18956323.

Chasan R, Anderson KV. The role of easter, an apparent serine protease, in organizing the dorsal-ventral pattern of the Drosophila embryo. Cell. 1989 Feb 10;56(3):391-400. doi: 10.1016/0092-8674(89)90242-0. PMID: 2492450.

Chasan R, Jin Y, Anderson KV. Activation of the easter zymogen is regulated by five other genes to define dorsal-ventral polarity in the Drosophila embryo. Development. 1992 Jun;115(2):607-16. doi: 10.1242/dev.115.2.607. PMID: 1425342.

Chen LY, Wang JC, Hyvert Y, Lin HP, Perrimon N, Imler JL, Hsu JC. Weckle is a zinc finger adaptor of the toll pathway in dorsoventral patterning of the Drosophila embryo. Curr Biol. 2006 Jun 20;16(12):1183-93. doi: 10.1016/j.cub.2006.05.050. PMID: 16782008.

Chen YT. The role of Toll signaling in dorsoventral axis formation in the milkweed bug *Oncopeltus fasciatus*, PhD thesis. Universität zu Köln. 2015

Cho YS, Stevens LM, Sieverman KJ, Nguyen J, Stein D. A ventrally localized protease in the Drosophila egg controls embryo dorsoventral polarity. Curr Biol. 2012 Jun 5;22(11):1013-8. doi: 10.1016/j.cub.2012.03.065. Epub 2012 May 10. PMID: 22578419; PMCID: PMC3371173.

Cho YS, Stevens LM, Stein D. Pipe-dependent ventral processing of Easter by Snake is the defining step in Drosophila embryo DV axis formation. Curr Biol. 2010 Jun 22;20(12):1133-7. doi: 10.1016/j.cub.2010.04.056. Epub 2010 Jun 3. PMID: 20605458; PMCID: PMC2902586.

Clement JH, Fettes P, Knöchel S, Lef J, Knöchel W. Bone morphogenetic protein 2 in the early development of Xenopus laevis. Mech Dev. 1995 Aug;52(2-3):357-70. doi: 10.1016/0925-4773(95)00413-u. PMID: 8541221.

Coffinier C, Ketpura N, Tran U, Geissert D, De Robertis EM. Mouse Crossveinless-2 is the vertebrate homolog of a Drosophila extracellular regulator of BMP signaling. Gene Expr Patterns. 2002 Dec;2(3-4):189-94. doi: 10.1016/s0925-4773(02)00420-3. PMID: 12617799.

Coleman JE. Structure and mechanism of alkaline phosphatase. Annu Rev Biophys Biomol Struct. 1992;21:441-83. doi: 10.1146/annurev.bb.21.060192.002301. PMID: 1525473.

Connors SA, Trout J, Ekker M, Mullins MC. The role of tolloid/mini fin in dorsoventral pattern formation of the zebrafish embryo. Development. 1999 Jun;126(14):3119-30. doi: 10.1242/dev.126.14.3119. PMID: 10375503.

Daigneault J, Klemetsaune L, Wasserman SA. The IRAK homolog Pelle is the functional counterpart of IκB kinase in the Drosophila Toll pathway. PLoS One. 2013 Sep 23;8(9):e75150. doi: 10.1371/journal.pone.0075150. PMID: 24086459; PMCID: PMC3781037.

Dale L, Evans W, Goodman SA. Xolloid-related: a novel BMP1/Tolloid-related metalloprotease is expressed during early Xenopus development. Mech Dev. 2002 Dec;119(2):177-90. doi: 10.1016/s0925-4773(02)00359-3. PMID: 12464431.

Dale L, Howes G, Price BM, Smith JC. Bone morphogenetic protein 4: a ventralizing factor in early Xenopus development. Development. 1992 Jun;115(2):573-85. doi: 10.1242/dev.115.2.573. PMID: 1425340.

De Gregorio E, Han SJ, Lee WJ, Baek MJ, Osaki T, Kawabata S, Lee BL, Iwanaga S, Lemaitre B, Brey PT. An immune-responsive Serpin regulates the melanization cascade in Drosophila. Dev Cell. 2002 Oct;3(4):581-92. doi: 10.1016/s1534-5807(02)00267-8. PMID: 12408809.

De Robertis EM. Evo-devo: variations on ancestral themes. Cell. 2008 Jan 25;132(2):185-95. doi: 10.1016/j.cell.2008.01.003. PMID: 18243095; PMCID: PMC2280037.

Dearden P, Grbic M, Falciani F, Akam M. Maternal expression and early zygotic regulation of the Hox3/zen gene in the grasshopper Schistocerca gregaria. Evol Dev. 2000 Sep-Oct;2(5):261-70. doi: 10.1046/j.1525-142x.2000.00065.x. PMID: 11252555.

DeLotto R, DeLotto Y, Steward R, Lippincott-Schwartz J. Nucleocytoplasmic shuttling mediates the dynamic maintenance of nuclear Dorsal levels during Drosophila embryogenesis. Development. 2007 Dec;134(23):4233-41. doi: 10.1242/dev.010934. Epub 2007 Oct 31. PMID: 17978003.

DeLotto R, Spierer P. A gene required for the specification of dorsal-ventral pattern in Drosophila appears to encode a serine protease. Nature. 1986 Oct 23;323(6090):688-92. doi: 10.1038/323688a0. PMID: 11486795.

DeLotto R. Gastrulation defective, a complement factor C2/B-like protease, interprets a ventral prepattern in Drosophila. EMBO Rep. 2001 Aug;2(8):721-6. doi: 10.1093/embo-reports/kve153. PMID: 11493599; PMCID: PMC1083990.

DeLotto Y, DeLotto R. Proteolytic processing of the Drosophila Spätzle protein by easter generates a dimeric NGF-like molecule with ventralising activity. Mech Dev. 1998 Mar;72(1-2):141-8. doi: 10.1016/s0925-4773(98)00024-0. PMID: 9533958.

Denes AS, Jékely G, Steinmetz PR, Raible F, Snyman H, Prud'homme B, Ferrier DE, Balavoine G, Arendt D. Molecular architecture of annelid nerve cord supports common origin of nervous system centralization in bilateria. Cell. 2007 Apr 20;129(2):277-88. doi: 10.1016/j.cell.2007.02.040. PMID: 17448990.

Dick A, Hild M, Bauer H, Imai Y, Maifeld H, Schier AF, Talbot WS, Bouwmeester T, Hammerschmidt M. Essential role of Bmp7 (snailhouse) and its prodomain in dorsoventral patterning of the zebrafish embryo. Development. 2000 Jan;127(2):343-54. doi: 10.1242/dev.127.2.343. PMID: 10603351.

Dissing M, Giordano H, DeLotto R. Autoproteolysis and feedback in a protease cascade directing Drosophila dorsal-ventral cell fate. EMBO J. 2001 May 15;20(10):2387-93. doi: 10.1093/emboj/20.10.2387. PMID: 11350927; PMCID: PMC125460.

Dosch R, Gawantka V, Delius H, Blumenstock C, Niehrs C. Bmp-4 acts as a morphogen in dorsoventral mesoderm patterning in Xenopus. Development. 1997 Jun;124(12):2325-34. doi: 10.1242/dev.124.12.2325. PMID: 9199359.

E. Bier, Evolution of development: Diversified dorsoventral patterning. Curr. Biol. 21, R591–R594 (2011).

Eimon PM, Harland RM. In Xenopus embryos, BMP heterodimers are not required for mesoderm induction, but BMP activity is necessary for dorsal/ventral patterning. Dev Biol. 1999 Dec 1;216(1):29-40. doi: 10.1006/dbio.1999.9496. PMID: 10588861.

Elalayli M, Hall JD, Fakhouri M, Neiswender H, Ellison TT, Han Z, Roon P, LeMosy EK. Palisade is required in the Drosophila ovary for assembly and function of the protective vitelline membrane. Dev Biol. 2008 Jul 15;319(2):359-69. doi: 10.1016/j.ydbio.2008.04.035. Epub 2008 May 8. PMID: 18514182; PMCID: PMC2536644.

Fainsod A, Steinbeisser H, De Robertis EM. On the function of BMP-4 in patterning the marginal zone of the Xenopus embryo. EMBO J. 1994 Nov 1;13(21):5015-25. doi: 10.1002/j.1460-2075.1994.tb06830.x. PMID: 7957067; PMCID: PMC395447.

Faure S, Lee MA, Keller T, ten Dijke P, Whitman M. Endogenous patterns of TGFbeta superfamily signaling during early Xenopus development. Development. 2000 Jul;127(13):2917-31. doi: 10.1242/dev.127.13.2917. PMID: 10851136.

Fekany-Lee K, Gonzalez E, Miller-Bertoglio V, Solnica-Krezel L. The homeobox gene bozozok promotes anterior neuroectoderm formation in zebrafish through negative regulation of BMP2/4 and Wnt pathways. Development. 2000 Jun;127(11):2333-45. doi: 10.1242/dev.127.11.2333. PMID: 10804176.

Fernandez NQ, Grosshans J, Goltz JS, Stein D. Separable and redundant regulatory determinants in Cactus mediate its dorsal group dependent degradation. Development. 2001 Aug;128(15):2963-74. doi: 10.1242/dev.128.15.2963. PMID: 11532919.

Franzenburg S, Fraune S, Künzel S, Baines JF, Domazet-Loso T, Bosch TC. MyD88-deficient Hydra reveal an ancient function of TLR signaling in sensing bacterial colonizers. Proc Natl Acad Sci U S A.

2012 Nov 20;109(47):19374-9. doi: 10.1073/pnas.1213110109. Epub 2012 Oct 29. PMID: 23112184; PMCID: PMC3511086.

Fritz BR, Sheets MD. Regulation of the mRNAs encoding proteins of the BMP signaling pathway during the maternal stages of Xenopus development. Dev Biol. 2001 Aug 1;236(1):230-43. doi: 10.1006/dbio.2001.0324. PMID: 11456457.

Fürthauer M, Reifers F, Brand M, Thisse B, Thisse C. sprouty4 acts in vivo as a feedback-induced antagonist of FGF signaling in zebrafish. Development. 2001 Jun;128(12):2175-86. doi: 10.1242/dev.128.12.2175. PMID: 11493538.

Fürthauer M, Thisse B, Thisse C. Three different noggin genes antagonize the activity of bone morphogenetic proteins in the zebrafish embryo. Dev Biol. 1999 Oct 1;214(1):181-96. doi: 10.1006/dbio.1999.9401. PMID: 10491267.

Fürthauer M, Thisse C, Thisse B. A role for FGF-8 in the dorsoventral patterning of the zebrafish gastrula. Development. 1997 Nov;124(21):4253-64. doi: 10.1242/dev.124.21.4253. PMID: 9334274.

Fürthauer M, Van Celst J, Thisse C, Thisse B. Fgf signalling controls the dorsoventral patterning of the zebrafish embryo. Development. 2004 Jun;131(12):2853-64. doi: 10.1242/dev.01156. Epub 2004 May 19. PMID: 15151985.

Galindo RL, Edwards DN, Gillespie SK, Wasserman SA. Interaction of the pelle kinase with the membrane-associated protein tube is required for transduction of the dorsoventral signal in Drosophila embryos. Development. 1995 Jul;121(7):2209-18. doi: 10.1242/dev.121.7.2209. PMID: 7635064.

Gaviño MA, Reddien PW. A Bmp/Admp regulatory circuit controls maintenance and regeneration of dorsal-ventral polarity in planarians. Curr Biol. 2011 Feb 22;21(4):294-9. doi: 10.1016/j.cub.2011.01.017. Epub 2011 Feb 3. PMID: 21295483; PMCID: PMC3079492.

Ge G, Greenspan DS. Developmental roles of the BMP1/TLD metalloproteinases. Birth Defects Res C Embryo Today. 2006 Mar;78(1):47-68. doi: 10.1002/bdrc.20060. PMID: 16622848.

Geisler R, Bergmann A, Hiromi Y, Nüsslein-Volhard C. cactus, a gene involved in dorsoventral pattern formation of Drosophila, is related to the I kappa B gene family of vertebrates. Cell. 1992 Nov 13;71(4):613-21. doi: 10.1016/0092-8674(92)90595-4. PMID: 1423618.

Genikhovich G, Fried P, Prünster MM, Schinko JB, Gilles AF, Fredman D, Meier K, Iber D, Technau U. Axis Patterning by BMPs: Cnidarian Network Reveals Evolutionary Constraints. Cell Rep. 2015 Mar 17;10(10):1646-1654. doi: 10.1016/j.celrep.2015.02.035. Epub 2015 Mar 12. PMID: 25772352; PMCID: PMC4460265.

Ghosh S, Gifford AM, Riviere LR, Tempst P, Nolan GP, Baltimore D. Cloning of the p50 DNA binding subunit of NF-kappa B: homology to rel and dorsal. Cell. 1990 Sep 7;62(5):1019-29. doi: 10.1016/0092-8674(90)90276-k. PMID: 2203532.

Gigliotti S, Graziani F, De Ponti L, Rafti F, Manzi A, Lavorgna G, Gargiulo G, Malva C. Sex-, tissue-, and stage-specific expression of a vitelline membrane protein gene from region 32 of the second chromosome of Drosophila melanogaster. Dev Genet. 1989;10(1):33-41. doi: 10.1002/dvg.1020100106. PMID: 2495206.

Gilmore TD, Wolenski FS. NF-κB: where did it come from and why? Immunol Rev. 2012 Mar;246(1):14-35. doi: 10.1111/j.1600-065X.2012.01096.x. PMID: 22435545.

Goff DJ, Nilson LA, Morisato D. Establishment of dorsal-ventral polarity of the Drosophila egg requires capicua action in ovarian follicle cells. Development. 2001 Nov;128(22):4553-62. doi: 10.1242/dev.128.22.4553. PMID: 11714680.

Goltsev Y, Fuse N, Frasch M, Zinzen RP, Lanzaro G, Levine M. Evolution of the dorsal-ventral patterning network in the mosquito, Anopheles gambiae. Development. 2007 Jul;134(13):2415-24. doi: 10.1242/dev.02863. Epub 2007 May 23. PMID: 17522157.

Gómez-Skarmeta J, de La Calle-Mustienes E, Modolell J. The Wnt-activated Xiro1 gene encodes a repressor that is essential for neural development and downregulates Bmp4. Development. 2001 Feb;128(4):551-60. doi: 10.1242/dev.128.4.551. PMID: 11171338.

Gonzalez EM, Fekany-Lee K, Carmany-Rampey A, Erter C, Topczewski J, Wright CV, Solnica-Krezel L. Head and trunk in zebrafish arise via coinhibition of BMP signaling by bozozok and chordino. Genes Dev. 2000 Dec 15;14(24):3087-92. doi: 10.1101/gad.852400. PMID: 11124801; PMCID: PMC317122.

Goodman SA, Albano R, Wardle FC, Matthews G, Tannahill D, Dale L. BMP1-related metalloproteinases promote the development of ventral mesoderm in early Xenopus embryos. Dev Biol. 1998 Mar 15;195(2):144-57. doi: 10.1006/dbio.1997.8840. PMID: 9520331.

Grabherr MG, Haas BJ, Yassour M, Levin JZ, Thompson DA, Amit I, Adiconis X, Fan L, Raychowdhury R, Zeng Q, Chen Z, Mauceli E, Hacohen N, Gnirke A, Rhind N, di Palma F, Birren BW, Nusbaum C, Lindblad-Toh K, Friedman N, Regev A. Full-length transcriptome assembly from RNA-Seq data without a reference genome. Nat Biotechnol. 2011 May 15;29(7):644-52. doi: 10.1038/nbt.1883. PMID: 21572440; PMCID: PMC3571712.

Grosshans J, Bergmann A, Haffter P, Nüsslein-Volhard C. Activation of the kinase Pelle by Tube in the dorsoventral signal transduction pathway of Drosophila embryo. Nature. 1994 Dec 8;372(6506):563-6. doi: 10.1038/372563a0. PMID: 7527496.

Hammerschmidt M, Pelegri F, Mullins MC, Kane DA, van Eeden FJ, Granato M, Brand M, Furutani-Seiki M, Haffter P, Heisenberg CP, Jiang YJ, Kelsh RN, Odenthal J, Warga RM, Nüsslein-Volhard C. dino and mercedes, two genes regulating dorsal development in the zebrafish embryo. Development. 1996 Dec;123:95-102. doi: 10.1242/dev.123.1.95. PMID: 9007232.

Hammonds AS, Bristow CA, Fisher WW, Weiszmann R, Wu S, Hartenstein V, Kellis M, Yu B, Frise E, Celniker SE. Spatial expression of transcription factors in Drosophila embryonic organ development. Genome Biol. 2013 Dec 20;14(12):R140. doi: 10.1186/gb-2013-14-12-r140. PMID: 24359758; PMCID: PMC4053779.

Hashimoto C, Gerttula S, Anderson KV. Plasma membrane localization of the Toll protein in the syncytial Drosophila embryo: importance of transmembrane signaling for dorsal-ventral pattern formation. Development. 1991 Apr;111(4):1021-8. doi: 10.1242/dev.111.4.1021. PMID: 1879347.

Hashimoto C, Hudson KL, Anderson KV. The Toll gene of Drosophila, required for dorsal-ventral embryonic polarity, appears to encode a transmembrane protein. Cell. 1988 Jan 29;52(2):269-79. doi: 10.1016/0092-8674(88)90516-8. PMID: 2449285.

Hashimoto C, Kim DR, Weiss LA, Miller JW, Morisato D. Spatial regulation of developmental signaling by a serpin. Dev Cell. 2003 Dec;5(6):945-50. doi: 10.1016/s1534-5807(03)00338-1. PMID: 14667416.

Hayden MS, Ghosh S. NF-κB, the first quarter-century: remarkable progress and outstanding questions. Genes Dev. 2012 Feb 1;26(3):203-34. doi: 10.1101/gad.183434.111. PMID: 22302935; PMCID: PMC3278889.

Hemmati-Brivanlou A, Kelly OG, Melton DA. Follistatin, an antagonist of activin, is expressed in the Spemann organizer and displays direct neuralizing activity. Cell. 1994 Apr 22;77(2):283-95. doi: 10.1016/0092-8674(94)90320-4. PMID: 8168135.

Hemmati-Brivanlou A, Thomsen GH. Ventral mesodermal patterning in Xenopus embryos: expression patterns and activities of BMP-2 and BMP-4. Dev Genet. 1995;17(1):78-89. doi: 10.1002/dvg.1020170109. PMID: 7554498.

Holland PW. Evolution of homeobox genes. Wiley Interdiscip Rev Dev Biol. 2013 Jan-Feb;2(1):31-45. doi: 10.1002/wdev.78. Epub 2012 Sep 10. PMID: 23799629.

Holley SA, Neul JL, Attisano L, Wrana JL, Sasai Y, O'Connor MB, De Robertis EM, Ferguson EL. The Xenopus dorsalizing factor noggin ventralizes Drosophila embryos by preventing DPP from activating its receptor. Cell. 1996 Aug 23;86(4):607-17. doi: 10.1016/s0092-8674(00)80134-8. PMID: 8752215.

Hong JW, Hendrix DA, Papatsenko D, Levine MS. How the Dorsal gradient works: insights from postgenome technologies. Proc Natl Acad Sci U S A. 2008 Dec 23;105(51):20072-6. doi: 10.1073/pnas.0806476105. Epub 2008 Dec 22. PMID: 19104040; PMCID: PMC2629255.

Huang JD, Dubnicoff T, Liaw GJ, Bai Y, Valentine SA, Shirokawa JM, Lengyel JA, Courey AJ. Binding sites for transcription factor NTF-1/Elf-1 contribute to the ventral repression of decapentaplegic. Genes Dev. 1995 Dec 15;9(24):3177-89. doi: 10.1101/gad.9.24.3177. PMID: 8543160.

Huang JD, Schwyter DH, Shirokawa JM, Courey AJ. The interplay between multiple enhancer and silencer elements defines the pattern of decapentaplegic expression. Genes Dev. 1993 Apr;7(4):694-704. doi: 10.1101/gad.7.4.694. PMID: 8458580.

Hughes CL, Kaufman TC. RNAi analysis of Deformed, proboscipedia and Sex combs reduced in the milkweed bug Oncopeltus fasciatus: novel roles for Hox genes in the hemipteran head. Development. 2000 Sep;127(17):3683-94. doi: 10.1242/dev.127.17.3683. PMID: 10934013.

Ip YT, Kraut R, Levine M, Rushlow CA. The dorsal morphogen is a sequence-specific DNA-binding protein that interacts with a long-range repression element in Drosophila. Cell. 1991 Jan 25;64(2):439-46. doi: 10.1016/0092-8674(91)90651-e. PMID: 1988156.

Ip YT, Levine M, Bier E. Neurogenic expression of snail is controlled by separable CNS and PNS promoter elements. Development. 1994 Jan;120(1):199-207. doi: 10.1242/dev.120.1.199. PMID: 8119127.

Ip YT, Park RE, Kosman D, Bier E, Levine M. The dorsal gradient morphogen regulates stripes of rhomboid expression in the presumptive neuroectoderm of the Drosophila embryo. Genes Dev. 1992 Sep;6(9):1728-39. doi: 10.1101/gad.6.9.1728. PMID: 1325394.

Jacobs CG, Rezende GL, Lamers GE, van der Zee M. The extraembryonic serosa protects the insect egg against desiccation. Proc Biol Sci. 2013 Jun 19;280(1764):20131082. doi: 10.1098/rspb.2013.1082. PMID: 23782888; PMCID: PMC3712428.

Jacobs CG, Spaink HP, van der Zee M. The extraembryonic serosa is a frontier epithelium providing the insect egg with a full-range innate immune response. Elife. 2014 Dec 9;3:e04111. doi: 10.7554/eLife.04111. PMID: 25487990; PMCID: PMC4358341.

Jiang H, Kanost MR. The clip-domain family of serine proteinases in arthropods. Insect Biochem Mol Biol. 2000 Feb;30(2):95-105. doi: 10.1016/s0965-1748(99)00113-7. PMID: 10696585.

Jiang J, Cai H, Zhou Q, Levine M. Conversion of a dorsal-dependent silencer into an enhancer: evidence for dorsal corepressors. EMBO J. 1993 Aug;12(8):3201-9. doi: 10.1002/j.1460-2075.1993.tb05989.x. PMID: 8344257; PMCID: PMC413587.

Jiang J, Levine M. Binding affinities and cooperative interactions with bHLH activators delimit threshold responses to the dorsal gradient morphogen. Cell. 1993 Mar 12;72(5):741-52. doi: 10.1016/0092-8674(93)90402-c. PMID: 8453668.

Jinek M, Doudna JA. A three-dimensional view of the molecular machinery of RNA interference. Nature. 2009 Jan 22;457(7228):405-12. doi: 10.1038/nature07755. PMID: 19158786.

Jones CM, Smith JC. Establishment of a BMP-4 morphogen gradient by long-range inhibition. Dev Biol. 1998 Feb 1;194(1):12-7. doi: 10.1006/dbio.1997.8752. PMID: 9473328.

Kamimura M, Matsumoto K, Koshiba-Takeuchi K, Ogura T. Vertebrate crossveinless 2 is secreted and acts as an extracellular modulator of the BMP signaling cascade. Dev Dyn. 2004 Jul;230(3):434-45. doi: 10.1002/dvdy.20069. PMID: 15188429.

Kamiyama S, Suda T, Ueda R, Suzuki M, Okubo R, Kikuchi N, Chiba Y, Goto S, Toyoda H, Saigo K, Watanabe M, Narimatsu H, Jigami Y, Nishihara S. Molecular cloning and identification of 3'-phosphoadenosine 5'-phosphosulfate transporter. J Biol Chem. 2003 Jul 11;278(28):25958-63. doi: 10.1074/jbc.M302439200. Epub 2003 Apr 25. PMID: 12716889.

Kanodia JS, Rikhy R, Kim Y, Lund VK, DeLotto R, Lippincott-Schwartz J, Shvartsman SY. Dynamics of the Dorsal morphogen gradient. Proc Natl Acad Sci U S A. 2009 Dec 22;106(51):21707-12. doi: 10.1073/pnas.0912395106. Epub 2009 Dec 8. PMID: 19996178; PMCID: PMC2799810.

Kanost MR, Gorman MJ. Phenoloxidases in insect immunity. 2008. Insect Immunology, (San Diego, CA: Academic Press & Elsevier;), 69–96.

Karaulanov E, Knöchel W, Niehrs C. Transcriptional regulation of BMP4 synexpression in transgenic Xenopus. EMBO J. 2004 Feb 25;23(4):844-56. doi: 10.1038/sj.emboj.7600101. Epub 2004 Feb 12. PMID: 14963489; PMCID: PMC381009.

Khokha MK, Yeh J, Grammer TC, Harland RM. Depletion of three BMP antagonists from Spemann's organizer leads to a catastrophic loss of dorsal structures. Dev Cell. 2005 Mar;8(3):401-11. doi: 10.1016/j.devcel.2005.01.013. PMID: 15737935.

Kidd S. Characterization of the Drosophila cactus locus and analysis of interactions between cactus and dorsal proteins. Cell. 1992 Nov 13;71(4):623-35. doi: 10.1016/0092-8674(92)90596-5. PMID: 1423619.

Kieran M, Blank V, Logeat F, Vandekerckhove J, Lottspeich F, Le Bail O, Urban MB, Kourilsky P, Baeuerle PA, Israël A. The DNA binding subunit of NF-kappa B is identical to factor KBF1 and homologous to the rel oncogene product. Cell. 1990 Sep 7;62(5):1007-18. doi: 10.1016/0092-8674(90)90275-j. PMID: 2203531.

Kirov N, Childs S, O'Connor M, Rushlow C. The Drosophila dorsal morphogen represses the tolloid gene by interacting with a silencer element. Mol Cell Biol. 1994 Jan;14(1):713-22. doi: 10.1128/mcb.14.1.713-722.1994. PMID: 8264640; PMCID: PMC358420.

Kirov N, Zhelnin L, Shah J, Rushlow C. Conversion of a silencer into an enhancer: evidence for a co-repressor in dorsal-mediated repression in Drosophila. EMBO J. 1993 Aug;12(8):3193-9. doi: 10.1002/j.1460-2075.1993.tb05988.x. PMID: 8344256; PMCID: PMC413585.

Kishimoto Y, Lee KH, Zon L, Hammerschmidt M, Schulte-Merker S. The molecular nature of zebrafish swirl: BMP2 function is essential during early dorsoventral patterning. Development. 1997 Nov;124(22):4457-66. doi: 10.1242/dev.124.22.4457. PMID: 9409664.

Kobayashi M, Habuchi H, Habuchi O, Saito M, Kimata K. Purification and characterization of heparan sulfate 2-sulfotransferase from cultured Chinese hamster ovary cells. J Biol Chem. 1996 Mar 29;271(13):7645-53. doi: 10.1074/jbc.271.13.7645. PMID: 8631801.

Kobayashi M, Habuchi H, Yoneda M, Habuchi O, Kimata K. Molecular cloning and expression of Chinese hamster ovary cell heparan-sulfate 2-sulfotransferase. J Biol Chem. 1997 May 23;272(21):13980-5. doi: 10.1074/jbc.272.21.13980. PMID: 9153262.

Kobayashi M, Sugumaran G, Liu J, Shworak NW, Silbert JE, Rosenberg RD. Molecular cloning and characterization of a human uronyl 2-sulfotransferase that sulfates iduronyl and glucuronyl residues in dermatan/chondroitin sulfate. J Biol Chem. 1999 Apr 9;274(15):10474-80. doi: 10.1074/jbc.274.15.10474. PMID: 10187838.

Konopová B, Zrzavý J. Ultrastructure, development, and homology of insect embryonic cuticles. J Morphol. 2005 Jun;264(3):339-62. doi: 10.1002/jmor.10338. PMID: 15838850.

Konrad KD, Goralski TJ, Mahowald AP, Marsh JL. The gastrulation defective gene of Drosophila melanogaster is a member of the serine protease superfamily. Proc Natl Acad Sci U S A. 1998 Jun 9;95(12):6819-24. doi: 10.1073/pnas.95.12.6819. PMID: 9618496; PMCID: PMC22648.

Konsolaki M, Schüpbach T. windbeutel, a gene required for dorsoventral patterning in Drosophila, encodes a protein that has homologies to vertebrate proteins of the endoplasmic reticulum. Genes Dev. 1998 Jan 1;12(1):120-31. doi: 10.1101/gad.12.1.120. PMID: 9420336; PMCID: PMC316405.

Koos DS, Ho RK. The nieuwkoid/dharma homeobox gene is essential for bmp2b repression in the zebrafish pregastrula. Dev Biol. 1999 Nov 15;215(2):190-207. doi: 10.1006/dbio.1999.9479. PMID: 10545230.

Kramer C, Mayr T, Nowak M, Schumacher J, Runke G, Bauer H, Wagner DS, Schmid B, Imai Y, Talbot WS, Mullins MC, Hammerschmidt M. Maternally supplied Smad5 is required for ventral specification in zebrafish embryos prior to zygotic Bmp signaling. Dev Biol. 2002 Oct 15;250(2):263-79. PMID: 12376102.

Kretzschmar M, Liu F, Hata A, Doody J, Massagué J. The TGF-beta family mediator Smad1 is phosphorylated directly and activated functionally by the BMP receptor kinase. Genes Dev. 1997 Apr 15;11(8):984-95. doi: 10.1101/gad.11.8.984. PMID: 9136927.

Kuo DH, Weisblat DA. A new molecular logic for BMP-mediated dorsoventral patterning in the leech Helobdella. Curr Biol. 2011 Aug 9;21(15):1282-8. doi: 10.1016/j.cub.2011.06.024. Epub 2011 Jul 21. PMID: 21782437; PMCID: PMC3152669.

Kuroda H, Fuentealba L, Ikeda A, Reversade B, De Robertis EM. Default neural induction: neuralization of dissociated Xenopus cells is mediated by Ras/MAPK activation. Genes Dev. 2005 May 1;19(9):1022-7. doi: 10.1101/gad.1306605. PMID: 15879552; PMCID: PMC1091736.

Kuroda H, Wessely O, De Robertis EM. Neural induction in Xenopus: requirement for ectodermal and endomesodermal signals via Chordin, Noggin, beta-Catenin, and Cerberus. PLoS Biol. 2004 May;2(5):E92. doi: 10.1371/journal.pbio.0020092. Epub 2004 May 11. PMID: 15138495; PMCID: PMC406387.

Langmead B, Trapnell C, Pop M, Salzberg SL. Ultrafast and memory-efficient alignment of short DNA sequences to the human genome. Genome Biol. 2009;10(3):R25. doi: 10.1186/gb-2009-10-3-r25. Epub 2009 Mar 4. PMID: 19261174; PMCID: PMC2690996.

Lapraz F, Besnardeau L, Lepage T. Patterning of the dorsal-ventral axis in echinoderms: insights into the evolution of the BMP-chordin signaling network. PLoS Biol. 2009 Nov;7(11):e1000248. doi: 10.1371/journal.pbio.1000248. Epub 2009 Nov 24. PMID: 19956794; PMCID: PMC2772021.

Law RH, Zhang Q, McGowan S, Buckle AM, Silverman GA, Wong W, Rosado CJ, Langendorf CG, Pike RN, Bird PI, Whisstock JC. An overview of the serpin superfamily. Genome Biol. 2006;7(5):216. doi: 10.1186/gb-2006-7-5-216. Epub 2006 May 30. PMID: 16737556; PMCID: PMC1779521.

Le Dréau G, Martí E. Dorsal-ventral patterning of the neural tube: a tale of three signals. Dev Neurobiol. 2012 Dec;72(12):1471-81. doi: 10.1002/dneu.22015. Epub 2012 Jul 20. PMID: 22821665.

Lécuyer E, Yoshida H, Parthasarathy N, Alm C, Babak T, Cerovina T, Hughes TR, Tomancak P, Krause HM. Global analysis of mRNA localization reveals a prominent role in organizing cellular architecture and function. Cell. 2007 Oct 5;131(1):174-87. doi: 10.1016/j.cell.2007.08.003. PMID: 17923096.

Lehming N, Thanos D, Brickman JM, Ma J, Maniatis T, Ptashne M. An HMG-like protein that can switch a transcriptional activator to a repressor. Nature. 1994 Sep 8;371(6493):175-9. doi: 10.1038/371175a0. PMID: 8072548.

Lekven AC, Thorpe CJ, Waxman JS, Moon RT. Zebrafish wnt8 encodes two wnt8 proteins on a bicistronic transcript and is required for mesoderm and neurectoderm patterning. Dev Cell. 2001 Jul;1(1):103-14. doi: 10.1016/s1534-5807(01)00007-7. PMID: 11703928.

Lemaire P, Garrett N, Gurdon JB. Expression cloning of Siamois, a Xenopus homeobox gene expressed in dorsal-vegetal cells of blastulae and able to induce a complete secondary axis. Cell. 1995 Apr 7;81(1):85-94. doi: 10.1016/0092-8674(95)90373-9. PMID: 7720076.

Lemaitre B, Nicolas E, Michaut L, Reichhart JM, Hoffmann JA. Pillars article: the dorsoventral regulatory gene cassette spätzle/Toll/cactus controls the potent antifungal response in Drosophila adults. Cell. 1996. 86: 973-983. J Immunol. 2012 Jun 1;188(11):5210-20. PMID: 22611248.

LeMosy EK, Tan YQ, Hashimoto C. Activation of a protease cascade involved in patterning the Drosophila embryo. Proc Natl Acad Sci U S A. 2001 Apr 24;98(9):5055-60. doi: 10.1073/pnas.081026598. Epub 2001 Apr 10. PMID: 11296245; PMCID: PMC33162.

LeMosy EK. Spatially dependent activation of the patterning protease, Easter. FEBS Lett. 2006 Apr 17;580(9):2269-72. doi: 10.1016/j.febslet.2006.03.036. Epub 2006 Mar 20. PMID: 16566925; PMCID: PMC2644372.

Leptin M, Grunewald B. Cell shape changes during gastrulation in Drosophila. Development. 1990 Sep;110(1):73-84. doi: 10.1242/dev.110.1.73. PMID: 2081472.

Leptin M. twist and snail as positive and negative regulators during Drosophila mesoderm development. Genes Dev. 1991 Sep;5(9):1568-76. doi: 10.1101/gad.5.9.1568. PMID: 1884999.

Leulier F, Lemaitre B. Toll-like receptors--taking an evolutionary approach. Nat Rev Genet. 2008 Mar;9(3):165-78. doi: 10.1038/nrg2303. PMID: 18227810.

Leung T, Bischof J, Söll I, Niessing D, Zhang D, Ma J, Jäckle H, Driever W. bozozok directly represses bmp2b transcription and mediates the earliest dorsoventral asymmetry of bmp2b expression in zebrafish. Development. 2003 Aug;130(16):3639-49. doi: 10.1242/dev.00558. PMID: 12835381.

Li B, Dewey CN. RSEM: accurate transcript quantification from RNA-Seq data with or without a reference genome. BMC Bioinformatics. 2011 Aug 4;12:323. doi: 10.1186/1471-2105-12-323. PMID: 21816040; PMCID: PMC3163565.

Liang HL, Nien CY, Liu HY, Metzstein MM, Kirov N, Rushlow C. The zinc-finger protein Zelda is a key activator of the early zygotic genome in Drosophila. Nature. 2008 Nov 20;456(7220):400-3. doi: 10.1038/nature07388. Epub 2008 Oct 19. PMID: 18931655; PMCID: PMC2597674.

Liberman LM, Reeves GT, Stathopoulos A. Quantitative imaging of the Dorsal nuclear gradient reveals limitations to threshold-dependent patterning in Drosophila. Proc Natl Acad Sci U S A. 2009 Dec 29;106(52):22317-22. doi: 10.1073/pnas.0906227106. Epub 2009 Dec 16. PMID: 20018754; PMCID: PMC2799780.

Liberman LM, Stathopoulos A. Design flexibility in cis-regulatory control of gene expression: synthetic and comparative evidence. Dev Biol. 2009 Mar 15;327(2):578-89. doi: 10.1016/j.ydbio.2008.12.020. Epub 2008 Dec 25. PMID: 19135437; PMCID: PMC2746413.

Ligoxygakis P, Roth S, Reichhart JM. A serpin regulates dorsal-ventral axis formation in the Drosophila embryo. Curr Biol. 2003 Dec 2;13(23):2097-102. doi: 10.1016/j.cub.2003.10.062. PMID: 14654000.

Little SC, Mullins MC. Extracellular modulation of BMP activity in patterning the dorsoventral axis. Birth Defects Res C Embryo Today. 2006 Sep;78(3):224-42. doi: 10.1002/bdrc.20079. PMID: 17061292.

Liu P, Kaufman TC. Morphology and husbandry of the large milkweed bug, Oncopeltus fasciatus. Cold Spring Harb Protoc. 2009 Aug;2009(8):pdb.emo127. doi: 10.1101/pdb.emo127. PMID: 20147229.

Liu PZ, Kaufman TC. even-skipped is not a pair-rule gene but has segmental and gap-like functions in Oncopeltus fasciatus, an intermediate germband insect. Development. 2005 May;132(9):2081-92. doi: 10.1242/dev.01807. Epub 2005 Mar 23. PMID: 15788450.

Liu PZ, Kaufman TC. hunchback is required for suppression of abdominal identity, and for proper germband growth and segmentation in the intermediate germband insect Oncopeltus fasciatus. Development. 2004 Apr;131(7):1515-27. doi: 10.1242/dev.01046. Epub 2004 Mar 3. PMID: 14998925.

Lüders F, Segawa H, Stein D, Selva EM, Perrimon N, Turco SJ, Häcker U. Slalom encodes an adenosine 3'-phosphate 5'-phosphosulfate transporter essential for development in Drosophila. EMBO J. 2003 Jul 15;22(14):3635-44. doi: 10.1093/emboj/cdg345. PMID: 12853478; PMCID: PMC165615.

Luschnig S, Moussian B, Krauss J, Desjeux I, Perkovic J, Nüsslein-Volhard C. An F1 genetic screen for maternal-effect mutations affecting embryonic pattern formation in Drosophila melanogaster. Genetics. 2004 May;167(1):325-42. doi: 10.1534/genetics.167.1.325. PMID: 15166158; PMCID: PMC1470860.

Markstein M, Zinzen R, Markstein P, Yee KP, Erives A, Stathopoulos A, Levine M. A regulatory code for neurogenic gene expression in the Drosophila embryo. Development. 2004 May;131(10):2387-94. doi: 10.1242/dev.01124. PMID: 15128669.

Martínez-Barberá JP, Toresson H, Da Rocha S, Krauss S. Cloning and expression of three members of the zebrafish Bmp family: Bmp2a, Bmp2b and Bmp4. Gene. 1997 Oct 1;198(1-2):53-9. doi: 10.1016/s0378-1119(97)00292-8. PMID: 9370264.

Metz A, Knöchel S, Büchler P, Köster M, Knöchel W. Structural and functional analysis of the BMP-4 promoter in early embryos of Xenopus laevis. Mech Dev. 1998 Jun;74(1-2):29-39. doi: 10.1016/s0925-4773(98)00059-8. PMID: 9651472.

Miller-Bertoglio VE, Fisher S, Sánchez A, Mullins MC, Halpern ME. Differential regulation of chordin expression domains in mutant zebrafish. Dev Biol. 1997 Dec 15;192(2):537-50. doi: 10.1006/dbio.1997.8788. PMID: 9441687.

Mintzer KA, Lee MA, Runke G, Trout J, Whitman M, Mullins MC. Lost-a-fin encodes a type I BMP receptor, Alk8, acting maternally and zygotically in dorsoventral pattern formation. Development. 2001 Mar;128(6):859-69. doi: 10.1242/dev.128.6.859. PMID: 11222141.

Misra S, Hecht P, Maeda R, Anderson KV. Positive and negative regulation of Easter, a member of the serine protease family that controls dorsal-ventral patterning in the Drosophila embryo. Development. 1998 Apr;125(7):1261-7. doi: 10.1242/dev.125.7.1261. PMID: 9477324.

Miyata T, Hiranaga M, Umezu M, Iwanaga S. Amino acid sequence of the coagulogen from Limulus polyphemus hemocytes. J Biol Chem. 1984 Jul 25;259(14):8924-33. PMID: 6378904.

Molina MD, Neto A, Maeso I, Gómez-Skarmeta JL, Saló E, Cebrià F. Noggin and noggin-like genes control dorsoventral axis regeneration in planarians. Curr Biol. 2011 Feb 22;21(4):300-5. doi: 10.1016/j.cub.2011.01.016. Epub 2011 Feb 3. PMID: 21295481.

Morisato D, Anderson KV. The spätzle gene encodes a component of the extracellular signaling pathway establishing the dorsal-ventral pattern of the Drosophila embryo. Cell. 1994 Feb 25;76(4):677-88. doi: 10.1016/0092-8674(94)90507-x. PMID: 8124709.

Moser M, Binder O, Wu Y, Aitsebaomo J, Ren R, Bode C, Bautch VL, Conlon FL, Patterson C. BMPER, a novel endothelial cell precursor-derived protein, antagonizes bone morphogenetic protein signaling

and endothelial cell differentiation. Mol Cell Biol. 2003 Aug;23(16):5664-79. doi: 10.1128/MCB.23.16.5664-5679.2003. PMID: 12897139; PMCID: PMC166349.

Muraoka O, Shimizu T, Yabe T, Nojima H, Bae YK, Hashimoto H, Hibi M. Sizzled controls dorso-ventral polarity by repressing cleavage of the Chordin protein. Nat Cell Biol. 2006 Apr;8(4):329-38. doi: 10.1038/ncb1379. Epub 2006 Mar 5. PMID: 16518392.

Muta T, Hashimoto R, Miyata T, Nishimura H, Toh Y, Iwanaga S. Proclotting enzyme from horseshoe crab hemocytes. cDNA cloning, disulfide locations, and subcellular localization. J Biol Chem. 1990 Dec 25;265(36):22426-33. PMID: 2266134.

Nakamura T, Yoshizaki M, Ogawa S, Okamoto H, Shinmyo Y, Bando T, Ohuchi H, Noji S, Mito T. Imaging of transgenic cricket embryos reveals cell movements consistent with a syncytial patterning mechanism. Curr Biol. 2010 Sep 28;20(18):1641-7. doi: 10.1016/j.cub.2010.07.044. Epub 2010 Aug 26. PMID: 20800488.

Nappi AJ, Christensen BM. Melanogenesis and associated cytotoxic reactions: applications to insect innate immunity. Insect Biochem Mol Biol. 2005 May;35(5):443-59. doi: 10.1016/j.ibmb.2005.01.014. PMID: 15804578.

Neuman-Silberberg FS, Schüpbach T. The Drosophila dorsoventral patterning gene gurken produces a dorsally localized RNA and encodes a TGF alpha-like protein. Cell. 1993 Oct 8;75(1):165-74. PMID: 7691414.

Neuman-Silberberg FS, Schüpbach T. The Drosophila TGF-alpha-like protein Gurken: expression and cellular localization during Drosophila oogenesis. Mech Dev. 1996 Oct;59(2):105-13. doi: 10.1016/0925-4773(96)00567-9. PMID: 8951789.

Nguyen VH, Schmid B, Trout J, Connors SA, Ekker M, Mullins MC. Ventral and lateral regions of the zebrafish gastrula, including the neural crest progenitors, are established by a bmp2b/swirl pathway of genes. Dev Biol. 1998 Jul 1;199(1):93-110. doi: 10.1006/dbio.1998.8927. PMID: 9676195.

Niehrs C. On growth and form: a Cartesian coordinate system of Wnt and BMP signaling specifies bilaterian body axes. Development. 2010 Mar;137(6):845-57. doi: 10.1242/dev.039651. PMID: 20179091.

Nikaido M, Tada M, Saji T, Ueno N. Conservation of BMP signaling in zebrafish mesoderm patterning. Mech Dev. 1997 Jan;61(1-2):75-88. doi: 10.1016/s0925-4773(96)00625-9. PMID: 9076679.

Nishimatsu S, Suzuki A, Shoda A, Murakami K, Ueno N. Genes for bone morphogenetic proteins are differentially transcribed in early amphibian embryos. Biochem Biophys Res Commun. 1992 Aug 14;186(3):1487-95. doi: 10.1016/s0006-291x(05)81574-8. PMID: 1510675.

Nolan GP, Ghosh S, Liou HC, Tempst P, Baltimore D. DNA binding and I kappa B inhibition of the cloned p65 subunit of NF-kappa B, a rel-related polypeptide. Cell. 1991 Mar 8;64(5):961-9. doi: 10.1016/0092-8674(91)90320-x. PMID: 2001591.

Nüsslein-Volhard C, Frohnhöfer HG, Lehmann R. Determination of anteroposterior polarity in Drosophila. Science. 1987 Dec 18;238(4834):1675-81. doi: 10.1126/science.3686007. PMID: 3686007.

Nüsslein-Volhard C, Lohs-Schardin M, Sander K, Cremer C. A dorso-ventral shift of embryonic primordia in a new maternal-effect mutant of Drosophila. Nature. 1980 Jan 31;283(5746):474-6. doi: 10.1038/283474a0. PMID: 6766208.

Nüsslein-Volhard C. Maternal effect mutations that alter the spatial coordinates of the embryo of Drosophila melanogaster. In: Subtelny S, Konigsberg IR, eds. Determinants of Spatial Organization: the Thirty-Seventh Symposium of the Society for Developmental Biology. New York: Academic Press; 1979, 185–211.

O'Connor MB, Umulis D, Othmer HG, Blair SS. Shaping BMP morphogen gradients in the Drosophila embryo and pupal wing. Development. 2006 Jan;133(2):183-93. doi: 10.1242/dev.02214. PMID: 16368928; PMCID: PMC6469686.

Oelgeschläger M, Kuroda H, Reversade B, De Robertis EM. Chordin is required for the Spemann organizer transplantation phenomenon in Xenopus embryos. Dev Cell. 2003 Feb;4(2):219-30. doi: 10.1016/s1534-5807(02)00404-5. PMID: 12586065.

Padgett RW, Wozney JM, Gelbart WM. Human BMP sequences can confer normal dorsal-ventral patterning in the Drosophila embryo. Proc Natl Acad Sci U S A. 1993 Apr 1;90(7):2905-9. doi: 10.1073/pnas.90.7.2905. PMID: 8464906; PMCID: PMC46205.

Panfilio KA, Liu PZ, Akam M, Kaufman TC. Oncopeltus fasciatus zen is essential for serosal tissue function in katatrepsis. Dev Biol. 2006 Apr 1;292(1):226-43. doi: 10.1016/j.ydbio.2005.12.028. Epub 2006 Feb 7. PMID: 16460723.

Panfilio KA, Vargas Jentzsch IM, Benoit JB, Erezyilmaz D, Suzuki Y, Colella S, Robertson HM, Poelchau MF, Waterhouse RM, Ioannidis P, Weirauch MT, Hughes DST, Murali SC, Werren JH, Jacobs CGC, Duncan EJ, Armisén D, Vreede BMI, Baa-Puyoulet P, Berger CS, Chang CC, Chao H, Chen MM, Chen YT, Childers CP, Chipman AD, Cridge AG, Crumière AJJ, Dearden PK, Didion EM, Dinh H, Doddapaneni HV, Dolan A, Dugan S, Extavour CG, Febvay G, Friedrich M, Ginzburg N, Han Y, Heger P, Holmes CJ, Horn T, Hsiao YM, Jennings EC, Johnston JS, Jones TE, Jones JW, Khila A, Koelzer S, Kovacova V, Leask M, Lee SL, Lee CY, Lovegrove MR, Lu HL, Lu Y, Moore PJ, Munoz-Torres MC, Muzny DM, Palli SR, Parisot N, Pick L, Porter ML, Qu J, Refki PN, Richter R, Rivera-Pomar R, Rosendale AJ, Roth S, Sachs L, Santos ME, Seibert J, Sghaier E, Shukla JN, Stancliffe RJ, Tidswell O, Traverso L, van der Zee M, Viala S, Worley KC, Zdobnov EM, Gibbs RA, Richards S. Molecular evolutionary trends and feeding ecology diversification in the Hemiptera, anchored by the milkweed bug genome. Genome Biol. 2019 Apr 2;20(1):64. doi: 10.1186/s13059-019-1660-0. PMID: 30935422; PMCID: PMC6444547.

Panfilio KA. Extraembryonic development in insects and the acrobatics of blastokinesis. Dev Biol. 2008 Jan 15;313(2):471-91. doi: 10.1016/j.ydbio.2007.11.004. Epub 2007 Nov 17. PMID: 18082679.

Papatsenko D, Levine M. Quantitative analysis of binding motifs mediating diverse spatial readouts of the Dorsal gradient in the Drosophila embryo. Proc Natl Acad Sci U S A. 2005 Apr 5;102(14):4966-71. doi: 10.1073/pnas.0409414102. Epub 2005 Mar 28. PMID: 15795372; PMCID: PMC555988.

Park Y, Zhang Z, Linhardt RJ, LeMosy EK. Distinct heparan sulfate compositions in wild-type and pipe-mutant eggshell matrix. Fly (Austin). 2008 Jul-Aug;2(4):175-9. doi: 10.4161/fly.6706. Epub 2008 Jul 31. PMID: 18719407; PMCID: PMC2784221.

Pearson MN, Groten C, Rohrmann GF. Identification of the lymantria dispar nucleopolyhedrovirus envelope fusion protein provides evidence for a phylogenetic division of the Baculoviridae. J Virol.

2000 Jul;74(13):6126-31. doi: 10.1128/jvi.74.13.6126-6131.2000. PMID: 10846096; PMCID: PMC112111.

Pechmann M, Benton MA, Kenny NJ, Posnien N, Roth S. A novel role for *Ets4* in axis specification and cell migration in the spider *Parasteatoda tepidariorum*. Elife. 2017 Aug 29;6:e27590. doi: 10.7554/eLife.27590. PMID: 28849761; PMCID: PMC5574703.

Pechmann M. Embryonic development and secondary axis induction in the Brazilian white knee tarantula Acanthoscurria geniculata, C. L. Koch, 1841 (Araneae; Mygalomorphae; Theraphosidae). Dev Genes Evol. 2020 Mar;230(2):75-94. doi: 10.1007/s00427-020-00653-w. Epub 2020 Feb 19. PMID: 32076811; PMCID: PMC7128004.

Pera EM, Ikeda A, Eivers E, De Robertis EM. Integration of IGF, FGF, and anti-BMP signals via Smad1 phosphorylation in neural induction. Genes Dev. 2003 Dec 15;17(24):3023-8. doi: 10.1101/gad.1153603. PMID: 14701872; PMCID: PMC305254.

Peri F, Bökel C, Roth S. Local Gurken signaling and dynamic MAPK activation during Drosophila oogenesis. Mech Dev. 1999 Mar;81(1-2):75-88. doi: 10.1016/s0925-4773(98)00228-7. PMID: 10330486.

Peters C, Schmidt B, Rommerskirch W, Rupp K, Zühlsdorf M, Vingron M, Meyer HE, Pohlmann R, von Figura K. Phylogenetic conservation of arylsulfatases. cDNA cloning and expression of human arylsulfatase B. J Biol Chem. 1990 Feb 25;265(6):3374-81. PMID: 2303452.

Petersen CP, Reddien PW. Wnt signaling and the polarity of the primary body axis. Cell. 2009 Dec 11;139(6):1056-68. doi: 10.1016/j.cell.2009.11.035. PMID: 20005801.

Piccolo S, Sasai Y, Lu B, De Robertis EM. Dorsoventral patterning in Xenopus: inhibition of ventral signals by direct binding of chordin to BMP-4. Cell. 1996 Aug 23;86(4):589-98. doi: 10.1016/s0092-8674(00)80132-4. PMID: 8752213; PMCID: PMC3070603.

Popodi E, Minoo P, Burke T, Waring GL. Organization and expression of a second chromosome follicle cell gene cluster in Drosophila. Dev Biol. 1988 Jun;127(2):248-56. doi: 10.1016/0012-1606(88)90312-0. PMID: 3132408.

Price JV, Clifford RJ, Schüpbach T. The maternal ventralizing locus torpedo is allelic to faint little ball, an embryonic lethal, and encodes the Drosophila EGF receptor homolog. Cell. 1989 Mar 24;56(6):1085-92. doi: 10.1016/0092-8674(89)90641-7. PMID: 2493993.

Rafiqi AM, Lemke S, Ferguson S, Stauber M, Schmidt-Ott U. Evolutionary origin of the amnioserosa in cyclorrhaphan flies correlates with spatial and temporal expression changes of zen. Proc Natl Acad Sci U S A. 2008 Jan 8;105(1):234-9. doi: 10.1073/pnas.0709145105. Epub 2008 Jan 2. PMID: 18172205; PMCID: PMC2224192.

Rafiqi AM, Park CH, Kwan CW, Lemke S, Schmidt-Ott U. BMP-dependent serosa and amnion specification in the scuttle fly Megaselia abdita. Development. 2012 Sep;139(18):3373-82. doi: 10.1242/dev.083873. Epub 2012 Aug 8. PMID: 22874914.

Ramel MC, Buckles GR, Baker KD, Lekven AC. WNT8 and BMP2B co-regulate non-axial mesoderm patterning during zebrafish gastrulation. Dev Biol. 2005 Nov 15;287(2):237-48. doi: 10.1016/j.ydbio.2005.08.012. Epub 2005 Oct 10. PMID: 16216234.

Ramel MC, Lekven AC. Repression of the vertebrate organizer by Wnt8 is mediated by Vent and Vox. Development. 2004 Aug;131(16):3991-4000. doi: 10.1242/dev.01277. Epub 2004 Jul 21. PMID: 15269175.

Rao Y, Vaessin H, Jan LY, Jan YN. Neuroectoderm in Drosophila embryos is dependent on the mesoderm for positioning but not for formation. Genes Dev. 1991 Sep;5(9):1577-88. doi: 10.1101/gad.5.9.1577. PMID: 1885000.

Rau JC, Beaulieu LM, Huntington JA, Church FC. Serpins in thrombosis, hemostasis and fibrinolysis. J Thromb Haemost. 2007 Jul;5 Suppl 1(Suppl 1):102-15. doi: 10.1111/j.1538-7836.2007.02516.x. PMID: 17635716; PMCID: PMC2670448.

Reach M, Galindo RL, Towb P, Allen JL, Karin M, Wasserman SA. A gradient of cactus protein degradation establishes dorsoventral polarity in the Drosophila embryo. Dev Biol. 1996 Nov 25;180(1):353-64. doi: 10.1006/dbio.1996.0308. PMID: 8948598.

Reddien PW, Bermange AL, Kicza AM, Sánchez Alvarado A. BMP signaling regulates the dorsal planarian midline and is needed for asymmetric regeneration. Development. 2007 Nov;134(22):4043-51. doi: 10.1242/dev.007138. Epub 2007 Oct 17. PMID: 17942485.

Reeves GT, Stathopoulos A. Graded dorsal and differential gene regulation in the Drosophila embryo. Cold Spring Harb Perspect Biol. 2009 Oct;1(4):a000836. doi: 10.1101/cshperspect.a000836. PMID: 20066095; PMCID: PMC2773625.

Reeves GT, Trisnadi N, Truong TV, Nahmad M, Katz S, Stathopoulos A. Dorsal-ventral gene expression in the Drosophila embryo reflects the dynamics and precision of the dorsal nuclear gradient. Dev Cell. 2012 Mar 13;22(3):544-57. doi: 10.1016/j.devcel.2011.12.007. Epub 2012 Feb 16. PMID: 22342544; PMCID: PMC3469262.

Reichhart JM. Tip of another iceberg: Drosophila serpins. Trends Cell Biol. 2005 Dec;15(12):659-65. doi: 10.1016/j.tcb.2005.10.001. Epub 2005 Nov 2. PMID: 16260136.
ROBBINS PW, LIPMANN F. Isolation and identification of active sulfate. J Biol Chem. 1957 Dec;229(2):837-51. PMID: 13502346.

Robinson MD, McCarthy DJ, Smyth GK. edgeR: a Bioconductor package for differential expression analysis of digital gene expression data. Bioinformatics. 2010 Jan 1;26(1):139-40. doi: 10.1093/bioinformatics/btp616. Epub 2009 Nov 11. PMID: 19910308; PMCID: PMC2796818.

Roth S, Hiromi Y, Godt D, Nüsslein-Volhard C. cactus, a maternal gene required for proper formation of the dorsoventral morphogen gradient in Drosophila embryos. Development. 1991 Jun;112(2):371-88. doi: 10.1242/dev.112.2.371. PMID: 1794309.

Roth S, Stein D, Nüsslein-Volhard C. A gradient of nuclear localization of the dorsal protein determines dorsoventral pattern in the Drosophila embryo. Cell. 1989 Dec 22;59(6):1189-202. doi: 10.1016/0092-8674(89)90774-5. PMID: 2688897.

Rozen S, Skaletsky H. Primer3 on the WWW for general users and for biologist programmers. Methods Mol Biol. 2000;132:365-86. doi: 10.1385/1-59259-192-2:365. PMID: 10547847.

Ruben SM, Dillon PJ, Schreck R, Henkel T, Chen CH, Maher M, Baeuerle PA, Rosen CA. Isolation of a rel-related human cDNA that potentially encodes the 65-kD subunit of NF-kappa B. Science. 1991

Mar 22;251(5000):1490-3. doi: 10.1126/science.2006423. Erratum in: Science. 1991 Oct 4;254(5028):11. PMID: 2006423.

Rushlow CA, Han K, Manley JL, Levine M. The graded distribution of the dorsal morphogen is initiated by selective nuclear transport in Drosophila. Cell. 1989 Dec 22;59(6):1165-77. doi: 10.1016/0092-8674(89)90772-1. PMID: 2598265.

Sachs L, Chen YT, Drechsler A, Lynch JA, Panfilio KA, Lässig M, Berg J, Roth S. Dynamic BMP signaling polarized by Toll patterns the dorsoventral axis in a hemimetabolous insect. Elife. 2015 May 12;4:e05502. doi: 10.7554/eLife.05502. PMID: 25962855; PMCID: PMC4423117.

Sachs L. BMP signaling in the dorsal-ventral patterning system of the milkweed bug *Oncopeltus fasciatus*, PhD thesis. Universität zu Köln. 2014

Sampath TK, Rashka KE, Doctor JS, Tucker RF, Hoffmann FM. Drosophila transforming growth factor beta superfamily proteins induce endochondral bone formation in mammals. Proc Natl Acad Sci U S A. 1993 Jul 1;90(13):6004-8. doi: 10.1073/pnas.90.13.6004. PMID: 8327474; PMCID: PMC46855.

Sasai Y, Lu B, Steinbeisser H, Geissert D, Gont LK, De Robertis EM. Xenopus chordin: a novel dorsalizing factor activated by organizer-specific homeobox genes. Cell. 1994 Dec 2;79(5):779-90. doi: 10.1016/0092-8674(94)90068-x. PMID: 8001117; PMCID: PMC3082463.

Saunders C, Cohen RS. The role of oocyte transcription, the 5'UTR, and translation repression and derepression in Drosophila gurken mRNA and protein localization. Mol Cell. 1999 Jan;3(1):43-54. doi: 10.1016/s1097-2765(00)80173-2. PMID: 10024878.

Schejter ED, Shilo BZ. The Drosophila EGF receptor homolog (DER) gene is allelic to faint little ball, a locus essential for embryonic development. Cell. 1989 Mar 24;56(6):1093-104. doi: 10.1016/0092-8674(89)90642-9. PMID: 2924351.

Scherer LJ, Harris DH, Petri WH. Drosophila vitelline membrane genes contain a 114 base pair region of highly conserved coding sequence. Dev Biol. 1988 Dec;130(2):786-8. doi: 10.1016/0012-1606(88)90367-3. PMID: 3143615.

Scherfer C, Tang H, Kambris Z, Lhocine N, Hashimoto C, Lemaitre B. Drosophila Serpin-28D regulates hemolymph phenoloxidase activity and adult pigmentation. Dev Biol. 2008 Nov 15;323(2):189-96. doi: 10.1016/j.ydbio.2008.08.030. Epub 2008 Sep 9. PMID: 18801354.

Schmid B, Fürthauer M, Connors SA, Trout J, Thisse B, Thisse C, Mullins MC. Equivalent genetic roles for bmp7/snailhouse and bmp2b/swirl in dorsoventral pattern formation. Development. 2000 Mar;127(5):957-67. doi: 10.1242/dev.127.5.957. PMID: 10662635.

Schmidt J, Francois V, Bier E, Kimelman D. Drosophila short gastrulation induces an ectopic axis in Xenopus: evidence for conserved mechanisms of dorsal-ventral patterning. Development. 1995 Dec;121(12):4319-28. doi: 10.1242/dev.121.12.4319. PMID: 8575332.

Schmidt JE, Suzuki A, Ueno N, Kimelman D. Localized BMP-4 mediates dorsal/ventral patterning in the early Xenopus embryo. Dev Biol. 1995 May;169(1):37-50. doi: 10.1006/dbio.1995.1124. PMID: 7750652.

Schmieder R, Edwards R. Fast identification and removal of sequence contamination from genomic and metagenomic datasets. PLoS One. 2011 Mar 9;6(3):e17288. doi: 10.1371/journal.pone.0017288. PMID: 21408061; PMCID: PMC3052304.

Schneider DS, Jin Y, Morisato D, Anderson KV. A processed form of the Spätzle protein defines dorsal-ventral polarity in the Drosophila embryo. Development. 1994 May;120(5):1243-50. doi: 10.1242/dev.120.5.1243. PMID: 8026333.

Schohl A, Fagotto F. Beta-catenin, MAPK and Smad signaling during early Xenopus development. Development. 2002 Jan;129(1):37-52. doi: 10.1242/dev.129.1.37. Erratum in: Development. 2007 Apr;134(7):1454. PMID: 11782399.

Schulte-Merker S, Lee KJ, McMahon AP, Hammerschmidt M. The zebrafish organizer requires chordino. Nature. 1997 Jun 26;387(6636):862-3. doi: 10.1038/43092. PMID: 9202118.

Schüpbach T, Wieschaus E. Female sterile mutations on the second chromosome of Drosophila melanogaster. I. Maternal effect mutations. Genetics. 1989 Jan;121(1):101-17. doi: 10.1093/genetics/121.1.101. PMID: 2492966; PMCID: PMC1203592.

Schüpbach T. Germ line and soma cooperate during oogenesis to establish the dorsoventral pattern of egg shell and embryo in Drosophila melanogaster. Cell. 1987 Jun 5;49(5):699-707. doi: 10.1016/0092-8674(87)90546-0. PMID: 3107840.

Seher TC, Narasimha M, Vogelsang E, Leptin M. Analysis and reconstitution of the genetic cascade controlling early mesoderm morphogenesis in the Drosophila embryo. Mech Dev. 2007 Mar;124(3):167-79. doi: 10.1016/j.mod.2006.12.004. Epub 2006 Dec 27. PMID: 17267182.

Sen J, Goltz JS, Konsolaki M, Schüpbach T, Stein D. Windbeutel is required for function and correct subcellular localization of the Drosophila patterning protein Pipe. Development. 2000 Dec;127(24):5541-50. doi: 10.1242/dev.127.24.5541. PMID: 11076773.

Sen J, Goltz JS, Stevens L, Stein D. Spatially restricted expression of pipe in the Drosophila egg chamber defines embryonic dorsal-ventral polarity. Cell. 1998 Nov 13;95(4):471-81. doi: 10.1016/s0092-8674(00)81615-3. PMID: 9827800.
Shen B, Manley JL. Pelle kinase is activated by autophosphorylation during Toll signaling in Drosophila. Development. 2002 Apr;129(8):1925-33. doi: 10.1242/dev.129.8.1925. PMID: 11934858.

Shen B, Manley JL. Phosphorylation modulates direct interactions between the Toll receptor, Pelle kinase and Tube. Development. 1998 Dec;125(23):4719-28. doi: 10.1242/dev.125.23.4719. PMID: 9806920.

Simpson P. Maternal-Zygotic Gene Interactions during Formation of the Dorsoventral Pattern in Drosophila Embryos. Genetics. 1983 Nov;105(3):615-32. doi: 10.1093/genetics/105.3.615. PMID: 17246169; PMCID: PMC1202177.

Slack JM, Holland PW, Graham CF. The zootype and the phylotypic stage. Nature. 1993 Feb 11;361(6412):490-2. doi: 10.1038/361490a0. PMID: 8094230.

Smith CL, DeLotto R. A common domain within the proenzyme regions of the Drosophila snake and easter proteins and Tachypleus proclotting enzyme defines a new subfamily of serine proteases. Protein Sci. 1992 Sep;1(9):1225-6. doi: 10.1002/pro.5560010915. PMID: 1304399; PMCID: PMC2142178.

Smith CL, DeLotto R. Ventralizing signal determined by protease activation in Drosophila embryogenesis. Nature. 1994 Apr 7;368(6471):548-51. doi: 10.1038/368548a0. PMID: 8139688.

Smith WC, Harland RM. Expression cloning of noggin, a new dorsalizing factor localized to the Spemann organizer in Xenopus embryos. Cell. 1992 Sep 4;70(5):829-40. doi: 10.1016/0092-8674(92)90316-5. PMID: 1339313.

Stappert D, Frey N, von Levetzow C, Roth S. Genome-wide identification of Tribolium dorsoventral patterning genes. Development. 2016 Jul 1;143(13):2443-54. doi: 10.1242/dev.130641. Epub 2016 Jun 10. PMID: 27287803.

Stappert D, Two novel, complementary next generation sequencing approaches to reveal the dorso-ventral gene regulatory network of Tribolium castaneum. PhD thesis, Universität zu Köln. 2014

Stathopoulos A, Levine M. Dorsal gradient networks in the Drosophila embryo. Dev Biol. 2002 Jun 1;246(1):57-67. doi: 10.1006/dbio.2002.0652. PMID: 12027434.

Stathopoulos A, Van Drenth M, Erives A, Markstein M, Levine M. Whole-genome analysis of dorsal-ventral patterning in the Drosophila embryo. Cell. 2002 Nov 27;111(5):687-701. doi: 10.1016/s0092-8674(02)01087-5. PMID: 12464180.

Steen PW, Tian S, Tully SE, Cravatt BF, LeMosy EK. Activation of Snake in a serine protease cascade that defines the dorsoventral axis is atypical and pipe-independent in Drosophila embryos. FEBS Lett. 2010 Aug 20;584(16):3557-60. doi: 10.1016/j.febslet.2010.07.020. Epub 2010 Jul 16. PMID: 20638387; PMCID: PMC2942767.

Stein D, Charatsi I, Cho YS, Zhang Z, Nguyen J, DeLotto R, Luschnig S, Moussian B. Localization and activation of the Drosophila protease easter require the ER-resident saposin-like protein seele. Curr Biol. 2010 Nov 9;20(21):1953-8. doi: 10.1016/j.cub.2010.09.069. Epub 2010 Oct 21. PMID: 20970335.

Stein D, Nüsslein-Volhard C. Multiple extracellular activities in Drosophila egg perivitelline fluid are required for establishment of embryonic dorsal-ventral polarity. Cell. 1992 Feb 7;68(3):429-40. doi: 10.1016/0092-8674(92)90181-b. PMID: 1739964.

Stein D, Roth S, Vogelsang E, Nüsslein-Volhard C. The polarity of the dorsoventral axis in the Drosophila embryo is defined by an extracellular signal. Cell. 1991 May 31;65(5):725-35. doi: 10.1016/0092-8674(91)90381-8. PMID: 1904007.

Stein DS, Stevens LM. Maternal control of the Drosophila dorsal-ventral body axis. Wiley Interdiscip Rev Dev Biol. 2014 Sep-Oct;3(5):301-30. doi: 10.1002/wdev.138. Epub 2014 May 29. PMID: 25124754; PMCID: PMC4724419.

Stern CD. Neural induction: old problem, new findings, yet more questions. Development. 2005 May;132(9):2007-21. doi: 10.1242/dev.01794. PMID: 15829523.

Steward R. Dorsal, an embryonic polarity gene in Drosophila, is homologous to the vertebrate proto-oncogene, c-rel. Science. 1987 Oct 30;238(4827):692-4. doi: 10.1126/science.3118464. PMID: 3118464.

Steward R. Relocalization of the dorsal protein from the cytoplasm to the nucleus correlates with its function. Cell. 1989 Dec 22;59(6):1179-88. doi: 10.1016/0092-8674(89)90773-3. PMID: 2598266.

Sun H, Towb P, Chiem DN, Foster BA, Wasserman SA. Regulated assembly of the Toll signaling complex drives Drosophila dorsoventral patterning. EMBO J. 2004 Jan 14;23(1):100-10. doi: 10.1038/sj.emboj.7600033. Epub 2003 Dec 18. PMID: 14685264; PMCID: PMC1271671.

Tang H, Kambris Z, Lemaitre B, Hashimoto C. A serpin that regulates immune melanization in the respiratory system of Drosophila. Dev Cell. 2008 Oct;15(4):617-26. doi: 10.1016/j.devcel.2008.08.017. PMID: 18854145; PMCID: PMC2671232.

Thio GL, Ray RP, Barcelo G, Schüpbach T. Localization of gurken RNA in Drosophila oogenesis requires elements in the 5' and 3' regions of the transcript. Dev Biol. 2000 May 15;221(2):435-46. doi: 10.1006/dbio.2000.9690. PMID: 10790337.

Thomsen GH. Antagonism within and around the organizer: BMP inhibitors in vertebrate body patterning. Trends Genet. 1997 Jun;13(6):209-11. doi: 10.1016/S0168-9525(97)01117-7. PMID: 9196324.

Timmer JR, Wang C, Niswander L. BMP signaling patterns the dorsal and intermediate neural tube via regulation of homeobox and helix-loop-helix transcription factors. Development. 2002 May;129(10):2459-72. doi: 10.1242/dev.129.10.2459. PMID: 11973277.

Tomancak P, Beaton A, Weiszmann R, Kwan E, Shu S, Lewis SE, et al. Systematic determination of patterns of gene expression during Drosophila embryogenesis. Genome Biol. 2002;3(12):RESEARCH0088. PMCID: 151190

Tomancak P, Berman BP, Beaton A, Weiszmann R, Kwan E, Hartenstein V, et al. Global analysis of patterns of gene expression during Drosophila embryogenesis. Genome Biol. 2007;8(7):R145. PMCID: 2323238

Towb P, Bergmann A, Wasserman SA. The protein kinase Pelle mediates feedback regulation in the Drosophila Toll signaling pathway. Development. 2001 Dec;128(23):4729-36. doi: 10.1242/dev.128.23.4729. PMID: 11731453.

Towb P, Galindo RL, Wasserman SA. Recruitment of Tube and Pelle to signaling sites at the surface of the Drosophila embryo. Development. 1998 Jul;125(13):2443-50. doi: 10.1242/dev.125.13.2443. PMID: 9609827.

Tsang M, Maegawa S, Kiang A, Habas R, Weinberg E, Dawid IB. A role for MKP3 in axial patterning of the zebrafish embryo. Development. 2004 Jun;131(12):2769-79. doi: 10.1242/dev.01157. Epub 2004 May 13. PMID: 15142973.

Valentine SA, Chen G, Shandala T, Fernandez J, Mische S, Saint R, Courey AJ. Dorsal-mediated repression requires the formation of a multiprotein repression complex at the ventral silencer. Mol Cell Biol. 1998 Nov;18(11):6584-94. doi: 10.1128/MCB.18.11.6584. PMID: 9774673; PMCID: PMC109243.

van der Zee M, Berns N, Roth S. Distinct functions of the Tribolium zerknüllt genes in serosa specification and dorsal closure. Curr Biol. 2005 Apr 12;15(7):624-36. doi: 10.1016/j.cub.2005.02.057. PMID: 15823534.

Vässin H, Bremer KA, Knust E, Campos-Ortega JA. The neurogenic gene Delta of Drosophila melanogaster is expressed in neurogenic territories and encodes a putative transmembrane protein with EGF-like repeats. EMBO J. 1987 Nov;6(11):3431-40. doi: 10.1002/j.1460-2075.1987.tb02666.x. PMID: 16453806; PMCID: PMC553800.

von Levetzow C. Konservierte und divergente Aspekte der twist-, snail- und concertina-Funktion im Käfer Tribolium castaneum. PhD thesis, Universität zu Köln. 2008

Wang S, Krinks M, Kleinwaks L, Moos M Jr. A novel Xenopus homologue of bone morphogenetic protein-7 (BMP-7). Genes Funct. 1997 Nov;1(4):259-71. doi: 10.1046/j.1365-4624.1997.00023.x. PMID: 9678902.

Wang Z, Gerstein M, Snyder M. RNA-Seq: a revolutionary tool for transcriptomics. Nat Rev Genet. 2009 Jan;10(1):57-63. doi: 10.1038/nrg2484. PMID: 19015660; PMCID: PMC2949280.

Weber AN, Tauszig-Delamasure S, Hoffmann JA, Lelièvre E, Gascan H, Ray KP, Morse MA, Imler JL, Gay NJ. Binding of the Drosophila cytokine Spätzle to Toll is direct and establishes signaling. Nat Immunol. 2003 Aug;4(8):794-800. doi: 10.1038/ni955. Epub 2003 Jul 20. PMID: 12872120.

Weisbrod A, Cohen M, Chipman AD. Evolution of the insect terminal patterning system--insights from the milkweed bug, Oncopeltus fasciatus. Dev Biol. 2013 Aug 1;380(1):125-31. doi: 10.1016/j.ydbio.2013.04.030. Epub 2013 May 8. PMID: 23665175.

Wilk R, Hu J, Blotsky D, Krause HM. Diverse and pervasive subcellular distributions for both coding and long noncoding RNAs. Genes Dev. 2016 Mar 1;30(5):594-609. doi: 10.1101/gad.276931.115. PMID: 26944682; PMCID: PMC4782052.

Wilson L, Maden M. The mechanisms of dorsoventral patterning in the vertebrate neural tube. Dev Biol. 2005 Jun 1;282(1):1-13. doi: 10.1016/j.ydbio.2005.02.027. PMID: 15936325.

Wilson MJ, Kenny NJ, Dearden PK. Components of the dorsal-ventral pathway also contribute to anterior-posterior patterning in honeybee embryos (Apis mellifera). Evodevo. 2014 Mar 12;5(1):11. doi: 10.1186/2041-9139-5-11. PMID: 24620747; PMCID: PMC3995682.

Wilson PA, Lagna G, Suzuki A, Hemmati-Brivanlou A. Concentration-dependent patterning of the Xenopus ectoderm by BMP4 and its signal transducer Smad1. Development. 1997 Aug;124(16):3177-84. doi: 10.1242/dev.124.16.3177. PMID: 9272958.

Wozney JM, Rosen V, Celeste AJ, Mitsock LM, Whitters MJ, Kriz RW, Hewick RM, Wang EA. Novel regulators of bone formation: molecular clones and activities. Science. 1988 Dec 16;242(4885):1528-34. doi: 10.1126/science.3201241. PMID: 3201241.

Xue Y, Zheng X, Huang L, Xu P, Ma Y, Min Z, Tao Q, Tao Y, Meng A. Organizer-derived Bmp2 is required for the formation of a correct Bmp activity gradient during embryonic development. Nat Commun. 2014 Apr 29;5:3766. doi: 10.1038/ncomms4766. PMID: 24777107; PMCID: PMC4071459.

Yu JK, Satou Y, Holland ND, Shin-I T, Kohara Y, Satoh N, Bronner-Fraser M, Holland LZ. Axial patterning in cephalochordates and the evolution of the organizer. Nature. 2007 Feb 8;445(7128):613-7. doi: 10.1038/nature05472. Epub 2007 Jan 21. PMID: 17237766.

Yu K, Srinivasan S, Shimmi O, Biehs B, Rashka KE, Kimelman D, O'Connor MB, Bier E. Processing of the Drosophila Sog protein creates a novel BMP inhibitory activity. Development. 2000 May;127(10):2143-54. doi: 10.1242/dev.127.10.2143. PMID: 10769238.

Zhang Z, Stevens LM, Stein D. Sulfation of eggshell components by Pipe defines dorsal-ventral polarity in the Drosophila embryo. Curr Biol. 2009 Jul 28;19(14):1200-5. doi: 10.1016/j.cub.2009.05.050. Epub 2009 Jun 18. PMID: 19540119; PMCID: PMC2733793.

Zhu X, Sen J, Stevens L, Goltz JS, Stein D. Drosophila pipe protein activity in the ovary and the embryonic salivary gland does not require heparan sulfate glycosaminoglycans. Development. 2005 Sep;132(17):3813-22. doi: 10.1242/dev.01962. Epub 2005 Jul 27. PMID: 16049108.

Zhu X, Stevens LM, Stein D. Synthesis of the sulfate donor PAPS in either the Drosophila germline or somatic follicle cells can support embryonic dorsal-ventral axis formation. Development. 2007 Apr;134(8):1465-9. doi: 10.1242/dev.003426. Epub 2007 Mar 7. PMID: 17344226.

Zimmerman LB, De Jesús-Escobar JM, Harland RM. The Spemann organizer signal noggin binds and inactivates bone morphogenetic protein 4. Cell. 1996 Aug 23;86(4):599-606. doi: 10.1016/s0092-8674(00)80133-6. PMID: 8752214.

Zou Z, Jiang H. Manduca sexta serpin-6 regulates immune serine proteinases PAP-3 and HP8. cDNA cloning, protein expression, inhibition kinetics, and function elucidation. J Biol Chem. 2005 Apr 8;280(14):14341-8. doi: 10.1074/jbc.M500570200. Epub 2005 Feb 3. PMID: 15691825; PMCID: PMC2047605.

Appendix

This appendix includes the output of the RNAseq analysis (see section 3.7 and Fig. 24) as tables in which the various transcriptomes of different knockdown conditions are compared to wild-type embryos. Green marks indicate upregulation compared to wild-type, red marks indicate downregulation compared to wild-type.

Table 5.: *Toll* knockdown compared to wild-type embryos

Gene ID	logFC	absolute FC	PValue	FDR
OFAS013274-RA	-9,380680613	666,6014352	6,53E-12	5,35E-09
OFAS025039-RD	-8,771158361	436,899717	1,06E-07	2,39E-05
OFAS008642-RC	-8,751758685	431,0641236	2,02E-05	0,001171561
OFAS011362-RA	-7,876915971	235,0650059	0,002076211	0,033095616
OFAS015006-RA	-7,257156219	152,9754379	0,000944283	0,019272483
OFAS008965-RA	-7,224278099	149,5286474	0,000877622	0,018195382
OFAS000081-RD	-7,023180316	130,0732346	0,001641506	0,028160063
OFAS000359-RA	-6,839790229	114,5465526	0,00360995	0,048315805
OFAS018886-RA	-5,80850466	56,04464629	1,21E-06	0,000139805
OFAS013548-RA	-4,478786021	22,29712849	0,001168425	0,022415625
OFAS013259-RA	-4,419178825	21,39465967	0,00339707	0,046318223
OFAS013434-RA	-4,0105144	16,11703438	0,002737578	0,039811864
OFAS027058-RA	-3,905401231	14,98452276	0,002735783	0,039811864
OFAS008467-RA	-3,485887703	11,20357846	5,30E-05	0,002347325
OFAS006907-RA	-3,41146731	10,64030286	5,41E-06	0,000427413
OFAS009611-RA	-3,396987119	10,53404133	6,40E-05	0,0026882
OFAS018884-RA	-3,213182116	9,273938221	2,69E-05	0,001440775
OFAS006070-RA	-3,127236967	8,737599423	0,000952233	0,019315418
OFAS007959-RA	-2,994755476	7,970970981	7,15E-09	2,84E-06

OFAS001225-RA	-2,826963329	7,095790073	3,76E-05	0,001861243
OFAS003526-RA	-2,585704744	6,003087698	0,000620119	0,014057813
OFAS015144-RA	-2,558612828	5,891409468	0,000174257	0,005693984
OFAS016797-RA	-2,5436957	5,830807526	5,40E-06	0,000427413
OFAS009879-RA	-2,511638276	5,70267287	3,56E-07	5,75E-05
OFAS004252-RA	-2,453818734	5,478643519	0,000545134	0,012800874
OFAS012223-RA	-2,374978975	5,187282623	0,000844388	0,017844447
OFAS017639-RA	-2,343590889	5,075644018	0,000496277	0,011887969
OFAS013115-RA	-2,295586168	4,90953425	6,85E-06	0,000513218
OFAS003596-RA	-2,266578606	4,811806428	0,001740059	0,029305897
OFAS009838-RA	-2,25972687	4,789008082	1,47E-08	4,68E-06
OFAS006404-RA	-2,247364361	4,748146211	0,000226095	0,006810408
OFAS001076-RA	-2,221561295	4,663979008	0,001365698	0,024638425
OFAS001719-RA	-2,16570857	4,486867464	0,000199051	0,006224751
OFAS012699-RA	-2,157312619	4,460831393	7,88E-05	0,003159418
OFAS015412-RA	-2,106574647	4,306675569	1,84E-05	0,001115244
OFAS016029-RA	-2,091852065	4,262949795	0,000141242	0,004844736
OFAS001714-RA	-2,072719508	4,206789144	7,91E-10	4,14E-07
OFAS004133-RA	-2,068704467	4,195097865	0,00325726	0,044878941
OFAS000070-RA	-2,067504419	4,191609793	0,00097087	0,019601405
OFAS002613-RA	-2,056841912	4,160745114	0,00142296	0,025332942
OFAS013487-RA	-2,048007622	4,135344792	1,75E-05	0,001091975
OFAS013256-RA	-2,035405615	4,099379675	4,93E-05	0,002293013
OFAS013435-RA	-2,026844138	4,075124506	0,001680155	0,028488773
OFAS016990-RA	-2,020579569	4,057467585	0,000582378	0,013420757
OFAS004111-RA	-2,010039031	4,027931171	3,60E-07	5,75E-05
OFAS003516-RA	-2,009375546	4,026079181	5,28E-07	7,44E-05
OFAS025328-RA	-2,00567715	4,015771411	1,59E-07	3,11E-05
OFAS013858-RA	-2,002906058	4,008065424	3,58E-05	0,001805351
OFAS011485-RA	-1,997454519	3,99294865	4,44E-06	0,000387786
OFAS017619-RA	-1,996289405	3,989725264	0,00052945	0,012535615
OFAS026013-RA	-1,995856902	3,988529371	2,01E-05	0,001170979
OFAS018215-RA	-1,976449237	3,935233487	1,53E-07	3,08E-05
OFAS017474-RA	-1,972353023	3,924076108	0,003617045	0,048361364
OFAS014100-RA	-1,930338151	3,811445247	0,000225783	0,006810408
OFAS005820-RA	-1,923879449	3,794420187	1,83E-06	0,000189089
OFAS012136-RA	-1,908988659	3,755457469	0,002578186	0,038363169
OFAS006330-RA	-1,90061008	3,733710525	0,000353737	0,009251539
OFAS019250-RA	-1,876971371	3,673031762	0,000791211	0,017010765
OFAS011729-RA	-1,851718054	3,609297475	2,57E-06	0,000248754
OFAS017120-RA	-1,846556766	3,596408168	0,002657246	0,039155591
OFAS007884-RA	-1,841482869	3,58378197	0,000399005	0,010151774
OFAS014108-RA	-1,841196898	3,583071663	8,59E-07	0,000108284
OFAS018334-RA	-1,832671324	3,561960022	0,001925147	0,031413696

OFAS013549-RA	-1,831364564	3,558735141	1,11E-05	0,000750675
OFAS015247-RA	-1,83129717	3,558568902	7,44E-06	0,000547442
OFAS014844-RA	-1,820443656	3,531897943	4,03E-08	1,15E-05
OFAS013253-RA	-1,812210137	3,511798668	0,000550987	0,012892113
OFAS005232-RA	-1,809333344	3,504802974	2,09E-09	9,44E-07
OFAS000859-RA	-1,805106528	3,49454961	7,85E-07	0,000101517
OFAS003248-RA	-1,804436352	3,492926663	0,000450699	0,011121495
OFAS011259-RA	-1,801559513	3,485968452	6,45E-05	0,002700677
OFAS006932-RA	-1,798929141	3,479618502	8,95E-07	0,00011129
OFAS018641-RA	-1,792991957	3,465328106	1,04E-06	0,000123538
OFAS005267-RA	-1,790005684	3,458162549	5,21E-08	1,39E-05
OFAS000026-RA	-1,780018225	3,434305131	1,14E-05	0,000767795
OFAS016897-RA	-1,77627887	3,425415201	0,003598445	0,048211072
OFAS011150-RA	-1,763977197	3,396331304	0,001175284	0,022514243
OFAS014334-RA	-1,751475026	3,367026385	3,05E-05	0,001591098
OFAS014464-RA	-1,750028149	3,36365129	2,24E-07	4,14E-05
OFAS014908-RA	-1,721020719	3,296695683	2,36E-06	0,000234446
OFAS009161-RA	-1,716408041	3,286172107	0,000995834	0,019894047
OFAS018881-RA	-1,713487671	3,279526815	0,000243011	0,007145068
OFAS018285-RA	-1,712656877	3,277638802	0,003711876	0,049101208
OFAS001654-RA	-1,700991193	3,25124256	0,001199865	0,02280032
OFAS014762-RA	-1,695534897	3,238969531	0,000612645	0,013965537
OFAS008195-RA	-1,694077951	3,235700218	0,000285429	0,007906928
OFAS009127-RA	-1,692191095	3,231471113	0,003702189	0,049077588
OFAS006765-RA	-1,685958743	3,217541469	0,000205293	0,006374299
OFAS015304-RA	-1,680259918	3,20485685	0,001913323	0,031337843
OFAS017495-RA	-1,675465309	3,194223605	7,20E-05	0,002938993
OFAS011055-RA	-1,671197883	3,184789197	6,54E-09	2,68E-06
OFAS013326-RA	-1,670107502	3,18238306	3,89E-06	0,00034682
OFAS017308-RA	-1,669104927	3,180172289	5,35E-08	1,40E-05
OFAS016387-RA	-1,667588958	3,176832352	0,000359604	0,009386244
OFAS017057-RA	-1,663724172	3,168333434	9,24E-06	0,000650642
OFAS004254-RA	-1,663656384	3,168184566	0,000506535	0,012111556
OFAS018794-RA	-1,660653407	3,161596834	4,93E-07	7,16E-05
OFAS006733-RA	-1,659955701	3,160068214	0,000186015	0,005930313
OFAS002296-RA	-1,658029879	3,155852722	3,17E-06	0,000292942
OFAS014761-RA	-1,655470745	3,150259654	7,19E-05	0,002938993
OFAS016293-RA	-1,64785314	3,133669737	4,01E-05	0,001975041
OFAS006046-RA	-1,647698705	3,133334308	4,27E-05	0,002065508
OFAS000075-RA	-1,647155277	3,132154279	3,36E-07	5,74E-05
OFAS018313-RA	-1,64705532	3,131937276	9,67E-06	0,000677907
OFAS009029-RA	-1,644811992	3,127071035	0,000243749	0,007145068
OFAS007728-RA	-1,637147331	3,110501778	0,003577275	0,048025655
OFAS001616-RA	-1,634361209	3,104500596	6,34E-07	8,56E-05

OFAS014793-RA	-1,629314974	3,093660694	6,67E-06	0,000507978
OFAS012738-RA	-1,627234816	3,089203297	0,000227441	0,006819596
OFAS015019-RA	-1,621871558	3,077740419	5,01E-05	0,002293794
OFAS011893-RA	-1,611383154	3,055446361	4,35E-07	6,55E-05
OFAS004581-RA	-1,609816042	3,052129216	5,16E-06	0,00041703
OFAS015136-RA	-1,60198677	3,035610668	0,001464503	0,025792173
OFAS018196-RA	-1,597577995	3,026348216	0,001872792	0,030983835
OFAS001596-RA	-1,590991368	3,012562908	6,06E-07	8,36E-05
OFAS015217-RA	-1,589502892	3,009456352	0,000316688	0,00850321
OFAS015643-RA	-1,588431229	3,007221696	2,11E-05	0,001218697
OFAS012033-RA	-1,575740006	2,980883528	1,46E-06	0,000162499
OFAS000019-RA	-1,572368182	2,973924831	2,58E-06	0,000248754
OFAS007391-RA	-1,570472346	2,970019383	2,24E-05	0,001257952
OFAS002255-RA	-1,566974091	2,962826386	7,14E-07	9,44E-05
OFAS027199-RA	-1,562736751	2,954137036	1,87E-06	0,00019101
OFAS013936-RA	-1,561181017	2,950953151	0,000131586	0,004634855
OFAS008572-RA	-1,55985561	2,948243348	2,81E-05	0,001489224
OFAS000597-RA	-1,555674703	2,939711755	5,13E-05	0,002300545
OFAS001526-RA	-1,553978302	2,936257111	2,62E-06	0,00025036
OFAS008708-RA	-1,553802373	2,935899072	1,80E-05	0,001097131
OFAS000060-RA	-1,542880208	2,913756278	1,73E-07	3,33E-05
OFAS004515-RA	-1,533551221	2,894975664	1,48E-06	0,000163159
OFAS018647-RA	-1,529359021	2,886575621	0,000748424	0,016313332
OFAS005227-RA	-1,527612856	2,883083969	0,00265958	0,039155591
OFAS008164-RA	-1,521072771	2,870043833	0,002188748	0,034060766
OFAS003850-RA	-1,519728653	2,86737114	0,002730669	0,039799788
OFAS000248-RA	-1,513821535	2,855654686	3,72E-05	0,001852211
OFAS013870-RA	-1,511785471	2,851627365	4,65E-06	0,000395923
OFAS004584-RA	-1,51146661	2,850997176	0,000846453	0,017844447
OFAS003165-RA	-1,50045127	2,829311985	0,001165663	0,022415625
OFAS002011-RA	-1,492995725	2,81472841	2,22E-05	0,001254064
OFAS016609-RA	-1,490765249	2,810380066	0,000661848	0,01479014
OFAS016222-RA	-1,488707753	2,806374906	5,12E-05	0,002300545
OFAS016178-RA	-1,487344411	2,803724145	8,12E-05	0,003216043
OFAS002081-RA	-1,486384126	2,801858554	1,58E-05	0,00101169
OFAS016656-RA	-1,480033325	2,789551769	2,25E-06	0,000224905
OFAS002759-RA	-1,473261798	2,776489226	7,46E-05	0,003035629
OFAS007882-RA	-1,468274745	2,766908134	7,61E-06	0,00055067
OFAS027140-RA	-1,465025576	2,760683647	0,000181406	0,005840189
OFAS007483-RA	-1,460790773	2,752591979	0,000153696	0,005163797
OFAS009528-RA	-1,455976238	2,743421391	0,000540475	0,012726471
OFAS008800-RA	-1,447323945	2,727017475	7,38E-06	0,000547442
OFAS017389-RA	-1,44351862	2,719834034	3,01E-06	0,000281865
OFAS006933-RA	-1,434530796	2,702942452	0,00031055	0,008407298

OFAS001335-RA	-1,433033296	2,700138287	0,000550299	0,012892113
OFAS027116-RA	-1,431819237	2,697867017	1,41E-05	0,000920767
OFAS017054-RA	-1,424594087	2,684389626	0,000530011	0,012535615
OFAS015973-RA	-1,421687193	2,678986281	0,001060468	0,020926678
OFAS017455-RA	-1,419495124	2,674918849	4,85E-06	0,000404529
OFAS018619-RA	-1,416666726	2,669679819	4,33E-05	0,002086323
OFAS011350-RA	-1,414233723	2,665181386	0,001317753	0,023981275
OFAS006661-RA	-1,408557718	2,654716344	3,59E-05	0,001805351
OFAS004673-RA	-1,407011004	2,651871748	1,59E-05	0,001012341
OFAS012229-RA	-1,400313809	2,639589911	1,12E-06	0,000130589
OFAS019013-RA	-1,393905819	2,627891697	2,55E-05	0,001389638
OFAS008904-RA	-1,389898537	2,620602498	1,42E-05	0,000920901
OFAS019579-RA	-1,381072115	2,604618571	0,00031348	0,008449539
OFAS004264-RA	-1,380930318	2,604362586	0,001890515	0,031159021
OFAS007454-RA	-1,380194043	2,603033796	0,00057534	0,013319231
OFAS011627-RA	-1,372108169	2,588485378	0,000306978	0,008327811
OFAS013419-RA	-1,371712143	2,587774926	0,000456342	0,011221395
OFAS005816-RA	-1,370921298	2,586356769	5,39E-05	0,002362035
OFAS003874-RA	-1,370088827	2,584864806	0,000138703	0,004814059
OFAS001343-RA	-1,368828106	2,582606969	0,001928407	0,031427764
OFAS015865-RA	-1,368420685	2,581877738	5,89E-06	0,000456146
OFAS005142-RA	-1,35689773	2,561338147	0,000238969	0,007132598
OFAS007377-RA	-1,354398106	2,556904197	0,001722832	0,02905312
OFAS012325-RA	-1,351948045	2,552565611	0,003726463	0,049221613
OFAS017316-RA	-1,348013809	2,545614236	0,001575069	0,027335277
OFAS006502-RA	-1,342948074	2,536691495	4,17E-07	6,36E-05
OFAS014788-RA	-1,341752219	2,534589694	1,05E-05	0,000727759
OFAS017855-RA	-1,341694942	2,534489069	1,34E-05	0,000886869
OFAS017890-RA	-1,339538794	2,530704034	0,000409978	0,010313637
OFAS006210-RA	-1,339480481	2,530601746	0,000342908	0,009004267
OFAS002351-RA	-1,332633669	2,518620347	9,94E-07	0,00011948
OFAS009020-RA	-1,329924785	2,513895684	0,000867085	0,018149231
OFAS008756-RA	-1,328915797	2,512138136	2,65E-05	0,00142104
OFAS013602-RA	-1,324857244	2,505080985	7,69E-05	0,003101103
OFAS016326-RA	-1,323375851	2,50251003	1,88E-05	0,00112442
OFAS010379-RA	-1,316416828	2,490467921	5,74E-05	0,002464577
OFAS004516-RA	-1,315701268	2,489232984	0,000560804	0,013005691
OFAS000216-RA	-1,3153206	2,488576265	0,002122098	0,033457288
OFAS014354-RA	-1,311164078	2,481416791	0,002876459	0,041299367
OFAS004704-RA	-1,309453638	2,4784766	6,71E-05	0,002772476
OFAS006401-RA	-1,302415885	2,466415541	0,000876199	0,018195382
OFAS016639-RA	-1,298433321	2,459616382	0,002116352	0,033457288
OFAS025239-RA	-1,296418062	2,456183015	1,69E-06	0,000179501
OFAS007629-RA	-1,295173254	2,454064647	0,000243443	0,007145068

OFAS002720-RA	-1,295147311	2,454020517	0,000142917	0,004876668
OFAS010514-RA	-1,292702615	2,449865616	0,001030628	0,020399266
OFAS009367-RA	-1,28827159	2,442352759	0,001367025	0,024638425
OFAS012251-RA	-1,285853932	2,43826331	0,000762367	0,01651124
OFAS006445-RA	-1,276204192	2,422008943	4,97E-05	0,002293794
OFAS012416-RA	-1,275546222	2,420904589	0,000204797	0,006373991
OFAS012027-RA	-1,273476902	2,41743467	0,000329147	0,0087304
OFAS025094-RA	-1,269086595	2,410089286	2,61E-05	0,001416288
OFAS006482-RA	-1,26812601	2,408485119	0,001210102	0,02281462
OFAS018229-RA	-1,261930593	2,39816445	0,000336646	0,008875389
OFAS002088-RA	-1,259512945	2,394149007	0,00014945	0,005047031
OFAS016276-RA	-1,251765803	2,3813271	0,000952283	0,019315418
OFAS015212-RA	-1,240742801	2,363201753	0,001256452	0,023330307
OFAS007617-RA	-1,237513912	2,357918597	6,81E-05	0,002796274
OFAS000191-RA	-1,235062823	2,353915974	0,00092544	0,019006327
OFAS008755-RA	-1,233951331	2,352103151	3,62E-05	0,001809854
OFAS018157-RA	-1,223996883	2,335929743	0,002806918	0,04041654
OFAS010942-RA	-1,221063553	2,331185087	0,001229628	0,023099034
OFAS011956-RA	-1,219109868	2,328030352	0,000274629	0,007738637
OFAS001859-RA	-1,207097985	2,308727635	0,000693377	0,015330608
OFAS011789-RA	-1,206089854	2,307114898	0,000183747	0,005886627
OFAS012141-RA	-1,205559762	2,306267346	0,000883672	0,018291875
OFAS013363-RA	-1,20540124	2,306013949	0,001820251	0,030267442
OFAS016277-RA	-1,193993312	2,287851341	0,000164254	0,005448672
OFAS009179-RA	-1,188575941	2,279276486	0,000407925	0,010313637
OFAS018618-RA	-1,188182339	2,278654731	0,000557427	0,012973291
OFAS000975-RA	-1,186346861	2,27575754	4,39E-05	0,002101211
OFAS004414-RA	-1,185553413	2,274506272	0,002108189	0,033442611
OFAS014024-RA	-1,183296217	2,270950432	0,001234665	0,023099034
OFAS001552-RA	-1,181358734	2,267902681	0,000632764	0,014319691
OFAS004207-RA	-1,17989342	2,265600391	0,000120003	0,004355684
OFAS004683-RA	-1,178306081	2,263109015	0,000298453	0,008181236
OFAS003944-RA	-1,174627106	2,257345277	9,29E-05	0,003558895
OFAS003210-RA	-1,174393371	2,256979588	0,000331066	0,008758709
OFAS011959-RA	-1,174368309	2,256940381	0,000940426	0,019245699
OFAS000524-RA	-1,171280132	2,25211443	0,002518717	0,037674374
OFAS009885-RA	-1,169534152	2,249390521	5,09E-05	0,002300545
OFAS002267-RA	-1,164047215	2,240851764	0,000262592	0,007512532
OFAS016978-RA	-1,162599267	2,238603881	0,003158141	0,043882418
OFAS017864-RA	-1,162563767	2,238548797	0,00291889	0,041799138
OFAS000018-RA	-1,157750856	2,231093317	0,000192327	0,006072444
OFAS003020-RA	-1,156070633	2,228496405	0,002954763	0,042037193
OFAS005018-RA	-1,155471648	2,227571359	0,000691227	0,015325124
OFAS005148-RA	-1,153479487	2,224497515	0,0008876	0,018344201

OFAS015288-RA	-1,146381571	2,213580086	0,002194752	0,034113678
OFAS014370-RA	-1,145302087	2,211924415	0,001283512	0,02364323
OFAS010695-RA	-1,14305083	2,208475504	0,002768864	0,040096618
OFAS017262-RA	-1,13923181	2,202637084	0,000592693	0,013600799
OFAS004113-RA	-1,136394535	2,198309527	0,002124434	0,033457288
OFAS016577-RA	-1,131149004	2,190331151	0,000173469	0,005682424
OFAS012637-RA	-1,127542727	2,18486286	0,000139612	0,004814059
OFAS009667-RA	-1,126390554	2,183118669	0,001565094	0,027204079
OFAS018483-RA	-1,123659111	2,178989298	0,000511573	0,012209736
OFAS016241-RA	-1,119162101	2,172207768	0,000175352	0,005701331
OFAS005022-RA	-1,115920489	2,167332482	0,003047232	0,042795151
OFAS017427-RA	-1,114417214	2,165075318	0,003472746	0,047202692
OFAS009368-RA	-1,10397735	2,1494646	0,000185262	0,005920712
OFAS018485-RA	-1,099647725	2,143023581	0,002353954	0,035784921
OFAS014188-RA	-1,08949833	2,128000264	0,000247298	0,007232924
OFAS014873-RA	-1,084811202	2,121097887	0,000794742	0,017033016
OFAS001752-RA	-1,073396507	2,104381842	0,001600054	0,02767748
OFAS005794-RA	-1,072692669	2,103355443	0,001508688	0,026499106
OFAS004482-RA	-1,07188271	2,102174906	0,00043863	0,01088517
OFAS001858-RA	-1,068943718	2,097896811	0,003533939	0,047645837
OFAS016999-RA	-1,068016325	2,096548674	0,000313239	0,008449539
OFAS001387-RA	-1,065132022	2,092361344	0,003007402	0,042601067
OFAS002430-RA	-1,05615712	2,079385319	0,000559008	0,012987031
OFAS011601-RA	-1,051904567	2,073265053	0,00190196	0,031229803
OFAS004084-RA	-1,05075861	2,071618877	0,002730673	0,039799788
OFAS018521-RA	-1,050003589	2,070534999	0,000302003	0,008251307
OFAS005661-RA	-1,04658326	2,065632006	0,000659376	0,01479014
OFAS017805-RA	-1,044958313	2,063306738	0,003784996	0,049793982
OFAS009578-RA	-1,043369037	2,061035046	0,000700545	0,015401406
OFAS001388-RA	-1,042856386	2,060302803	0,003504805	0,047418571
OFAS008388-RA	-1,040337419	2,056708622	0,003039184	0,042779174
OFAS011919-RA	-1,039434421	2,055421709	0,00137876	0,024774035
OFAS003945-RA	-1,037402064	2,05252823	0,002084728	0,033150718
OFAS004911-RA	-1,033933028	2,047598746	0,000927459	0,019017992
OFAS012987-RA	-1,032095108	2,04499187	0,003668791	0,048903524
OFAS025199-RA	-1,031301959	2,043867906	0,000865062	0,018135848
OFAS001414-RA	-1,029616402	2,04148137	0,002256582	0,034807983
OFAS017706-RA	-1,029267193	2,040987283	0,002850271	0,040995714
OFAS012622-RA	-1,027876245	2,03902045	0,001784161	0,0298187
OFAS025143-RA	-1,026775948	2,037465948	0,002587077	0,038390109
OFAS006484-RA	-1,014879802	2,020734529	0,001408884	0,025150698
OFAS004939-RA	-1,007993446	2,011112025	0,000993025	0,019894047
OFAS002084-RA	-1,005663898	2,007867263	0,000225351	0,006810408
OFAS002748-RA	-1,001021986	2,001417275	0,00192075	0,031381038

OFAS012553-RA	-1,000929382	2,001288812	0,000441197	0,010923607
OFAS005422-RB	1,001103482	2,001530336	0,001827186	0,030344256
OFAS003521-RA	1,002190951	2,003039611	0,002387806	0,036003939
OFAS018044-RA	1,003998137	2,005550282	0,000612851	0,013965537
OFAS014080-RA	1,010941512	2,015225821	0,001305926	0,023898816
OFAS003283-RA	1,011000073	2,015307623	0,003005268	0,042601067
OFAS013938-RA	1,012393886	2,017255588	0,000277671	0,007771823
OFAS008118-RA	1,012937931	2,018016445	0,00063395	0,014321795
OFAS015539-RA	1,013357224	2,01860303	0,001286165	0,02364323
OFAS005973-RA	1,013516588	2,018826022	0,000265622	0,007566191
OFAS003506-RA	1,014160605	2,019727424	0,000663684	0,01479014
OFAS025019-RA	1,014501376	2,02020455	0,002948349	0,042035219
OFAS011540-RA	1,01544954	2,021532699	0,000410602	0,010313637
OFAS010516-RA	1,018541125	2,025869334	0,000372762	0,009595869
OFAS000552-RA	1,020094871	2,028052319	0,001314328	0,023952209
OFAS002649-RA	1,025255227	2,035319421	0,000776142	0,016726623
OFAS007394-RA	1,025698412	2,035944751	0,000725578	0,015925035
OFAS011287-RA	1,026449245	2,03700461	0,00218298	0,034060766
OFAS013260-RA	1,026849906	2,037570399	8,85E-05	0,003435377
OFAS009375-RA	1,027430845	2,038391046	0,000190999	0,006045068
OFAS007531-RA	1,028827772	2,040365727	0,000151463	0,005101862
OFAS009104-RA	1,029147017	2,040817276	0,000338458	0,008905239
OFAS003877-RA	1,031585838	2,044270117	0,001134848	0,021971698
OFAS012981-RA	1,034335763	2,048170423	0,000106643	0,004003851
OFAS003903-RA	1,03516378	2,049346282	0,003019089	0,042646618
OFAS012657-RA	1,035924192	2,050426731	0,002229066	0,034442745
OFAS004950-RA	1,036362712	2,051050072	0,001798382	0,029979901
OFAS016862-RA	1,037380933	2,052498167	0,000219319	0,006683113
OFAS008991-RA	1,038001883	2,053381772	0,001005315	0,020049692
OFAS002857-RA	1,038623747	2,054267059	0,000281277	0,007824994
OFAS000683-RA	1,038689892	2,054361245	8,52E-05	0,003342135
OFAS003477-RA	1,038792912	2,054507948	0,000206904	0,006409145
OFAS017453-RA	1,040691221	2,057213064	0,000750739	0,016313332
OFAS009913-RA	1,042252902	2,059441152	0,00022481	0,006810408
OFAS006706-RA	1,048407206	2,06824516	0,000458127	0,011221395
OFAS007006-RA	1,052739314	2,074464996	0,000133103	0,004663228
OFAS004766-RA	1,055558783	2,078523102	0,002031855	0,032706871
OFAS007522-RA	1,055672792	2,078687364	0,000540994	0,012726471
OFAS009867-RA	1,056075272	2,079267353	0,000259872	0,007457699
OFAS016010-RA	1,056687013	2,080149204	0,00048228	0,011616382
OFAS005895-RA	1,057064502	2,080693557	0,001539093	0,026913239
OFAS013395-RA	1,057140324	2,080802913	0,00098392	0,019743194
OFAS017897-RA	1,060897693	2,08622924	6,29E-05	0,002665295
OFAS012686-RA	1,060948073	2,086302093	0,00011844	0,004321483

OFAS017200-RA	1,061147395	2,086590356	0,000275993	0,007760367
OFAS005060-RA	1,061498818	2,087098685	0,001889588	0,031159021
OFAS015721-RA	1,062625548	2,088729325	0,000654056	0,014725261
OFAS008279-RA	1,063777078	2,090397172	0,000370832	0,00956499
OFAS001824-RA	1,06526744	2,092557751	8,85E-05	0,003435377
OFAS015537-RA	1,067483691	2,095774785	0,000277407	0,007771823
OFAS003474-RA	1,068895127	2,097826153	0,002062303	0,032954086
OFAS003902-RA	1,069231666	2,098315572	0,001526657	0,026778838
OFAS008288-RA	1,071228759	2,101222239	0,00119728	0,02280032
OFAS010871-RA	1,071524109	2,101652448	0,001380222	0,024774035
OFAS011120-RA	1,072069814	2,102447557	0,00012986	0,004598808
OFAS007355-RA	1,076402829	2,108771575	5,99E-05	0,002558391
OFAS013854-RA	1,076519832	2,108942605	0,001302875	0,023876332
OFAS015503-RA	1,077259172	2,110023654	0,000116573	0,004285822
OFAS018235-RA	1,077263563	2,110030076	0,000526378	0,012494811
OFAS000235-RA	1,077418991	2,110257411	0,000123065	0,004454468
OFAS001132-RA	1,079500155	2,113303766	0,002527385	0,037760921
OFAS008638-RA	1,080893254	2,115345406	0,002005437	0,032361126
OFAS018653-RA	1,082457935	2,117640858	0,001626446	0,028004364
OFAS012209-RA	1,082897964	2,118286846	0,002579406	0,038363169
OFAS006973-RA	1,083511347	2,119187658	0,000331552	0,008758709
OFAS002245-RA	1,083724721	2,119501109	0,001434082	0,025461758
OFAS007027-RA	1,084621174	2,120818521	0,000209079	0,006446034
OFAS009204-RA	1,085099572	2,121521901	0,000405503	0,010277187
OFAS001407-RA	1,086025322	2,122883678	0,000383822	0,009803554
OFAS001323-RA	1,088484696	2,126505662	0,000468371	0,011364939
OFAS019103-RA	1,089187559	2,127541921	0,000169145	0,005568619
OFAS012560-RA	1,092141082	2,131901941	4,41E-05	0,002103007
OFAS001688-RA	1,092910557	2,133039315	0,000400644	0,010173713
OFAS000995-RA	1,09412602	2,134837146	0,0013119	0,023946767
OFAS006013-RA	1,098144047	2,140791136	8,07E-05	0,003206197
OFAS005618-RA	1,098553599	2,141398949	0,000951356	0,019315418
OFAS005882-RA	1,098722068	2,141649022	0,00321565	0,044492774
OFAS015513-RA	1,098972189	2,142020354	0,000314045	0,008449539
OFAS003834-RA	1,099722914	2,143135272	5,24E-05	0,002334253
OFAS009859-RA	1,102377998	2,147083052	0,001131393	0,021971698
OFAS008555-RA	1,103876817	2,149314821	0,000227245	0,006819596
OFAS007943-RA	1,104199982	2,149796323	0,000241314	0,007145068
OFAS005149-RA	1,104582	2,150365653	0,00010045	0,003793061
OFAS002328-RA	1,105113964	2,151158703	0,000922121	0,018967905
OFAS006970-RA	1,110382872	2,159029374	0,000915659	0,018894306
OFAS001759-RA	1,113102955	2,163103887	0,000582799	0,013420757
OFAS004332-RA	1,113242892	2,163313712	0,000860636	0,018071987
OFAS015082-RA	1,114507564	2,165210912	9,59E-05	0,003651732

OFAS013233-RA	1,114549709	2,165274165	0,002072894	0,033082985
OFAS008345-RA	1,114801576	2,165652213	0,000457611	0,011221395
OFAS004510-RA	1,115961948	2,167394766	0,001418404	0,025286195
OFAS009572-RA	1,116492635	2,168192176	5,46E-05	0,002370219
OFAS014172-RA	1,116898608	2,16880239	0,000460876	0,011245544
OFAS009012-RA	1,12011003	2,173635496	0,000740106	0,01616268
OFAS010224-RA	1,120481206	2,174194799	0,001200658	0,02280032
OFAS012630-RA	1,121466045	2,175679495	0,000841345	0,017809601
OFAS006193-RA	1,122543547	2,177305046	0,000367305	0,009511464
OFAS014440-RA	1,122750873	2,177617963	0,002305479	0,035373168
OFAS013536-RA	1,123192475	2,178284624	0,000215893	0,006609466
OFAS012764-RA	1,124022363	2,179538008	0,001895657	0,031165366
OFAS000916-RA	1,124242012	2,179869866	8,96E-05	0,003454685
OFAS006463-RA	1,124430174	2,180154193	0,000791923	0,017010765
OFAS014757-RA	1,124854876	2,180796082	8,86E-05	0,003435377
OFAS013908-RA	1,126189706	2,182814763	0,002729903	0,039799788
OFAS013352-RA	1,126825742	2,183777305	0,000278299	0,007771823
OFAS009430-RA	1,129809256	2,188298061	0,001068071	0,021045008
OFAS015098-RA	1,130975122	2,190067176	0,003506723	0,047418571
OFAS006534-RA	1,131079732	2,190225984	0,002132806	0,033548808
OFAS008589-RA	1,131330845	2,190607244	0,000127616	0,004556281
OFAS001818-RA	1,131506295	2,190873665	0,002350428	0,035784921
OFAS012020-RA	1,133470823	2,193859025	0,000125419	0,004490058
OFAS007964-RA	1,134676636	2,195693432	0,001126917	0,021940556
OFAS000699-RA	1,135853638	2,197485488	0,001020247	0,020285729
OFAS004577-RA	1,136098736	2,197858848	2,14E-05	0,001223289
OFAS007708-RA	1,136251822	2,198092079	0,002797019	0,040334789
OFAS005560-RA	1,136342536	2,198230294	0,000472259	0,011416981
OFAS001599-RA	1,136959803	2,199171024	8,27E-05	0,003265403
OFAS014817-RA	1,137237634	2,199594576	0,000123997	0,004463553
OFAS019581-RA	1,137823145	2,200487452	5,05E-05	0,002299567
OFAS008489-RA	1,140495333	2,204567014	0,000436787	0,010880653
OFAS003849-RA	1,140781147	2,205003808	0,000251174	0,007281895
OFAS010056-RA	1,141644775	2,206324165	0,000376513	0,009673427
OFAS015594-RA	1,1437359	2,209524457	0,000159811	0,005328241
OFAS009697-RA	1,144327355	2,21043047	2,20E-05	0,001249751
OFAS007727-RA	1,144811728	2,211172729	3,09E-05	0,001605326
OFAS001478-RA	1,145415027	2,21209758	5,70E-05	0,002457398
OFAS012855-RA	1,146475188	2,213723732	0,0002839	0,007881237
OFAS003556-RA	1,146685831	2,214046973	2,62E-05	0,001416288
OFAS001078-RA	1,147487488	2,215277586	0,000370469	0,00956499
OFAS010073-RA	1,148517385	2,216859572	0,000278773	0,007771823
OFAS017913-RA	1,149461384	2,218310606	0,001618159	0,027935091
OFAS001248-RA	1,151262156	2,221081229	0,000323123	0,008640561

OFAS006456-RA	1,152289126	2,22266285	0,000973519	0,019624647
OFAS007559-RA	1,152345288	2,222749376	1,85E-05	0,001115244
OFAS006141-RA	1,152701197	2,22329779	0,001765549	0,029657269
OFAS001693-RA	1,152815154	2,223473414	0,0001768	0,00572003
OFAS027118-RA	1,15414458	2,225523261	0,000243056	0,007145068
OFAS017903-RA	1,154816133	2,22655945	0,001312202	0,023946767
OFAS014465-RA	1,155033174	2,226894442	0,000948846	0,019315418
OFAS006176-RA	1,155558415	2,227705333	0,002410948	0,036269405
OFAS005865-RA	1,156423967	2,229042258	0,000225827	0,006810408
OFAS016321-RA	1,156598126	2,229311358	0,000579398	0,01338951
OFAS001030-RA	1,157378101	2,230516934	0,001984182	0,032063851
OFAS017896-RA	1,161162851	2,236376129	0,000382671	0,00979325
OFAS005490-RA	1,161990211	2,237659019	0,002400597	0,036155201
OFAS002863-RA	1,163000716	2,239226888	0,000515704	0,01228595
OFAS008783-RA	1,169723181	2,249685267	0,002111765	0,033457288
OFAS018041-RA	1,171063324	2,251776007	2,51E-05	0,001375694
OFAS006697-RA	1,171081749	2,251804765	0,000698993	0,015393126
OFAS011930-RA	1,171542008	2,252523266	6,36E-05	0,002678011
OFAS010538-RA	1,172041221	2,253302839	0,000292064	0,008055337
OFAS014754-RA	1,174521242	2,257179641	0,000422657	0,010548714
OFAS010001-RA	1,176338864	2,260025208	0,000175127	0,005701331
OFAS008447-RA	1,178211315	2,262960363	0,000106547	0,004003851
OFAS018459-RA	1,180629584	2,266756755	4,99E-05	0,002293794
OFAS016982-RA	1,181069352	2,267447822	0,000822511	0,01746737
OFAS009849-RA	1,185900004	2,275052762	9,97E-05	0,003777183
OFAS014301-RA	1,186618338	2,276185818	5,14E-05	0,002300545
OFAS007007-RA	1,188189114	2,278665431	3,74E-05	0,001856516
OFAS011638-RA	1,188427404	2,27904183	0,000137197	0,004793838
OFAS000793-RA	1,188632913	2,279366497	0,000193831	0,006091895
OFAS015355-RA	1,189084076	2,280079418	0,000260106	0,007457699
OFAS000821-RA	1,1914622	2,283840978	4,07E-05	0,001998622
OFAS008817-RA	1,192108571	2,284864437	6,48E-05	0,002703886
OFAS009257-RA	1,193559483	2,28716347	5,01E-05	0,002293794
OFAS016699-RA	1,195879907	2,290845093	0,000123837	0,004463553
OFAS015764-RA	1,196165494	2,291298619	0,000459144	0,011224195
OFAS018183-RA	1,200264269	2,297817579	0,000242218	0,007145068
OFAS016597-RA	1,200833093	2,298723738	5,76E-05	0,002464577
OFAS001523-RA	1,200896252	2,298824376	0,001469723	0,025849376
OFAS008119-RA	1,202107966	2,300755961	0,00087075	0,018167889
OFAS005651-RA	1,20300306	2,302183866	0,001907283	0,031278011
OFAS005339-RA	1,203785975	2,303433543	0,001753666	0,029497152
OFAS015913-RA	1,205107895	2,305545112	0,000132988	0,004663228
OFAS010404-RA	1,205414286	2,306034802	0,001937182	0,031531549
OFAS000446-RA	1,205692685	2,306479845	0,00118499	0,022633992

OFAS002807-RA	1,207811861	2,309870324	0,000969934	0,019601405
OFAS013272-RA	1,208180013	2,31045984	0,001269393	0,02349274
OFAS009565-RA	1,210560501	2,314275311	0,000107516	0,004025098
OFAS000121-RA	1,213220549	2,31854632	2,44E-05	0,001342979
OFAS017944-RA	1,217512117	2,325453541	7,61E-05	0,00308707
OFAS008299-RA	1,22593176	2,339064687	0,000322819	0,008640561
OFAS003871-RA	1,228402336	2,343073703	4,58E-06	0,000391888
OFAS016732-RA	1,230605242	2,346654164	0,001337357	0,024203575
OFAS003389-RA	1,234129834	2,352394192	0,000693814	0,015330608
OFAS006188-RA	1,234186559	2,352486688	3,57E-05	0,001805351
OFAS004160-RA	1,234276213	2,352632884	4,20E-05	0,002046993
OFAS007369-RA	1,234774356	2,353445357	0,001136901	0,021971698
OFAS002198-RA	1,238105449	2,358885593	7,66E-05	0,003096704
OFAS009186-RA	1,238321284	2,359238521	0,000870134	0,018167889
OFAS009213-RA	1,240242417	2,362382242	0,000267058	0,007590596
OFAS003010-RA	1,241176288	2,363911932	0,00069526	0,015336686
OFAS003051-RA	1,244106864	2,368718674	0,001671145	0,028429173
OFAS003994-RA	1,249580194	2,377722241	4,77E-05	0,002232467
OFAS015936-RA	1,253337694	2,383923092	1,42E-05	0,000920901
OFAS007711-RA	1,254027806	2,385063713	8,02E-05	0,003193116
OFAS015369-RA	1,254639245	2,386074758	4,53E-05	0,002142209
OFAS012627-RA	1,255586182	2,387641413	0,000795559	0,017033016
OFAS007106-RA	1,256507581	2,389166802	0,000379186	0,009723054
OFAS001400-RA	1,256521433	2,389189742	0,000683709	0,015209907
OFAS011614-RA	1,258443024	2,392374133	3,16E-05	0,001629735
OFAS012231-RA	1,260444537	2,395695481	0,000253551	0,007333952
OFAS001889-RA	1,261397826	2,397279006	9,40E-05	0,00359106
OFAS009136-RA	1,261835536	2,398006444	0,0035437	0,047672594
OFAS004096-RA	1,265664388	2,404379106	1,99E-05	0,001166791
OFAS025038-RA	1,268830501	2,409661508	0,000154453	0,005175952
OFAS000044-RA	1,270852237	2,413040679	4,81E-06	0,000403805
OFAS014877-RA	1,271379465	2,413922678	0,003206307	0,044437254
OFAS002955-RA	1,271966395	2,414904932	0,000118731	0,004321483
OFAS009909-RA	1,272756168	2,416227283	0,00012912	0,004585001
OFAS003326-RA	1,275629225	2,421043876	0,000139482	0,004814059
OFAS014051-RA	1,276473805	2,422461614	0,000161006	0,005354486
OFAS012925-RA	1,277022029	2,423382325	0,001641936	0,028160063
OFAS006629-RA	1,278054624	2,425117457	2,91E-05	0,001531453
OFAS013787-RA	1,280522163	2,429268849	0,000256783	0,007394784
OFAS008342-RA	1,280590861	2,429384529	1,37E-05	0,000901571
OFAS010554-RA	1,280929383	2,42995464	0,000273804	0,007732001
OFAS011593-RA	1,281204386	2,430417875	0,000306128	0,008321987
OFAS017296-RA	1,282193619	2,432084946	3,47E-05	0,001767512
OFAS018306-RA	1,288317683	2,442430792	0,000271928	0,007695608

OFAS008926-RA	1,290532331	2,446182991	0,003493779	0,047418571
OFAS009969-RA	1,292987502	2,450349437	0,000287714	0,007953417
OFAS000123-RA	1,293909567	2,451916021	4,27E-05	0,002065508
OFAS004446-RA	1,295787691	2,455110044	9,65E-05	0,003666605
OFAS019512-RA	1,295989092	2,455452803	8,17E-06	0,000584715
OFAS017983-RA	1,298759156	2,460171953	1,81E-06	0,00018788
OFAS003681-RA	1,301341218	2,464578986	9,96E-06	0,000694475
OFAS007284-RA	1,303846768	2,468862976	4,48E-06	0,000388783
OFAS006476-RA	1,307544714	2,475199334	0,001136072	0,021971698
OFAS010480-RA	1,308709029	2,47719773	5,36E-05	0,002362035
OFAS010795-RA	1,310432376	2,480158593	0,003077429	0,043126796
OFAS015370-RA	1,314090282	2,486454931	8,79E-06	0,0006258
OFAS007109-RA	1,31482926	2,487728871	0,003234343	0,044657106
OFAS018907-RA	1,315764508	2,489342101	1,89E-05	0,00112442
OFAS012561-RA	1,31763933	2,492579173	0,000519851	0,012362261
OFAS009004-RA	1,318083087	2,493345981	4,92E-06	0,000405259
OFAS015914-RA	1,319177894	2,495238805	0,000966147	0,019566338
OFAS003826-RA	1,320736985	2,497936815	8,58E-07	0,000108284
OFAS014152-RA	1,321188543	2,498718783	4,46E-05	0,002117756
OFAS002909-RA	1,322035762	2,500186581	4,39E-05	0,002101211
OFAS012876-RA	1,322307957	2,500658338	0,00198222	0,032063851
OFAS001571-RA	1,325917887	2,506923352	0,003349016	0,045901832
OFAS017237-RA	1,326006315	2,507077015	0,000324797	0,008650038
OFAS003476-RA	1,327583285	2,509818929	1,52E-06	0,00016511
OFAS001819-RA	1,329856243	2,513776252	0,000243686	0,007145068
OFAS011632-RA	1,330536398	2,514961645	0,001251098	0,023318826
OFAS003960-RA	1,335493464	2,523617857	0,000390473	0,009954011
OFAS012182-RA	1,34084951	2,533004271	7,60E-06	0,00055067
OFAS000090-RA	1,345804543	2,541719003	3,29E-05	0,001693009
OFAS007507-RA	1,34740864	2,544546648	1,52E-06	0,00016511
OFAS001436-RA	1,34940482	2,548069839	0,001918618	0,031381038
OFAS014385-RA	1,351908971	2,552496478	0,001165422	0,022415625
OFAS009205-RA	1,352168255	2,55295526	0,001977591	0,032063851
OFAS017726-RA	1,352549486	2,553629966	0,000663711	0,01479014
OFAS006187-RA	1,352671872	2,553846604	0,003367284	0,04598344
OFAS015334-RA	1,356864156	2,561278541	0,000159392	0,005327832
OFAS014879-RA	1,356931665	2,561398395	0,001442218	0,025571557
OFAS001262-RA	1,361495674	2,569514287	1,90E-05	0,001127671
OFAS001723-RA	1,36225119	2,570860253	3,01E-05	0,001579533
OFAS025161-RA	1,363656181	2,573365145	0,000254229	0,007337375
OFAS007659-RA	1,366202611	2,577911275	5,24E-06	0,000418271
OFAS015951-RA	1,367859858	2,580874265	4,88E-06	0,000404529
OFAS006457-RA	1,368129508	2,581356695	7,90E-06	0,000569046
OFAS007919-RA	1,368135147	2,581366784	0,001210117	0,02281462

OFAS014397-RA	1,36929172	2,583437031	0,002354163	0,035784921
OFAS017850-RA	1,374191575	2,592226129	0,000730819	0,01598652
OFAS002156-RA	1,379716236	2,602171838	4,95E-06	0,000405402
OFAS015219-RA	1,380071794	2,602813233	0,000124781	0,004479449
OFAS007014-RA	1,381155749	2,604769567	0,000591891	0,013600799
OFAS002446-RA	1,384964953	2,61165613	0,000131241	0,004634855
OFAS005878-RA	1,390570382	2,621823164	0,001407689	0,025150698
OFAS003124-RA	1,391313571	2,623174115	0,000995993	0,019894047
OFAS016140-RA	1,39544698	2,630700446	6,70E-05	0,002772476
OFAS010091-RA	1,395794833	2,631334819	0,003208246	0,044437254
OFAS012037-RA	1,396503322	2,632627351	8,38E-05	0,003296215
OFAS017962-RA	1,39710902	2,63373286	0,000188367	0,00597622
OFAS003828-RA	1,398156606	2,635645991	1,78E-05	0,001097095
OFAS003266-RA	1,402353554	2,643324518	0,000242384	0,007145068
OFAS012291-RA	1,40301014	2,644527797	0,001581927	0,027417976
OFAS000799-RA	1,405035523	2,648243028	1,35E-06	0,000152354
OFAS010587-RA	1,406910088	2,651686256	0,000797604	0,017048957
OFAS011205-RA	1,410749584	2,658752682	1,78E-06	0,000186341
OFAS015040-RA	1,414313117	2,665328061	8,90E-06	0,0006307
OFAS012375-RA	1,414730292	2,666098888	0,000293246	0,008055337
OFAS002777-RA	1,415740576	2,667966545	0,000145306	0,004932484
OFAS003009-RA	1,41599801	2,668442659	2,00E-05	0,001170979
OFAS016688-RA	1,419753295	2,67539757	3,80E-07	5,95E-05
OFAS014008-RA	1,419783555	2,675453685	9,00E-07	0,00011129
OFAS017648-RA	1,421483321	2,678607731	2,10E-07	3,93E-05
OFAS003889-RA	1,4277475	2,690263526	2,18E-05	0,001243496
OFAS002990-RA	1,428280898	2,691258364	1,28E-06	0,000146925
OFAS025203-RA	1,435996227	2,705689385	0,001124193	0,021920097
OFAS012132-RA	1,437371839	2,708270496	2,48E-06	0,000242326
OFAS012028-RA	1,43809826	2,709634498	0,000175876	0,005704203
OFAS003425-RA	1,438728536	2,710818525	0,002185335	0,034060766
OFAS018707-RA	1,439248526	2,71179576	1,79E-05	0,001097131
OFAS015187-RA	1,439667573	2,712583548	0,001007226	0,020057271
OFAS000582-RA	1,44640366	2,725278484	3,60E-05	0,001805351
OFAS014611-RA	1,448779904	2,729770954	2,27E-05	0,001271062
OFAS018022-RA	1,462743106	2,756319458	0,000416632	0,010418195
OFAS010561-RA	1,463957228	2,758640056	1,31E-05	0,000872928
OFAS001805-RA	1,464495364	2,759669242	3,30E-06	0,000302153
OFAS000642-RA	1,46749782	2,76541849	6,74E-05	0,002777972
OFAS012298-RA	1,471018992	2,772176264	0,00311298	0,043485478
OFAS011918-RA	1,471315336	2,772745756	1,49E-05	0,000963486
OFAS000131-RA	1,477231542	2,784139581	0,002122795	0,033457288
OFAS016644-RA	1,485204223	2,799567999	1,07E-05	0,000734533
OFAS002317-RA	1,49388445	2,816462866	0,000653533	0,014725261

OFAS000007-RA	1,494559476	2,817780975	6,84E-06	0,000513218
OFAS001193-RA	1,495630173	2,819872969	1,89E-05	0,00112442
OFAS007952-RA	1,500621738	2,829646314	0,002169535	0,034004093
OFAS008521-RA	1,501048972	2,830484399	0,000484299	0,011643619
OFAS016773-RA	1,502475494	2,833284537	0,000461899	0,011249564
OFAS007517-RA	1,508529439	2,845198758	4,76E-06	0,000402467
OFAS007524-RA	1,514525674	2,857048792	5,65E-06	0,000443255
OFAS017349-RA	1,514859988	2,857710928	7,55E-06	0,00055067
OFAS017479-RA	1,520100293	2,868109873	3,82E-06	0,000342749
OFAS010776-RA	1,520684414	2,869271354	3,44E-07	5,74E-05
OFAS012883-RA	1,524967153	2,877801638	3,91E-07	6,03E-05
OFAS000459-RA	1,527477615	2,882813717	0,000876782	0,018195382
OFAS010790-RA	1,529394157	2,886645923	0,003051024	0,042802533
OFAS010937-RA	1,530054751	2,887967989	0,002622876	0,0388226
OFAS008316-RA	1,533562737	2,894998773	0,002383034	0,035973386
OFAS003965-RA	1,542705976	2,91340441	1,14E-07	2,49E-05
OFAS002626-RA	1,543448405	2,914904069	0,001625613	0,028004364
OFAS012972-RA	1,546566604	2,921211072	4,95E-08	1,35E-05
OFAS003575-RA	1,546814044	2,921712138	0,001094906	0,021509074
OFAS014443-RA	1,547984308	2,924083093	4,07E-06	0,000357939
OFAS008893-RA	1,549666207	2,927493986	0,001646745	0,028168795
OFAS002228-RA	1,552390283	2,933026859	0,000179561	0,00579505
OFAS018015-RA	1,55290497	2,934073415	5,46E-05	0,002370219
OFAS015911-RA	1,561091459	2,95076997	1,49E-07	3,05E-05
OFAS009569-RA	1,563023751	2,95472477	3,81E-07	5,95E-05
OFAS006041-RA	1,564688389	2,958136015	0,003223267	0,044551123
OFAS004384-RA	1,56515427	2,959091422	9,32E-07	0,000114158
OFAS016598-RA	1,566978951	2,962836367	2,82E-05	0,001489224
OFAS015160-RA	1,568517971	2,96599871	7,55E-08	1,85E-05
OFAS012929-RA	1,575821333	2,981051571	0,000619587	0,014057813
OFAS000798-RA	1,576840704	2,983158648	0,000323904	0,008643806
OFAS018785-RA	1,580378529	2,990483026	0,002323192	0,035555278
OFAS008271-RA	1,582641181	2,995176833	8,76E-05	0,00342664
OFAS016199-RA	1,584619658	2,999287163	0,000770043	0,016649955
OFAS008163-RA	1,587375918	3,005022761	7,22E-08	1,82E-05
OFAS000750-RA	1,588665632	3,007710337	5,02E-05	0,002293794
OFAS012269-RA	1,593254418	3,017292204	0,000470651	0,011399141
OFAS004801-RA	1,593361223	3,017515586	1,94E-05	0,001142687
OFAS013203-RA	1,597397981	3,025970622	2,34E-07	4,25E-05
OFAS017738-RA	1,600422827	3,03232172	7,63E-08	1,85E-05
OFAS015935-RA	1,603310943	3,038398173	1,55E-07	3,08E-05
OFAS010689-RA	1,606679935	3,045501754	1,37E-08	4,56E-06
OFAS009814-RA	1,609977283	3,052470352	6,78E-06	0,000513218
OFAS006621-RA	1,610275146	3,05310064	1,07E-08	3,91E-06

OFAS013038-RA	1,613101306	3,059087358	1,39E-07	2,94E-05
OFAS006428-RA	1,614299101	3,061628214	1,64E-05	0,001036603
OFAS014228-RA	1,621047798	3,075983572	0,000115842	0,004275705
OFAS008429-RA	1,624416681	3,083174792	3,03E-08	8,81E-06
OFAS003479-RA	1,62902517	3,093039311	8,50E-08	1,99E-05
OFAS015368-RA	1,629909744	3,094936361	2,10E-07	3,93E-05
OFAS006395-RA	1,633475675	3,102595623	1,10E-05	0,000750675
OFAS017400-RA	1,637571503	3,111416443	2,36E-05	0,001305781
OFAS015952-RA	1,638112281	3,11258294	1,79E-05	0,001097131
OFAS006170-RA	1,658037183	3,155868699	4,87E-07	7,16E-05
OFAS025047-RA	1,661354949	3,163134603	3,41E-07	5,74E-05
OFAS015481-RA	1,661688593	3,163866208	9,99E-08	2,30E-05
OFAS001929-RA	1,663674561	3,168224485	5,10E-05	0,002300545
OFAS007918-RA	1,666639755	3,174742883	0,002178933	0,034060766
OFAS006333-RA	1,672200434	3,187003126	6,53E-08	1,68E-05
OFAS000586-RA	1,674845066	3,19285064	0,000138115	0,004813101
OFAS025129-RC	1,674849523	3,192860504	2,31E-05	0,001290484
OFAS004215-RA	1,677419722	3,198553738	0,000251196	0,007281895
OFAS007519-RA	1,678136571	3,200143436	5,21E-06	0,000418271
OFAS005877-RA	1,696830838	3,241880334	0,001429662	0,025417723
OFAS009679-RA	1,70147525	3,25233361	2,18E-06	0,000219999
OFAS001667-RA	1,713491135	3,279534688	9,89E-07	0,00011948
OFAS018780-RA	1,717017442	3,287560494	0,000208087	0,006430582
OFAS002231-RA	1,72091563	3,296455555	0,000757366	0,016430069
OFAS016910-RA	1,724326094	3,304257441	2,87E-07	5,02E-05
OFAS003669-RA	1,733491828	3,325316884	1,65E-05	0,001041099
OFAS014102-RA	1,743343768	3,348102668	0,000271646	0,007695608
OFAS018423-RA	1,746718644	3,355944004	0,000410468	0,010313637
OFAS016415-RA	1,751365101	3,366769844	0,00221781	0,0343475
OFAS013306-RA	1,761238318	3,389889667	0,001278539	0,023608484
OFAS011857-RA	1,765139669	3,399069048	0,00012825	0,00456647
OFAS001867-RA	1,773504881	3,418835199	9,13E-09	3,52E-06
OFAS005162-RA	1,774877408	3,422089301	5,43E-05	0,002370219
OFAS011610-RA	1,793180566	3,465781172	2,64E-05	0,00142104
OFAS003630-RA	1,797438618	3,476025385	0,001206162	0,02281462
OFAS011012-RA	1,816675527	3,522685129	0,000874007	0,018195382
OFAS003052-RA	1,817954393	3,52580917	6,32E-05	0,002673198
OFAS016631-RA	1,818583249	3,527346369	1,26E-08	4,33E-06
OFAS008275-RA	1,824575876	3,542028637	2,74E-06	0,000258737
OFAS006630-RA	1,830735932	3,557184814	1,28E-09	6,20E-07
OFAS001915-RA	1,831033739	3,557919179	0,00293001	0,041912574
OFAS001636-RA	1,83129822	3,558571492	3,63E-09	1,53E-06
OFAS002741-RA	1,833406386	3,563775323	4,82E-05	0,002249023
OFAS001728-RA	1,839943803	3,579960832	7,01E-10	3,83E-07

OFAS012526-RA	1,846301224	3,5957712	0,003413709	0,046496704
OFAS008580-RA	1,855249141	3,618142278	0,002035039	0,032717928
OFAS006331-RA	1,856688699	3,621754354	1,42E-07	2,95E-05
OFAS013421-RA	1,861116089	3,632885986	0,002135544	0,0335516
OFAS004857-RA	1,867549909	3,649123325	2,42E-06	0,000238803
OFAS004761-RA	1,868011396	3,650290789	3,46E-07	5,74E-05
OFAS002217-RA	1,872338612	3,661255897	1,73E-05	0,001084446
OFAS006784-RA	1,872857017	3,662571736	0,000194338	0,006091895
OFAS007992-RA	1,879736055	3,68007726	1,82E-08	5,68E-06
OFAS008121-RA	1,886203206	3,696610927	9,11E-05	0,003501548
OFAS018941-RA	1,889486691	3,705033767	8,15E-08	1,94E-05
OFAS006934-RA	1,889491699	3,705046628	0,000215419	0,006609466
OFAS012566-RA	1,897303566	3,725163031	1,89E-06	0,00019222
OFAS002899-RA	1,908590049	3,754419996	1,37E-06	0,000153385
OFAS015854-RA	1,911980815	3,763254386	2,71E-07	4,86E-05
OFAS013853-RA	1,915083034	3,771355198	0,002052969	0,032885151
OFAS010013-RA	1,920351451	3,785152565	4,97E-07	7,16E-05
OFAS027123-RA	1,925510247	3,79871176	8,01E-05	0,003193116
OFAS015884-RA	1,925640134	3,799053776	6,91E-07	9,24E-05
OFAS011693-RA	1,933341541	3,819388145	9,47E-09	3,54E-06
OFAS002511-RA	1,942691326	3,844221129	0,002544866	0,037935587
OFAS004958-RA	1,949642593	3,862788246	3,27E-10	2,04E-07
OFAS013440-RA	1,953157869	3,872211806	5,65E-05	0,002444164
OFAS012927-RA	1,955048661	3,877290045	0,000265291	0,007566191
OFAS009424-RA	1,957648041	3,88428226	7,68E-07	0,000100644
OFAS011640-RA	1,959487574	3,889238138	1,11E-07	2,48E-05
OFAS004445-RA	1,982554465	3,951921979	1,51E-09	7,07E-07
OFAS000476-RA	1,993728241	3,982648734	0,000847077	0,017844447
OFAS011856-RA	1,996950893	3,991555007	0,00315107	0,043862682
OFAS012406-RA	2,002554977	4,007090176	3,12E-06	0,000290179
OFAS002165-RA	2,004426668	4,012292179	0,001035507	0,020464934
OFAS011901-RA	2,010123929	4,028168208	0,00010871	0,004058214
OFAS015105-RA	2,036222727	4,101702134	0,001941476	0,031562229
OFAS006474-RA	2,041443855	4,11657313	2,76E-05	0,001468815
OFAS005680-RA	2,045627021	4,128526659	0,003363029	0,04598344
OFAS016542-RA	2,048751414	4,13747735	6,90E-13	7,53E-10
OFAS003217-RQ	2,064291982	4,182286753	5,07E-07	7,22E-05
OFAS013462-RA	2,092450651	4,264718897	0,000602948	0,013787843
OFAS014486-RA	2,094143163	4,269725029	4,52E-06	0,000389635
OFAS005525-RA	2,104189274	4,299560733	2,18E-08	6,66E-06
OFAS008377-RA	2,107559762	4,309617301	2,14E-05	0,001223289
OFAS011609-RA	2,121883215	4,352617411	4,73E-07	7,04E-05
OFAS001524-RA	2,132132232	4,383648838	0,000166697	0,005515719
OFAS010508-RA	2,13961384	4,406440852	2,77E-10	1,82E-07

OFAS004760-RA	2,15687653	4,459483203	1,76E-05	0,001091975
OFAS003478-RA	2,16489452	4,484336436	5,68E-07	7,91E-05
OFAS017793-RA	2,176009311	4,519018025	2,34E-12	2,19E-09
OFAS013957-RA	2,20845998	4,621816496	0,002080283	0,033120232
OFAS012467-RA	2,242451905	4,732006008	2,76E-09	1,21E-06
OFAS018996-RA	2,261544307	4,795044841	0,001279251	0,023608484
OFAS004098-RA	2,27169463	4,828900142	0,001872622	0,030983835
OFAS005511-RA	2,272041155	4,83006015	0,000188354	0,00597622
OFAS010513-RA	2,287689942	4,88273656	5,35E-13	6,38E-10
OFAS000117-RA	2,289060831	4,887378479	1,20E-10	8,74E-08
OFAS027001-RA	2,302472721	4,933025419	6,17E-05	0,002625192
OFAS017703-RA	2,36786557	5,161768969	2,34E-05	0,0012968
OFAS014448-RA	2,385119331	5,223871218	2,63E-08	7,83E-06
OFAS019613-RA	2,389593987	5,240098705	0,000367213	0,009511464
OFAS007119-RA	2,407725992	5,306372638	7,74E-05	0,003109948
OFAS010127-RA	2,413970288	5,329389541	0,003680757	0,048913749
OFAS006269-RA	2,42884184	5,384609938	0,000553308	0,012923343
OFAS007213-RA	2,430779425	5,391846498	0,00222028	0,0343475
OFAS016851-RA	2,478133426	5,571761196	3,51E-07	5,75E-05
OFAS014485-RA	2,495551867	5,639439836	1,61E-06	0,000172923
OFAS002949-RA	2,544645081	5,834645812	0,000325549	0,008652484
OFAS025131-RA	2,546646325	5,842744998	2,30E-13	3,35E-10
OFAS000751-RA	2,565843125	5,921009319	0,00014789	0,005007236
OFAS014678-RA	2,578779549	5,974340851	4,61E-12	4,02E-09
OFAS003243-RA	2,607330809	6,093752092	0,000811403	0,017259434
OFAS006229-RA	2,614410093	6,123727532	1,17E-05	0,000783176
OFAS007927-RA	2,625989681	6,173076545	0,000687191	0,015261469
OFAS015035-RA	2,670949947	6,368483838	0,003362861	0,04598344
OFAS027088-RA	2,686889327	6,439235113	0,00156133	0,027204079
OFAS012689-RA	2,690067337	6,453435279	6,02E-10	3,43E-07
OFAS018690-RA	2,748877747	6,72194038	0,000302269	0,008251307
OFAS009851-RA	2,750694263	6,730409393	2,17E-12	2,19E-09
OFAS014828-RA	2,754964679	6,750361102	9,18E-16	1,72E-12
OFAS007054-RA	2,766182923	6,803055803	5,92E-06	0,000456146
OFAS003579-RA	2,801487217	6,971587535	4,70E-20	2,05E-16
OFAS005712-RA	2,877821733	7,350394758	6,27E-07	8,56E-05
OFAS010383-RA	2,887330038	7,398998665	2,74E-06	0,000258737
OFAS001620-RA	2,89229179	7,424489288	0,001113586	0,021745626
OFAS012563-RA	2,939665121	7,672331846	0,00011851	0,004321483
OFAS016064-RA	2,946406275	7,708265558	0,000600255	0,013750258
OFAS010146-RA	2,984930138	7,916869871	1,52E-05	0,000976256
OFAS010788-RA	3,040129879	8,225651096	6,06E-06	0,000463983
OFAS007566-RA	3,135875154	8,790073045	0,003704322	0,049077588
OFAS011521-RA	3,156407302	8,916066035	2,14E-17	4,66E-14

OFAS003578-RA	3,268014511	9,633195941	0,003457342	0,047042117
OFAS005298-RA	3,268293163	9,635056745	2,75E-07	4,88E-05
OFAS013816-RA	3,415051805	10,66677244	1,71E-06	0,000180351
OFAS013925-RA	3,461516077	11,01590469	0,002951416	0,042035219
OFAS017747-RA	3,516440351	11,44337219	0,00047391	0,011435812
OFAS009045-RA	3,677817758	12,79774533	0,001639658	0,028160063
OFAS006898-RA	3,692056707	12,92468045	0,002187651	0,034060766
OFAS012313-RA	3,701619322	13,01063366	0,00232173	0,035555278
OFAS004834-RA	3,745527281	13,41269537	0,000249404	0,007278266
OFAS017508-RA	3,785202909	13,78667746	4,70E-05	0,002209455
OFAS004772-RA	4,064795651	16,73498846	0,002669289	0,039254429
OFAS014843-RA	4,133845361	17,55542918	5,01E-06	0,000407462
OFAS007819-RA	4,186063133	18,20248018	0,000110503	0,004101766
OFAS018822-RA	4,264422428	19,21848128	0,000365697	0,009507405
OFAS019586-RA	4,272428801	19,32543256	0,001459084	0,025766016
OFAS006230-RA	4,327938305	20,08349299	0,000193983	0,006091895
OFAS009525-RA	4,376281361	20,76787012	0,000981859	0,019732044
OFAS007556-RA	4,469830503	22,15914793	0,000364406	0,009492677
OFAS005913-RA	4,510460188	22,79207215	3,41E-05	0,001744581
OFAS003694-RA	4,606629151	24,36315642	0,003538075	0,047645837
OFAS000424-RA	4,627405749	24,71655467	1,39E-08	4,56E-06
OFAS015448-RA	4,658766607	25,25971764	0,003109772	0,043485478
OFAS016360-RA	4,803981524	27,93460517	3,36E-06	0,000305441
OFAS010103-RA	4,824187441	28,32860081	0,001795523	0,02997036
OFAS018039-RA	5,107154026	34,46724367	5,03E-33	6,59E-29
OFAS013935-RA	5,203063553	36,83648639	0,000304818	0,008303605
OFAS008143-RA	5,285673448	39,00733275	3,15E-11	2,43E-08
OFAS005473-RA	5,303789328	39,5002349	0,000218502	0,006673725
OFAS007134-RA	5,454773129	43,85815231	5,38E-05	0,002362035
OFAS018980-RA	5,699686639	51,97286337	3,12E-05	0,001617222
OFAS015885-RA	5,737609741	53,35715136	0,000109439	0,004073787
OFAS011291-RA	5,940665509	61,42123043	3,40E-06	0,000307252
OFAS001002-RA	6,342203317	81,13223448	1,25E-08	4,33E-06
OFAS010968-RA	6,572155373	95,15155795	0,003628292	0,048462299
OFAS003056-RA	6,599093683	96,94493925	0,003791396	0,049828147
OFAS004367-RA	6,599676264	96,98409487	0,00350557	0,047418571
OFAS007220-RA	6,608386669	97,57141658	1,06E-09	5,32E-07
OFAS016540-RA	6,634070588	99,32400894	0,003755632	0,049530078
OFAS009202-RA	6,654448446	100,7369011	0,003658397	0,048814641
OFAS009484-RA	6,656173888	100,857453	0,003130741	0,043656407
OFAS002913-RA	6,679035956	102,4684495	0,003330526	0,045696215
OFAS005364-RA	6,696789051	103,7371659	0,003680025	0,048913749
OFAS000516-RA	6,710224107	104,7077274	0,002901023	0,041588731
OFAS019208-RA	6,713773328	104,9656395	0,002688772	0,039408255

OFAS008244-RA	6,726052905	105,8628732	0,002375381	0,035973386
OFAS010020-RA	6,742041681	107,0426317	0,002543987	0,037935587
OFAS010399-RA	6,742650111	107,0877845	0,002755394	0,039982204
OFAS005450-RA	6,756416615	108,1145299	0,003153373	0,043862682
OFAS014945-RA	6,758307698	108,2563392	0,002973522	0,042258196
OFAS014931-RA	6,76709172	108,9174816	0,00319385	0,044331582
OFAS019486-RA	6,768215517	109,0023567	0,003044944	0,042795151
OFAS004534-RA	6,773163247	109,3768226	0,003514771	0,047478401
OFAS011349-RA	6,787919039	110,5012622	0,002357188	0,035789373
OFAS016383-RA	6,796383953	111,1515266	0,001837316	0,03047386
OFAS002290-RA	6,801429464	111,5409354	0,001812303	0,030173585
OFAS010148-RA	6,801507625	111,5469785	0,002949584	0,042035219
OFAS025098-RA	6,802518448	111,6251612	0,001777257	0,029741242
OFAS015899-RA	6,81937989	112,9374295	0,002877686	0,041299367
OFAS018586-RA	6,84028109	114,5855323	0,002122657	0,033457288
OFAS006464-RA	6,863026874	116,4064246	0,001651554	0,028177486
OFAS008235-RA	6,865314091	116,5911192	0,001601124	0,02767748
OFAS017702-RA	6,869898285	116,9621791	0,001543616	0,026932096
OFAS009785-RA	6,882756586	118,0092867	0,001984567	0,032063851
OFAS001970-RA	6,901167719	119,5249274	0,00238196	0,035973386
OFAS002884-RA	6,916072941	120,7662018	0,001352528	0,024444382
OFAS015845-RA	6,920936538	121,1740144	0,00301472	0,042646618
OFAS003957-RA	6,922797813	121,3304464	0,001257055	0,023330307
OFAS003058-RA	6,925641613	121,5698455	0,001565434	0,027204079
OFAS011766-RA	6,92944222	121,8905289	0,002780343	0,04021063
OFAS008626-RA	6,940595719	122,8365186	0,001286547	0,02364323
OFAS010810-RA	6,946810417	123,3668028	0,002718936	0,039761408
OFAS018990-RA	6,999087905	127,9191019	0,001263563	0,023417921
OFAS000155-RA	7,00521892	128,463876	0,001235183	0,023099034
OFAS009090-RA	7,01734169	129,5478884	0,00123578	0,023099034
OFAS006772-RA	7,02069131	129,8490195	0,003567004	0,047936875
OFAS003024-RA	7,024502827	130,1925267	0,001875233	0,030985094
OFAS018838-RA	7,031299665	130,807338	0,001767712	0,029657269
OFAS008625-RA	7,051094909	132,6145176	0,00124966	0,023318826
OFAS019232-RA	7,051160778	132,6205725	0,001328191	0,024091227
OFAS025196-RA	7,076217807	134,9440735	0,003330053	0,045696215
OFAS014209-RA	7,076972821	135,014713	0,003020382	0,042646618
OFAS015434-RA	7,086921217	135,9489518	0,001156314	0,02231397
OFAS014137-RA	7,089582408	136,1999542	0,003026048	0,042680632
OFAS013891-RA	7,098751415	137,0683257	0,002644004	0,039057938
OFAS001502-RA	7,147693684	141,7980305	0,002211139	0,034327674
OFAS025056-RA	7,201564557	147,1929289	0,001102709	0,021629933
OFAS004200-RA	7,211368316	148,1965771	0,002012099	0,0324287
OFAS013392-RA	7,214162744	148,4839046	0,001194961	0,022791237

OFAS007790-RA	7,223590212	149,4573681	0,001951312	0,03168283
OFAS001822-RA	7,231172947	150,2449767	0,002328202	0,035555278
OFAS003105-RA	7,245447293	151,7389125	0,001684713	0,028507448
OFAS019496-RA	7,251100888	152,3347095	0,002583363	0,038378462
OFAS008581-RA	7,287174131	156,1917163	0,001371628	0,024687425
OFAS019383-RA	7,322388469	160,0510652	0,00116707	0,022415625
OFAS004071-RA	7,335078393	161,4650817	0,001023127	0,020312173
OFAS025325-RA	7,335329677	161,4932077	1,26E-30	8,24E-27
OFAS004797-RA	7,340621999	162,0867105	0,001540482	0,026913239
OFAS012971-RA	7,373319561	165,8022255	0,001134563	0,021971698
OFAS011050-RA	7,374656665	165,9559638	0,000941501	0,019245699
OFAS014661-RA	7,419546922	171,2009529	0,000826275	0,017518898
OFAS014357-RA	7,45016068	174,8726282	0,000772623	0,016678225
OFAS006506-RA	7,485538998	179,2139335	0,001107255	0,021654267
OFAS007326-RA	7,512574782	182,6040283	0,000614846	0,013986677
OFAS017442-RA	7,521039238	183,678536	0,000662852	0,01479014
OFAS013300-RA	7,574727992	190,6427678	0,002379087	0,035973386
OFAS009262-RA	7,590408088	192,7260914	0,000537707	0,012694736
OFAS005108-RA	7,629029693	197,9551366	0,000663394	0,01479014
OFAS017794-RA	7,652069587	201,1418659	0,000249983	0,007278957
OFAS003217-RP	7,656536729	201,7656442	0,000411664	0,010313637
OFAS010787-RA	7,68615599	205,95081	0,000214657	0,006602462
OFAS008693-RA	7,702894809	208,3542631	0,000554361	0,0129249
OFAS018435-RA	7,715747418	210,2187318	0,000437817	0,01088517
OFAS016604-RA	7,739007868	213,6355411	0,000200906	0,006267802
OFAS012525-RA	7,769764963	218,238975	0,00034887	0,009142495
OFAS004798-RA	7,780413324	219,8557301	0,000141181	0,004844736
OFAS025039-RA	7,784414326	220,4662986	0,000143927	0,004898374
OFAS001256-RB	7,802274937	223,2126433	0,000139368	0,004814059
OFAS000931-RA	7,805853848	223,767057	0,000112361	0,004158954
OFAS009060-RA	7,80919179	224,2853829	0,000167645	0,005533137
OFAS000423-RA	7,893959558	237,8584647	3,26E-18	8,54E-15
OFAS000303-RA	7,92544812	243,1070835	6,50E-05	0,002704012
OFAS012155-RA	7,937920623	245,2179235	5,26E-05	0,002335566
OFAS017538-RA	7,959260294	248,8720308	8,90E-05	0,003440377
OFAS007110-RA	8,004358179	256,7745093	4,63E-05	0,002180061
OFAS002031-RA	8,040231756	263,2394233	4,18E-05	0,002044812
OFAS019021-RA	8,11761938	277,7454332	1,20E-05	0,000803881
OFAS006375-RA	8,138701882	281,834005	1,10E-05	0,000750675
OFAS010970-RA	8,179268232	289,871208	7,40E-06	0,000547442
OFAS025309-RA	8,18490852	291,0066921	0,000488378	0,011720181
OFAS009689-RA	8,306570637	316,6116732	3,92E-06	0,00034682
OFAS008080-RA	8,322546682	320,1372365	0,000141965	0,004856818
OFAS000707-RA	8,35534414	327,4984209	5,76E-06	0,000449612

OFAS009524-RA	8,41905122	342,2842787	1,29E-06	0,000146925
OFAS016399-RA	8,457709883	351,5801681	7,90E-07	0,000101517
OFAS006666-RA	8,829777328	455,0172179	0,001539084	0,026913239
OFAS006887-RA	8,845199246	459,9072869	1,09E-06	0,000128456
OFAS027101-RB	8,940096266	491,1760026	1,26E-07	2,71E-05
OFAS017061-RA	9,028755892	522,3076021	4,86E-08	1,35E-05
OFAS012456-RA	9,241805492	605,4254414	3,86E-10	2,30E-07
OFAS000627-RA	9,39588935	673,6658467	1,60E-10	1,10E-07
OFAS025129-RB	9,768811487	872,3791546	4,85E-13	6,35E-10
OFAS000425-RA	9,803906649	893,8609736	2,22E-13	3,35E-10
OFAS017000-RA	10,89638104	1906,064259	0,00011677	0,004285822
OFAS025202-RC	11,32883907	2572,292637	1,12E-19	3,66E-16

Table 6.: *sog* knockdown compared to wild-type embryos

Gene ID	logFC	absolute FC	PValue	FDR
OFAS013274-RA	-9,518720766	733,5343753	2,26E-05	0,008971197
OFAS003756-RA	-7,912222883	240,8886957	0,00012996	0,028868681
OFAS013549-RA	-2,394150739	5,25667572	6,11E-07	0,000728241
OFAS001343-RA	-1,976223807	3,934618632	5,17E-05	0,015764513
OFAS012325-RA	-1,973991653	3,928535651	0,000279699	0,046330279
OFAS009029-RA	-1,89769746	3,726180239	0,000261948	0,044494138
OFAS006046-RA	-1,87672037	3,67239278	1,63E-05	0,007652
OFAS000859-RA	-1,8373611	3,573557744	1,44E-05	0,006984783
OFAS017308-RA	-1,768811553	3,407731228	4,14E-06	0,003680394
OFAS018794-RA	-1,763868041	3,396074342	9,58E-06	0,00570717
OFAS008572-RA	-1,759565786	3,385962009	0,000260852	0,044494138
OFAS015643-RA	-1,748183532	3,359353304	0,000227143	0,040779966
OFAS004704-RA	-1,723104707	3,301461236	4,36E-06	0,003680394
OFAS002720-RA	-1,698621715	3,245907111	5,91E-06	0,003686926
OFAS000019-RA	-1,695750515	3,239453649	1,82E-05	0,00823743
OFAS017054-RA	-1,694869085	3,237475074	0,000217526	0,040153391
OFAS027199-RA	-1,649521786	3,137296291	3,32E-05	0,011442297
OFAS018641-RA	-1,62250173	3,079085075	0,000171326	0,034544668
OFAS016222-RA	-1,611555368	3,05581111	6,59E-05	0,018761879
OFAS011893-RA	-1,603055265	3,037859747	1,35E-05	0,006984783
OFAS010379-RA	-1,59752896	3,026245356	6,39E-05	0,018612218
OFAS025094-RA	-1,568042931	2,96502225	2,22E-05	0,008971197
OFAS017389-RA	-1,550966964	2,930134653	7,57E-05	0,020069982
OFAS001752-RA	-1,504929297	2,83810762	0,000108389	0,026306304
OFAS004673-RA	-1,490130807	2,809144441	2,17E-05	0,008971197
OFAS005534-RA	-1,474243729	2,778379612	0,00018256	0,035710991
OFAS000060-RA	-1,439406462	2,712092646	0,000127406	0,028789432
OFAS005794-RA	-1,417224973	2,670713044	0,000248126	0,043359212

OFAS014873-RA	-1,366560981	2,578551717	0,000115316	0,027478689
OFAS016999-RA	-1,288936009	2,44347782	0,000302548	0,048953091
OFAS004207-RA	-1,269737683	2,411177205	0,000282803	0,046330279
OFAS006621-RA	1,253062155	2,383467833	0,000177083	0,035164293
OFAS014284-RA	1,320169503	2,496954449	0,000157951	0,032858882
OFAS007517-RA	1,356161395	2,560031204	0,000227053	0,040779966
OFAS025047-RA	1,457467333	2,746258316	7,66E-05	0,020069982
OFAS001193-RA	1,530672336	2,889204527	0,000125679	0,028789432
OFAS013440-RA	1,700041347	3,249102701	0,000118176	0,027657401
OFAS003960-RA	1,702849209	3,255432463	0,000140447	0,03067827
OFAS014678-RA	1,752310594	3,368977035	0,000264806	0,044494138
OFAS001867-RA	1,761312448	3,390063855	3,42E-06	0,00344781
OFAS016773-RA	1,762189867	3,392126253	5,61E-06	0,003686926
OFAS016539-RA	1,763450582	3,395091795	3,31E-05	0,011442297
OFAS015914-RA	1,832506934	3,561554171	2,12E-05	0,008971197
OFAS014828-RA	1,853219064	3,613054618	4,93E-06	0,003686926
OFAS003010-RA	1,869094769	3,653032956	6,96E-05	0,018998467
OFAS011857-RA	1,894102013	3,716905509	0,000143939	0,030925688
OFAS025203-RA	1,943048063	3,845171812	0,00010232	0,025302121
OFAS006160-RA	1,95841998	3,886361168	1,16E-05	0,006605835
OFAS025201-RA	1,964200341	3,901963657	0,000162268	0,033229475
OFAS014486-RA	1,999489426	3,998584638	5,83E-06	0,003686926
OFAS006356-RA	2,111943477	4,322732246	3,86E-05	0,012056473
OFAS010790-RA	2,438571151	5,421045631	2,64E-07	0,0003846
OFAS010201-RA	2,793086377	6,931109816	3,07E-07	0,000402031
OFAS012335-RA	2,799963157	6,964226653	2,71E-05	0,009880973
OFAS009424-RA	2,992726482	7,959768554	1,13E-07	0,000212399
OFAS000625-RA	3,031929358	8,179027745	3,43E-05	0,011518867
OFAS016851-RA	3,139876288	8,814485047	6,45E-10	1,69E-06
OFAS018840-RA	3,454677216	10,96380915	7,96E-11	2,61E-07
OFAS018575-RA	3,52770246	11,53305216	6,77E-05	0,018891262
OFAS009423-RA	3,54755079	11,69281824	2,43E-05	0,009373334
OFAS000423-RA	3,788493504	13,81815892	4,49E-06	0,003680394
OFAS012688-RA	3,809741324	14,02317695	0,000201006	0,038316846
OFAS016360-RA	4,044900544	16,50579296	0,00021359	0,039990226
OFAS006554-RB	4,07965606	16,90825722	0,000243548	0,043134385
OFAS000425-RA	4,10405106	17,19659538	0,000201729	0,038316846
OFAS009422-RA	4,799155582	27,84131757	2,60E-05	0,009728546
OFAS025131-RA	6,020031434	64,89482066	3,23E-24	4,23E-20
OFAS017060-RA	7,875624507	234,8546759	0,00015133	0,031989104
OFAS025039-RA	7,918040713	241,8620678	9,72E-05	0,024487349
OFAS002031-RA	8,173535113	288,721576	3,52E-05	0,011522586
OFAS006375-RA	8,272571817	309,2375745	1,41E-05	0,006984783
OFAS007134-RA	8,345409599	325,2509812	3,85E-05	0,012056473

OFAS002508-RA	8,366490558	330,0385089	1,43E-05	0,006984783
OFAS008080-RA	8,457257916	351,4700425	7,86E-05	0,02020795
OFAS000081-RA	8,912352914	481,8208163	2,90E-06	0,00316523
OFAS006887-RA	8,979797383	504,8802327	5,57E-06	0,003686926
OFAS001445-RB	9,114216133	554,1820348	6,38E-05	0,018612218
OFAS000627-RA	9,529029713	738,7947033	2,37E-09	5,17E-06
OFAS025035-RA	10,4844479	1432,627577	2,03E-17	8,89E-14
OFAS009692-RA	10,93421664	1956,713262	1,96E-07	0,000321103
OFAS025202-RC	11,46249327	2821,982399	1,93E-18	1,27E-14

Table 7.: *tld* knockdown compared to wild-type embryos

Gene ID	logFC	absolute FC	PValue	FDR
OFAS027173-RB	-9,539771552	744,3160584	4,24E-08	1,47E-06
OFAS013274-RA	-8,705567148	417,4811208	1,64E-06	3,71E-05
OFAS007530-RA	-8,460845091	352,3450391	1,02E-09	5,32E-08
OFAS017534-RA	-8,278134906	310,4323087	4,49E-11	3,13E-09
OFAS014948-RA	-8,250911818	304,6294937	6,51E-10	3,50E-08
OFAS000081-RD	-7,941033954	245,7476745	1,50E-08	5,83E-07
OFAS012345-RA	-7,51185245	182,5126246	1,81E-05	0,000295689
OFAS008236-RA	-7,461252628	176,2222923	4,49E-05	0,000641487
OFAS011098-RA	-7,445118139	174,2624762	1,78E-06	3,97E-05
OFAS014349-RA	-7,437608534	173,3577512	4,54E-06	8,93E-05
OFAS002203-RA	-7,344530137	162,5263848	0,0004792	0,004711549
OFAS027074-RA	-7,321481731	159,9505043	1,91E-05	0,000309276
OFAS025039-RD	-7,295821105	157,130682	0,004594247	0,029204582
OFAS010406-RA	-7,286710101	156,1414866	2,14E-05	0,000338766
OFAS025039-RE	-7,104879877	137,6518203	0,004924285	0,030894324
OFAS008838-RA	-7,043634808	131,9305447	5,52E-05	0,000764656
OFAS001035-RA	-7,019216311	129,7163308	0,00011269	0,0014081
OFAS005875-RA	-6,872412283	117,1661717	7,76E-05	0,001025242
OFAS004317-RA	-6,838754094	114,4643154	0,000183648	0,002139502
OFAS015405-RA	-6,792470546	110,8504292	0,00015777	0,001879007
OFAS019216-RA	-6,697155319	103,7635058	0,002095402	0,015698037
OFAS002482-RA	-6,64253974	99,90879229	0,001119856	0,009463277
OFAS005188-RA	-6,634877066	99,37954737	0,000247305	0,00271491
OFAS012088-RA	-6,594156017	96,61370948	0,000371469	0,003828378
OFAS019097-RA	-6,562267277	94,5016279	0,000611077	0,005760116
OFAS016648-RA	-6,559583345	94,32598433	0,005809069	0,035374396
OFAS018910-RA	-6,556393431	94,11765245	0,000382112	0,003913583
OFAS005625-RA	-6,555170002	94,03787298	0,00238191	0,017435898
OFAS010993-RA	-6,506165068	90,89727049	0,000813103	0,007262932
OFAS000346-RA	-6,502767464	90,68345571	0,000854038	0,007568351
OFAS006124-RA	-6,432915198	86,39735241	0,000950307	0,008236288

OFAS018547-RA	-6,389835709	83,85562798	1,33E-08	5,21E-07
OFAS002201-RA	-6,351879703	81,6782303	4,93E-12	4,62E-10
OFAS016926-RA	-6,341862887	81,11309212	0,003323253	0,02256261
OFAS014016-RA	-6,271457287	77,2496926	0,006873089	0,040355082
OFAS019570-RA	-6,263270867	76,81258876	0,00221836	0,016442144
OFAS010861-RA	-6,204305457	73,73641942	0,007163334	0,041680392
OFAS014065-RA	-6,203741295	73,70759063	0,005185757	0,032264271
OFAS009744-RA	-6,189146196	72,96568307	0,001997133	0,015121627
OFAS010240-RA	-6,185502739	72,78164422	0,005551074	0,03407988
OFAS017241-RA	-6,182330371	72,6217792	0,006249025	0,037611427
OFAS003761-RA	-6,148415102	70,9344771	0,004518324	0,028830803
OFAS005620-RA	-6,103915797	68,77993262	2,02E-10	1,26E-08
OFAS004190-RA	-6,033491149	65,50309405	0,006947585	0,040618045
OFAS016772-RA	-5,985145842	63,34442916	0,004063271	0,026556168
OFAS002443-RA	-5,977110843	62,99261698	0,00597196	0,036284304
OFAS005630-RA	-5,937710283	61,29554356	0,000421268	0,004256922
OFAS001543-RA	-5,905452443	59,94021871	0,007796591	0,044613457
OFAS005621-RA	-5,815304336	56,30941807	0,007260181	0,042080308
OFAS010693-RA	-5,746699338	53,69438553	0,008539745	0,047889411
OFAS001584-RA	-5,725179668	52,89940784	1,37E-05	0,000233496
OFAS016131-RA	-5,615569467	49,02920511	2,34E-05	0,000365366
OFAS000452-RB	-5,45601036	43,89578045	0,005189541	0,032272905
OFAS014901-RA	-5,361326895	41,10741921	0,000103943	0,001317138
OFAS008064-RA	-5,343059698	40,59020434	1,91E-05	0,000309276
OFAS000706-RA	-5,089384287	34,04531288	0,000235662	0,002619112
OFAS007500-RA	-5,034025464	32,7636791	0,002704838	0,019246785
OFAS001503-RA	-4,967225581	31,28123529	1,54E-24	1,68E-21
OFAS017164-RA	-4,902871462	29,91654077	3,51E-07	9,56E-06
OFAS013656-RA	-4,894845924	29,75058071	8,93E-05	0,001150529
OFAS026013-RA	-4,869156512	29,22551438	4,17E-21	2,01E-18
OFAS011686-RA	-4,86068489	29,05440269	0,005125048	0,031930801
OFAS019497-RA	-4,775207535	27,38297965	0,001162448	0,009774141
OFAS003261-RA	-4,731440502	26,56473658	2,58E-06	5,52E-05
OFAS013259-RA	-4,714498819	26,25460925	1,57E-08	6,04E-07
OFAS004484-RA	-4,66930402	25,44488948	4,49E-07	1,19E-05
OFAS016605-RA	-4,655565384	25,20373051	0,000430283	0,00432531
OFAS010364-RA	-4,63955744	24,92561922	0,0025477	0,018351611
OFAS017394-RA	-4,588876548	24,06520067	0,004303156	0,027786917
OFAS008145-RA	-4,564842082	23,66760934	5,72E-27	9,64E-24
OFAS004074-RA	-4,533350542	23,15658402	0,000722798	0,006609697
OFAS005523-RA	-4,513003127	22,83228158	0,00020844	0,002369357
OFAS007990-RA	-4,487818937	22,4371719	0,000345204	0,003615783
OFAS007015-RA	-4,461762027	22,03556566	2,53E-07	7,09E-06
OFAS019578-RA	-4,447564095	21,8197716	0,000133733	0,001630208

OFAS006074-RA	-4,431731582	21,58162485	0,007185152	0,041755835
OFAS017687-RA	-4,377444118	20,78461497	0,000184085	0,0021413
OFAS016393-RA	-4,369589549	20,67176327	1,88E-05	0,000306158
OFAS008830-RA	-4,35814832	20,50847511	0,000152976	0,001833264
OFAS002251-RA	-4,342761962	20,29091421	0,001221905	0,010204006
OFAS018583-RA	-4,299937012	19,6974506	2,12E-13	2,77E-11
OFAS014111-RA	-4,267709811	19,26232321	9,90E-24	8,34E-21
OFAS001783-RA	-4,229888901	18,76391416	1,09E-11	9,04E-10
OFAS009121-RA	-4,180594811	18,13361696	0,003225806	0,022023113
OFAS019431-RA	-4,175399783	18,0684367	0,00029249	0,003126856
OFAS008827-RA	-4,134885321	17,56808849	4,98E-07	1,30E-05
OFAS010166-RA	-4,133633839	17,55285546	4,09E-08	1,43E-06
OFAS019481-RA	-4,106954362	17,23123692	0,000187537	0,00217582
OFAS017733-RA	-4,10300773	17,18416362	0,001454129	0,011742879
OFAS003847-RA	-4,100594052	17,15543797	0,004762362	0,030145217
OFAS014107-RA	-4,063572596	16,72080726	6,85E-17	1,67E-14
OFAS009659-RA	-4,052397275	16,59178587	0,002867608	0,020086674
OFAS008126-RA	-4,048581846	16,54796431	6,42E-22	3,60E-19
OFAS013548-RA	-4,041000379	16,46123166	5,83E-05	0,000801105
OFAS011792-RA	-4,020076392	16,22421075	4,41E-11	3,11E-09
OFAS013811-RA	-3,989962843	15,88907069	9,94E-11	6,50E-09
OFAS016229-RA	-3,94119953	15,36099251	1,76E-05	0,000288738
OFAS014939-RA	-3,935770122	15,30329192	0,003410444	0,02299233
OFAS001625-RA	-3,935495999	15,30038445	0,003214126	0,021954499
OFAS012438-RA	-3,934659025	15,29151057	3,49E-06	7,13E-05
OFAS014149-RA	-3,919338359	15,12998193	0,006093393	0,036872421
OFAS000914-RA	-3,914024222	15,07435347	3,13E-06	6,49E-05
OFAS019143-RA	-3,885255639	14,77673511	0,000120336	0,001483005
OFAS007941-RA	-3,867709132	14,59810433	2,12E-18	6,48E-16
OFAS018296-RA	-3,797755054	13,90715156	0,002116312	0,015801952
OFAS009834-RA	-3,79147469	13,8467423	1,59E-07	4,76E-06
OFAS010978-RA	-3,78997955	13,83239963	0,004194137	0,027252785
OFAS017883-RA	-3,766464335	13,60876587	6,13E-17	1,56E-14
OFAS012737-RA	-3,74572543	13,41453769	0,001312993	0,010850316
OFAS004572-RA	-3,738419361	13,34677577	1,46E-09	7,26E-08
OFAS005228-RA	-3,735602414	13,32074083	4,00E-05	0,000584168
OFAS018424-RA	-3,706815435	13,05757816	2,87E-17	7,58E-15
OFAS008498-RA	-3,689594161	12,90263804	0,006743754	0,03984139
OFAS008728-RA	-3,688798547	12,89552449	0,000786451	0,007081211
OFAS017619-RA	-3,680969063	12,82573024	1,42E-23	1,12E-20
OFAS014439-RA	-3,593507143	12,07128322	1,68E-30	5,66E-27
OFAS004539-RA	-3,544935866	11,67164389	0,00329268	0,022400203
OFAS007013-RA	-3,544602375	11,6689462	8,75E-19	2,92E-16
OFAS010415-RA	-3,521083044	11,48025708	0,005801106	0,035357872

OFAS012777-RA	-3,520315656	11,47415221	1,09E-09	5,63E-08
OFAS004083-RA	-3,517762659	11,45386548	4,37E-06	8,67E-05
OFAS001888-RA	-3,513709565	11,42173225	0,000379371	0,003891946
OFAS007333-RA	-3,5076733	11,37404333	6,27E-14	8,96E-12
OFAS013297-RA	-3,50413946	11,34621703	0,00290264	0,020279339
OFAS013385-RA	-3,488832545	11,22647067	3,72E-31	1,67E-27
OFAS003542-RA	-3,487777509	11,2182638	0,002518732	0,01819159
OFAS007534-RA	-3,485409801	11,19986782	8,23E-06	0,000149662
OFAS019026-RA	-3,482394223	11,17648187	3,30E-06	6,82E-05
OFAS001267-RA	-3,481252614	11,16764138	0,000216842	0,002440155
OFAS015302-RA	-3,475741204	11,12505994	1,40E-11	1,12E-09
OFAS004763-RA	-3,450484416	10,93199209	0,003653058	0,024420195
OFAS008007-RA	-3,445410095	10,89360907	1,77E-09	8,63E-08
OFAS017236-RA	-3,440047194	10,85318965	2,06E-07	5,97E-06
OFAS001167-RA	-3,439052228	10,84570724	1,36E-21	6,79E-19
OFAS009611-RA	-3,427870295	10,76197008	1,18E-11	9,62E-10
OFAS016443-RA	-3,427619858	10,76010207	0,000337405	0,003546388
OFAS009515-RA	-3,421750179	10,71641298	0,007053556	0,041148288
OFAS000988-RA	-3,420806307	10,70940414	0,000159902	0,001897686
OFAS006280-RA	-3,410619099	10,63404889	7,80E-06	0,000143374
OFAS000801-RA	-3,394860217	10,51852289	0,000627603	0,00588296
OFAS010515-RA	-3,389637125	10,48051078	0,001100975	0,009350649
OFAS011298-RA	-3,380866572	10,41699005	4,21E-07	1,13E-05
OFAS019499-RA	-3,377318335	10,39140146	6,98E-09	2,95E-07
OFAS002372-RA	-3,368176849	10,3257656	7,83E-05	0,001031348
OFAS017911-RA	-3,357362701	10,24865513	2,20E-10	1,35E-08
OFAS002735-RA	-3,311289257	9,92652843	1,34E-12	1,44E-10
OFAS019018-RA	-3,295482527	9,818363137	0,00017783	0,002081121
OFAS008829-RA	-3,273314975	9,668653418	0,001818277	0,013912044
OFAS013810-RA	-3,26243898	9,596038727	0,002383036	0,017435898
OFAS013227-RA	-3,249063731	9,507484826	6,98E-05	0,000934291
OFAS001499-RA	-3,246668794	9,491715073	9,14E-05	0,001174543
OFAS017493-RA	-3,225906974	9,356098007	1,02E-15	1,97E-13
OFAS016316-RA	-3,224183139	9,344925347	0,0055249	0,033975409
OFAS004328-RA	-3,215732919	9,290349809	3,25E-10	1,86E-08
OFAS025328-RA	-3,214730513	9,283896974	1,46E-19	5,47E-17
OFAS005242-RA	-3,199898998	9,188943507	0,000377005	0,003876537
OFAS017265-RA	-3,191795068	9,137471923	0,000688611	0,006344734
OFAS016511-RA	-3,191141138	9,133331122	0,001793752	0,013783133
OFAS011734-RA	-3,184345732	9,090412311	1,88E-24	1,81E-21
OFAS017590-RA	-3,167900064	8,987376644	1,36E-11	1,09E-09
OFAS000088-RA	-3,158069987	8,926347597	7,46E-06	0,000138113
OFAS014433-RA	-3,150987665	8,882634724	8,89E-19	2,92E-16
OFAS011261-RA	-3,147422176	8,860709207	1,74E-08	6,63E-07

OFAS015995-RA	-3,143763735	8,83826835	1,59E-23	1,19E-20
OFAS009942-RA	-3,132628294	8,770312771	0,000322759	0,003412532
OFAS002449-RA	-3,130408236	8,756827155	0,001528628	0,012205466
OFAS014741-RA	-3,129661638	8,752296655	0,000971693	0,008363388
OFAS009406-RA	-3,128336744	8,7442627	6,31E-09	2,71E-07
OFAS008484-RA	-3,125990324	8,730052464	0,00834555	0,047141586
OFAS018186-RA	-3,121423844	8,702463414	0,005083299	0,031714701
OFAS008706-RA	-3,11611563	8,670502635	1,97E-14	3,05E-12
OFAS008565-RA	-3,112333314	8,647800933	0,000159021	0,001892237
OFAS008833-RA	-3,103971169	8,597821563	0,000471861	0,004656388
OFAS011641-RA	-3,103007503	8,592080456	0,005173649	0,032203812
OFAS009129-RA	-3,092277917	8,52841662	2,59E-06	5,54E-05
OFAS006633-RA	-3,083879927	8,478916555	0,000533897	0,005170087
OFAS011419-RA	-3,071802066	8,408229604	0,006482334	0,038609888
OFAS015864-RA	-3,066955495	8,380030502	0,000236856	0,002628043
OFAS018733-RA	-3,055231727	8,312207836	0,003072827	0,021204398
OFAS006152-RA	-3,054503596	8,308013705	0,000132032	0,001610929
OFAS013670-RA	-3,049123078	8,277086747	1,01E-22	6,47E-20
OFAS008614-RA	-3,041195123	8,231726921	1,16E-05	0,000203486
OFAS019105-RA	-3,040950345	8,230330387	7,54E-07	1,85E-05
OFAS013106-RA	-3,020971483	8,117139921	3,07E-13	3,83E-11
OFAS009696-RA	-3,020819845	8,116286797	2,07E-05	0,000330666
OFAS012308-RA	-3,006191155	8,034404823	3,84E-06	7,74E-05
OFAS008595-RA	-2,991143545	7,95103982	0,0064516	0,03849977
OFAS005170-RA	-2,987443186	7,930672378	2,20E-05	0,000346381
OFAS015095-RA	-2,981241268	7,896652845	0,000692487	0,006375803
OFAS017495-RA	-2,968854894	7,829145707	1,15E-20	4,70E-18
OFAS027060-RA	-2,966240439	7,814970562	0,000301789	0,003216063
OFAS000844-RA	-2,965564616	7,811310539	0,000878627	0,007739197
OFAS013112-RA	-2,963872553	7,802154424	0,001705478	0,013263733
OFAS007651-RA	-2,961828009	7,791105275	8,99E-22	4,84E-19
OFAS009334-RA	-2,957407225	7,76726789	4,03E-19	1,43E-16
OFAS001187-RA	-2,953189594	7,744593915	0,00056169	0,005377374
OFAS002828-RA	-2,951941677	7,737897813	0,000529997	0,005139712
OFAS004252-RA	-2,950703928	7,731261992	5,58E-11	3,81E-09
OFAS001084-RA	-2,93777278	7,662274865	0,000425873	0,004290578
OFAS006533-RA	-2,936479257	7,655407934	2,73E-07	7,58E-06
OFAS002265-RA	-2,930898028	7,625849337	0,005708084	0,034885613
OFAS012551-RA	-2,925593329	7,597861055	0,001741232	0,013479535
OFAS010862-RA	-2,913196953	7,532856014	0,008869359	0,049286415
OFAS013906-RA	-2,892038037	7,423183523	0,002782553	0,019623554
OFAS025166-RA	-2,885547348	7,389861614	3,11E-13	3,84E-11
OFAS012400-RA	-2,874912415	7,335586993	1,15E-28	3,10E-25
OFAS025131-RA	-2,868095562	7,301007501	2,35E-23	1,58E-20

OFAS012718-RA	-2,863405596	7,277311654	1,40E-09	6,99E-08
OFAS013419-RA	-2,859568258	7,257980886	3,17E-26	4,27E-23
OFAS015509-RA	-2,856670273	7,243416195	1,68E-06	3,79E-05
OFAS010658-RA	-2,842959742	7,174905063	4,74E-09	2,07E-07
OFAS012685-RA	-2,825577605	7,088977764	1,71E-17	4,59E-15
OFAS011260-RA	-2,825539003	7,08878809	0,008353253	0,04715772
OFAS006511-RA	-2,811658115	7,020910392	0,00217501	0,016168535
OFAS006844-RA	-2,810603626	7,015780571	0,003306363	0,02248193
OFAS010119-RA	-2,808096785	7,003600466	6,18E-09	2,66E-07
OFAS002565-RA	-2,79571896	6,943769028	0,000273657	0,002951284
OFAS015747-RA	-2,793148617	6,931408843	0,001570779	0,012460773
OFAS005912-RA	-2,781901847	6,877583959	4,70E-14	6,88E-12
OFAS018615-RA	-2,777501612	6,856639217	1,03E-07	3,24E-06
OFAS001431-RB	-2,756813459	6,759017077	0,000516455	0,005019231
OFAS008709-RA	-2,754110059	6,746363522	0,000362104	0,003753616
OFAS016674-RA	-2,748968095	6,722361354	1,08E-05	0,000190517
OFAS005889-RA	-2,744640062	6,70222473	2,14E-07	6,20E-06
OFAS006992-RA	-2,744047896	6,699474314	5,96E-21	2,55E-18
OFAS014037-RA	-2,739710048	6,679360805	0,00249646	0,018079204
OFAS006442-RA	-2,731838976	6,643018701	1,18E-09	6,00E-08
OFAS004034-RA	-2,730032122	6,634704089	4,76E-10	2,64E-08
OFAS005753-RA	-2,729648117	6,632938349	2,68E-06	5,69E-05
OFAS006281-RA	-2,728010229	6,625412267	3,88E-05	0,000568135
OFAS009575-RA	-2,7130864	6,55722955	3,12E-12	3,03E-10
OFAS001066-RA	-2,705203388	6,52149798	0,00018918	0,002188856
OFAS019549-RA	-2,698709229	6,49220803	0,000216011	0,002436913
OFAS002111-RA	-2,689109271	6,449151098	1,32E-17	3,70E-15
OFAS006789-RA	-2,686547534	6,437709756	1,22E-20	4,85E-18
OFAS005629-RA	-2,677684779	6,398282882	0,000116573	0,001452575
OFAS001655-RA	-2,676050172	6,391037585	7,76E-09	3,24E-07
OFAS010449-RA	-2,675468241	6,388460192	6,73E-17	1,67E-14
OFAS008956-RA	-2,67426556	6,383136766	0,001481421	0,011920393
OFAS005938-RA	-2,671122067	6,369243673	3,09E-08	1,10E-06
OFAS017665-RA	-2,667875084	6,354924934	0,007858598	0,044881625
OFAS012890-RA	-2,665862115	6,346064195	1,71E-07	5,03E-06
OFAS007912-RA	-2,66408739	6,33826241	0,000340051	0,003570011
OFAS000345-RA	-2,663006307	6,333514616	0,006780617	0,039989017
OFAS016445-RA	-2,662038249	6,329266211	9,55E-06	0,000170762
OFAS011732-RA	-2,65865426	6,314437664	6,83E-09	2,89E-07
OFAS018511-RA	-2,658366426	6,313177991	0,007292566	0,042231669
OFAS010061-RA	-2,643165194	6,247007206	0,000315733	0,003346451
OFAS003392-RA	-2,641879578	6,241442847	1,03E-06	2,45E-05
OFAS014686-RA	-2,639073361	6,229314282	0,002811022	0,019772568
OFAS003298-RA	-2,638021571	6,224774485	0,002320396	0,017079635

OFAS018545-RA	-2,63504243	6,211933694	3,44E-10	1,97E-08
OFAS011790-RA	-2,62752814	6,179662893	1,62E-24	1,68E-21
OFAS011262-RA	-2,62353569	6,162585213	3,68E-14	5,45E-12
OFAS012161-RA	-2,623485392	6,162370362	0,002118786	0,01581166
OFAS003262-RA	-2,599080879	6,059004927	0,003708711	0,024743108
OFAS012210-RA	-2,591088587	6,025531845	2,25E-11	1,72E-09
OFAS002738-RA	-2,581421483	5,98529138	2,84E-19	1,03E-16
OFAS014763-RA	-2,578245767	5,972130816	0,008685961	0,048567829
OFAS009622-RA	-2,563746245	5,912409701	6,65E-05	0,00089544
OFAS007940-RA	-2,561367571	5,902669524	3,06E-08	1,09E-06
OFAS011152-RA	-2,558842593	5,892347816	9,33E-14	1,30E-11
OFAS018831-RA	-2,553302286	5,86976313	0,001563209	0,012422668
OFAS017014-RA	-2,54162533	5,822445902	0,004223447	0,027403582
OFAS002286-RA	-2,536649805	5,802400207	1,52E-11	1,21E-09
OFAS002618-RA	-2,52280567	5,746986539	9,45E-15	1,57E-12
OFAS019517-RA	-2,518480458	5,729782827	0,000681798	0,006307569
OFAS013990-RA	-2,51752739	5,725998888	2,44E-06	5,25E-05
OFAS010922-RA	-2,515359411	5,717400727	0,000462286	0,004568598
OFAS025266-RA	-2,513818279	5,711296483	0,001552223	0,012357892
OFAS001144-RA	-2,511596116	5,702506223	0,001602619	0,01266859
OFAS013929-RA	-2,509829402	5,69552725	1,14E-05	0,00019969
OFAS014271-RA	-2,508416602	5,689952473	4,16E-05	0,000604694
OFAS001726-RA	-2,498653292	5,651576228	2,80E-10	1,64E-08
OFAS008256-RA	-2,497889993	5,648586889	2,97E-16	6,45E-14
OFAS007177-RA	-2,490666417	5,620375097	8,54E-06	0,000154165
OFAS004923-RA	-2,489462957	5,615688673	1,94E-06	4,25E-05
OFAS013066-RA	-2,483534003	5,592657584	3,68E-05	0,000543604
OFAS000911-RA	-2,477710428	5,570127796	0,004908999	0,03083138
OFAS019008-RA	-2,473247856	5,552924789	8,16E-06	0,000148514
OFAS002182-RA	-2,470504001	5,542373744	7,25E-07	1,80E-05
OFAS016778-RA	-2,469970083	5,540322981	3,25E-06	6,72E-05
OFAS005668-RA	-2,468572251	5,534957545	0,000744416	0,006779775
OFAS018664-RA	-2,465977821	5,525012855	0,00139294	0,011343956
OFAS005681-RA	-2,458500572	5,496451708	0,000127292	0,001560166
OFAS002709-RA	-2,457759365	5,493628545	0,000664853	0,006166341
OFAS011707-RA	-2,454930891	5,482868569	0,000130839	0,001597821
OFAS004790-RA	-2,449962268	5,464018122	6,53E-05	0,000880399
OFAS015212-RA	-2,446128761	5,449518488	1,16E-17	3,41E-15
OFAS005881-RA	-2,442907732	5,437365208	0,000576719	0,005493925
OFAS013291-RA	-2,441211503	5,430976057	0,000801132	0,007179803
OFAS015347-RA	-2,440037062	5,426556713	3,24E-12	3,12E-10
OFAS012259-RA	-2,440029642	5,426528805	0,005135113	0,03197872
OFAS015991-RA	-2,439933278	5,426166354	0,000609248	0,005753208
OFAS000398-RA	-2,438827074	5,422007368	0,008437045	0,047437798

OFAS019594-RA	-2,43862268	5,421239261	1,01E-06	2,42E-05
OFAS002403-RA	-2,437385814	5,416593459	2,93E-05	0,0004426
OFAS010819-RA	-2,434679433	5,406441888	6,25E-06	0,000118327
OFAS004006-RA	-2,43423077	5,4047608	3,03E-06	6,34E-05
OFAS016078-RA	-2,433234728	5,401030623	0,0052514	0,032562291
OFAS000719-RA	-2,426498151	5,375869628	4,72E-07	1,24E-05
OFAS015491-RA	-2,420650857	5,354125134	0,000193652	0,002231392
OFAS009841-RA	-2,414464251	5,331214577	0,001799729	0,013813303
OFAS011007-RA	-2,411133888	5,318922028	2,41E-12	2,44E-10
OFAS011494-RA	-2,409148762	5,311608305	0,008968171	0,049712454
OFAS007589-RA	-2,407041894	5,303857055	2,40E-05	0,000372905
OFAS014729-RA	-2,406171618	5,300658577	2,79E-05	0,000423769
OFAS006513-RA	-2,401410683	5,283195085	0,002713594	0,019278538
OFAS003318-RA	-2,399375543	5,27574759	1,99E-15	3,63E-13
OFAS019615-RA	-2,398303301	5,271827999	0,002762973	0,019543371
OFAS000929-RA	-2,390617088	5,243816088	6,32E-14	8,96E-12
OFAS001996-RA	-2,39060891	5,243786364	1,42E-06	3,25E-05
OFAS010835-RA	-2,389395211	5,239376766	9,59E-06	0,000171387
OFAS001629-RA	-2,386786921	5,229912905	0,000345623	0,003617362
OFAS013606-RA	-2,37674189	5,193625144	5,55E-09	2,40E-07
OFAS009865-RA	-2,364568218	5,149984955	6,02E-05	0,000820701
OFAS010595-RA	-2,361292655	5,138305452	4,85E-07	1,27E-05
OFAS008739-RA	-2,352476217	5,107000561	0,00224652	0,016608468
OFAS005642-RA	-2,350782563	5,101008707	5,33E-10	2,89E-08
OFAS012117-RA	-2,348166272	5,091766537	1,68E-05	0,00027642
OFAS011627-RA	-2,347048795	5,087824107	2,32E-14	3,56E-12
OFAS008914-RA	-2,345300138	5,08166101	5,16E-07	1,34E-05
OFAS008863-RA	-2,341560956	5,068507395	2,23E-05	0,000350213
OFAS010736-RA	-2,339518712	5,061337616	0,002666191	0,019032109
OFAS005696-RA	-2,338976121	5,059434426	2,75E-12	2,73E-10
OFAS019250-RA	-2,329791683	5,02732753	8,08E-11	5,33E-09
OFAS001343-RA	-2,320003021	4,993332653	1,43E-15	2,70E-13
OFAS012979-RA	-2,319627977	4,99203475	5,16E-16	1,04E-13
OFAS004425-RA	-2,317473552	4,984585541	0,001555274	0,012366904
OFAS000344-RA	-2,310735208	4,961358501	0,00303886	0,021034656
OFAS012306-RA	-2,310308333	4,959890714	0,001501716	0,012046825
OFAS014307-RA	-2,309829658	4,958245334	3,18E-10	1,83E-08
OFAS019389-RA	-2,292034535	4,897462805	5,16E-08	1,74E-06
OFAS025091-RA	-2,290389681	4,89188226	4,07E-17	1,06E-14
OFAS004733-RA	-2,285180957	4,874252394	3,95E-08	1,38E-06
OFAS013669-RA	-2,283508405	4,868604827	8,00E-11	5,33E-09
OFAS015192-RA	-2,281325482	4,861243776	0,002808156	0,019772542
OFAS005968-RA	-2,277234714	4,847479222	8,75E-12	7,51E-10
OFAS009729-RA	-2,267598626	4,815209695	0,008198833	0,046461203

OFAS008273-RA	-2,261173814	4,793813603	2,57E-14	3,85E-12
OFAS002986-RA	-2,258823467	4,786010184	4,26E-11	3,02E-09
OFAS002707-RA	-2,258203956	4,783955453	0,004909674	0,03083138
OFAS002556-RA	-2,254467205	4,771580477	0,00106444	0,009068949
OFAS001196-RA	-2,254269704	4,770927304	3,47E-11	2,53E-09
OFAS003149-RA	-2,25332009	4,767788009	0,001778214	0,013694991
OFAS016845-RA	-2,248665477	4,752430329	0,002549128	0,018352088
OFAS006425-RA	-2,247818263	4,749640313	0,006910337	0,040482695
OFAS014541-RA	-2,243651203	4,735941312	0,000960774	0,008295913
OFAS018405-RA	-2,233199118	4,701754195	5,30E-08	1,77E-06
OFAS002796-RA	-2,23296053	4,7009767	1,97E-05	0,000316723
OFAS008509-RA	-2,225840679	4,677834041	0,004288235	0,027717141
OFAS004516-RA	-2,223783775	4,671169431	1,82E-15	3,36E-13
OFAS007297-RA	-2,22106802	4,66238461	0,003015394	0,02091522
OFAS013549-RA	-2,21841059	4,653804448	3,75E-11	2,70E-09
OFAS012647-RA	-2,215197031	4,643449779	0,002098543	0,015704099
OFAS008708-RA	-2,214023762	4,639675034	8,24E-12	7,21E-10
OFAS016897-RA	-2,213664695	4,638520427	2,27E-07	6,52E-06
OFAS009045-RA	-2,209193953	4,624168449	7,33E-12	6,50E-10
OFAS008640-RA	-2,206143271	4,614400645	1,30E-14	2,08E-12
OFAS005869-RA	-2,205424952	4,612103702	4,18E-07	1,13E-05
OFAS002474-RA	-2,203077647	4,604605783	0,000555322	0,005335365
OFAS013478-RA	-2,201584003	4,599841031	4,38E-05	0,000629256
OFAS016453-RA	-2,199424428	4,592960666	0,000952205	0,008243057
OFAS003598-RA	-2,198613286	4,59037904	0,001111996	0,009414575
OFAS005746-RA	-2,196023659	4,582146735	3,19E-09	1,47E-07
OFAS000994-RA	-2,193895593	4,575392761	1,86E-06	4,11E-05
OFAS007448-RA	-2,192982957	4,572499325	0,007824281	0,044714922
OFAS001382-RA	-2,192718704	4,571661874	0,000293576	0,003135978
OFAS009408-RA	-2,189268622	4,560742197	1,21E-11	9,82E-10
OFAS012538-RA	-2,175498347	4,517417791	1,18E-07	3,66E-06
OFAS003063-RA	-2,174190274	4,513323763	1,20E-05	0,000209246
OFAS017287-RA	-2,165717977	4,486896722	0,000119322	0,001477274
OFAS007075-RA	-2,158968479	4,465954271	5,49E-08	1,82E-06
OFAS003659-RA	-2,157380421	4,461041041	3,37E-15	5,97E-13
OFAS017097-RA	-2,156125509	4,457162344	0,000108139	0,001362614
OFAS015002-RA	-2,155120226	4,454057634	1,66E-07	4,91E-06
OFAS007234-RA	-2,154853942	4,453235607	4,37E-05	0,000629209
OFAS000180-RA	-2,152746482	4,446735158	0,000290461	0,003110108
OFAS012198-RA	-2,144687911	4,421965935	0,003110953	0,021433899
OFAS004725-RA	-2,143679895	4,418877372	0,003513896	0,023618853
OFAS005151-RA	-2,140930369	4,410463778	2,04E-11	1,58E-09
OFAS000357-RA	-2,140356769	4,408710573	5,34E-06	0,000102554
OFAS016029-RA	-2,139806407	4,407029051	9,89E-07	2,38E-05

OFAS015362-RA	-2,138801018	4,403958939	0,000212576	0,002405565
OFAS018940-RA	-2,132238036	4,383970336	0,000632165	0,005913375
OFAS016756-RA	-2,125907806	4,364776571	1,88E-05	0,000305788
OFAS002695-RA	-2,120585772	4,348704781	1,34E-08	5,23E-07
OFAS003593-RA	-2,11737559	4,339039111	0,00045522	0,004515326
OFAS003124-RA	-2,110230111	4,317601552	4,36E-16	9,03E-14
OFAS025228-RH	-2,105792773	4,304342184	0,005055187	0,031568552
OFAS005042-RA	-2,104064343	4,299188427	0,000877949	0,007739197
OFAS010424-RA	-2,100768032	4,289376731	2,19E-16	5,07E-14
OFAS006082-RA	-2,10007432	4,287314705	1,63E-08	6,25E-07
OFAS011555-RA	-2,098990406	4,284094802	0,000351395	0,003666376
OFAS009220-RA	-2,097439679	4,279492381	2,78E-16	6,15E-14
OFAS008769-RA	-2,094208406	4,269918122	2,47E-10	1,49E-08
OFAS016020-RA	-2,094104002	4,269609132	1,31E-05	0,000224037
OFAS019062-RA	-2,090867646	4,260041975	0,00221914	0,016442144
OFAS007029-RA	-2,088988738	4,254497479	2,54E-05	0,000390212
OFAS012775-RA	-2,088673261	4,253567243	2,82E-10	1,64E-08
OFAS003007-RA	-2,086715098	4,247797812	7,01E-05	0,000936187
OFAS006225-RA	-2,085434489	4,244028925	2,45E-13	3,17E-11
OFAS007784-RA	-2,085138447	4,243158138	0,005192643	0,032277296
OFAS013173-RA	-2,0832787	4,237691899	1,92E-05	0,000309975
OFAS008156-RA	-2,077984681	4,222170039	6,69E-09	2,84E-07
OFAS007798-RA	-2,074233461	4,211206032	2,03E-05	0,000325383
OFAS009790-RA	-2,070891416	4,201461943	0,002594973	0,018612506
OFAS002481-RA	-2,068590462	4,194766372	0,000775951	0,007000708
OFAS009675-RA	-2,06647148	4,188609763	0,000260737	0,002833685
OFAS017242-RA	-2,06050147	4,171312708	0,000110856	0,001389054
OFAS008713-RA	-2,059499946	4,168417973	0,006761301	0,039910044
OFAS002599-RA	-2,058447284	4,165377597	0,006611427	0,039201386
OFAS017557-RA	-2,057937815	4,163906909	0,007557768	0,043487028
OFAS003248-RA	-2,057745732	4,163352556	2,46E-05	0,000380757
OFAS003429-RA	-2,056480336	4,159702456	0,006652345	0,039405052
OFAS016740-RA	-2,051996033	4,146793002	0,000937955	0,008170728
OFAS002254-RA	-2,051439606	4,145193951	0,003130798	0,021505279
OFAS014272-RA	-2,048602802	4,137051169	4,41E-05	0,000631888
OFAS006764-RA	-2,043919459	4,123643059	1,50E-05	0,000252276
OFAS016672-RA	-2,041732583	4,117397064	5,37E-12	4,99E-10
OFAS006322-RA	-2,041210833	4,115908279	5,91E-07	1,51E-05
OFAS013348-RA	-2,038941228	4,109438347	0,001071411	0,009122568
OFAS018271-RA	-2,038398493	4,107892686	0,004543015	0,028933526
OFAS006933-RA	-2,036357977	4,102086679	9,84E-13	1,08E-10
OFAS011797-RA	-2,035422755	4,099428377	6,27E-07	1,59E-05
OFAS002922-RA	-2,032770913	4,091900069	6,20E-07	1,57E-05
OFAS001549-RA	-2,032637509	4,091521716	0,00495234	0,031018868

OFAS016492-RA	-2,032026831	4,089790182	0,002674863	0,019073799
OFAS000897-RA	-2,031538955	4,088407373	5,03E-08	1,70E-06
OFAS012928-RA	-2,023039791	4,064392672	0,000431943	0,004332298
OFAS012254-RA	-2,020538214	4,05735128	0,001635868	0,012863478
OFAS007635-RA	-2,017518869	4,048868728	2,34E-09	1,11E-07
OFAS002088-RA	-2,014005899	4,039021705	3,12E-16	6,68E-14
OFAS018823-RA	-2,011589363	4,032261946	0,002201613	0,016330244
OFAS006932-RA	-2,009860253	4,027432063	1,11E-11	9,20E-10
OFAS009423-RA	-2,009102917	4,025318437	5,52E-10	2,99E-08
OFAS016074-RA	-2,007667418	4,021315189	1,50E-06	3,42E-05
OFAS000872-RA	-2,006853893	4,019048237	2,73E-06	5,78E-05
OFAS006893-RA	-2,006592625	4,018320465	1,79E-09	8,65E-08
OFAS012500-RA	-2,004442625	4,012336558	1,28E-05	0,000220379
OFAS015859-RA	-1,996728702	3,990940311	2,37E-07	6,73E-06
OFAS002702-RA	-1,993806072	3,982863598	8,53E-05	0,00110952
OFAS019019-RA	-1,993608907	3,982319319	3,78E-08	1,33E-06
OFAS000873-RA	-1,989366983	3,970627392	0,006214104	0,037434694
OFAS012694-RA	-1,986200588	3,961922302	0,000762277	0,006905095
OFAS006155-RA	-1,983707817	3,955082579	0,001968051	0,014935016
OFAS025123-RA	-1,981636777	3,949408989	0,0048819	0,03074089
OFAS017940-RA	-1,973866345	3,928194446	0,001004364	0,008617055
OFAS015308-RA	-1,966509209	3,908213304	0,006823997	0,040156944
OFAS017390-RA	-1,966252811	3,907518792	0,000117469	0,001462392
OFAS000203-RA	-1,964260386	3,902126062	0,002182131	0,016212524
OFAS006907-RA	-1,95754366	3,884001235	0,000727905	0,006651884
OFAS008318-RA	-1,953759525	3,873826997	1,24E-05	0,000215291
OFAS002278-RA	-1,950130396	3,86409455	0,00168148	0,013121724
OFAS014523-RA	-1,944092258	3,847955881	0,000628538	0,005887629
OFAS004638-RA	-1,936670502	3,828211405	0,00399322	0,026225586
OFAS007821-RA	-1,934023178	3,821193135	0,00105932	0,009036757
OFAS005814-RA	-1,932791386	3,817931942	0,002338042	0,01718136
OFAS001872-RA	-1,932176532	3,816305146	8,50E-05	0,001106356
OFAS019355-RA	-1,929545875	3,809352714	0,002048577	0,015418748
OFAS002112-RA	-1,925768236	3,799391124	1,02E-08	4,11E-07
OFAS009063-RA	-1,924569304	3,796235002	6,63E-09	2,83E-07
OFAS006720-RA	-1,914575223	3,770027961	1,16E-11	9,53E-10
OFAS008084-RA	-1,914432456	3,769654901	0,000414503	0,004199136
OFAS007454-RA	-1,913617664	3,767526513	7,01E-09	2,95E-07
OFAS019065-RA	-1,912494036	3,764593356	2,86E-06	6,02E-05
OFAS010194-RA	-1,909038935	3,755588342	1,76E-07	5,15E-06
OFAS001821-RA	-1,903154071	3,740300211	5,96E-08	1,97E-06
OFAS002720-RA	-1,902839051	3,739483586	9,06E-13	1,00E-10
OFAS013379-RA	-1,900964051	3,73462672	0,002760697	0,019541034
OFAS001466-RA	-1,900493845	3,733409721	3,42E-13	4,19E-11

OFAS006986-RA	-1,898744334	3,728885075	0,002135424	0,015927002
OFAS010091-RA	-1,897911454	3,726732981	7,15E-13	8,37E-11
OFAS008218-RA	-1,897103024	3,724645249	0,004466982	0,028624642
OFAS014024-RA	-1,894570102	3,718111672	1,97E-09	9,48E-08
OFAS015412-RA	-1,888620654	3,702810335	3,77E-10	2,13E-08
OFAS010499-RA	-1,886188836	3,696574106	2,37E-06	5,12E-05
OFAS011682-RA	-1,88618336	3,696560075	6,87E-08	2,26E-06
OFAS018716-RA	-1,885606409	3,695082073	7,87E-05	0,001036375
OFAS003599-RA	-1,882164696	3,686277541	1,01E-08	4,07E-07
OFAS013326-RA	-1,881419361	3,684373604	3,92E-11	2,81E-09
OFAS011258-RA	-1,879346768	3,679084389	6,09E-05	0,000827625
OFAS002865-RA	-1,879148311	3,678578327	0,000590046	0,005605022
OFAS008255-RA	-1,877163065	3,673519836	1,61E-07	4,78E-06
OFAS013187-RA	-1,873687415	3,664680476	0,00040104	0,004076988
OFAS011829-RA	-1,87034641	3,656203597	0,001281396	0,010641432
OFAS005743-RA	-1,869876353	3,655012531	2,02E-07	5,88E-06
OFAS005306-RA	-1,862523875	3,636432696	2,11E-06	4,58E-05
OFAS005669-RA	-1,860530098	3,631410686	0,000223532	0,002502889
OFAS008828-RA	-1,857189285	3,623011248	3,34E-07	9,16E-06
OFAS016069-RA	-1,856852148	3,622164703	0,00093896	0,008170728
OFAS016687-RA	-1,85684851	3,622155569	9,38E-12	7,95E-10
OFAS001758-RA	-1,854155212	3,615399848	0,001801964	0,013822584
OFAS005728-RA	-1,850773936	3,606936279	8,14E-06	0,000148514
OFAS010253-RA	-1,850534642	3,606338059	5,69E-06	0,000108836
OFAS016467-RA	-1,850298765	3,60574848	9,71E-06	0,000173229
OFAS001225-RA	-1,847467826	3,598680012	0,003036809	0,021031266
OFAS001857-RA	-1,847117731	3,597806836	2,91E-12	2,86E-10
OFAS000070-RA	-1,846479355	3,596215199	0,001684949	0,013126816
OFAS010767-RA	-1,844162175	3,590443786	0,000109862	0,001380446
OFAS005555-RA	-1,843050222	3,587677528	1,22E-09	6,18E-08
OFAS008610-RA	-1,841429735	3,583649981	4,97E-07	1,30E-05
OFAS007235-RA	-1,840719675	3,581886629	0,000764393	0,006915796
OFAS000215-RA	-1,840215596	3,580635334	0,001961168	0,014894676
OFAS012424-RA	-1,83983441	3,57968939	6,22E-05	0,000844391
OFAS016894-RA	-1,837454108	3,573788132	2,36E-11	1,80E-09
OFAS003979-RA	-1,83546523	3,568864753	2,88E-05	0,000436377
OFAS007265-RA	-1,834724349	3,567032471	5,48E-08	1,82E-06
OFAS013042-RA	-1,832016238	3,560343006	0,000188492	0,002185019
OFAS005411-RA	-1,828698546	3,552164873	0,000329062	0,003476439
OFAS005404-RA	-1,826789935	3,547468651	0,003116633	0,021440777
OFAS018554-RA	-1,823242194	3,538755764	4,74E-09	2,07E-07
OFAS004640-RA	-1,81991563	3,530605507	0,000231105	0,00257272
OFAS003294-RA	-1,819342397	3,529202952	3,29E-12	3,14E-10
OFAS014780-RA	-1,819190529	3,528831463	8,00E-05	0,001051697

OFAS019135-RA	-1,819069019	3,528534263	0,004919244	0,03087708
OFAS008996-RA	-1,817880685	3,525629041	2,20E-07	6,34E-06
OFAS000043-RA	-1,81575588	3,520440305	0,0030022	0,020866681
OFAS015897-RA	-1,815118453	3,51888521	1,71E-06	3,84E-05
OFAS013523-RA	-1,813921391	3,515966663	7,31E-05	0,000975234
OFAS002087-RA	-1,811416326	3,509866909	2,65E-10	1,57E-08
OFAS012482-RA	-1,810196587	3,506900716	0,000164685	0,001949304
OFAS001654-RA	-1,808362091	3,502444261	1,05E-06	2,48E-05
OFAS010870-RA	-1,808023389	3,501622087	0,00105158	0,008982111
OFAS007656-RA	-1,804676541	3,493508234	0,002196015	0,016297699
OFAS008571-RA	-1,804085526	3,492077377	6,99E-10	3,73E-08
OFAS008800-RA	-1,804063977	3,492025217	8,35E-13	9,37E-11
OFAS017776-RA	-1,80393966	3,491724323	0,004459158	0,028588702
OFAS007487-RA	-1,79799777	3,477372865	0,004359669	0,028044286
OFAS002984-RA	-1,795570896	3,471528212	2,57E-11	1,93E-09
OFAS003619-RA	-1,792147381	3,463300044	2,04E-12	2,08E-10
OFAS000859-RA	-1,787081468	3,451160256	1,25E-10	8,09E-09
OFAS011746-RA	-1,785377108	3,44708556	0,00088637	0,007778115
OFAS016365-RA	-1,78337823	3,442312871	2,29E-07	6,56E-06
OFAS019565-RA	-1,781100763	3,436883055	0,001374441	0,011236489
OFAS011434-RA	-1,780848345	3,436281781	4,37E-06	8,67E-05
OFAS013798-RA	-1,78034049	3,435072359	4,58E-09	2,02E-07
OFAS003560-RA	-1,77763292	3,428631654	4,09E-06	8,19E-05
OFAS018446-RA	-1,774708825	3,421689443	6,66E-06	0,000124775
OFAS004264-RA	-1,774110936	3,420271704	5,49E-07	1,41E-05
OFAS009978-RA	-1,767186448	3,403894795	2,48E-14	3,76E-12
OFAS010912-RA	-1,762493812	3,392840976	2,41E-07	6,81E-06
OFAS007848-RA	-1,759480666	3,38576224	1,64E-09	8,09E-08
OFAS007068-RA	-1,759413256	3,385604043	1,35E-05	0,000230032
OFAS013253-RA	-1,758900647	3,384401306	2,34E-05	0,000365366
OFAS005751-RA	-1,758156486	3,382656038	0,000227664	0,002540705
OFAS016736-RA	-1,756046116	3,377711518	0,000223032	0,002501451
OFAS002772-RA	-1,755532736	3,37650978	0,005317752	0,032933385
OFAS008105-RA	-1,754118129	3,373200629	5,50E-05	0,000763387
OFAS014794-RA	-1,749213052	3,361751423	9,36E-06	0,000167934
OFAS018922-RA	-1,745116345	3,352218864	1,54E-09	7,63E-08
OFAS011837-RA	-1,743869213	3,349322305	0,004600686	0,029231715
OFAS008904-RA	-1,740798965	3,342202077	8,06E-11	5,33E-09
OFAS019034-RA	-1,740600333	3,341741952	1,06E-11	8,87E-10
OFAS016609-RA	-1,73860498	3,337123271	1,60E-07	4,77E-06
OFAS017950-RA	-1,736330011	3,331865148	3,64E-06	7,41E-05
OFAS007959-RA	-1,735907082	3,330888549	0,001504387	0,012054787
OFAS014550-RA	-1,735750589	3,330527257	0,002475624	0,01796695
OFAS012587-RA	-1,734873708	3,328503553	0,001238352	0,010328549

OFAS025192-RA	-1,732700745	3,323493989	0,006851773	0,040302785
OFAS016026-RA	-1,731885123	3,321615597	0,001783434	0,01371951
OFAS012811-RA	-1,728514622	3,313864519	0,008009653	0,045523217
OFAS006786-RA	-1,725375925	3,306662782	0,000109186	0,001374521
OFAS025145-RA	-1,72177134	3,29841137	9,20E-08	2,94E-06
OFAS017015-RA	-1,719706766	3,293694544	0,000104538	0,00132254
OFAS015350-RA	-1,718398502	3,290709111	3,64E-06	7,41E-05
OFAS016193-RA	-1,717843703	3,289443888	0,00467987	0,029692815
OFAS001596-RA	-1,715393602	3,283862231	5,17E-10	2,82E-08
OFAS018870-RA	-1,715305793	3,283662365	0,007954471	0,04530517
OFAS013391-RA	-1,713647464	3,279890075	0,000866051	0,007654651
OFAS016585-RA	-1,707974828	3,267018961	0,002583937	0,018545305
OFAS014728-RA	-1,707290752	3,265470222	0,006823387	0,040156944
OFAS006833-RA	-1,705096427	3,260507248	0,007784187	0,044580359
OFAS014878-RA	-1,700032918	3,24908372	4,86E-08	1,66E-06
OFAS016399-RA	-1,697965214	3,244430393	1,78E-07	5,21E-06
OFAS009226-RA	-1,695823059	3,239616543	6,90E-07	1,72E-05
OFAS000885-RA	-1,693149023	3,233617475	1,52E-05	0,00025534
OFAS008371-RA	-1,690868804	3,228510691	0,000210309	0,002384564
OFAS002661-RA	-1,68941543	3,22525992	9,40E-09	3,85E-07
OFAS002727-RA	-1,68528982	3,216049963	4,89E-06	9,46E-05
OFAS016788-RA	-1,683873925	3,212895204	0,000944358	0,008190924
OFAS012027-RA	-1,683460092	3,211973727	9,01E-09	3,72E-07
OFAS017076-RA	-1,679762309	3,203751633	2,43E-09	1,15E-07
OFAS008629-RA	-1,678035614	3,199919504	0,001330384	0,010973399
OFAS005641-RA	-1,678019485	3,19988373	1,23E-06	2,88E-05
OFAS017651-RA	-1,676486876	3,196486223	1,46E-08	5,68E-07
OFAS014012-RA	-1,676158017	3,195757675	7,79E-09	3,24E-07
OFAS002174-RA	-1,674814322	3,192782602	0,000173102	0,002039969
OFAS002723-RA	-1,674373612	3,19180743	0,007231633	0,041969018
OFAS005424-RA	-1,672622002	3,187934532	0,008847731	0,04918652
OFAS008605-RA	-1,671536719	3,185537275	0,001326414	0,010947791
OFAS007987-RA	-1,670846372	3,184013321	0,00019283	0,002225724
OFAS016782-RA	-1,670594124	3,183456661	5,47E-05	0,000759937
OFAS000870-RA	-1,668607896	3,179076858	7,55E-06	0,000139424
OFAS007528-RA	-1,668101844	3,177961935	0,000792312	0,007119709
OFAS000667-RA	-1,661463151	3,163371846	1,95E-05	0,000314472
OFAS015789-RA	-1,661419503	3,163276141	1,61E-11	1,27E-09
OFAS014139-RA	-1,661332079	3,16308446	3,04E-08	1,09E-06
OFAS007270-RA	-1,654267856	3,147634129	3,24E-09	1,48E-07
OFAS010655-RA	-1,652078655	3,142861409	0,000251042	0,002746986
OFAS006889-RA	-1,647126125	3,132090991	1,81E-06	4,02E-05
OFAS010414-RA	-1,645562481	3,128698157	0,000199052	0,002281897
OFAS010222-RA	-1,64167444	3,120277716	0,000430701	0,004326285

OFAS007547-RA	-1,639365399	3,11528769	0,008374691	0,047236586
OFAS007882-RA	-1,637917994	3,112163799	3,55E-10	2,02E-08
OFAS018992-RA	-1,631931124	3,099275757	1,69E-06	3,82E-05
OFAS008572-RA	-1,630287427	3,095746689	3,69E-08	1,30E-06
OFAS013907-RA	-1,628934313	3,092844527	0,000281367	0,00302959
OFAS006162-RA	-1,627479276	3,089726796	9,09E-05	0,001170853
OFAS015283-RA	-1,626548068	3,087733133	2,18E-08	8,12E-07
OFAS005816-RA	-1,626275897	3,087150672	4,29E-10	2,40E-08
OFAS004362-RA	-1,623597642	3,081424924	6,86E-05	0,00092042
OFAS009323-RA	-1,623404249	3,081011888	0,00021801	0,002451252
OFAS009940-RA	-1,622237581	3,078521365	0,004012944	0,026325269
OFAS009196-RA	-1,619960404	3,073666002	0,00311245	0,021433899
OFAS018425-RA	-1,61994029	3,073623149	4,38E-05	0,000629256
OFAS010357-RA	-1,612570834	3,057962752	1,20E-05	0,000209246
OFAS016222-RA	-1,608446067	3,049232307	1,27E-08	5,01E-07
OFAS007569-RA	-1,606933182	3,046036401	0,003207135	0,021917865
OFAS016421-RA	-1,606073359	3,044221552	9,93E-10	5,21E-08
OFAS008857-RA	-1,605588642	3,043198926	2,98E-05	0,000448028
OFAS000135-RA	-1,605101754	3,042172065	0,001405248	0,011423467
OFAS002679-RA	-1,605097612	3,042163332	0,000260859	0,002833685
OFAS006080-RA	-1,602071971	3,035789946	0,000212697	0,002405565
OFAS018840-RA	-1,602064265	3,035773732	1,54E-07	4,62E-06
OFAS025233-RA	-1,601738192	3,035087674	0,002070034	0,01555123
OFAS017191-RA	-1,599904931	3,031233377	0,006738862	0,039829957
OFAS000847-RA	-1,593214798	3,017209343	0,004391427	0,028194721
OFAS010376-RA	-1,592619328	3,01596425	7,26E-08	2,37E-06
OFAS016677-RA	-1,591559428	3,013749335	0,003657652	0,024438773
OFAS010366-RA	-1,591395916	3,013407784	0,001375252	0,011236489
OFAS012656-RA	-1,590173145	3,010854821	0,001108686	0,009392451
OFAS004922-RA	-1,588312884	3,006975023	4,18E-06	8,35E-05
OFAS004385-RA	-1,584132411	2,998274373	2,19E-10	1,35E-08
OFAS006964-RA	-1,581435515	2,992674796	1,08E-07	3,38E-06
OFAS008302-RA	-1,575823508	2,981056064	1,44E-08	5,63E-07
OFAS010181-RA	-1,575659965	2,980718153	2,36E-07	6,73E-06
OFAS010660-RA	-1,575170406	2,979706859	3,13E-09	1,44E-07
OFAS000973-RA	-1,574894682	2,979137439	0,005219412	0,03242873
OFAS015743-RA	-1,574216104	2,977736518	1,49E-05	0,000250198
OFAS014999-RA	-1,57220783	2,973594304	0,000177133	0,002076567
OFAS003285-RA	-1,571469901	2,972073719	3,10E-11	2,28E-09
OFAS001387-RA	-1,570818712	2,970732518	1,52E-07	4,58E-06
OFAS016802-RA	-1,566446474	2,961743031	0,00269526	0,019198915
OFAS013599-RA	-1,563905042	2,956530258	0,001375573	0,011236489
OFAS004584-RA	-1,561624314	2,951860029	2,06E-05	0,000329272
OFAS006026-RA	-1,560666751	2,949901436	1,05E-06	2,48E-05

OFAS003008-RA	-1,560018125	2,948575479	7,42E-05	0,00098715
OFAS016305-RA	-1,559277049	2,947061258	1,95E-06	4,27E-05
OFAS003165-RA	-1,558177675	2,94481637	8,79E-05	0,001136138
OFAS002677-RA	-1,556271194	2,940927449	1,22E-09	6,19E-08
OFAS003955-RA	-1,555587245	2,939533552	7,87E-07	1,93E-05
OFAS012648-RA	-1,554892247	2,938117815	5,55E-05	0,000767658
OFAS012245-RA	-1,553796986	2,935888109	0,001266542	0,010531064
OFAS006078-RA	-1,548257573	2,924637004	0,007596092	0,043651605
OFAS002633-RA	-1,546819424	2,921723034	1,34E-06	3,09E-05
OFAS011844-RA	-1,544950935	2,917941451	0,00035786	0,003725176
OFAS018593-RA	-1,544627338	2,917287028	0,000126702	0,00155435
OFAS011760-RA	-1,543935989	2,915889379	2,76E-05	0,00042042
OFAS010812-RA	-1,54336727	2,914740145	6,92E-06	0,000129016
OFAS017273-RA	-1,543239947	2,914482919	0,000123569	0,001519569
OFAS011578-RA	-1,542952786	2,913902866	0,000302874	0,003225075
OFAS004042-RA	-1,536997487	2,90189936	1,48E-07	4,49E-06
OFAS000449-RA	-1,534106378	2,896089882	0,000210104	0,002384564
OFAS006472-RA	-1,533785776	2,895446372	0,000682563	0,006308069
OFAS007043-RA	-1,533527742	2,894928552	5,02E-10	2,77E-08
OFAS010708-RA	-1,53318326	2,894237392	0,005238403	0,032501743
OFAS002807-RA	-1,530424244	2,88870773	9,30E-09	3,82E-07
OFAS009307-RA	-1,529883748	2,887625697	0,007758802	0,044453876
OFAS027116-RA	-1,525997863	2,87985837	9,43E-08	2,99E-06
OFAS002920-RA	-1,522498075	2,87288068	3,75E-06	7,59E-05
OFAS003966-RA	-1,519137812	2,866197078	2,75E-05	0,000419321
OFAS015512-RA	-1,518248327	2,864430486	0,000577218	0,005494793
OFAS012123-RA	-1,514421903	2,856843295	0,000665159	0,006166341
OFAS013774-RA	-1,512457405	2,852955818	0,00238917	0,017471289
OFAS004392-RA	-1,510110739	2,848319015	5,62E-10	3,03E-08
OFAS011377-RA	-1,509448026	2,847010918	0,005120171	0,031915179
OFAS001368-RA	-1,507425243	2,843021961	0,000126166	0,001549184
OFAS011114-RA	-1,506851925	2,841892386	2,09E-08	7,83E-07
OFAS009832-RA	-1,504707288	2,837670911	0,006045053	0,036645751
OFAS005227-RA	-1,503897204	2,836077986	0,001005588	0,008622069
OFAS001708-RA	-1,498500502	2,825488862	0,002452138	0,017844573
OFAS002374-RA	-1,497612422	2,823750111	0,000426827	0,00429698
OFAS018498-RA	-1,497580956	2,823688523	0,003251698	0,022166168
OFAS006360-RA	-1,495142283	2,818919507	5,05E-07	1,32E-05
OFAS008091-RA	-1,492995099	2,814727188	0,000259828	0,002827051
OFAS000972-RA	-1,490409412	2,809686978	0,000110667	0,001387972
OFAS006475-RA	-1,489073527	2,807086512	1,17E-08	4,64E-07
OFAS002350-RA	-1,488754833	2,806466489	8,59E-05	0,00111432
OFAS002225-RA	-1,488118858	2,805229604	2,88E-08	1,05E-06
OFAS017246-RA	-1,488049576	2,805094893	5,85E-05	0,000801972

OFAS012838-RA	-1,486415903	2,801920269	0,006131226	0,037018202
OFAS006476-RA	-1,481311193	2,79202371	6,64E-07	1,66E-05
OFAS010763-RA	-1,476926038	2,783550077	6,16E-05	0,000835907
OFAS008164-RA	-1,476710537	2,783134318	8,89E-05	0,001147659
OFAS004468-RA	-1,474520537	2,778912747	0,00044145	0,004411221
OFAS013245-RA	-1,47277482	2,775552187	0,004903477	0,030821204
OFAS002644-RA	-1,471279377	2,772676646	0,000563883	0,005386882
OFAS000318-RA	-1,470137376	2,770482734	2,41E-05	0,000372905
OFAS012460-RA	-1,468991071	2,7682823	2,63E-07	7,34E-06
OFAS004391-RA	-1,468353907	2,767059961	7,48E-08	2,43E-06
OFAS009625-RA	-1,465783381	2,762134134	1,54E-06	3,50E-05
OFAS002415-RA	-1,464192555	2,759090072	1,69E-09	8,27E-08
OFAS012497-RA	-1,462097951	2,755087142	1,50E-06	3,42E-05
OFAS013198-RA	-1,460287759	2,751632421	4,15E-05	0,000603901
OFAS012714-RA	-1,459769655	2,750644426	9,84E-06	0,000175413
OFAS008596-RA	-1,459357513	2,749858747	0,001620808	0,012768617
OFAS009223-RA	-1,458992771	2,749163616	1,28E-05	0,000220379
OFAS004368-RA	-1,4574167	2,746161935	0,003970307	0,026138822
OFAS007117-RA	-1,456942876	2,74526016	7,71E-06	0,00014204
OFAS006252-RA	-1,456378393	2,744186233	0,00393731	0,025972363
OFAS004043-RA	-1,446509369	2,725478177	0,006598104	0,039152627
OFAS013243-RA	-1,445566097	2,72369677	1,24E-05	0,000215291
OFAS003115-RA	-1,445392379	2,723368824	0,007637972	0,04385485
OFAS015324-RA	-1,444433547	2,721559443	2,15E-05	0,000340118
OFAS002227-RA	-1,441162815	2,715396388	2,34E-10	1,43E-08
OFAS010771-RA	-1,440689482	2,714505641	0,006450274	0,03849977
OFAS011396-RA	-1,439057615	2,711436934	0,000950811	0,008236288
OFAS014464-RA	-1,438586102	2,710550906	2,80E-07	7,76E-06
OFAS002691-RD	-1,437841639	2,709152562	0,003913634	0,025866852
OFAS016370-RA	-1,43744076	2,708399878	0,008254908	0,046700384
OFAS014591-RA	-1,434863272	2,70356543	0,00061091	0,005760116
OFAS014980-RA	-1,432945466	2,699973908	0,000525425	0,005102725
OFAS015865-RA	-1,429689603	2,693887499	9,14E-08	2,93E-06
OFAS002110-RA	-1,429041216	2,692677064	0,000759973	0,006888849
OFAS002308-RA	-1,427141715	2,689134127	0,001520973	0,012151545
OFAS013568-RA	-1,426493354	2,687925876	0,000443392	0,004420791
OFAS005018-RA	-1,422885073	2,681211586	1,71E-08	6,53E-07
OFAS017316-RA	-1,421672812	2,678959577	5,29E-05	0,000737408
OFAS012030-RA	-1,42156199	2,678753798	2,98E-05	0,000447757
OFAS011777-RA	-1,421137301	2,677965363	2,73E-06	5,78E-05
OFAS007293-RA	-1,420812014	2,677361626	3,10E-09	1,43E-07
OFAS011231-RA	-1,418424363	2,672934274	0,006707677	0,039663043
OFAS005144-RA	-1,418206682	2,672530998	0,002455083	0,017855981
OFAS004289-RA	-1,413812996	2,664404265	0,006987613	0,040798937

OFAS000976-RA	-1,411452675	2,660048731	0,001338393	0,011019654
OFAS012526-RA	-1,408145477	2,653957884	1,66E-05	0,000274071
OFAS009506-RA	-1,407239602	2,652291974	4,53E-07	1,20E-05
OFAS001605-RA	-1,406666815	2,651239155	0,001668943	0,013054472
OFAS012166-RA	-1,405563446	2,649212272	0,003105315	0,021417235
OFAS007645-RA	-1,404797934	2,64780694	0,002245632	0,016608468
OFAS002613-RA	-1,40424434	2,646791111	0,007699324	0,044141824
OFAS014908-RA	-1,404196242	2,646702873	8,54E-06	0,000154165
OFAS014206-RA	-1,402090253	2,642842138	0,005961335	0,036236092
OFAS017904-RA	-1,399729725	2,638521474	0,006882391	0,040377092
OFAS007744-RA	-1,396588109	2,632782075	0,005516371	0,03394496
OFAS014084-RA	-1,391757089	2,623980665	4,27E-05	0,000618382
OFAS010152-RA	-1,390803128	2,622246169	0,003535967	0,02373168
OFAS016955-RA	-1,389450815	2,619789353	0,000258988	0,002820185
OFAS000216-RA	-1,387526191	2,616296759	9,97E-06	0,000177454
OFAS012125-RA	-1,386744675	2,614879881	0,001773313	0,013672882
OFAS013784-RA	-1,386091868	2,613696938	5,93E-07	1,51E-05
OFAS015003-RA	-1,385038231	2,611788785	0,002791793	0,019678412
OFAS013409-RA	-1,382945372	2,608002716	0,001478549	0,011904397
OFAS009161-RA	-1,380519311	2,603620739	0,001082644	0,009200763
OFAS000684-RA	-1,379922634	2,602544143	2,04E-06	4,45E-05
OFAS014247-RA	-1,378930984	2,600755875	4,62E-05	0,000657258
OFAS002596-RA	-1,371830659	2,587987517	6,54E-07	1,65E-05
OFAS011097-RA	-1,370881329	2,586285116	2,24E-05	0,000351444
OFAS005820-RA	-1,370791134	2,58612343	0,000331878	0,003497964
OFAS013351-RA	-1,369345997	2,583534227	0,004268517	0,027616199
OFAS011115-RA	-1,369220839	2,583310108	0,005424829	0,033458083
OFAS009128-RA	-1,368342148	2,58173719	7,39E-05	0,000985105
OFAS005016-RA	-1,367869702	2,580891876	0,000646727	0,006032833
OFAS008315-RA	-1,36653202	2,578499954	0,003380458	0,022836787
OFAS014219-RA	-1,366000847	2,577550775	1,55E-06	3,52E-05
OFAS016290-RA	-1,365677781	2,576973643	0,004991034	0,031240345
OFAS011720-RA	-1,36556101	2,576765072	1,20E-07	3,71E-06
OFAS013343-RA	-1,361964852	2,570350054	0,001431695	0,0115895
OFAS008905-RA	-1,360509823	2,567759035	5,77E-06	0,000109997
OFAS008508-RA	-1,358455659	2,564105564	0,000499805	0,004882071
OFAS007390-RA	-1,356454476	2,560551323	2,30E-07	6,57E-06
OFAS016629-RA	-1,355617915	2,559066991	0,00866322	0,048480917
OFAS006766-RA	-1,355329773	2,558555934	1,25E-05	0,000215291
OFAS012196-RA	-1,350947969	2,550796786	0,002144196	0,015974637
OFAS011677-RA	-1,350598862	2,550179613	0,00338059	0,022836787
OFAS009712-RA	-1,350211805	2,549495524	4,72E-05	0,000669707
OFAS001575-RA	-1,349177405	2,547668213	4,39E-05	0,000630039
OFAS013702-RA	-1,347348065	2,544439811	3,22E-08	1,14E-06

OFAS013217-RA	-1,347106838	2,544014403	1,70E-05	0,000279901
OFAS017128-RA	-1,346577392	2,543080961	1,24E-07	3,82E-06
OFAS014762-RA	-1,343103905	2,536965508	0,000839048	0,007455128
OFAS010790-RA	-1,343014441	2,536808191	1,44E-07	4,38E-06
OFAS004515-RA	-1,340929924	2,533145462	1,43E-07	4,33E-06
OFAS019166-RA	-1,339919148	2,531371321	0,001391429	0,011338505
OFAS001948-RA	-1,334778366	2,522367289	0,000486918	0,004773502
OFAS015773-RA	-1,332573418	2,518515165	3,53E-06	7,21E-05
OFAS009134-RA	-1,332035909	2,517577009	1,84E-08	6,96E-07
OFAS009147-RA	-1,331586341	2,516792612	0,006900242	0,040446587
OFAS014235-RA	-1,331009151	2,515785901	0,006368448	0,038176676
OFAS001814-RA	-1,330089431	2,514182596	3,23E-05	0,000484096
OFAS015402-RA	-1,329699144	2,513502535	3,75E-06	7,59E-05
OFAS007077-RA	-1,329425405	2,513025665	1,29E-06	2,98E-05
OFAS001154-RA	-1,329380283	2,512947068	0,002820767	0,019810076
OFAS006848-RA	-1,32630871	2,507602564	0,000200348	0,002294798
OFAS004079-RA	-1,324900588	2,505156248	0,002625352	0,018780398
OFAS002414-RA	-1,323560887	2,502831015	0,002699534	0,019219198
OFAS018853-RA	-1,323400105	2,502552101	3,72E-05	0,000547818
OFAS000846-RA	-1,319704262	2,49614936	0,000447937	0,004459309
OFAS009179-RA	-1,318595284	2,494231345	1,14E-05	0,000201009
OFAS006006-RA	-1,318521997	2,494104644	0,000648738	0,00604322
OFAS000104-RA	-1,318255928	2,493644712	0,001118007	0,009453582
OFAS017993-RA	-1,31731122	2,492012354	0,008723653	0,048717911
OFAS010327-RA	-1,316436244	2,490501438	0,0001708	0,002018132
OFAS010075-RA	-1,316207044	2,490105804	0,000576077	0,005491688
OFAS007594-RA	-1,315110304	2,488213541	0,007411682	0,042774362
OFAS003123-RA	-1,313743992	2,48585818	0,007495255	0,043201151
OFAS002694-RA	-1,311376606	2,481782364	0,004754868	0,030126092
OFAS017399-RA	-1,31128562	2,481625851	2,49E-06	5,35E-05
OFAS015227-RA	-1,30912801	2,477917251	6,47E-06	0,000121713
OFAS007386-RA	-1,308131039	2,476205484	0,003386054	0,022850775
OFAS013299-RA	-1,307043394	2,474339381	8,24E-05	0,001078332
OFAS007372-RA	-1,304998359	2,470834463	0,002779364	0,01961133
OFAS010375-RA	-1,301729135	2,46524176	1,46E-06	3,34E-05
OFAS005434-RA	-1,299206084	2,4609342	2,46E-06	5,28E-05
OFAS009447-RA	-1,294474782	2,452876814	0,008469396	0,047534486
OFAS006214-RA	-1,292355847	2,449276835	3,44E-05	0,000511527
OFAS006354-RA	-1,291671677	2,448115589	3,28E-05	0,000489719
OFAS009594-RA	-1,290787478	2,446615647	0,000173514	0,002041251
OFAS003310-RA	-1,288405537	2,442579531	0,000182499	0,002130205
OFAS004386-RA	-1,287331075	2,440761071	3,63E-07	9,81E-06
OFAS001560-RA	-1,287161045	2,440473429	0,000343312	0,003598766
OFAS015557-RA	-1,287102986	2,440375219	3,71E-05	0,000546997

OFAS000406-RA	-1,286610046	2,439541534	0,000311558	0,003309169
OFAS006987-RA	-1,286526189	2,43939974	2,81E-05	0,000427296
OFAS009898-RA	-1,286154619	2,438771547	0,00408206	0,026666029
OFAS000116-RA	-1,282028416	2,431806464	1,64E-05	0,000272164
OFAS011722-RA	-1,281832711	2,431476605	9,92E-05	0,001267186
OFAS000248-RA	-1,281423116	2,430786384	2,96E-05	0,000447212
OFAS016079-RA	-1,279795183	2,428045039	7,74E-06	0,000142435
OFAS012699-RA	-1,279404583	2,42738775	0,003359087	0,022737134
OFAS004511-RA	-1,279207991	2,427057	0,000139983	0,001691091
OFAS003036-RA	-1,278880486	2,426506098	0,005259489	0,032587542
OFAS018366-RA	-1,278723322	2,426241774	0,00295694	0,020605269
OFAS016375-RA	-1,278268026	2,425476206	3,35E-05	0,0004987
OFAS016172-RA	-1,27774063	2,424589702	2,30E-07	6,57E-06
OFAS005315-RA	-1,276523348	2,422544803	3,93E-06	7,90E-05
OFAS002233-RA	-1,274754449	2,419576324	0,003026178	0,020968556
OFAS002041-RA	-1,273102834	2,416807948	2,40E-07	6,80E-06
OFAS013535-RA	-1,270600528	2,41261971	1,97E-06	4,29E-05
OFAS011924-RA	-1,269702096	2,411117729	0,001660583	0,01301982
OFAS015103-RA	-1,268887635	2,409756938	0,000438446	0,004387722
OFAS003473-RA	-1,267937927	2,408171146	1,20E-05	0,000209262
OFAS004704-RA	-1,266756171	2,406199347	6,64E-07	1,66E-05
OFAS012534-RA	-1,264638091	2,402669299	6,61E-06	0,000123951
OFAS003400-RA	-1,264572529	2,402560114	0,000955371	0,00825985
OFAS016889-RA	-1,264522032	2,402476021	6,49E-05	0,000876239
OFAS004863-RA	-1,264007424	2,401619214	6,71E-06	0,00012554
OFAS025201-RA	-1,258007901	2,391652692	1,02E-06	2,42E-05
OFAS009667-RA	-1,257733308	2,391197523	5,39E-05	0,000750205
OFAS001551-RA	-1,256068233	2,388439334	0,000330439	0,00348825
OFAS004263-RA	-1,255454442	2,387423394	0,000216302	0,00243724
OFAS014185-RA	-1,255271472	2,387120628	4,99E-05	0,000702018
OFAS001462-RA	-1,253479136	2,384156824	0,004716402	0,029910518
OFAS016226-RA	-1,251209585	2,380409177	2,82E-06	5,94E-05
OFAS003319-RA	-1,248731087	2,376323231	0,000145475	0,00175116
OFAS016828-RA	-1,247297931	2,373963791	0,008605378	0,048217323
OFAS010016-RA	-1,245351619	2,370763282	4,96E-07	1,30E-05
OFAS012590-RA	-1,244366441	2,369144904	4,37E-05	0,000629209
OFAS011884-RA	-1,243836859	2,368275402	6,16E-06	0,000116986
OFAS001813-RA	-1,241886678	2,365076219	0,002521043	0,018198526
OFAS013668-RA	-1,241657565	2,364700654	0,008236314	0,046614767
OFAS025215-RA	-1,235699884	2,35495564	0,002524994	0,018217286
OFAS005805-RA	-1,232837343	2,350287658	0,000222653	0,002499285
OFAS013782-RA	-1,229721479	2,345217097	8,65E-06	0,000155928
OFAS019129-RA	-1,228263994	2,342849034	0,001625764	0,012798969
OFAS012006-RA	-1,225360426	2,338138557	6,07E-05	0,000826002

OFAS012608-RA	-1,222906638	2,334165147	0,00105329	0,008991008
OFAS003131-RA	-1,222481933	2,333478109	0,000778426	0,007018336
OFAS012980-RA	-1,218829398	2,327577811	0,006051237	0,036666742
OFAS017643-RA	-1,21650827	2,323836022	0,005687797	0,034777403
OFAS003216-RA	-1,216266448	2,323446536	3,12E-06	6,48E-05
OFAS006881-RA	-1,215401083	2,322053292	0,000414614	0,004199136
OFAS018926-RA	-1,210176478	2,313659369	0,000382352	0,003913583
OFAS010913-RA	-1,208261849	2,310590903	3,33E-06	6,86E-05
OFAS018047-RA	-1,205387593	2,305992136	1,90E-06	4,19E-05
OFAS014270-RA	-1,205065836	2,3054779	4,27E-06	8,49E-05
OFAS002371-RA	-1,203769127	2,303406644	0,00173199	0,013435086
OFAS013018-RA	-1,203289854	2,302641563	0,005920455	0,036003853
OFAS013241-RA	-1,20322443	2,302537144	3,97E-06	7,98E-05
OFAS012229-RA	-1,202509906	2,301397049	3,46E-06	7,09E-05
OFAS005733-RA	-1,200697983	2,29850847	0,00100698	0,008628511
OFAS005713-RA	-1,198556049	2,295098464	0,003909666	0,025853316
OFAS017919-RA	-1,198138246	2,294433902	0,002503696	0,018110936
OFAS019528-RA	-1,197578801	2,293544344	0,000311331	0,003309169
OFAS006599-RA	-1,195889487	2,290860306	7,61E-06	0,000140433
OFAS012036-RA	-1,193014263	2,286299274	0,004484832	0,028671423
OFAS011371-RA	-1,191981264	2,284662823	0,000631622	0,005912401
OFAS003516-RA	-1,191083992	2,283242338	0,00084475	0,007499469
OFAS004254-RA	-1,190244378	2,281913931	0,001669848	0,013054472
OFAS001354-RA	-1,186095447	2,275360986	0,008714239	0,048685526
OFAS018413-RA	-1,185436045	2,27432124	0,007920841	0,045132713
OFAS009290-RA	-1,1850397	2,273696513	9,90E-05	0,00126475
OFAS002985-RA	-1,183887961	2,271882089	2,23E-06	4,84E-05
OFAS008212-RA	-1,181874218	2,268713162	0,008045019	0,045704937
OFAS005163-RA	-1,180661731	2,266807264	0,005988365	0,036351182
OFAS003307-RA	-1,179106714	2,264365289	0,007502529	0,04322458
OFAS014654-RA	-1,177520844	2,261877574	8,16E-05	0,001068741
OFAS006232-RA	-1,175951828	2,259418985	0,001107532	0,009392451
OFAS000026-RA	-1,175103964	2,258091527	0,001545492	0,012325503
OFAS001040-RA	-1,1740365	2,256421361	0,002372496	0,017377666
OFAS005697-RA	-1,1738603	2,256145796	0,002075122	0,015572088
OFAS001264-RA	-1,173616565	2,255764666	0,00024164	0,002669589
OFAS006251-RA	-1,172961724	2,254741003	0,000537039	0,00519305
OFAS017081-RA	-1,172600792	2,254176985	0,004322836	0,027860575
OFAS010496-RA	-1,170851255	2,251445032	0,008626965	0,048318179
OFAS011080-RA	-1,169919506	2,249991429	7,66E-05	0,001016129
OFAS002369-RA	-1,169763341	2,249747892	0,000539625	0,005206836
OFAS000119-RA	-1,16965276	2,249575457	0,000395068	0,004019588
OFAS014310-RA	-1,169365584	2,249127713	1,63E-05	0,000270496
OFAS014608-RA	-1,168210212	2,247327235	0,000436541	0,004371897

OFAS008638-RA	-1,168085771	2,247133398	3,04E-06	6,36E-05
OFAS005232-RA	-1,167145966	2,245670041	7,87E-06	0,00014432
OFAS005099-RA	-1,164510547	2,241571545	0,001653722	0,012973576
OFAS015476-RA	-1,163679647	2,240280915	0,001975935	0,01496954
OFAS001188-RA	-1,163377349	2,239811542	2,88E-05	0,000436287
OFAS017057-RA	-1,160595071	2,235496165	8,12E-06	0,000148332
OFAS006429-RA	-1,157466005	2,230652845	0,000554175	0,005331951
OFAS003130-RA	-1,156904556	2,229784917	0,008838383	0,049175144
OFAS025199-RA	-1,155892204	2,228220806	2,29E-06	4,97E-05
OFAS005267-RA	-1,155669343	2,227876628	5,25E-05	0,00073337
OFAS014761-RA	-1,153730697	2,224884891	0,000223727	0,002502988
OFAS015257-RA	-1,15043911	2,219814481	0,000714007	0,006547086
OFAS019538-RA	-1,150125421	2,219331874	8,50E-05	0,001106356
OFAS008841-RA	-1,149626801	2,218564967	2,76E-05	0,000420885
OFAS004956-RA	-1,148463964	2,216777486	0,001037257	0,008876652
OFAS016712-RA	-1,145939949	2,212902594	4,68E-06	9,14E-05
OFAS004859-RA	-1,144552153	2,210774923	0,001832349	0,013999854
OFAS008573-RA	-1,142525182	2,20767099	7,94E-05	0,001044063
OFAS017803-RA	-1,139330777	2,202788187	0,000893129	0,007832322
OFAS014816-RA	-1,139013462	2,202303746	0,001619757	0,012768617
OFAS008606-RA	-1,136834944	2,198980704	8,69E-05	0,001126681
OFAS002332-RA	-1,136695968	2,198768884	0,003065689	0,021177607
OFAS007423-RA	-1,1359422	2,197620389	0,002364411	0,017346739
OFAS002941-RA	-1,134883015	2,196007551	0,001189347	0,009969197
OFAS002205-RA	-1,133585004	2,194032664	8,77E-05	0,001135229
OFAS013159-RA	-1,13016969	2,188844839	0,003609031	0,024185897
OFAS004159-RA	-1,12917353	2,187333996	2,62E-05	0,000402444
OFAS005579-RA	-1,128650836	2,186541659	0,000816672	0,007284819
OFAS017972-RA	-1,125409422	2,181634503	0,000179996	0,002104645
OFAS004634-RA	-1,125073709	2,181126899	0,004513613	0,028828053
OFAS017523-RA	-1,124904169	2,180870596	4,88E-05	0,000689822
OFAS018685-RA	-1,123752117	2,179129776	0,001553043	0,012357892
OFAS000268-RA	-1,12342632	2,178637728	0,000240431	0,002661141
OFAS004393-RA	-1,121526029	2,175769957	6,46E-06	0,000121713
OFAS007810-RA	-1,121499073	2,175729303	0,000486902	0,004773502
OFAS011485-RA	-1,120746223	2,174594227	0,003945002	0,026010364
OFAS000566-RA	-1,118505703	2,171219681	0,000160635	0,001904707
OFAS009964-RA	-1,117884108	2,170284398	0,000164179	0,001945027
OFAS013272-RA	-1,115941496	2,167364041	6,02E-06	0,000114675
OFAS001679-RA	-1,114478919	2,165167922	8,55E-05	0,001110748
OFAS013602-RA	-1,114348231	2,164971796	0,000658735	0,006119421
OFAS010947-RA	-1,113057426	2,163035624	0,008464702	0,047527944
OFAS016166-RA	-1,112040223	2,161511068	0,00055083	0,005303557
OFAS013035-RA	-1,111664727	2,160948555	0,002138207	0,015938931

OFAS007902-RA	-1,10975967	2,158096938	0,005796963	0,035348613
OFAS000626-RA	-1,109433721	2,157609413	1,25E-05	0,000215291
OFAS005258-RA	-1,109421286	2,157590817	1,92E-05	0,000309975
OFAS002726-RA	-1,107182053	2,154244578	0,002978469	0,020733842
OFAS008483-RA	-1,106586085	2,153354858	0,006634375	0,039315896
OFAS015225-RA	-1,106276014	2,152892098	0,000994346	0,008536546
OFAS000225-RA	-1,104617728	2,150418907	3,84E-05	0,000563954
OFAS003863-RA	-1,104596972	2,150387969	0,000135797	0,001647909
OFAS014108-RA	-1,104365801	2,150043429	0,000270581	0,002925144
OFAS008316-RA	-1,103360361	2,148545547	0,000454138	0,004508225
OFAS008502-RA	-1,102362096	2,147059386	0,003005661	0,020879964
OFAS003850-RA	-1,101077695	2,145148755	0,004469014	0,028624642
OFAS001500-RA	-1,10014923	2,143768662	0,008947689	0,04961934
OFAS016815-RA	-1,098219682	2,140903371	0,000194085	0,002234464
OFAS005098-RA	-1,097263901	2,139485499	1,67E-05	0,000276319
OFAS015208-RA	-1,096441652	2,138266469	0,000134654	0,001639958
OFAS015361-RA	-1,095291704	2,136562771	0,000560931	0,005373926
OFAS017455-RA	-1,091143116	2,130427736	1,80E-05	0,000294582
OFAS011486-RA	-1,087044035	2,124383214	0,004104796	0,026768056
OFAS013644-RA	-1,086912126	2,124188986	0,000699989	0,006431684
OFAS001581-RA	-1,085874178	2,122661285	8,27E-05	0,001079451
OFAS004113-RA	-1,085809483	2,122566101	0,001718665	0,013343179
OFAS012877-RA	-1,084808742	2,121094271	0,002448269	0,017826047
OFAS010895-RA	-1,084708538	2,120946952	0,000960413	0,008295913
OFAS025037-RA	-1,084315577	2,120369328	0,004136764	0,026918942
OFAS015281-RA	-1,080892892	2,115344875	0,002758886	0,019538486
OFAS017620-RA	-1,080290793	2,114462234	1,43E-05	0,000242016
OFAS008890-RA	-1,079713482	2,113616277	0,004018607	0,026328127
OFAS002598-RA	-1,078246454	2,111468104	2,70E-05	0,00041401
OFAS010945-RA	-1,077996753	2,111102684	0,000337526	0,003546388
OFAS004195-RA	-1,076973263	2,109605538	2,52E-05	0,000388929
OFAS011464-RA	-1,07634946	2,108693568	0,000220995	0,002482733
OFAS000451-RA	-1,0760105	2,10819819	0,000487679	0,004777482
OFAS011729-RA	-1,075505987	2,107461078	0,001733476	0,013435086
OFAS016945-RA	-1,074921864	2,106607975	0,000461965	0,004568598
OFAS004846-RA	-1,074596112	2,10613237	0,002157308	0,01605466
OFAS001434-RA	-1,073373022	2,104347587	0,008447318	0,047450114
OFAS002962-RA	-1,071697287	2,10190474	0,000857576	0,007584729
OFAS008112-RA	-1,071185644	2,101159445	7,67E-05	0,001016493
OFAS005867-RA	-1,070007688	2,099444555	0,00205411	0,015448831
OFAS007826-RA	-1,069650926	2,09892545	0,008229377	0,046595086
OFAS012033-RA	-1,067490963	2,095785348	0,000117592	0,001462565
OFAS011198-RA	-1,067262454	2,095453423	0,000195954	0,002250209
OFAS008087-RA	-1,066005027	2,093627859	0,001382902	0,011275843

OFAS016739-RA	-1,06577552	2,093294827	0,000385301	0,003940774
OFAS004414-RA	-1,064320274	2,091184386	0,000117732	0,001462961
OFAS013753-RA	-1,064276901	2,091121517	3,01E-05	0,000451506
OFAS015912-RA	-1,062510027	2,08856208	0,001754729	0,013560643
OFAS016387-RA	-1,06070328	2,085948124	0,001460544	0,011780558
OFAS003005-RA	-1,056154771	2,079381933	0,000246984	0,002713601
OFAS018149-RA	-1,054662844	2,077232703	0,000668493	0,006192986
OFAS005012-RA	-1,05310546	2,074991549	6,03E-05	0,000821548
OFAS006035-RA	-1,051988492	2,073385663	0,000386654	0,003951615
OFAS016423-RA	-1,046303672	2,065231735	0,005457948	0,033646941
OFAS018029-RA	-1,045899827	2,064653708	0,000248261	0,002723192
OFAS017281-RA	-1,044685569	2,062916703	0,000331349	0,003495118
OFAS003064-RA	-1,044245851	2,062288045	0,001650749	0,012957803
OFAS018264-RA	-1,044203915	2,062228098	0,000118804	0,001473379
OFAS014250-RA	-1,042358967	2,059592564	0,00196163	0,014894676
OFAS016169-RA	-1,04154915	2,058436793	0,002233405	0,016529653
OFAS004955-RA	-1,039718244	2,055826114	0,001434327	0,011603834
OFAS017266-RA	-1,039018243	2,054828863	0,004255626	0,027559271
OFAS014171-RA	-1,037823665	2,05312813	0,00017412	0,002046594
OFAS006977-RA	-1,037230696	2,052284438	5,35E-05	0,000745412
OFAS010654-RA	-1,036226873	2,050856961	0,006807195	0,040093097
OFAS015435-RA	-1,033667076	2,047221319	0,00286328	0,020066798
OFAS016686-RA	-1,03319728	2,046554775	0,000154967	0,001852174
OFAS004817-RA	-1,032256824	2,045221112	8,26E-05	0,001079083
OFAS016279-RA	-1,032072409	2,044959696	0,000810457	0,007244098
OFAS015980-RA	-1,029477112	2,041284277	0,000251297	0,00274754
OFAS013347-RA	-1,028644778	2,04010694	0,008766514	0,048876218
OFAS003270-RA	-1,027465898	2,038440573	0,001509509	0,012088639
OFAS011226-RA	-1,022681703	2,031691991	0,004255357	0,027559271
OFAS004865-RA	-1,021576874	2,030136699	9,55E-05	0,001224589
OFAS015254-RA	-1,020579158	2,028733214	0,001501497	0,012046825
OFAS016326-RA	-1,017951015	2,025040856	0,000409091	0,004152569
OFAS010221-RA	-1,017816705	2,02485234	0,000941589	0,008177433
OFAS002450-RA	-1,017530076	2,02445009	0,001125546	0,009505397
OFAS016591-RA	-1,01594816	2,022231496	0,000578944	0,005507324
OFAS018957-RA	-1,015615598	2,021765396	0,004213079	0,02734948
OFAS009387-RA	-1,015570849	2,021702686	0,004847522	0,030572918
OFAS014702-RA	-1,015255233	2,02126045	0,007865032	0,044881625
OFAS027199-RA	-1,014594619	2,020335121	5,14E-05	0,000721169
OFAS014085-RA	-1,014131303	2,019686403	0,003264176	0,022228743
OFAS005547-RA	-1,013885773	2,019342704	0,000102559	0,001304446
OFAS003098-RA	-1,013644484	2,019005001	0,003253342	0,022166168
OFAS014370-RA	-1,010568763	2,014705213	0,000816344	0,007284819
OFAS000648-RA	-1,01023869	2,014244324	6,24E-05	0,000845213

OFAS005026-RA	-1,008043104	2,011181248	0,002888464	0,020201252
OFAS013595-RA	-1,007744825	2,010765478	0,008677147	0,048538694
OFAS012996-RA	-1,006039211	2,008389672	0,00797538	0,045366709
OFAS004933-RA	-1,003687344	2,005118283	0,002941508	0,020518961
OFAS003357-RA	-1,003449986	2,004788419	0,000173476	0,002041251
OFAS002466-RA	-1,00325446	2,004516733	0,00024945	0,002734008
OFAS005534-RA	-1,00255653	2,003547245	5,79E-05	0,000796721
OFAS002430-RA	-1,00117786	2,001633527	5,51E-05	0,000763607
OFAS003627-RA	1,001705055	2,002365106	4,54E-05	0,000646714
OFAS006540-RA	1,002425367	2,003365101	0,007970975	0,045360807
OFAS009240-RA	1,004173353	2,005793871	7,38E-06	0,000136797
OFAS007611-RA	1,004423201	2,006141268	0,000115775	0,001443973
OFAS025257-RA	1,004952537	2,006877472	5,84E-05	0,000801663
OFAS003835-RA	1,006551144	2,009102465	0,001816667	0,013911599
OFAS008521-RA	1,007031002	2,009770829	0,000118899	0,001473379
OFAS000224-RA	1,007795096	2,010835544	0,000875886	0,007726383
OFAS008479-RA	1,008403308	2,011683452	0,000462259	0,004568598
OFAS001923-RA	1,010812163	2,015045147	1,25E-05	0,000215291
OFAS017547-RA	1,011265615	2,015678594	0,000135118	0,001644121
OFAS016336-RA	1,013075043	2,018208244	0,000368644	0,003802171
OFAS005060-RA	1,013334263	2,018570903	0,000617572	0,005801047
OFAS008279-RA	1,015883043	2,022140223	0,000139713	0,001689353
OFAS003923-RA	1,018679332	2,026063417	0,000788245	0,007092626
OFAS013938-RA	1,020572941	2,028724471	1,86E-05	0,000303461
OFAS019393-RA	1,022304817	2,031161307	0,002323956	0,017096498
OFAS007060-RA	1,022529878	2,031478192	0,007336954	0,042452222
OFAS017134-RA	1,023793614	2,033258456	2,53E-05	0,000389348
OFAS003683-RA	1,024916068	2,034840999	0,000619285	0,005813076
OFAS016982-RA	1,025945604	2,036293621	6,24E-05	0,000845213
OFAS009424-RA	1,026840448	2,037557041	0,005786987	0,035303763
OFAS014720-RA	1,027370495	2,038305778	2,27E-05	0,000356032
OFAS010403-RA	1,027497336	2,038484993	0,004536762	0,028915435
OFAS006203-RA	1,028693817	2,040176286	0,000152276	0,001829758
OFAS013395-RA	1,029522972	2,041349167	0,000793975	0,007129896
OFAS016644-RA	1,029708033	2,041611037	6,78E-05	0,000911178
OFAS005712-RA	1,032766941	2,045944402	0,002407817	0,01758034
OFAS014603-RA	1,033351453	2,04677349	0,002838223	0,019911906
OFAS012662-RA	1,03347294	2,046945853	0,003758982	0,02502891
OFAS014770-RA	1,035268609	2,049495197	0,003345619	0,022668755
OFAS006552-RA	1,036181707	2,050792757	0,000980025	0,008424335
OFAS019315-RA	1,036467918	2,051199646	0,003163246	0,021694971
OFAS009317-RA	1,036813957	2,051691697	9,42E-06	0,00016874
OFAS005878-RA	1,039473747	2,055477738	0,000372626	0,003837361
OFAS016888-RA	1,040332968	2,056702276	0,000395095	0,004019588

OFAS011499-RA	1,045392643	2,063927999	0,005001568	0,031291744
OFAS009146-RA	1,049324359	2,069560407	0,002042753	0,015406429
OFAS009186-RA	1,050397684	2,071100675	0,000322186	0,003409148
OFAS011853-RA	1,050416004	2,071126975	1,19E-06	2,79E-05
OFAS012884-RA	1,050691503	2,071522518	0,007516058	0,043284012
OFAS007210-RA	1,050897873	2,071818859	0,000768804	0,006950198
OFAS003061-RA	1,051264299	2,072345142	0,000718694	0,006581107
OFAS010901-RA	1,051436147	2,072592006	0,003008701	0,020890314
OFAS014296-RA	1,053433347	2,075463193	0,00178776	0,013744937
OFAS009738-RA	1,054323002	2,076743447	4,92E-05	0,000694423
OFAS016560-RA	1,054766628	2,07738214	4,54E-06	8,93E-05
OFAS013783-RA	1,055188188	2,077989247	0,000360124	0,003740074
OFAS002171-RA	1,056236424	2,079499624	0,001971287	0,014942733
OFAS001735-RA	1,056410173	2,07975008	0,000870444	0,007683407
OFAS013745-RA	1,057355907	2,081113872	0,000193243	0,002228579
OFAS010554-RA	1,057489354	2,08130638	0,000834724	0,007421601
OFAS007531-RA	1,057752231	2,081685655	2,26E-06	4,91E-05
OFAS000821-RA	1,060498637	2,085652258	2,02E-05	0,000323675
OFAS006428-RA	1,060499839	2,085653997	0,00015948	0,001895595
OFAS009912-RA	1,060727066	2,085982516	0,001909685	0,014541246
OFAS004952-RA	1,062736064	2,088889336	0,000311755	0,003309169
OFAS007857-RA	1,063429057	2,089892966	0,002809551	0,019772542
OFAS006098-RA	1,065429577	2,092792936	0,002722817	0,019323681
OFAS008246-RA	1,065561705	2,092984612	1,65E-05	0,000273331
OFAS004025-RA	1,066007048	2,093630792	2,83E-05	0,000428654
OFAS009849-RA	1,066273822	2,094017968	3,08E-05	0,000461184
OFAS000793-RA	1,06790831	2,096391711	8,25E-05	0,001079083
OFAS002710-RA	1,067991319	2,096512336	0,002071873	0,015556373
OFAS014172-RA	1,068532604	2,097299075	4,15E-05	0,000603901
OFAS001229-RA	1,068556434	2,097333717	0,000191241	0,002209274
OFAS006693-RA	1,068575028	2,097360748	0,00565363	0,034615632
OFAS012695-RA	1,071030602	2,100933652	1,81E-06	4,02E-05
OFAS015484-RA	1,071433267	2,101520117	0,000200949	0,002297784
OFAS017821-RA	1,072467209	2,103026761	0,001356344	0,011132791
OFAS012627-RA	1,073067103	2,103901413	0,00013078	0,001597821
OFAS008063-RA	1,073395216	2,10437996	0,000899256	0,007875802
OFAS005068-RA	1,075191408	2,107001598	0,002533717	0,018260657
OFAS000286-RA	1,075628819	2,107640517	0,00028397	0,003050303
OFAS027194-RA	1,077805132	2,110822303	0,002672797	0,01906916
OFAS000223-RA	1,081150682	2,115722892	8,81E-05	0,00113793
OFAS009877-RA	1,08305732	2,11852084	0,000560322	0,005371911
OFAS006954-RA	1,084470425	2,120596925	2,06E-05	0,000329329
OFAS006207-RA	1,084777095	2,121047743	0,000202107	0,002309055
OFAS006934-RA	1,08488996	2,121213684	0,000747306	0,006787733

OFAS000063-RA	1,086887149	2,12415221	0,001668723	0,013054472
OFAS006329-RA	1,087328579	2,124802249	6,53E-06	0,000122632
OFAS004114-RA	1,088676932	2,126789033	0,00028965	0,003103885
OFAS019613-RA	1,089154226	2,127492765	0,006012909	0,036467306
OFAS010814-RA	1,089891952	2,128580942	0,001450974	0,011724426
OFAS002859-RA	1,090053362	2,128819103	1,97E-05	0,000317498
OFAS008983-RA	1,091192085	2,130500049	4,73E-06	9,22E-05
OFAS000149-RA	1,095890392	2,137449585	8,77E-06	0,000157788
OFAS000628-RA	1,096649154	2,138574037	2,46E-05	0,000379814
OFAS008210-RA	1,096678676	2,1386178	6,47E-06	0,000121713
OFAS018082-RA	1,09807381	2,140686915	0,000317449	0,00336166
OFAS014047-RA	1,09911577	2,142233545	5,01E-05	0,000704182
OFAS012132-RA	1,099947573	2,143469031	6,34E-06	0,000119688
OFAS005478-RA	1,103331508	2,148502578	0,00056722	0,005414919
OFAS001947-RA	1,10394284	2,149413184	0,006537716	0,038869827
OFAS001534-RA	1,10571049	2,152048349	0,000683882	0,00631384
OFAS016600-RA	1,107140019	2,154181814	4,92E-05	0,000694423
OFAS007754-RA	1,108400393	2,156064582	5,83E-07	1,49E-05
OFAS003556-RA	1,108639848	2,15642247	3,08E-06	6,42E-05
OFAS017521-RA	1,109220708	2,157290867	0,001777814	0,013694991
OFAS014153-RA	1,111366966	2,160502598	0,000918922	0,008021959
OFAS016910-RA	1,112121091	2,161632231	3,59E-05	0,000532495
OFAS009163-RA	1,113708658	2,164012238	0,003980734	0,026186236
OFAS013200-RA	1,113971191	2,164406068	4,52E-05	0,000645099
OFAS002817-RA	1,114864747	2,165747042	5,64E-05	0,000777806
OFAS016479-RA	1,119675922	2,172981545	0,000745342	0,006783622
OFAS017897-RA	1,120253156	2,173851146	6,13E-07	1,56E-05
OFAS007981-RA	1,125055392	2,181099207	0,001896581	0,014449632
OFAS003015-RA	1,126675734	2,183550252	1,92E-05	0,000309975
OFAS004332-RA	1,126731138	2,183634109	2,24E-05	0,000351767
OFAS011307-RA	1,127713404	2,185121354	0,00012011	0,001481573
OFAS007521-RA	1,130505902	2,189354997	7,87E-06	0,00014432
OFAS012298-RA	1,131729264	2,191212291	0,002407998	0,01758034
OFAS012657-RA	1,131762486	2,191262751	3,77E-05	0,000553908
OFAS015180-RA	1,133280993	2,193570376	0,000107976	0,00136183
OFAS008896-RA	1,133564304	2,194001184	0,004199059	0,02727161
OFAS003052-RA	1,135387445	2,196775506	3,61E-05	0,000534597
OFAS018008-RA	1,137460205	2,199933944	2,14E-05	0,000338766
OFAS017896-RA	1,137805142	2,200459993	6,87E-06	0,000128315
OFAS005162-RA	1,138947872	2,202203625	0,001641413	0,012899556
OFAS003960-RA	1,139963985	2,203755217	4,34E-05	0,000627719
OFAS008761-RA	1,140581796	2,204699143	0,000137607	0,001665381
OFAS010594-RA	1,141494137	2,206093805	1,06E-07	3,31E-06
OFAS016597-RA	1,141984449	2,206843693	1,88E-06	4,15E-05

OFAS025143-RA	1,142166062	2,207121517	4,52E-05	0,000645099
OFAS003382-RA	1,142470049	2,207586623	0,002563923	0,018448742
OFAS013699-RA	1,144621812	2,21088167	0,000111282	0,001393094
OFAS007716-RA	1,144751004	2,211079661	0,006946031	0,040618045
OFAS004990-RA	1,146035221	2,213048734	0,001136608	0,009586793
OFAS001142-RA	1,147058942	2,214619647	0,000165068	0,001952125
OFAS003894-RA	1,147327318	2,215031657	0,000180867	0,002112986
OFAS013069-RA	1,148252506	2,216452593	6,77E-05	0,000910265
OFAS000624-RA	1,148287684	2,21650664	0,005361023	0,033140422
OFAS015764-RA	1,151150473	2,220909296	1,40E-05	0,000237413
OFAS011887-RA	1,153953367	2,225228312	6,67E-05	0,000897648
OFAS017886-RA	1,155031899	2,226892474	0,00162096	0,012768617
OFAS018112-RA	1,155951952	2,228313087	4,51E-07	1,19E-05
OFAS001979-RA	1,156204102	2,22870258	0,000172808	0,002039969
OFAS017630-RA	1,157572447	2,230817427	0,005345663	0,033070496
OFAS002626-RA	1,158226301	2,231828702	0,002833636	0,019890088
OFAS015761-RA	1,161151021	2,236357792	0,001739569	0,013474405
OFAS012037-RA	1,16163369	2,237106113	5,19E-06	9,97E-05
OFAS003911-RA	1,163099496	2,239380212	0,008700819	0,048630721
OFAS015334-RA	1,165932276	2,24378163	1,90E-05	0,000308065
OFAS000409-RA	1,166857048	2,245220362	4,24E-05	0,00061561
OFAS010446-RA	1,167441961	2,246130828	0,00245799	0,017858214
OFAS000594-RA	1,168369981	2,247576127	0,000739698	0,00674136
OFAS000739-RA	1,168425445	2,247662535	0,000273563	0,002951284
OFAS017296-RA	1,170396575	2,250735578	8,15E-06	0,000148514
OFAS002955-RA	1,170859183	2,251457404	1,41E-06	3,23E-05
OFAS009117-RA	1,171715428	2,252794048	1,02E-07	3,22E-06
OFAS008704-RA	1,171741869	2,252835337	1,73E-07	5,08E-06
OFAS010279-RA	1,171950511	2,253161164	0,000477824	0,004701458
OFAS017703-RA	1,173106577	2,2549674	0,00046051	0,004561081
OFAS006626-RA	1,173212278	2,25513262	1,62E-05	0,000269408
OFAS000123-RA	1,17334387	2,255338326	3,62E-05	0,000536176
OFAS003712-RA	1,175010301	2,257944932	0,000720614	0,006594207
OFAS009636-RA	1,177662386	2,262099496	1,35E-05	0,000230688
OFAS015355-RA	1,183107293	2,270653066	2,41E-05	0,000372905
OFAS016738-RA	1,183276082	2,270918739	5,95E-05	0,000812981
OFAS017845-RA	1,185429272	2,274310564	0,006114989	0,036959718
OFAS000601-RA	1,186801029	2,276474074	4,03E-07	1,09E-05
OFAS005740-RA	1,188220793	2,278715468	7,79E-05	0,001028939
OFAS007549-RA	1,18956763	2,28084377	3,53E-07	9,57E-06
OFAS014962-RA	1,189799461	2,281210315	1,72E-06	3,86E-05
OFAS017421-RA	1,19006325	2,28162746	1,41E-07	4,32E-06
OFAS003569-RA	1,191085574	2,283244842	0,000512894	0,004991826
OFAS005686-RA	1,191975265	2,284653323	6,93E-05	0,000927298

OFAS004161-RA	1,194647217	2,28888855	3,65E-06	7,42E-05
OFAS012425-RA	1,195179936	2,289733884	2,45E-07	6,92E-06
OFAS008412-RA	1,195561663	2,290339812	5,58E-05	0,000770181
OFAS000150-RA	1,197655263	2,293665903	2,97E-06	6,25E-05
OFAS000056-RA	1,197724298	2,293775661	4,53E-08	1,56E-06
OFAS007995-RA	1,198579603	2,295135934	0,000196252	0,002251721
OFAS006413-RA	1,199066208	2,295910189	1,33E-05	0,000227322
OFAS015368-RA	1,199912358	2,297257149	4,54E-06	8,93E-05
OFAS010108-RA	1,203329305	2,30270453	3,47E-07	9,47E-06
OFAS006195-RA	1,204447975	2,304490747	9,31E-07	2,25E-05
OFAS005300-RA	1,204461059	2,304511647	1,60E-05	0,000267306
OFAS016159-RA	1,205160912	2,305629839	8,51E-06	0,000154054
OFAS004857-RA	1,206753676	2,308176707	0,000102748	0,001304446
OFAS006791-RA	1,207552382	2,309454914	5,07E-07	1,32E-05
OFAS003479-RA	1,207688267	2,309672449	4,50E-06	8,91E-05
OFAS008375-RA	1,207798021	2,309848165	1,29E-06	2,98E-05
OFAS012866-RA	1,208274571	2,310611278	6,81E-07	1,70E-05
OFAS014092-RA	1,20830163	2,310654616	0,000542678	0,005228806
OFAS001430-RA	1,208931813	2,311664154	0,008820948	0,049118712
OFAS008985-RA	1,209882739	2,313188347	9,97E-05	0,001270034
OFAS017349-RA	1,211284487	2,315436973	0,00021223	0,002404322
OFAS000121-RA	1,211365163	2,315566457	5,20E-07	1,35E-05
OFAS000604-RA	1,212872964	2,317987785	7,04E-06	0,000131227
OFAS025157-RA	1,213049212	2,318270981	1,36E-05	0,000231037
OFAS025111-RA	1,214709763	2,320940862	0,000145698	0,001752283
OFAS025224-RA	1,216343044	2,323569897	1,20E-05	0,000209246
OFAS003120-RA	1,218528249	2,327092001	0,003419982	0,023045098
OFAS017790-RA	1,219776963	2,32910707	7,51E-07	1,85E-05
OFAS001563-RA	1,219925243	2,329346468	0,000770163	0,006953144
OFAS009101-RA	1,221558541	2,331985052	0,00317674	0,021754287
OFAS010689-RA	1,221871893	2,332491613	8,37E-08	2,70E-06
OFAS016764-RA	1,222262818	2,33312373	1,71E-06	3,85E-05
OFAS000444-RA	1,22516759	2,337826053	2,67E-06	5,69E-05
OFAS006591-RA	1,226205469	2,339508497	0,00236646	0,017352324
OFAS006453-RA	1,22680055	2,340473694	0,003106851	0,021417235
OFAS018941-RA	1,226842839	2,3405423	1,23E-06	2,88E-05
OFAS006596-RA	1,227179421	2,341088415	6,51E-05	0,000879044
OFAS001407-RA	1,233444229	2,35127654	2,57E-07	7,19E-06
OFAS012228-RA	1,234956631	2,353742717	0,000555304	0,005335365
OFAS005152-RA	1,236324074	2,355974745	5,62E-07	1,45E-05
OFAS005792-RA	1,237637573	2,358120714	4,74E-05	0,000671513
OFAS012291-RA	1,239457381	2,361097112	0,00025187	0,002749428
OFAS012113-RA	1,240226057	2,362355453	9,15E-05	0,001174654
OFAS000906-RA	1,240274599	2,36243494	5,02E-08	1,70E-06

OFAS009004-RA	1,240317284	2,362504838	1,39E-07	4,27E-06
OFAS014334-RA	1,241950093	2,365180181	0,001620272	0,012768617
OFAS009230-RA	1,242080325	2,365393694	5,40E-08	1,80E-06
OFAS009966-RA	1,242135009	2,365483354	3,06E-06	6,39E-05
OFAS008223-RA	1,243368043	2,367505936	0,006786739	0,040007601
OFAS003283-RA	1,245534619	2,371064024	2,80E-06	5,91E-05
OFAS013679-RA	1,246374078	2,372444073	0,00082307	0,007331117
OFAS008487-RA	1,246682711	2,372951659	0,001674403	0,013082484
OFAS011083-RA	1,247337464	2,374028846	0,000104688	0,001322838
OFAS017706-RA	1,248446354	2,375854281	4,25E-05	0,000615684
OFAS013397-RA	1,250619295	2,379435414	4,80E-05	0,000679648
OFAS000055-RA	1,250777323	2,379696063	0,001043047	0,008914872
OFAS009814-RA	1,251143926	2,380300844	1,57E-05	0,000261618
OFAS011188-RA	1,251670903	2,381170462	4,88E-05	0,000690107
OFAS008893-RA	1,251784605	2,381358134	0,000354488	0,003692923
OFAS014196-RA	1,253233488	2,383750908	0,00362778	0,024275312
OFAS010146-RA	1,256433587	2,389044269	0,004875609	0,030717703
OFAS017644-RA	1,260246152	2,395366071	1,78E-06	3,97E-05
OFAS002899-RA	1,262277454	2,398741101	1,53E-05	0,000256502
OFAS007955-RA	1,26367336	2,401063169	4,67E-06	9,13E-05
OFAS014060-RA	1,264452677	2,40236053	0,000377665	0,00388036
OFAS012689-RA	1,264769433	2,402888046	0,000215807	0,002436643
OFAS010001-RA	1,266945295	2,406514799	4,26E-07	1,14E-05
OFAS000603-RA	1,268404518	2,408950114	1,04E-06	2,45E-05
OFAS001809-RA	1,268473924	2,409066008	4,60E-05	0,000654351
OFAS007370-RA	1,269339541	2,410511881	7,95E-06	0,000145464
OFAS006970-RA	1,270807335	2,412965579	1,03E-06	2,45E-05
OFAS015124-RA	1,271430048	2,414007315	4,46E-05	0,000637765
OFAS012630-RA	1,272513695	2,415821222	0,000153503	0,001836315
OFAS008301-RA	1,272625527	2,416008494	3,47E-07	9,47E-06
OFAS000280-RA	1,273078679	2,416767484	3,55E-08	1,26E-06
OFAS014477-RA	1,274648323	2,419398344	0,004329415	0,0278763
OFAS009665-RA	1,275579979	2,420961236	1,27E-06	2,94E-05
OFAS017484-RA	1,277314424	2,423873527	0,005369796	0,033179428
OFAS017548-RA	1,277944846	2,424932932	0,001704926	0,013263733
OFAS017817-RA	1,278450491	2,425782986	0,004234019	0,027458949
OFAS014264-RA	1,280810558	2,429754508	0,000177725	0,002081121
OFAS008360-RA	1,281753655	2,43134337	0,001683967	0,013126753
OFAS008589-RA	1,282208924	2,432110747	4,43E-07	1,18E-05
OFAS002691-RA	1,286313712	2,439040497	1,56E-05	0,000261313
OFAS011714-RA	1,286806358	2,439873512	9,49E-07	2,28E-05
OFAS002857-RA	1,287001977	2,440204364	2,15E-08	8,03E-07
OFAS013853-RA	1,287166764	2,440483104	0,000979453	0,008424335
OFAS016093-RA	1,289190183	2,44390835	0,003800824	0,025282516

OFAS010813-RA	1,289364778	2,44420413	1,42E-07	4,33E-06
OFAS016688-RA	1,292791235	2,450016108	2,54E-08	9,34E-07
OFAS007096-RA	1,292910867	2,450219278	4,20E-06	8,39E-05
OFAS000234-RA	1,29400982	2,45208641	2,20E-05	0,000346381
OFAS025038-RA	1,296676943	2,456623796	1,82E-05	0,000297248
OFAS000058-RA	1,297305462	2,457694274	0,00096637	0,008338886
OFAS015040-RA	1,299382068	2,461234409	1,66E-07	4,92E-06
OFAS004220-RA	1,301482597	2,464820518	0,000804403	0,00719476
OFAS009388-RA	1,302431713	2,466442601	1,25E-07	3,85E-06
OFAS011761-RA	1,303116528	2,467613644	0,000310754	0,003306362
OFAS011857-RA	1,3033141	2,467951598	3,73E-05	0,000547818
OFAS013002-RA	1,303939321	2,469021366	0,000104566	0,00132254
OFAS000553-RA	1,303990182	2,469108411	5,03E-05	0,000705816
OFAS004958-RA	1,304518141	2,470012155	4,38E-07	1,17E-05
OFAS002217-RA	1,307132886	2,474492871	1,24E-05	0,000215291
OFAS015594-RA	1,307883262	2,475780242	5,00E-06	9,64E-05
OFAS008299-RA	1,308428278	2,476715709	4,78E-06	9,30E-05
OFAS016685-RA	1,308896495	2,477519641	2,27E-05	0,000356032
OFAS001925-RA	1,310053016	2,479506515	1,29E-05	0,000220453
OFAS015593-RA	1,310648479	2,480530126	0,001081908	0,009200316
OFAS000699-RA	1,310871679	2,480913919	6,94E-07	1,72E-05
OFAS000868-RA	1,311025218	2,481177965	6,06E-07	1,54E-05
OFAS009293-RA	1,311107948	2,48132025	0,000109458	0,001376662
OFAS000446-RA	1,312985306	2,484551257	0,000258167	0,002813522
OFAS006188-RA	1,31466592	2,487447231	1,87E-07	5,45E-06
OFAS005074-RA	1,315391837	2,488699148	5,31E-07	1,37E-05
OFAS003581-RA	1,31568722	2,489208745	6,59E-07	1,66E-05
OFAS000945-RA	1,319094089	2,495093862	0,000101341	0,001290229
OFAS004318-RA	1,32011621	2,496862213	1,29E-05	0,000220453
OFAS019361-RA	1,320327354	2,497227665	0,008357458	0,047161693
OFAS007508-RA	1,320828228	2,498094803	0,000597771	0,005666414
OFAS000007-RA	1,320953074	2,498310989	1,07E-05	0,000188802
OFAS014434-RA	1,321322158	2,498950213	6,39E-05	0,000863868
OFAS006176-RA	1,321519542	2,499292132	1,25E-05	0,000215391
OFAS009114-RA	1,323228045	2,502253657	1,38E-05	0,000234358
OFAS013580-RA	1,324472657	2,504413282	1,21E-06	2,84E-05
OFAS007727-RA	1,325989411	2,50704764	8,10E-09	3,36E-07
OFAS013817-RA	1,326859663	2,508560379	0,000242824	0,002678822
OFAS013778-RA	1,327368568	2,509445419	0,000152739	0,001833264
OFAS010828-RA	1,328128852	2,510768217	0,00011546	0,001441374
OFAS012942-RA	1,328816534	2,511965299	2,19E-05	0,000345294
OFAS015760-RA	1,329017597	2,512315405	1,25E-06	2,91E-05
OFAS007016-RA	1,331450002	2,516554779	0,000500177	0,00488216
OFAS010349-RA	1,336379126	2,525167567	0,003185587	0,021796628

OFAS018649-RA	1,336510264	2,525397108	1,58E-07	4,72E-06
OFAS003356-RA	1,33844277	2,528782173	2,98E-06	6,26E-05
OFAS014631-RA	1,339965199	2,531452122	0,000425068	0,004288891
OFAS013352-RA	1,340119004	2,531722014	2,16E-07	6,24E-06
OFAS009913-RA	1,343663984	2,537950592	8,27E-07	2,01E-05
OFAS019324-RA	1,34671696	2,543326994	1,02E-06	2,42E-05
OFAS002812-RA	1,348521917	2,546510943	3,06E-05	0,000458318
OFAS015163-RA	1,349224816	2,547751938	0,003070946	0,021202276
OFAS007007-RA	1,349765176	2,548706373	2,37E-08	8,75E-07
OFAS013380-RA	1,350885552	2,550686432	0,001198482	0,010033286
OFAS014916-RA	1,351437675	2,551662773	2,61E-08	9,60E-07
OFAS010561-RA	1,351448278	2,551681525	7,39E-08	2,41E-06
OFAS008201-RA	1,351686862	2,552103542	0,008922623	0,049500715
OFAS016065-RA	1,354266417	2,556670813	6,03E-06	0,000114675
OFAS025035-RB	1,354881758	2,557761522	2,87E-08	1,05E-06
OFAS018867-RA	1,355670828	2,55916085	0,007960735	0,045321683
OFAS005362-RA	1,355680591	2,55917817	3,31E-09	1,51E-07
OFAS017726-RA	1,356409106	2,560470799	2,72E-06	5,78E-05
OFAS012455-RA	1,356580276	2,560774607	7,27E-06	0,000134989
OFAS017387-RA	1,357047476	2,561604019	2,34E-05	0,000365614
OFAS014754-RA	1,358301015	2,563830729	5,39E-06	0,000103206
OFAS000733-RA	1,361789573	2,57003779	3,81E-08	1,34E-06
OFAS018041-RA	1,362730406	2,57171435	5,73E-08	1,90E-06
OFAS015217-RA	1,36355503	2,573184726	0,007134444	0,041531265
OFAS016860-RA	1,364134548	2,574218559	1,40E-05	0,000236165
OFAS012566-RA	1,365810831	2,577211311	1,89E-06	4,16E-05
OFAS006192-RA	1,365974547	2,577503786	0,00806	0,045770744
OFAS009968-RA	1,367959396	2,581052338	6,85E-07	1,71E-05
OFAS009549-RA	1,368582703	2,582167706	8,30E-07	2,01E-05
OFAS025167-RA	1,371990553	2,588274361	0,000117907	0,001463781
OFAS005143-RA	1,372615436	2,589395678	4,65E-06	9,11E-05
OFAS001636-RA	1,37278905	2,589707304	9,85E-08	3,11E-06
OFAS001148-RA	1,376025473	2,595523361	0,000200924	0,002297784
OFAS004093-RA	1,377552807	2,598272612	0,004735963	0,030020434
OFAS006962-RA	1,378091026	2,599242117	3,34E-07	9,16E-06
OFAS011856-RA	1,378667955	2,600281754	0,008829754	0,049147435
OFAS002181-RA	1,37937061	2,601548512	4,21E-07	1,13E-05
OFAS015369-RA	1,381253138	2,604945408	1,85E-07	5,41E-06
OFAS015984-RA	1,382024318	2,60633823	2,38E-06	5,12E-05
OFAS013536-RA	1,383381425	2,608791101	3,22E-07	8,88E-06
OFAS002314-RA	1,383459956	2,608933111	0,00436727	0,028079773
OFAS001203-RA	1,384033316	2,609970166	4,27E-08	1,48E-06
OFAS002198-RA	1,386876251	2,615118373	1,00E-06	2,40E-05
OFAS001805-RA	1,389945451	2,620687717	1,15E-07	3,57E-06

OFAS012206-RA	1,391718991	2,623911373	1,15E-08	4,56E-07
OFAS012584-RA	1,392815533	2,625906474	5,74E-06	0,000109595
OFAS006269-RA	1,393893048	2,627868433	0,002400068	0,017541464
OFAS017225-RA	1,394023944	2,628106872	1,48E-06	3,39E-05
OFAS001394-RA	1,394478334	2,628934749	0,000340304	0,003570011
OFAS014465-RA	1,395360564	2,630542873	2,40E-07	6,80E-06
OFAS009330-RA	1,395785034	2,631316947	2,08E-05	0,000330885
OFAS002348-RA	1,397105737	2,633726866	6,89E-05	0,000923781
OFAS016862-RA	1,397925611	2,635224022	5,06E-10	2,78E-08
OFAS018024-RA	1,400280899	2,639529699	0,000228016	0,002542527
OFAS015444-RA	1,402159856	2,642969647	4,69E-05	0,0006658
OFAS010128-RA	1,403978592	2,646303611	0,000442429	0,004417728
OFAS006973-RA	1,40432459	2,646938344	3,01E-08	1,08E-06
OFAS010062-RA	1,405167677	2,648485622	2,97E-05	0,000447757
OFAS015537-RA	1,405707898	2,64947754	2,88E-08	1,05E-06
OFAS004094-RA	1,406559957	2,651042791	3,98E-05	0,000580784
OFAS007832-RA	1,409780672	2,656967668	2,51E-07	7,06E-06
OFAS011610-RA	1,409820198	2,657040462	0,000429554	0,004321201
OFAS007121-RA	1,41022818	2,657791958	2,40E-10	1,46E-08
OFAS008817-RA	1,410261469	2,657853285	3,08E-09	1,43E-07
OFAS007507-RA	1,412051887	2,661153789	8,06E-10	4,29E-08
OFAS009554-RA	1,41308703	2,66306387	0,008988419	0,049804196
OFAS015370-RA	1,414394161	2,665477789	2,42E-08	8,92E-07
OFAS009969-RA	1,417887592	2,671939964	2,61E-06	5,56E-05
OFAS017738-RA	1,418354616	2,672805054	2,15E-09	1,02E-07
OFAS011156-RA	1,419022333	2,674042385	1,04E-06	2,46E-05
OFAS013472-RA	1,420744405	2,677236159	6,47E-07	1,63E-05
OFAS000438-RA	1,421429753	2,678508274	3,27E-05	0,0004889
OFAS025031-RA	1,423151252	2,681706319	0,000381917	0,003913583
OFAS002766-RA	1,425107132	2,685344407	0,000182975	0,002133916
OFAS007054-RA	1,425747076	2,686535823	5,84E-05	0,000801663
OFAS001206-RA	1,426585203	2,688097008	0,001564551	0,012426005
OFAS004767-RA	1,428109566	2,690938774	1,72E-06	3,86E-05
OFAS012045-RA	1,428142588	2,691000368	0,000448248	0,004459309
OFAS014095-RA	1,42986198	2,694209392	0,000914701	0,007995476
OFAS009568-RA	1,430529302	2,695455892	2,40E-05	0,000372905
OFAS019548-RA	1,431618521	2,6974917	8,49E-06	0,000153836
OFAS027062-RA	1,433060737	2,700189645	1,08E-08	4,31E-07
OFAS001031-RA	1,433154235	2,700364644	0,002005079	0,015139243
OFAS019468-RA	1,433984745	2,701919599	2,11E-05	0,000336598
OFAS001169-RA	1,434531548	2,702943861	0,00431408	0,027830775
OFAS008915-RA	1,436783893	2,70716701	3,91E-08	1,37E-06
OFAS025108-RA	1,436863667	2,707316708	0,001512961	0,012109085
OFAS005676-RA	1,438496201	2,710382005	0,000454169	0,004508225

OFAS017552-RA	1,439922759	2,713063395	4,82E-06	9,35E-05
OFAS001263-RA	1,440031238	2,713267403	4,38E-07	1,17E-05
OFAS003849-RA	1,44258676	2,718077817	6,11E-09	2,64E-07
OFAS000161-RA	1,442811635	2,71850152	4,73E-07	1,25E-05
OFAS000293-RA	1,443267829	2,719361272	0,000643432	0,006006257
OFAS016713-RA	1,443773651	2,720314873	5,29E-07	1,37E-05
OFAS002165-RA	1,444117978	2,720964206	1,24E-05	0,000215291
OFAS001030-RA	1,445341184	2,723272185	3,57E-06	7,28E-05
OFAS014629-RA	1,446333721	2,725146372	0,006408567	0,038348909
OFAS025036-RA	1,446734601	2,725903709	2,64E-07	7,36E-06
OFAS014643-RA	1,448522063	2,729283127	8,26E-07	2,01E-05
OFAS002199-RA	1,448692968	2,729606463	0,000183772	0,002139502
OFAS016118-RA	1,45126287	2,734473101	1,06E-05	0,000187377
OFAS014102-RA	1,45151532	2,734951635	0,000176682	0,002073086
OFAS016413-RA	1,455429556	2,74238202	0,002004905	0,015139243
OFAS001524-RA	1,457006157	2,745380579	0,000359311	0,003734501
OFAS025130-RA	1,45809608	2,747455434	0,001593918	0,012614612
OFAS002493-RA	1,459640793	2,750398747	3,15E-11	2,30E-09
OFAS007925-RA	1,463001393	2,756812968	0,002742204	0,019440783
OFAS010776-RA	1,463076827	2,756957116	3,22E-09	1,48E-07
OFAS010888-RA	1,463235979	2,757261268	0,001138186	0,009594094
OFAS009754-RA	1,463866935	2,758467408	6,62E-09	2,83E-07
OFAS006356-RA	1,465796553	2,762159353	1,87E-05	0,000304319
OFAS001400-RA	1,466375825	2,763268639	8,59E-07	2,08E-05
OFAS005318-RA	1,470420067	2,771025653	0,003644276	0,024373581
OFAS016651-RA	1,471114812	2,772360391	2,57E-10	1,54E-08
OFAS001193-RA	1,471265344	2,772649676	4,25E-06	8,47E-05
OFAS006457-RA	1,472238323	2,774520232	1,14E-07	3,56E-06
OFAS016574-RA	1,476784057	2,783276151	2,61E-06	5,56E-05
OFAS005233-RA	1,476901903	2,783503511	4,52E-10	2,52E-08
OFAS027093-RA	1,478194975	2,785999453	0,002301146	0,016975049
OFAS025077-RA	1,48015363	2,789784396	0,005222814	0,032434902
OFAS009124-RA	1,482677459	2,794669074	0,000140145	0,001691538
OFAS019323-RA	1,483546657	2,79635332	0,000573082	0,005467007
OFAS017298-RA	1,483918036	2,79707325	4,77E-08	1,63E-06
OFAS018707-RA	1,486291186	2,80167806	7,59E-07	1,86E-05
OFAS000620-RA	1,489664148	2,808235933	8,06E-07	1,97E-05
OFAS012609-RA	1,492989286	2,814715848	4,81E-06	9,33E-05
OFAS008762-RA	1,498467555	2,825424336	4,58E-08	1,57E-06
OFAS003723-RA	1,499016013	2,82649866	2,40E-05	0,000372905
OFAS001186-RA	1,50117662	2,830734849	0,0001889	0,002187867
OFAS000947-RA	1,502888125	2,834095012	0,000110427	0,001386258
OFAS005149-RA	1,503983214	2,836247072	5,17E-10	2,82E-08
OFAS015481-RA	1,508660076	2,845456405	2,94E-09	1,37E-07

OFAS000618-RA	1,515250552	2,858484669	2,71E-07	7,55E-06
OFAS017200-RA	1,517621988	2,863187177	7,28E-11	4,90E-09
OFAS002146-RA	1,519897061	2,867705872	0,001107283	0,009392451
OFAS007156-RA	1,520918669	2,869737286	0,000362264	0,003753616
OFAS011624-RA	1,522393769	2,872672982	1,02E-08	4,11E-07
OFAS005856-RA	1,523684592	2,875244399	0,004014261	0,026325269
OFAS007943-RA	1,526450639	2,88076233	1,64E-09	8,09E-08
OFAS007227-RA	1,526885385	2,881630558	8,41E-06	0,00015272
OFAS000738-RA	1,529862127	2,887582421	0,000210253	0,002384564
OFAS006135-RA	1,52999562	2,887849623	0,003925857	0,025934915
OFAS018974-RA	1,530041277	2,887941016	0,000562871	0,005381033
OFAS004764-RA	1,53090603	2,88967257	8,32E-13	9,37E-11
OFAS011364-RA	1,532756052	2,893380484	2,90E-07	8,02E-06
OFAS004267-RA	1,534218659	2,896315285	7,46E-07	1,84E-05
OFAS012764-RA	1,534792744	2,897468032	6,24E-08	2,06E-06
OFAS000955-RA	1,535961036	2,899815346	3,06E-10	1,77E-08
OFAS001759-RA	1,539497903	2,906933167	4,04E-09	1,80E-07
OFAS009524-RA	1,539771852	2,907485208	0,008895198	0,049409615
OFAS004046-RA	1,539794299	2,907530446	3,66E-06	7,43E-05
OFAS025161-RA	1,541688654	2,911350736	6,28E-07	1,59E-05
OFAS015884-RA	1,544685702	2,917405048	2,98E-08	1,08E-06
OFAS019552-RA	1,545345798	2,918740193	0,000288737	0,003096571
OFAS000365-RA	1,546038569	2,920142086	8,68E-06	0,000156227
OFAS011522-RA	1,546038863	2,920142682	0,00024562	0,002703025
OFAS016415-RA	1,54650532	2,921086985	1,51E-05	0,000254125
OFAS016364-RA	1,546697553	2,921476233	0,001884347	0,01437268
OFAS004996-RA	1,549674569	2,927510955	4,91E-08	1,67E-06
OFAS003715-RA	1,550236586	2,928651619	0,000603853	0,005708
OFAS012780-RA	1,550354818	2,928891639	1,91E-06	4,20E-05
OFAS003017-RA	1,550498509	2,929183368	1,76E-08	6,68E-07
OFAS011593-RA	1,553615995	2,935519815	4,34E-07	1,16E-05
OFAS005704-RA	1,555567623	2,939493573	7,34E-09	3,08E-07
OFAS003757-RA	1,555857955	2,940085183	1,63E-12	1,71E-10
OFAS015304-RA	1,56188335	2,952390085	0,00045846	0,00454412
OFAS009682-RA	1,563606457	2,955918428	4,04E-05	0,000588493
OFAS009697-RA	1,564201862	2,957138597	5,63E-12	5,15E-10
OFAS008350-RA	1,56433362	2,957408677	0,005526364	0,033975409
OFAS010390-RA	1,565066386	2,95891117	1,83E-11	1,42E-09
OFAS007240-RA	1,56639999	2,961647605	1,25E-06	2,91E-05
OFAS003676-RA	1,56738331	2,963666909	0,008919222	0,049500715
OFAS010788-RA	1,567485918	2,963877699	0,000123641	0,001519569
OFAS003943-RA	1,568959279	2,966906123	6,40E-12	5,74E-10
OFAS011291-RA	1,572434501	2,974061542	0,001932428	0,014706103
OFAS017055-RA	1,572737595	2,974686424	0,000718083	0,006579984

OFAS005526-RA	1,573652428	2,976573312	0,000195752	0,002249815
OFAS010247-RA	1,573742331	2,976758805	0,000434112	0,004350807
OFAS016009-RA	1,574523174	2,978370381	1,13E-05	0,000198424
OFAS016071-RA	1,579763632	2,989208712	1,75E-06	3,91E-05
OFAS007535-RA	1,581896069	2,993630307	4,42E-09	1,96E-07
OFAS016010-RA	1,585287181	3,00067523	1,33E-10	8,58E-09
OFAS015469-RA	1,58573686	3,001610666	7,47E-05	0,000992689
OFAS016887-RA	1,586581643	3,003368801	1,02E-06	2,42E-05
OFAS008681-RA	1,58679196	3,003806666	2,14E-05	0,0003396
OFAS002154-RA	1,587607061	3,005504252	0,000424759	0,004288891
OFAS017887-RA	1,594695837	3,020308332	5,75E-05	0,000791731
OFAS006378-RA	1,595860452	3,022747461	9,71E-05	0,001243809
OFAS025078-RA	1,596207149	3,02347395	0,005017938	0,031379587
OFAS009889-RA	1,597743149	3,026694679	1,44E-05	0,000243253
OFAS017176-RA	1,59953137	3,030448594	0,000364085	0,00376958
OFAS006830-RA	1,600002538	3,031438465	0,000532808	0,005163254
OFAS004160-RA	1,600154204	3,031757169	1,03E-09	5,34E-08
OFAS010688-RA	1,600707364	3,032919832	8,35E-12	7,26E-10
OFAS006943-RA	1,602012688	3,035665204	0,00264821	0,018913782
OFAS018519-RA	1,602863968	3,037456963	2,06E-08	7,74E-07
OFAS004950-RA	1,603932937	3,03970841	3,94E-09	1,76E-07
OFAS005775-RA	1,604027475	3,039907604	5,45E-08	1,82E-06
OFAS014222-RA	1,604812333	3,041561832	1,48E-09	7,37E-08
OFAS018690-RA	1,606222538	3,04453635	1,07E-06	2,53E-05
OFAS018780-RA	1,607712964	3,047683239	4,53E-06	8,93E-05
OFAS011519-RA	1,610651353	3,053896891	7,51E-05	0,000996991
OFAS015951-RA	1,612992745	3,058857174	9,54E-09	3,89E-07
OFAS003477-RA	1,613250025	3,059402716	3,94E-11	2,81E-09
OFAS004446-RA	1,613298902	3,059506369	1,52E-07	4,58E-06
OFAS001309-RA	1,614953505	3,063017277	0,001418809	0,011526751
OFAS008926-RA	1,615446813	3,064064811	2,36E-05	0,000367979
OFAS008020-RA	1,61594062	3,06511376	0,003329553	0,022593991
OFAS018044-RA	1,618583069	3,070732987	6,11E-11	4,15E-09
OFAS004169-RA	1,619691833	3,073093865	0,004883853	0,03074089
OFAS008806-RA	1,622447379	3,078969079	1,89E-12	1,95E-10
OFAS003391-RA	1,622535907	3,07915802	2,30E-06	4,97E-05
OFAS013816-RA	1,625900634	3,08634777	8,73E-05	0,001130389
OFAS000749-RA	1,626876611	3,088436377	0,004538028	0,028915435
OFAS012124-RA	1,628383249	3,091663383	0,000879063	0,007739197
OFAS005361-RA	1,630992048	3,097259039	7,58E-13	8,65E-11
OFAS011969-RA	1,635579001	3,10712224	0,003806932	0,025310646
OFAS003506-RA	1,636273289	3,108617884	1,53E-10	9,70E-09
OFAS010871-RA	1,637131361	3,110467346	3,84E-09	1,73E-07
OFAS001681-RA	1,638279455	3,112943637	1,64E-10	1,03E-08

OFAS004761-RA	1,645051125	3,127589403	3,01E-08	1,08E-06
OFAS014283-RA	1,650231495	3,13884001	2,07E-10	1,28E-08
OFAS011567-RA	1,652324791	3,143397654	0,000135594	0,001646935
OFAS007850-RA	1,655159783	3,149580712	4,67E-09	2,05E-07
OFAS008217-RA	1,65525849	3,14979621	9,90E-09	4,03E-07
OFAS009572-RA	1,657088902	3,153795033	2,45E-12	2,46E-10
OFAS006245-RA	1,660997384	3,162350732	0,000802855	0,007185684
OFAS015503-RA	1,661210048	3,16281692	2,05E-13	2,74E-11
OFAS012907-RA	1,66448379	3,170002087	1,56E-08	6,04E-07
OFAS007922-RA	1,666825911	3,175152557	0,000443276	0,004420791
OFAS011348-RA	1,667765378	3,177220855	1,66E-11	1,30E-09
OFAS008361-RA	1,667771697	3,177234771	2,79E-05	0,000423769
OFAS025144-RA	1,668473869	3,178781535	9,39E-08	2,98E-06
OFAS011901-RA	1,671081186	3,184531595	0,000213169	0,002408883
OFAS018731-RA	1,672741655	3,18819894	4,80E-06	9,33E-05
OFAS011609-RA	1,672905413	3,188560848	2,52E-09	1,18E-07
OFAS012557-RA	1,677107938	3,197862568	1,35E-05	0,000230032
OFAS018874-RA	1,679634914	3,203468743	0,00041608	0,004207655
OFAS006474-RA	1,681322246	3,207217614	3,77E-06	7,61E-05
OFAS013701-RA	1,683492942	3,212046864	0,001037025	0,008876652
OFAS007964-RA	1,686205777	3,21809246	2,48E-09	1,17E-07
OFAS011640-RA	1,686299169	3,218300789	2,26E-07	6,50E-06
OFAS014397-RA	1,688513706	3,223244674	3,44E-05	0,000511527
OFAS016223-RA	1,68936083	3,225137858	0,001949747	0,014821156
OFAS017068-RA	1,692747369	3,232717342	0,001766169	0,013641225
OFAS000296-RA	1,694051385	3,235640637	2,71E-10	1,60E-08
OFAS005358-RA	1,700659225	3,250494527	2,10E-11	1,61E-09
OFAS018996-RA	1,703171346	3,256159444	0,001197271	0,010029375
OFAS016699-RA	1,704674749	3,259554392	5,35E-09	2,32E-07
OFAS007607-RA	1,704708234	3,259630045	2,08E-09	9,97E-08
OFAS013654-RA	1,704786828	3,259807627	8,95E-06	0,000160766
OFAS012659-RA	1,70488649	3,260032823	0,002440838	0,017781552
OFAS001032-RA	1,707038832	3,264900062	3,73E-08	1,31E-06
OFAS013787-RA	1,709268628	3,269950117	1,04E-07	3,25E-06
OFAS003871-RA	1,709484795	3,27044011	1,56E-12	1,64E-10
OFAS003750-RB	1,718530813	3,291010918	0,006371367	0,038177188
OFAS012754-RA	1,721997898	3,298929387	2,89E-05	0,000436377
OFAS015332-RA	1,722601791	3,300310566	0,000407414	0,004138659
OFAS018459-RA	1,722610937	3,300331487	1,03E-09	5,34E-08
OFAS017480-RA	1,725344687	3,306591186	4,48E-11	3,13E-09
OFAS003826-RA	1,725782745	3,307595347	5,81E-12	5,25E-10
OFAS004096-RA	1,726201027	3,30855446	5,71E-12	5,19E-10
OFAS016199-RA	1,732242451	3,3224384	4,55E-06	8,93E-05
OFAS006629-RA	1,733412233	3,325133429	5,27E-11	3,62E-09

OFAS025047-RA	1,735888604	3,330845887	3,47E-09	1,57E-07
OFAS011206-RA	1,738058992	3,335860575	7,09E-14	9,95E-12
OFAS011205-RA	1,741918776	3,344797281	6,53E-13	7,72E-11
OFAS002156-RA	1,743278856	3,347952027	1,51E-10	9,61E-09
OFAS027123-RA	1,743580421	3,348651919	0,000103387	0,001311327
OFAS002155-RA	1,743987516	3,349596966	0,000186894	0,002170225
OFAS014018-RA	1,746086505	3,354473868	4,74E-08	1,62E-06
OFAS010489-RA	1,749462506	3,362332748	0,000229302	0,002554749
OFAS004760-RA	1,753923942	3,372746628	1,65E-10	1,04E-08
OFAS015214-RA	1,755088316	3,37546981	7,33E-05	0,000977968
OFAS010970-RA	1,756431529	3,378613986	0,001866154	0,014241976
OFAS019428-RA	1,756737574	3,379330783	0,00631479	0,037888737
OFAS007369-RA	1,760327658	3,387750572	9,25E-09	3,81E-07
OFAS003103-RA	1,76253365	3,392934666	0,008904406	0,049440374
OFAS018647-RA	1,762979307	3,393982925	1,05E-05	0,000186228
OFAS009851-RA	1,764868797	3,398430919	2,80E-10	1,64E-08
OFAS006794-RA	1,765249438	3,399327681	1,93E-06	4,24E-05
OFAS006721-RA	1,766747343	3,402858929	0,000272214	0,002940438
OFAS013038-RA	1,768988008	3,408148051	4,69E-11	3,24E-09
OFAS019599-RA	1,771621031	3,414373848	0,005676834	0,034726136
OFAS003254-RA	1,771711625	3,414588259	0,001420103	0,01153031
OFAS006213-RA	1,777284023	3,427802583	2,73E-05	0,000417078
OFAS015161-RA	1,781824943	3,438608678	0,008399529	0,047305516
OFAS005338-RA	1,786515089	3,449805654	0,002708694	0,019263387
OFAS006403-RA	1,791109718	3,460809949	3,34E-05	0,000498675
OFAS017962-RA	1,791536629	3,461834196	8,51E-08	2,73E-06
OFAS011407-RA	1,793777675	3,4672159	0,000847131	0,007512082
OFAS027001-RA	1,794005982	3,467764632	2,60E-10	1,55E-08
OFAS025336-RA	1,794049308	3,467868777	1,34E-06	3,09E-05
OFAS010013-RA	1,795241795	3,470736394	6,99E-11	4,73E-09
OFAS025155-RA	1,800694557	3,483879093	1,22E-05	0,000211613
OFAS011111-RA	1,803715507	3,491181851	1,56E-07	4,69E-06
OFAS006678-RA	1,803883595	3,491588631	0,003952167	0,026044857
OFAS012275-RA	1,80500653	3,4943074	0,000378939	0,003890483
OFAS013024-RA	1,807356021	3,500002666	1,39E-07	4,27E-06
OFAS015250-RA	1,810819796	3,508415938	2,98E-13	3,79E-11
OFAS009415-RA	1,813747845	3,515543741	1,14E-12	1,24E-10
OFAS006630-RA	1,81733441	3,524294316	1,86E-12	1,93E-10
OFAS025279-RA	1,823677609	3,539823946	2,51E-11	1,90E-09
OFAS027157-RA	1,825624839	3,54460493	0,00112941	0,009532052
OFAS004992-RA	1,82696676	3,547903475	0,004819547	0,03044995
OFAS002223-RA	1,829283794	3,553606147	0,000415144	0,004201348
OFAS005004-RA	1,832242402	3,560901187	1,40E-05	0,000236165
OFAS025309-RC	1,832339241	3,561140214	0,004401505	0,028245964

OFAS001824-RA	1,833098714	3,563015387	4,23E-15	7,39E-13
OFAS007155-RA	1,833977485	3,565186345	1,29E-08	5,10E-07
OFAS018263-RA	1,835678071	3,569391308	0,001514785	0,012116478
OFAS009565-RA	1,835698898	3,569442838	4,33E-09	1,92E-07
OFAS002685-RA	1,835810452	3,569718849	0,00096781	0,008345965
OFAS003478-RA	1,835965723	3,570103063	3,01E-08	1,08E-06
OFAS017885-RA	1,836903774	3,572425124	0,001487128	0,011959176
OFAS015482-RA	1,845455929	3,593665003	2,81E-11	2,09E-09
OFAS009566-RA	1,847171496	3,597940917	2,54E-10	1,53E-08
OFAS011688-RA	1,860325576	3,630895921	0,000527867	0,005122745
OFAS006414-RA	1,861638904	3,634202737	0,001319423	0,01089677
OFAS003892-RA	1,86414817	3,640529173	1,78E-09	8,63E-08
OFAS018776-RA	1,874013406	3,665508639	3,89E-09	1,75E-07
OFAS007516-RA	1,875796539	3,670041913	2,98E-10	1,73E-08
OFAS014757-RA	1,884631097	3,692584914	5,61E-14	8,12E-12
OFAS013127-RA	1,893699546	3,715868755	1,51E-05	0,000253864
OFAS014423-RA	1,896793185	3,723845416	0,000712871	0,006545584
OFAS016294-RA	1,898847413	3,729151511	9,96E-05	0,001270034
OFAS001965-RA	1,901638557	3,736373185	2,70E-12	2,69E-10
OFAS000061-RA	1,902402642	3,738352579	2,06E-05	0,000329329
OFAS001929-RA	1,904311485	3,743302101	1,10E-08	4,40E-07
OFAS016489-RA	1,907189914	3,750778099	8,01E-07	1,96E-05
OFAS027006-RA	1,90861917	3,754495778	0,002644725	0,018898908
OFAS000619-RA	1,915420781	3,772238205	9,20E-11	6,05E-09
OFAS006040-RA	1,917407971	3,777437724	0,002044074	0,015407768
OFAS009681-RA	1,917775746	3,778400801	1,78E-06	3,97E-05
OFAS007140-RA	1,918489534	3,780270663	0,000495518	0,00484722
OFAS018013-RA	1,925047298	3,79749298	0,001422692	0,011537424
OFAS003099-RA	1,926350753	3,800925514	0,002947424	0,020549587
OFAS004681-RA	1,927299488	3,803425874	7,69E-12	6,77E-10
OFAS001728-RA	1,939760558	3,8364197	9,97E-09	4,05E-07
OFAS008653-RA	1,944576397	3,849247393	1,30E-09	6,54E-08
OFAS014677-RA	1,945738284	3,852348666	4,55E-06	8,93E-05
OFAS018015-RA	1,948266074	3,859104402	3,47E-09	1,57E-07
OFAS018022-RA	1,948442353	3,859575964	3,59E-07	9,72E-06
OFAS008119-RA	1,949056401	3,861219048	2,61E-09	1,22E-07
OFAS013676-RA	1,951948935	3,868968371	2,29E-08	8,50E-07
OFAS015132-RA	1,962893758	3,898431427	0,004105628	0,026768056
OFAS015183-RA	1,965484313	3,905437879	6,18E-13	7,43E-11
OFAS018348-RA	1,967769266	3,911628248	7,52E-11	5,04E-09
OFAS004766-RA	1,97108901	3,920639545	3,43E-12	3,25E-10
OFAS003908-RA	1,971979455	3,923060149	7,39E-07	1,83E-05
OFAS016773-RA	1,972254275	3,923807525	7,58E-15	1,28E-12
OFAS001523-RA	1,972788011	3,925259437	1,26E-09	6,34E-08

OFAS006784-RA	1,975024818	3,931350022	3,63E-11	2,63E-09
OFAS011028-RA	1,982543941	3,951893152	0,002846357	0,019958578
OFAS017364-RA	1,98363175	3,954874048	6,53E-16	1,29E-13
OFAS006841-RA	1,991779248	3,977272052	0,000227209	0,002537738
OFAS012227-RA	2,00092643	4,002569433	7,09E-08	2,32E-06
OFAS003834-RA	2,006707284	4,018639835	2,23E-15	4,00E-13
OFAS001808-RA	2,011464756	4,03191369	1,05E-09	5,44E-08
OFAS010202-RA	2,015928693	4,044408419	0,00649674	0,038670388
OFAS000956-RA	2,020868354	4,058279851	2,01E-05	0,0003227
OFAS004445-RA	2,022567441	4,063062172	9,62E-15	1,58E-12
OFAS016488-RA	2,023815442	4,066578439	0,002003564	0,015139243
OFAS015160-RA	2,026496013	4,07414129	1,36E-12	1,46E-10
OFAS016180-RA	2,031092733	4,087143035	0,004327705	0,0278763
OFAS012518-RA	2,032882404	4,092216304	0,000769833	0,006953144
OFAS011585-RA	2,038343535	4,107736202	3,03E-06	6,34E-05
OFAS001784-RA	2,046824011	4,131953479	4,35E-05	0,000628541
OFAS016318-RA	2,066984802	4,190100369	2,12E-05	0,000337302
OFAS011303-RA	2,068223892	4,193700672	1,20E-17	3,45E-15
OFAS002811-RA	2,069356779	4,196995099	6,78E-07	1,70E-05
OFAS000425-RA	2,070042528	4,198990511	6,22E-06	0,000117842
OFAS027117-RA	2,084576273	4,24150503	0,003599837	0,024136292
OFAS006722-RA	2,093370098	4,267437719	0,001428093	0,011574256
OFAS004856-RA	2,095604679	4,274052648	0,000504714	0,004922877
OFAS009072-RA	2,099048821	4,284268271	1,51E-12	1,61E-10
OFAS005339-RA	2,101021837	4,290131402	4,13E-08	1,44E-06
OFAS001439-RA	2,101737206	4,292259218	2,03E-10	1,26E-08
OFAS025241-RA	2,103239758	4,296731891	0,000127603	0,001562556
OFAS013955-RA	2,119782404	4,346283867	1,16E-05	0,000204021
OFAS002072-RA	2,122620861	4,354843461	3,80E-10	2,14E-08
OFAS003009-RA	2,127689726	4,370170981	1,95E-14	3,05E-12
OFAS008150-RA	2,131398381	4,381419587	0,006066694	0,036743869
OFAS004552-RA	2,144463252	4,421277392	0,002986404	0,020767611
OFAS017508-RA	2,147165409	4,429566171	0,000206086	0,002346033
OFAS016732-RA	2,150946355	4,441190192	5,25E-08	1,76E-06
OFAS009678-RA	2,153868103	4,450193611	1,33E-06	3,07E-05
OFAS001776-RA	2,15659732	4,458620226	0,003747095	0,024974455
OFAS005298-RA	2,174976981	4,515785565	1,13E-09	5,81E-08
OFAS015055-RA	2,175466616	4,517318436	0,006116051	0,036959718
OFAS025035-RA	2,177100215	4,522436402	7,53E-09	3,15E-07
OFAS003579-RA	2,185302163	4,548220388	1,32E-11	1,06E-09
OFAS017290-RA	2,192256547	4,57019761	1,11E-13	1,51E-11
OFAS014517-RA	2,197392063	4,586494987	1,61E-07	4,78E-06
OFAS013440-RA	2,197578575	4,58708797	7,38E-13	8,57E-11
OFAS017060-RA	2,205089947	4,611032861	0,003862062	0,025576192

OFAS013451-RA	2,217015989	4,649307956	5,56E-12	5,13E-10
OFAS012316-RA	2,225994937	4,678334239	0,002368997	0,017361474
OFAS013458-RC	2,227002662	4,681603203	0,000515756	0,005016055
OFAS015219-RA	2,227696055	4,683853834	1,38E-17	3,78E-15
OFAS002741-RA	2,231062926	4,694797481	3,42E-07	9,35E-06
OFAS017400-RA	2,232436537	4,699269596	1,38E-10	8,87E-09
OFAS014828-RA	2,233128518	4,701524116	4,82E-15	8,33E-13
OFAS004582-RA	2,233140445	4,701562986	0,005883171	0,035809452
OFAS013661-RA	2,233815722	4,703764143	9,22E-07	2,23E-05
OFAS003010-RA	2,236650055	4,713014286	9,28E-12	7,91E-10
OFAS018141-RA	2,247492966	4,748569491	1,63E-08	6,24E-07
OFAS001522-RA	2,251019134	4,760189919	0,001181455	0,009915386
OFAS002909-RA	2,254196807	4,770686244	9,01E-16	1,76E-13
OFAS025325-RA	2,256124955	4,777066483	4,54E-13	5,51E-11
OFAS003185-RA	2,260676063	4,792159951	8,35E-08	2,70E-06
OFAS018388-RA	2,266108223	4,810237818	0,000475146	0,004685369
OFAS003578-RA	2,268974756	4,819804923	0,001293593	0,010703131
OFAS014649-RA	2,2786085	4,852097363	0,005587023	0,034238947
OFAS007519-RA	2,294197124	4,904809567	4,90E-16	1,00E-13
OFAS015721-RA	2,297048346	4,914512607	2,31E-16	5,26E-14
OFAS025253-RA	2,300650843	4,92679978	0,000265034	0,0028744
OFAS012406-RA	2,302175343	4,932008695	1,45E-10	9,26E-09
OFAS019296-RA	2,304865788	4,941214851	0,000119916	0,001480922
OFAS012115-RA	2,306908266	4,948215271	0,005565007	0,034124096
OFAS025262-RA	2,308892895	4,955026918	0,000555941	0,005337513
OFAS010344-RA	2,310738965	4,961371422	4,06E-10	2,28E-08
OFAS010480-RA	2,311713708	4,964724658	6,96E-17	1,67E-14
OFAS014584-RA	2,312890323	4,968775376	9,99E-18	2,99E-15
OFAS001373-RA	2,314723933	4,975094512	0,001343411	0,011046419
OFAS019098-RA	2,318377646	4,987710211	0,000647386	0,006034803
OFAS012028-RA	2,318387039	4,987742683	2,79E-16	6,15E-14
OFAS003472-RA	2,321225825	4,997566709	1,09E-05	0,000191777
OFAS010285-RA	2,322568395	5,002219604	9,70E-10	5,10E-08
OFAS007517-RA	2,322963805	5,003590788	1,02E-16	2,40E-14
OFAS015216-RA	2,33030893	5,029130291	0,005252996	0,032562291
OFAS015722-RA	2,333664248	5,040840298	0,000203794	0,002324393
OFAS009081-RA	2,341374195	5,067851304	1,60E-08	6,15E-07
OFAS014421-RA	2,341603929	5,068658369	1,07E-13	1,47E-11
OFAS007052-RA	2,34297914	5,07349224	1,67E-05	0,000275643
OFAS016293-RA	2,344191759	5,077758419	1,05E-05	0,000186063
OFAS006623-RA	2,362454559	5,142445356	0,00838125	0,047236586
OFAS009413-RA	2,368453574	5,163873194	2,16E-05	0,000342035
OFAS014452-RA	2,381493674	5,210759515	0,001430985	0,0115895
OFAS004743-RA	2,382227418	5,213410343	0,000509958	0,004970434

OFAS003630-RA	2,388890272	5,237543323	9,27E-08	2,95E-06
OFAS014678-RA	2,389712194	5,240528069	2,87E-11	2,13E-09
OFAS007493-RA	2,39545372	5,261425473	0,001520007	0,012151032
OFAS010964-RA	2,397136848	5,267567325	5,11E-09	2,23E-07
OFAS025218-RA	2,397845908	5,27015688	0,004265228	0,027608177
OFAS001435-RA	2,399607982	5,27659766	4,29E-12	4,04E-10
OFAS011632-RA	2,401123297	5,282142774	8,38E-10	4,44E-08
OFAS015915-RA	2,401408229	5,283186098	0,000603616	0,005708
OFAS004834-RA	2,403625355	5,29131151	5,84E-07	1,49E-05
OFAS017442-RA	2,410425447	5,31631079	0,004145794	0,026964675
OFAS002031-RA	2,413751735	5,328582258	0,007199223	0,04181696
OFAS015971-RA	2,419089971	5,348335509	0,000189311	0,002188856
OFAS010757-RA	2,427232621	5,378607156	0,002773028	0,019576879
OFAS001607-RA	2,428307896	5,382617455	3,36E-06	6,92E-05
OFAS025295-RA	2,444223316	5,442325767	0,000295487	0,003153895
OFAS005171-RA	2,451954022	5,471566835	0,002108671	0,015762374
OFAS000707-RA	2,456213595	5,487745571	0,001240892	0,010332855
OFAS014254-RA	2,462004394	5,509816967	3,86E-06	7,77E-05
OFAS009360-RA	2,463096433	5,513989167	8,50E-12	7,34E-10
OFAS016542-RA	2,46427844	5,518508657	4,64E-21	2,15E-18
OFAS010481-RA	2,471628635	5,546695914	0,000291956	0,00312363
OFAS019265-RA	2,476948971	5,567188649	0,000906924	0,007937792
OFAS003842-RA	2,47944598	5,576832654	0,000431024	0,004326298
OFAS012078-RA	2,483423654	5,592229829	1,54E-15	2,88E-13
OFAS012215-RA	2,500746546	5,659782237	0,002598581	0,018618556
OFAS009689-RA	2,502738781	5,667603299	0,000122339	0,001506319
OFAS007110-RA	2,505014577	5,676550782	0,003960975	0,026090138
OFAS019021-RA	2,536519058	5,801874376	0,000782857	0,007053567
OFAS000128-RA	2,543262789	5,82905813	1,82E-06	4,03E-05
OFAS001207-RA	2,543851911	5,8314389	0,00555083	0,03407988
OFAS009136-RA	2,544409273	5,833692219	3,58E-16	7,54E-14
OFAS010675-RA	2,552264992	5,865544303	1,97E-13	2,65E-11
OFAS007467-RA	2,559772982	5,896148997	0,002419499	0,01764518
OFAS017728-RA	2,574111878	5,955042803	0,002193093	0,016284988
OFAS008143-RA	2,585372927	6,001707159	1,78E-08	6,72E-07
OFAS011892-RA	2,587488821	6,010515874	9,32E-07	2,25E-05
OFAS013748-RA	2,588374738	6,014207892	2,12E-13	2,77E-11
OFAS018990-RA	2,59263236	6,031982989	0,007316292	0,04235086
OFAS025228-RF	2,600186826	6,063651446	6,43E-12	5,74E-10
OFAS000476-RA	2,60786071	6,095990734	1,29E-07	3,95E-06
OFAS017944-RA	2,647190947	6,264463446	6,07E-21	2,55E-18
OFAS007559-RA	2,64746123	6,265637176	1,50E-18	4,69E-16
OFAS018865-RA	2,657537904	6,309553448	0,000128736	0,001574993
OFAS001243-RA	2,669416783	6,36171959	0,004841863	0,030566615

OFAS000751-RA	2,677723631	6,398455193	1,91E-08	7,18E-07
OFAS018895-RA	2,68407866	6,426702367	0,00094021	0,008170728
OFAS003217-RQ	2,712576149	6,554910805	1,22E-10	7,92E-09
OFAS001867-RA	2,721782104	6,596871963	1,36E-21	6,79E-19
OFAS012688-RA	2,727433863	6,622765899	6,21E-06	0,00011784
OFAS006621-RA	2,732428314	6,645732918	2,89E-27	5,57E-24
OFAS007134-RA	2,767259421	6,808133945	0,00014389	0,001735179
OFAS017066-RA	2,781396681	6,875176168	4,37E-05	0,000629209
OFAS002704-RA	2,811169857	7,018534677	8,53E-08	2,73E-06
OFAS012563-RA	2,815057143	7,037471345	1,02E-11	8,57E-10
OFAS018328-RA	2,826421665	7,09312644	4,94E-06	9,55E-05
OFAS002889-RA	2,833934742	7,130161436	0,00342407	0,023061112
OFAS025129-RC	2,836502354	7,142862522	2,79E-11	2,08E-09
OFAS013852-RA	2,850284907	7,211427691	3,12E-12	3,03E-10
OFAS002810-RA	2,861114406	7,265763497	4,51E-06	8,92E-05
OFAS013356-RA	2,86301958	7,275364754	0,001342302	0,011045091
OFAS002344-RA	2,879351041	7,358190567	0,000389217	0,003974795
OFAS025096-RA	2,887269564	7,398688521	2,72E-05	0,000416609
OFAS004606-RA	2,88985719	7,411970761	0,004812185	0,030431989
OFAS000242-RA	2,897008942	7,448804729	1,70E-09	8,31E-08
OFAS008078-RA	2,901189929	7,470422968	5,78E-21	2,55E-18
OFAS001932-RA	2,919843707	7,567641297	4,36E-05	0,000628913
OFAS015230-RA	2,947031675	7,711607769	0,008762594	0,048876218
OFAS010513-RA	2,949573724	7,725207711	9,33E-28	2,10E-24
OFAS025019-RA	2,952124371	7,738877755	4,39E-26	5,37E-23
OFAS004828-RA	2,962467675	7,794560484	0,001547862	0,012337101
OFAS006743-RA	2,979207788	7,885530347	0,000855728	0,007573362
OFAS000803-RA	2,980464817	7,892404052	0,005025963	0,031415186
OFAS014843-RA	2,994893776	7,971735132	7,94E-08	2,58E-06
OFAS012524-RA	3,007294208	8,040550104	0,003879083	0,025676286
OFAS016411-RA	3,013772105	8,076734438	0,003026197	0,020968556
OFAS012916-RA	3,032264589	8,180928481	2,44E-05	0,000378485
OFAS025203-RA	3,032760602	8,183741653	4,51E-11	3,13E-09
OFAS018807-RA	3,04235486	8,238346806	0,002693809	0,019198734
OFAS017538-RA	3,051803229	8,292477711	0,000300831	0,003208384
OFAS001170-RA	3,065463888	8,371370837	0,001214725	0,010156641
OFAS018980-RA	3,074437275	8,423602012	3,59E-05	0,000532495
OFAS025056-RA	3,08990791	8,514417953	0,008814214	0,049101515
OFAS005922-RA	3,091043151	8,521120492	0,004842551	0,030566615
OFAS000750-RA	3,097390925	8,558695529	8,75E-13	9,74E-11
OFAS016417-RA	3,09853733	8,565499204	0,003162434	0,021694971
OFAS009725-RA	3,113688004	8,655925029	2,90E-08	1,05E-06
OFAS004367-RA	3,123260672	8,713550383	0,004093246	0,026713187
OFAS009205-RA	3,134712155	8,782989962	1,74E-14	2,76E-12

OFAS018838-RA	3,141308193	8,823237953	0,008162872	0,046276886
OFAS004196-RA	3,154862272	8,906522634	0,000186551	0,002168108
OFAS009484-RA	3,181902124	9,075028189	0,005749049	0,03510412
OFAS009422-RA	3,188048042	9,113770506	5,02E-08	1,70E-06
OFAS006183-RA	3,202128672	9,203155928	0,001261351	0,010494378
OFAS010235-RA	3,219885751	9,317130824	0,000156852	0,001869733
OFAS018562-RA	3,238513327	9,438210359	0,000281831	0,003032158
OFAS008461-RA	3,241968804	9,460843425	0,004940536	0,030981855
OFAS004008-RA	3,257258593	9,561643341	0,007441991	0,042930888
OFAS002071-RA	3,259308331	9,575237897	2,50E-05	0,000385627
OFAS025045-RA	3,271932857	9,659395172	0,004953347	0,031018868
OFAS007886-RA	3,283912521	9,739937545	0,003990391	0,026219787
OFAS000424-RA	3,324930458	10,02083247	1,64E-05	0,000272701
OFAS001839-RA	3,331296019	10,06514478	0,000119947	0,001480922
OFAS013809-RA	3,36574463	10,30837221	0,006312237	0,037888737
OFAS005241-RA	3,371875638	10,35227282	0,003758554	0,02502891
OFAS014852-RA	3,38462432	10,44415827	0,000256222	0,002794584
OFAS025202-RC	3,401334113	10,56582938	0,003333706	0,022610786
OFAS025204-RA	3,415649694	10,67119393	0,003497127	0,02351787
OFAS003398-RA	3,43110076	10,78609515	0,002287936	0,016896104
OFAS000474-RA	3,471277714	11,0906938	3,11E-07	8,60E-06
OFAS009472-RA	3,526922264	11,52681688	0,000697704	0,00641507
OFAS009561-RA	3,568361351	11,86270695	0,007134621	0,041531265
OFAS000806-RA	3,584454163	11,99577251	3,45E-06	7,09E-05
OFAS012335-RA	3,604245375	12,16146711	1,06E-08	4,24E-07
OFAS007659-RA	3,617056319	12,26994025	1,10E-32	7,41E-29
OFAS004198-RA	3,631194673	12,39077631	5,86E-05	0,000801972
OFAS018014-RA	3,74317712	13,39086378	0,000413519	0,004194354
OFAS017570-RA	3,779855009	13,73566648	0,006612142	0,039201386
OFAS013331-RA	3,781329363	13,74971074	0,000206214	0,002346033
OFAS000081-RA	3,827940025	14,20119102	1,33E-06	3,07E-05
OFAS012430-RA	3,855222778	14,47230465	0,004150514	0,026982345
OFAS004427-RA	3,862790273	14,54841694	0,003523145	0,02366921
OFAS016027-RA	3,907008027	15,00122101	0,008404016	0,047305516
OFAS013130-RA	3,919849969	15,13534828	0,000336501	0,003543919
OFAS013695-RA	3,925727253	15,19713278	3,40E-06	7,00E-05
OFAS004341-RA	3,926046847	15,2004997	0,003814795	0,025350413
OFAS014661-RA	3,948623712	15,4402447	0,000156816	0,001869733
OFAS018531-RA	3,954960811	15,50821581	1,34E-22	8,21E-20
OFAS014766-RA	3,96822163	15,6514198	0,002315719	0,017054528
OFAS007044-RA	3,993257652	15,92539943	0,002977463	0,020733842
OFAS025318-RA	4,104942347	17,2072226	0,000614639	0,005781508
OFAS014486-RA	4,127500586	17,47839232	7,61E-27	1,14E-23
OFAS008234-RA	4,169306329	17,99228269	7,38E-06	0,000136797

OFAS025098-RA	4,205592027	18,4505514	0,00075816	0,006877046
OFAS014485-RA	4,228083878	18,74045243	2,30E-23	1,58E-20
OFAS006464-RA	4,306352379	19,78523614	0,000235859	0,00261914
OFAS008580-RA	4,348748276	20,37528418	3,07E-13	3,83E-11
OFAS025063-RA	4,408877692	21,24244158	6,42E-13	7,65E-11
OFAS010201-RA	4,428876301	21,53895424	7,79E-20	3,00E-17
OFAS025181-RA	4,462406507	22,04541158	6,91E-15	1,18E-12
OFAS016612-RA	4,529591505	23,09632654	0,000425683	0,004290578
OFAS005108-RA	5,08756273	34,00235415	1,05E-05	0,000185811
OFAS017312-RA	5,120474757	34,78696129	0,003408925	0,02299233
OFAS025156-RA	5,251330621	38,08974228	1,16E-18	3,71E-16
OFAS011568-RA	5,362876713	41,15160267	1,23E-14	1,99E-12
OFAS006666-RA	5,487450411	44,86288244	0,004299428	0,027776162
OFAS001998-RA	5,520989399	45,91804769	0,006572884	0,039054587
OFAS015252-RA	5,552691718	46,93823594	0,007118503	0,04149123
OFAS015062-RA	5,580819835	47,86236679	0,006666384	0,039453513
OFAS017532-RA	5,580994826	47,86817259	0,007665014	0,043991367
OFAS013850-RA	5,638185374	49,80385025	0,007794696	0,044613457
OFAS017473-RA	5,685692014	51,47114651	0,00456127	0,029022345
OFAS010410-RA	5,696535254	51,85945912	0,00393364	0,025960866
OFAS014136-RA	5,70013873	51,98915243	0,006460011	0,038519851
OFAS006594-RA	5,734370248	53,23747521	0,006414873	0,038369602
OFAS006551-RA	5,763982068	54,34148432	0,003665766	0,024480849
OFAS006509-RA	5,778487062	54,8905946	0,004248139	0,027537266
OFAS005280-RA	5,783733701	55,09057825	0,005347256	0,033070496
OFAS014007-RA	5,805028346	55,90976383	0,006444993	0,03849977
OFAS015342-RA	5,82717388	56,77460584	0,003732981	0,024892698
OFAS014098-RA	5,830325244	56,89875751	2,14E-09	1,02E-07
OFAS015498-RA	5,859628415	58,06626829	0,005343341	0,033070496
OFAS009365-RA	5,870630163	58,51076449	0,00856405	0,048005723
OFAS008804-RA	5,878944645	58,84894493	0,003063039	0,021177607
OFAS007252-RA	5,885551202	59,11905085	0,00403774	0,026427774
OFAS013855-RA	5,898686054	59,65975112	0,006924526	0,040518401
OFAS013103-RA	5,924153746	60,7222669	0,00319622	0,021854357
OFAS008012-RA	5,947276723	61,70334186	0,007699129	0,044141824
OFAS016912-RA	5,983175073	63,25795765	0,006764855	0,039913535
OFAS018202-RA	5,985502628	63,36009652	0,00611312	0,036959718
OFAS000459-RA	5,986606092	63,40857685	9,76E-24	8,34E-21
OFAS015061-RA	6,034941514	65,56897848	0,005553477	0,03407988
OFAS008639-RA	6,061121784	66,76970607	0,0083798	0,047236586
OFAS004623-RA	6,088588485	68,0530768	0,004498985	0,028748259
OFAS016460-RA	6,091032622	68,16846641	0,008799806	0,049041532
OFAS018484-RA	6,101341102	68,65729446	0,002616483	0,018726901
OFAS008433-RA	6,154222356	71,22058376	0,004088934	0,026697982

OFAS009453-RA	6,156022743	71,30951779	0,004310885	0,027823488
OFAS008179-RA	6,212446489	74,15368532	0,004851321	0,030578987
OFAS004874-RA	6,219454993	74,51479475	0,005029649	0,031423644
OFAS009546-RA	6,226938835	74,90233741	0,00289029	0,02020353
OFAS000423-RA	6,243350185	75,75925218	1,68E-22	9,84E-20
OFAS000317-RA	6,260561665	76,6684796	0,002581247	0,018543678
OFAS017000-RA	6,283549457	77,89989383	0,002002264	0,015139243
OFAS006742-RA	6,305005937	79,06711815	2,58E-13	3,31E-11
OFAS011762-RA	6,308773316	79,27385975	0,001398998	0,011379913
OFAS009957-RA	6,48035077	89,2853004	0,003539885	0,023746144
OFAS012803-RA	6,558286999	94,24126496	0,000510734	0,00497439
OFAS004366-RA	6,579703798	95,65071168	0,001818791	0,013912044
OFAS007178-RA	6,605395662	97,36934028	0,002048965	0,015418748
OFAS007797-RA	6,724166708	105,7245572	0,000392947	0,004006808
OFAS012869-RA	6,74565168	107,3108157	0,001213732	0,01015464
OFAS014349-RB	6,893916664	118,9256965	8,07E-05	0,001059183
OFAS002691-RB	7,131538402	140,2190351	0,001715512	0,013326381
OFAS011853-RB	7,334443928	161,3940886	0,000884302	0,007770091
OFAS025226-RA	7,391548323	167,9104631	5,06E-06	9,74E-05
OFAS008868-RA	7,421454019	171,427413	0,00080106	0,007179803
OFAS000241-RA	7,424358855	171,7729262	5,00E-06	9,64E-05
OFAS008080-RA	8,351071907	326,5300389	3,13E-06	6,49E-05
OFAS007884-RA	8,63445562	397,4020819	7,45E-13	8,58E-11
OFAS006887-RA	8,860597715	464,8423538	9,25E-10	4,89E-08
OFAS001445-RB	8,993945108	509,855674	4,04E-06	8,10E-05
OFAS006554-RB	9,713696796	839,680571	4,33E-19	1,49E-16
OFAS009692-RA	10,81521487	1801,789636	8,47E-08	2,73E-06
OFAS005422-RA	11,56605286	3031,997532	2,36E-41	3,18E-37

Danksagungen

Zuerst möchte ich Prof. Dr. Siegfried Roth für die Möglichkeit danken diese Arbeit in seinem Labor bearbeiten zu dürfen. Bedanken möchte ich mich außerdem bei ihm für die ausgezeichnete Betreuung und die anregenden Hilfestellungen.

Herrn Prof. Dr. Matthias Hammerschmidt möchte ich Danken für das Erstellen des Zweitgutachtens.

Großer Dank gebührt auch Dr. Nathan J. Kenny für die großartige Hilfestellung bei der Durchführung der Transkriptomanalyse.

Bedanken möchte ich mich außerdem bei der AG von Prof. Dr. Matthias Hammerschmidt für die freundliche Zurverfügungstellung Ihres Zebrafisch *cordin* Plasmiden.

Dr. Kristen Panfilio möchte ich danken für das Teilen Ihrer Erfahrung über die Embryogenese und die experimentelle Arbeit von und mit *Oncopeltus faciatus*.

Dr. Matthias Pechmann und Dr. Matthew A. Benton möchte ich danken für die extrem wertvollen Diskussionen über die Laborarbeit im Allgemeinen und unzähligen Hilfestellung bei diversen experimentellen Herausforderungen.

Dr. Lena Sachs und Dr. Yen-Ta Chen möchte ich danken für die Einführung in die experimentelle Laborarbeit mit *Oncopeltus faciatus*.

Ich möchte mich ganz herzlich bedanken bei Dr. Nadine Frey, Dr. Daniela Gurská und Dr. Muhammad Salim Hakeemi für die gemeinsam verbrachte Zeit im Büro Und Labor, sowie bei den unendlich vielen Hilfestellungen während meiner gesamten Promotionszeit.

Dank gebührt auch Oliver Karst für die Zusammenarbeit im Büro und Labor während der gesamten Promotion.

Ich danke natürlich auch meiner gesamten Familie und all meinen Freunden die mich im Verlauf der Promotion bedingungslos unterstützt haben. Mein größter Dank gilt meinem Sohn Finn für das Lächeln das er mir jeden Tag schenkt.

Erklärung zur Dissertation

Ich versichere, dass ich die von mir vorgelegte Dissertation selbständig angefertigt, die benutzten Quellen und Hilfsmittel vollständig angegeben und die Stellen der Arbeit − einschließlich Tabellen, Karten und Abbildungen −, die anderen Werken im Wortlaut oder dem Sinn nach entnommen sind, in jedem Einzelfall als Entlehnung kenntlich gemacht habe; dass diese Dissertation noch keiner anderen Fakultät oder Universität zur Prüfung vorgelegen hat; dass sie − abgesehen von unten angegebenen Teilpublikationen − noch nicht veröffentlicht worden ist, sowie, dass ich eine solche Veröffentlichung vor Abschluss des Promotionsverfahrens nicht vornehmen werde. Die Bestimmungen der Promotionsordnung sind mir bekannt. Die von mir vorgelegte Dissertation ist von Prof. Dr. Siegfried Roth betreut worden.

Teilpublikationen: keine

---------- ----------

(Ort, Datum) (Kai Hans Conrads)

Lebenslauf

Persönliche Informationen

Name:	Kai Hans Conrads
Geburtstag:	29. September 1987
Geburtsort:	Neuss
Nationalität:	deutsch

Schulbildung

07/1994 – 07/1998	Albert-Schweizer-Grundschule, Neuss
08/1998 – 07/2007	Abitur am Gymnasium Norf, Neuss

Zivildienst

08/2007 – 07/2008	Träger: Lebenshilfe Rhein-Kreis Neuss

Studienverlauf

07/2008 – 07/2012	B.Sc. in Biologie an der Universität zu Köln Thesis: „Analysis of Fog signaling in *Nasonia vitripennis*“
10/2012 – 09/2015	M.Sc. in Biologie an der Heinrich-Heine-Universität Düsseldorf Thesis: „Embryonic patterning in the bean beetle *Callsosbruchus maculatus*“

Promotion

Seit 10/2015	Promotion an der Universität zu Köln Institut für Entwicklungsbiologie Betreuer: Prof. Dr. Siehfried Roth

Beruflicher Werdegang

Seit 06/2021	klinischer Monitor bei IQVIA RDS GmbH

Pulikation

Benton MA, Frey N, Nunes da Fonseca R, von Levetzow C, Stappert D, Hakeemi MS, Conrads KH, Pechmann M, Panfilio K, Lynch J, Roth S.
Fog signaling has diverse roles in epithelial morphogenesis in insects (eLife 2019)

Benton MA, Pechmann M, Frey N, Stappert D, Conrads KH, Chen YT, Stamataki E, Pavlopoulos A, Roth S.
Toll Genes Have an Ancestral Role in Axis Elongation (Current Biology 2016)

Benton MA, Kenny NJ, Conrads KH, Roth S, Lynch JA.
Deep, Staged Transcriptome Resources for the Novel Coleopteran Models *Atrachya menetriesi* and *Callosobruchus maculatus* (PLoS One 2016)